

1995

# Statistical Methods for Detecting and Characterizing Departures from Additivity in Multi-Dimensional Drug/Chemical Mixtures

Kathryn S. Dawson  
kathystat@gmail.com

Follow this and additional works at: <http://scholarscompass.vcu.edu/etd>

 Part of the [Life Sciences Commons](#)

© The Author

---


Downloaded from

<http://scholarscompass.vcu.edu/etd/4507>

This Dissertation is brought to you for free and open access by the Graduate School at VCU Scholars Compass. It has been accepted for inclusion in Theses and Dissertations by an authorized administrator of VCU Scholars Compass. For more information, please contact [libcompass@vcu.edu](mailto:libcompass@vcu.edu).


Virginia Commonwealth University  
School of Medicine

This is to certify that the dissertation prepared by Kathryn S. Dawson entitled "Statistical Methods for Detecting and Characterizing Departures from Additivity in Multi-Dimensional Drug/Chemical Mixtures" has been approved by her committee as satisfactory completion of the dissertation requirement of Doctor of Philosophy.

  
Walter H. Carter, Jr., Ph.D., Co-Director of Dissertation

  
Chris Gennings, Ph.D., Co-Director of Dissertation

  
Janet S. Knisely, Ph.D., School of Medicine

  
Vernon M. Chinchilli, Ph.D., Center for Biostatistics and Epidemiology  
College of Medicine  
Pennsylvania State University

  
Richard A. Carchman, Ph.D., Philip Morris USA

  
Walter H. Carter, Jr., Ph.D., Department Chairman

  
Hermes A. Kontos, M.D., Ph.D., Dean, School of Medicine

  
William L. Dewey, Ph.D., Dean, School of Graduate Studies

Date

*July 27, 1995*

**Statistical Methods for Detecting and Characterizing  
Departures from Additivity in Multi-Dimensional  
Drug/Chemical Mixtures**

A dissertation submitted in partial fulfillment of the requirements for the degree of Doctor of Philosophy at Virginia Commonwealth University.

by

Kathryn S. Dawson  
B.A. William Paterson College, 1973  
Wayne, New Jersey  
M.A. University of Maine, 1975  
Orono, Maine  
M.S. Virginia Commonwealth University, 1985  
Richmond, Virginia

Co-Directors:

Dr. Walter Hans Carter, Jr.  
Professor  
Department of Biostatistics

Dr. Chris Gennings  
Assistant Professor  
Department of Biostatistics

Virginia Commonwealth University  
Richmond, Virginia

August, 1995

## Acknowledgments

"...but those who hope in the Lord will renew their strength.  
They will soar on wings like eagles;  
they will run and not grow weary,  
they will walk and not be faint."  
Isaiah 40:31

I would like sincerely to thank my co-advisors, Hans Carter and Chris Gennings. I feel very fortunate to have had the opportunity to work so closely with them. Without Hans's patience and guidance it is doubtful that this project would have been completed. Chris's encouraging words were often a timely, needed motivation. Thanks also to Vern Chinchilli not only for serving on my committee, and coming such a long distance for my defense, but also for being such an excellent teacher in several of my graduate courses. I learned so much in these classes. I want to give a special thanks to Janet Knisely for serving on the committee and for being such a good friend during the last six years. I would also like to thank Rich Carchman for serving on my committee.

I am grateful to all of the past and current members of the Department of Biostatistics for their support and friendship during the time that I have worked on this dissertation. I would especially like to thank everyone who celebrated with me when this project was completed. I was deeply moved by this show of friendship and will always remember it.

Thanks also to the faculty and staff of the Department of Substance Abuse Medicine. Their support and patience throughout my graduate studies has been greatly appreciated.

I thank Barbara Robinson for her unwavering and loyal friendship during the last several years. She was always there when I needed a friend.

Lastly, a special thanks to my parents whose friendship, love and answered prayers saw me through.



## Table of Contents

|   | Page |
|---|------|
| List of Tables . . . . .  | vi   |
| List of Figures . . . . .   | viii |
| Abstract . . . . .  | xi   |
| Chapter 1 Introduction . . . . .  | 1    |
| 1.1 Motivation and Background . . . . .   | 1    |
| 1.2 Prospectus . . . . .  | 13   |
| Chapter 2 Two Graphical Techniques Useful in Detecting Correlation<br>Structure Repeated Measures Data with Fixed Effects . . . . . | 16   |
| 2.1 Introduction . . . . .  | 16   |
| 2.2 A Linear Repeated Measures Model with Fixed Effects Based<br>on the Mixed Model . . . . .                                       | 19   |
| 2.2.1 A Repeated Measures Model with Fixed Effects . . . . .  | 20   |
| 2.3 Properties of the Centered and Scaled Observations . . . . .  | 23   |
| 2.4 Draftman's Display . . . . .  | 25   |
| 2.5 Parallel Axis Display . . . . .   | 25   |
| 2.6 Example . . . . .   | 34   |
| Chapter 3 The Logistic Model . . . . .  | 46   |
| 3.1 Introduction . . . . .  | 46   |
| 3.2 Notation and Model Assumptions . . . . .  | 46   |
| 3.3 Estimation . . . . .  | 50   |
| 3.4 Distributional Properties . . . . .   | 52   |
| 3.5 Goodness-of-Fit Tests . . . . .   | 54   |
| 3.6 Inference . . . . .   | 58   |
| 3.7 Confidence Regions . . . . .  | 62   |
| 3.8 Example . . . . .   | 65   |

|           |   |     |
|-----------|---|-----|
| Chapter 4 | Additivity, Deviations from Additivity, and Isobolograms  | 70  |
| 4.1       | Introduction  | 70  |
| 4.2       | Types of Dose-Response Relationships  | 71  |
| 4.3       | Types of Interactions   | 75  |
| 4.3.1     | Homergic Combinations   | 76  |
| 4.3.2     | Heterergic Combinations: Predictive & Inert   | 81  |
| 4.3.3     | Heterergic Combinations: Predictive & Nonpredictive   | 83  |
| 4.3.4     | Coalitive Combinations  | 84  |
| 4.3.5     | Summary   | 84  |
| 4.4       | Non-monotonic Single Agent Dose-Response Curves   | 85  |
| 4.5       | Isobolograms  | 86  |
| 4.6       | Alternative Definitions of Additivity   | 93  |
| 4.7       | Additivity and Deviations from Additivity for Combinations of Any Number of Agents                        | 97  |
| Chapter 5 | The Dose-Response Surface Approach to Characterizing and Detecting Interactions                           | 103 |
| 5.1       | Introduction  | 103 |
| 5.2       | A Single Agent Dose-Response Curve  | 104 |
| 5.3       | Two Agent Model with Single Interaction Term  | 107 |
| 5.4       | Isobolograms Based on the Two Agent Model with Single Interaction Term                                    | 113 |
| 5.4.1     | Isobolograms for Homergic Two Agent Combinations  | 115 |
| 5.4.2     | Isobolograms for Heterergic Combination of an Active, Predictive Agent and an Inert Agent                 | 119 |
| 5.4.3     | Isobolograms for Coalitive Combinations   | 120 |
| 5.5       | Two Agent Model with More than One Interaction Term   | 126 |
| 5.6       | Logistic Dose-Response Models for N Agent Studies   | 129 |
| 5.6.1     | Point-Wise Interpretation of the Interactions in an N Agent Model   | 131 |
| 5.6.2     | Interactions in an N Agent Model at Varying Doses of a Single Agent                                       | 135 |
| 5.6.3     | Pair-wise Interactions in an N Agent Model  | 136 |
| Chapter 6 | A Point-Wise Test to Detect Interactions  | 148 |
| 6.1       | Introduction  | 148 |
| 6.2       | Characterizing the Interactions When the Response-Surface Model is Based on a Transformation of the Doses | 149 |
| 6.3       | The Interaction Index Test  | 151 |
| 6.4       | Example   | 155 |

|            |   |     |
|------------|---|-----|
| Chapter 7  | Detecting and Characterizing Interactions Based on a Ray Designed Experiment . . . . .      | 162 |
| 7.1        | Introduction . . . . .  | 162 |
| 7.2        | The Model . . . . .   | 163 |
| 7.3        | Two Agent Example . . . . .   | 169 |
| 7.4        | Statistical Tests for Detecting Deviations from Additivity . . . . .                        | 173 |
| 7.4.1      | Likelihood Ratio Test for Nonadditivity . . . . .   | 177 |
| 7.4.2      | Wald Test for Nonadditivity . . . . .   | 179 |
| 7.4.3      | Score Test for Nonadditivity . . . . .  | 180 |
| 7.5        | Characterizing and Testing for Deviations from Additivity Along Each Non-axis Ray . . . . . | 181 |
| 7.5.1      | Two Agent Example . . . . .   | 183 |
| 7.5.2      | Four Agent Example . . . . .  | 185 |
| 7.6        | Isobolograms for an N Agent Ray Designed Experiment . . . . .                               | 192 |
| 7.7        | Summary . . . . .   | 196 |
| Chapter 8  | Extensions an Summary Comments . . . . .  | 199 |
| 8.1        | Extensions . . . . .  | 199 |
| 8.2        | Summary Comments . . . . .  | 200 |
| References | . . . . .   | 202 |
| Appendix A | . . . . .   | 208 |
| Appendix B | . . . . .   | 211 |
| Appendix C | . . . . .   | 214 |
| Vita       | . . . . .   | 221 |

## List of Tables

| Table  | Page |
|--|------|
| 2.1 Covariance Structures . . . . .  | 22   |
| 2.2 Tumor Size (mm <sup>3</sup> ) over course of the Experiment (Koziol) . . . . .   | 35   |
| 2.3 Preliminary Analysis Results Using Proc Mixed in SAS® . . . . .  | 43   |
| 3.1 Chloral Hydrate and Ethanol Study: Loss of Righting Reflex in Mice: Data and Goodness of Fit Statistics . . . . .  | 67   |
| 3.2 Chloral Hydrate and Ethanol Study: Loss of Righting Reflex in Mice - Analysis Results . . . . .  | 68   |
| 4.1 Comparison Method Applied to Homergic Combinations . . . . .   | 79   |
| 5.1 Parallel Axis Representation of X <sub>i</sub> X <sub>j</sub> Isobol . . . . .   | 143  |
| 6.1 Simulated Two Agent Dose-Response Study Data . . . . .   | 156  |
| 6.2 Simulated Two Agent Dose-Response Analysis Results for Model $\text{logit}[P(\mathbf{X};\boldsymbol{\beta})] = \beta_0 + \beta_1 X_1 + \beta_2 X_2 + \beta_{12} X_1 X_2$ . . . . .   | 157  |
| 6.3 Simulated Two Agent Dose-Response Analysis Results for Model $\text{logit}[P(\mathbf{X};\boldsymbol{\beta})] = \beta_0 + \beta_1 \log_{10}(X_1 + 1) + \beta_2 \log_{10}(X_2 + 1) + \beta_{12} \log_{10}(X_1 + 1) \log_{10}(X_2 + 1)$ . . . . . | 159  |
| 6.4 Simulated Two Agent Dose-Response Study Interaction Index Test Results . . . . .   | 160  |
| 7.1 Two Agent Simulated Data . . . . .   | 172  |
| 7.2 Two Agent Simulated Data Analysis Results . . . . .  | 174  |
| 7.3 Two Agent Simulated Data Observed and Predicted Responses and Goodness-of-Fit Statistics . . . . .   | 175  |

|     |  |     |
|-----|--|-----|
| 7.4 | Two Agent Simulated Data Simultaneous Tests for Deviations from Additivity . . . . . | 184 |
| 7.5 | 4 Agent Simulated Data . . . . .   | 188 |
| 7.6 | 4 Agent Simulated Data Analysis Results . . . . .                                    | 189 |
| 7.7 | 4 Agent Simulated Data Simultaneous Tests fro Deviations from Additivity . . . . .   | 190 |

## List of Figures

| Figure   | Page |
|--|------|
| 1.1 Dose-Response Surface and their Corresponding Contours ( $\pi = 0.5$ ) . . . . .   | 4    |
| 1.2 Isobologram ( $\pi = 0.5$ ) from Gessner and Cabana's Study (1970) of Chloral Hydrate and Ethanol . . . . .  | 6    |
| 1.3 "Conjectures based solely on low-dimensional examples are false in high dimensions", What's Happening in Mathematics, p.25, (1993) . . . . .                                   | 12   |
| 1.4 Parallel Axis N-Dimensional Representation of Point Interior to N-Dimensional Sphere . . . . .   | 14   |
| 2.1 Five Dimensional Point (3,7,5,8,2) Plotted in a Parallel Coordinate System . . . . .   | 18   |
| 2.2 Ordering of Scatter Plots in a Draftman's Display to View Correlation Structure . . . . .  | 26   |
| 2.3 Simulated Four Dimensional Normal Data with Various Correlation Structures Plotted in a Draftman's Display . . . . .   | 27   |
| 2.4 Comparing the Diagonal Elements of the Covariance Matrix in a Parallel Axis System using Simulated Four Dimensional Normal Data with Different Correlation Structure . . . . . | 29   |
| 2.5 Simulated Bivariate Normal Data with Various Correlation Coefficients plotted in both a Parallel Axis System and a Scatter Plot . . . . .                                      | 31   |
| 2.6 Ordering of the Parallel Axis Plots to View Correlation Structure . . . . .  | 32   |
| 2.7 Simulated 4-Dimensional Normal Data with Various Correlation Structure Plotted in a Parallel Axis System . . . . .   | 33   |
| 2.8 Observed Koziol Data Plotted Over Time . . . . .   | 36   |
| 2.9 Centered Observed and Transformed Koziol Data Plotted in a Parallel Axis System . . . . .  | 38   |

|      |  |     |
|------|--|-----|
| 2.10 | Centered Ln Transformed Koziol Data by Group . . . . .   | 39  |
| 2.11 | Centered and Scaled Ln Transformed Koziol Data in a Parallel Axis System . . . . .   | 40  |
| 2.12 | Centered and Scaled Ln Transformed Koziol Data in a Draftman's Display   | 41  |
| 2.13 | Ln Transformed Koziol Data Plotted Over Time . . . . .   | 44  |
| 4.1  | Single Agent Dose-Response Curves . . . . .  | 72  |
| 4.2  | Types of Two Agent Combinations . . . . .  | 74  |
| 4.3  | Isobolograms for a Two Agent Study . . . . .   | 87  |
| 4.4  | Isobolograms for the Heterergic Combination of a Predictive Agent and an Inert Agent . . . . .                                   | 89  |
| 4.5  | The Use of the Potentiation Coefficient . . . . .  | 91  |
| 4.6  | Comparison of Total of Doses at $(x_1, x_2)$ and $(z_1, z_2)$ . . . . .  | 92  |
| 4.7  | Three Agent Isobologram . . . . .  | 103 |
| 5.1  | Examples of Single Agent Logistic Dose-Response Curves . . . . .   | 106 |
| 5.2  | Examples of Two Agent Logistic Dose-Response Surfaces . . . . .  | 109 |
| 5.3  | Chloral Hydrate and Ethanol Dose-Response Surface, Carter (1988) .   | 114 |
| 5.4  | Homergic Combinations . . . . .  | 117 |
| 5.5  | Heterergic Combinations . . . . .  | 121 |
| 5.6  | Coalitive Combinations . . . . .   | 123 |
| 5.7  | Isobologram and Associated Dose-Response Surface with Regions of Synergism and Antagonism . . . . .                              | 128 |
| 5.8  | Regions of Synergism and Antagonism for Model given in (5.6.5) and $X_i = 0.5, 1.0, 1.5, 2.0, 2.5; i=1,2,3,4$ . . . . .          | 133 |
| 5.9  | Regions of Synergism and Antagonism for Model given in (5.6.5) and $X_1 = 0.25, X_2 = 0.25, X_3, X_4 = 1, 1.5, 2, 2.5$ . . . . . | 134 |

|      |   |     |
|------|---|-----|
| 5.10 | Full Model Versus Model Under Additivity Over Levels of $X_1$ at Fixed Levels of $X_2$ , $X_3$ , and $X_4$ - Model given in (5.6.5) | 137 |
| 5.11 | Draftman's Display of Pairwise Isobols ( $\pi = 0.5$ ) - Model Given in (5.6.5)   | 139 |
| 5.12 | Parallel Axis Display of Pairwise Isobols ( $\pi = 0.5$ ) - Model Given in (5.6.5)  | 144 |
| 7.1  | Experimental Design for Two-Agent Simulated Data  | 171 |
| 7.2  | Two Agent Simulated Data - Full Model versus Expected Under Additivity  | 186 |
| 7.3  | Four Agent Simulated Data - Full Model versus Expected Under Additivity   | 191 |
| 7.4  | Isobologram ( $\pi = 0.5$ ) for Two Agent Simulated Data  | 194 |
| 7.5  | Parallel Isobologram ( $\pi = 0.5$ ) for Two Agent Simulated Data   | 195 |
| 7.6  | Parallel Isobologram ( $\pi = 0.5$ ) for Four Agent Simulated Data with Rays Ordered by Increasing Size of Observed p-value         | 197 |



Statistical Methods for Detecting and Characterizing  
Departures from Additivity in Multi-Dimensional Drug/Chemical Mixtures

Abstract

A dissertation submitted in partial fulfillment of the requirements for the degree of Doctor of Philosophy in the Department of Biostatistics at the Medical College of Virginia, Virginia Commonwealth University.

Kathryn S. Dawson

Medical College of Virginia

Virginia Commonwealth University

Research Co-Directors: Dr. Walter Hans Carter, Jr.

Dr. Chris Gennings

In studies of the effects of multiple drug or chemical combinations, one goal may be to detect and characterize the interactions between the agents. The techniques currently applied to this problem have limitations when the experiments involve more than 2 agents. Certain response-surface techniques require an unrealistic number of observations for studies involving a large number of agents. Current graphical methods are impossible to use in studies of 3 or more agents. In this research two statistical techniques are described that can be applied to studies with an unlimited number of agents. In the first approach, dose combinations are collected along rays or at fixed ratios. Using properties of this experimental design, an additive model is derived. Comparing the fitted dose-response curve along each ray to the curve predicted under additivity, synergistic and antagonistic

interactions between the agents can be detected. Statistical testing procedures are given to determine if these are significant interactions, not due to random fluctuations in the data. Graphical techniques that enhance the interpretation of the results are described. The second approach developed in this research is a point-wise test which determines if the agents interact in a nonadditive manner. This test can be applied to each dose combination of interest. After applying a multiple comparison adjustment to the resulting p-values, departures from additivity can then be characterized. These approaches are likely to be more economical than current techniques, implying that a larger number of agents can be studied in combination for the same experimental effort.

# **Chapter 1**

## **Introduction**

### **1.1 Motivation and Background**

A goal of studies that examine the effects of combinations of chemicals or drugs is to describe how the agents interact. Specifically, based on knowledge of each agent's dose-response relationship, an additive response, or the response assuming the agents do not interact, can be determined. If the observed response differs from the additive response, then the manner in which it differs can be assessed. This type of information may be useful in several ways. For example, if it can be determined that the chemicals that comprise an insecticide interact to enhance the effect, less of the chemicals in combination may be needed to observe the desired response.

One purpose of this dissertation is to derive statistical and graphical methods for detecting and characterizing the interactions in studies that contain a large number of agents. While many methods exist for analyzing two agent combinations, not all are applicable to studies that involve 3 or more agents. This can possibly be explained by limitations inherent in the two agent methods. Certain of these methods are dependent on 2-dimensional graphical displays which are not generalizable to dimensions higher than 2 or 3. In addition, while other analytic methods can be applied, at least theoretically, to studies that involve any number of agents, the size of the experiment needed to adequately determine the results is unreasonably large. Calabrese, (1991, p. 4) has noted, however, that "humans are not exposed to single agents; the environment provides exposure to

complex daily mixture of agents; health standards have long ignored the issue of multiple exposures; and this should be an area of high priority". Berenbaum (1989) also gave several examples of situations where it is important to study the effects of combinations of more than 2 agents, i.e. in the treatment of certain cancers 4 - 6 agents are jointly applied, since in combination, they have been shown to be more effective than each agent alone. Clearly there is a need for methods that can be applied to studies that involve a large number of agents.

In the following discussion several terms will be used that will only be briefly defined in this chapter. These terms and derivations, however, will be thoroughly discussed in Chapter 4. In fact, one aim of this dissertation is to unify certain definitions that have been used to describe interactions. It has been noted in this field of study that there has been a lack of consistency in terminology. Calabrese (1991, p. 13) writes, " there are different words describing phenomena that seem to be the same but are often employed in totally different ways by different authors. Such lack of communication and frequent anarchy creates a high baseline of confusion within the scientific and regulatory communities but also the general public". For example, all of the following terms have been used to describe an interaction where the response is greater than additive: synergy, potentiation, superadditivity, positive interaction.

While the focus in this research is on combinations of a large number of agents it will be useful to review certain methods that have been applied to the study of two agents. In general the literature on this subject can be grouped into two broad, not necessarily exclusive, categories. The first group is dependent on an assumed knowledge of the mechanism of action of the agents considered in the study. As noted by Berenbaum (1989), authors who have considered this approach include Bliss (1939), Finney (1952), Hewlett and Plackett (1964), Ashford and Smith (1964), and Chou and Talalay (1984).

An alternative approach, and the approach considered in this dissertation, is mechanism-free. The results are based only on the observed effects. In general, it is assumed that an underlying dose-response surface exists. By examining the isobols, or contours from this surface, the types of interactions between the agents can be described.

In 1953 Loewe graphically described a 3-dimensional dose-response surface. When the agents interacted in an additive manner, the resulting surface was described by Loewe as a "tense sail". Loewe noted that an "inflated" sail, or synergism, indicates less of the agents in combination are needed to reach a given response. A "sagging sail", or an antagonism, implies more is needed. Loewe demonstrated that when isobols, or contours from these surfaces for a fixed value of the response, were examined, the resulting 2-dimensional plot differentiated the types of interactions between the agents. Illustrations of these surfaces and their associated isobols are shown in Figure 1.1. A plot of the isobol is referred to as an isobologram. Note that, assuming additivity, the isobol is a straight line. The equation of this line of additivity is given by

$$\frac{X_1}{ED_1(\pi)} + \frac{X_2}{ED_2(\pi)} = 1 \quad (1.1.1)$$

where  $\pi$  is the fixed response of interest,  $X_i$  is a dose of the  $i$ th agent, and  $ED_i(\pi)$  is the effective dose of the  $i$ th agent,  $i = 1, 2$ . Berenbaum (1977, 1981, 1989) validated the usefulness of this approach by demonstrating that (1.1.1) holds for combinations of two agents that clearly do not interact: the sham combination of an agent with itself. He also derived the interaction index given as

$$\frac{X_1}{ED_1(\pi)} + \frac{X_2}{ED_2(\pi)} \begin{cases} > 1 & \text{Synergism} \\ = 1 & \text{Additivity} \\ < 1 & \text{Antagonism} \end{cases} \quad (1.1.2)$$

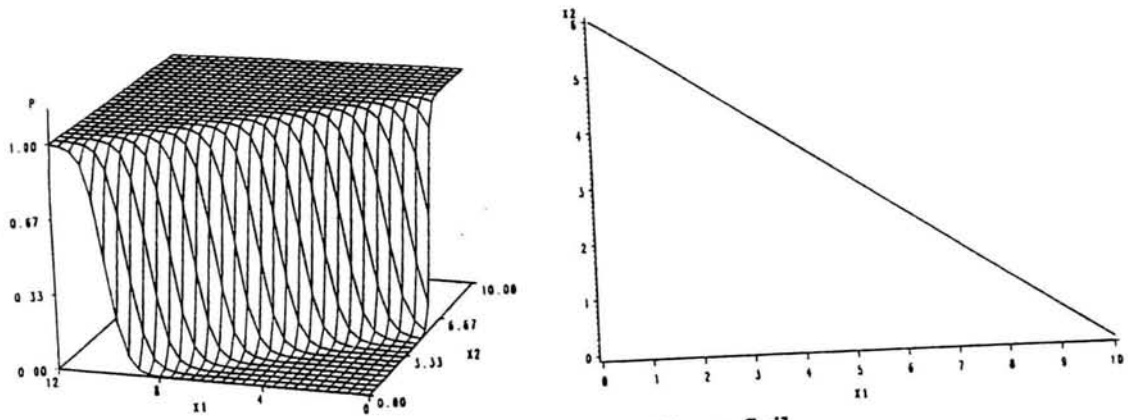


Figure 1.1 (a): Additivity - Tense Sail

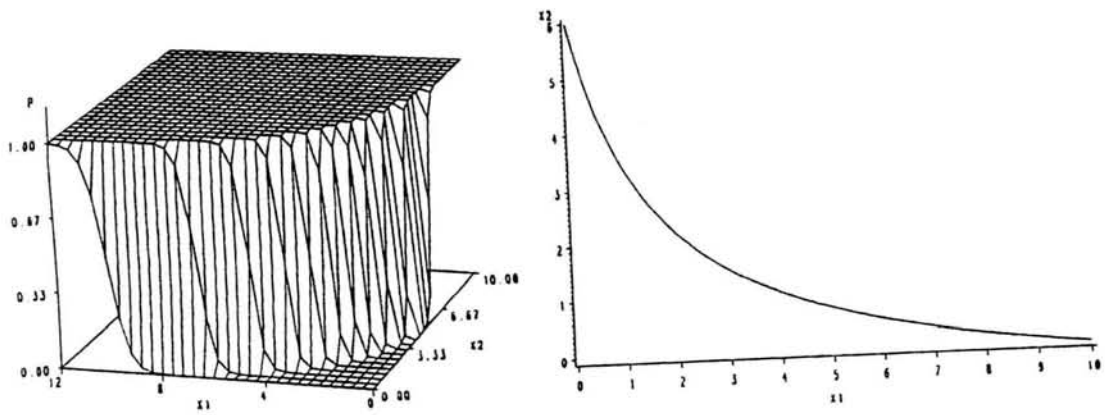


Figure 1.2 (b): Synergism - Inflated Sail

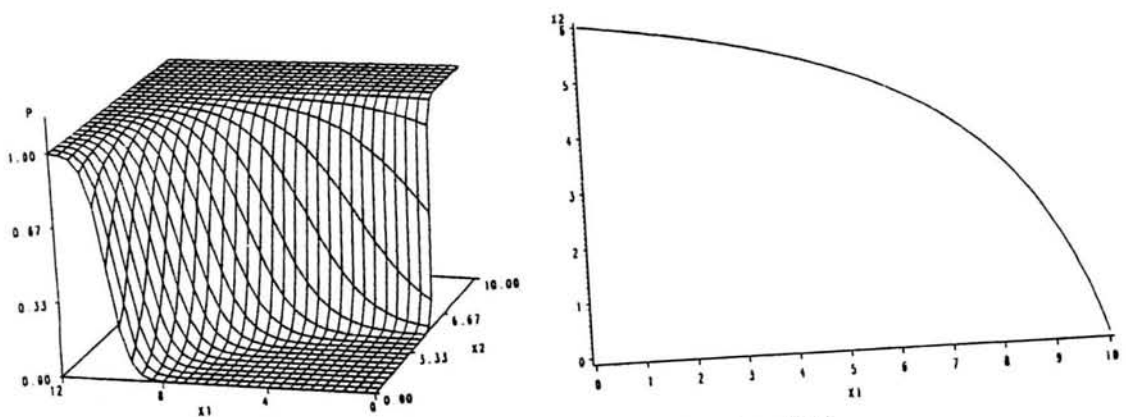


Figure 1.1 (c): Antagonism - Sagging Sail

Figure 1.1: Dose-Response Surface and their Corresponding Contours ( $\pi = 0.5$ )

By applying (1.1.2) at a given dose combination with observed response  $\pi$ , the type of interaction can be described. Berenbaum noted, however, that "Whether the degree of synergy so measured is statistically significant or clinically relevant are matters for investigation by appropriate statistical, experimental, and clinical methods" (1978, p.130). Hence, the methods of Loewe and Berenbaum can be considered exploratory in nature since the conclusions drawn, based on these methods, may be attributable to random variability in the data.

Gessner and Cabana (1970) incorporated statistical techniques when they used isobolograms to study the joint effects of chloral hydrate and ethanol. Dose combinations were taken at fixed levels of one agent and varying doses of the other. The loss of righting reflex (yes/no) in mice was then observed. Using probit analysis, the dose associated with a 50% response was estimated and confidence intervals placed about the dose combination. The results are shown in Figure 1.2. Synergism is suggested at low doses of ethanol and high doses of chloral hydrate since the predicted dose combinations fall below the line of additivity. Note, however, that while multiple confidence intervals were derived, no multiple testing adjustment in their statistical methods was made.

The additive expression given in (1.1.1) has been used in several other alternative ways. For example, at a fixed value of the response, Tallarida (1992) applied (1.1.1) to estimate additive dose combinations. Modeling a probit transformation of the response as a function of  $\log(\text{dose})$ , dose-response curves were estimated for each agent alone. An expected dose combination under additivity was then determined and compared to the observation combination. A statistical test was applied to determine if these values significantly differed.

Under the assumption that each individual agent's dose-response curve is known, Berenbaum (1985) also demonstrated that (1.1.1) can be used to determine a response

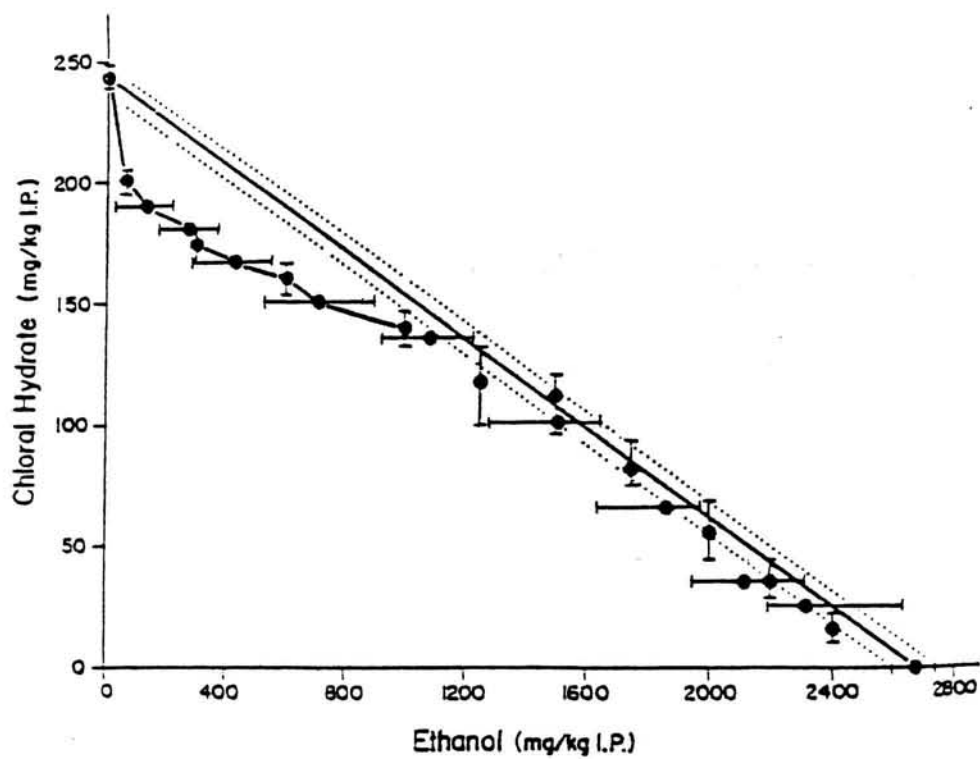


**Figure 1.2:** Isobologram ( $\pi = 0.5$ ) from Gessner and Cabana's Study (1970) of Chloral Hydrate and Ethanol



under the assumption of additivity at a given dose combination  $(x_1, x_2)$ . Kelly and Rice (1990) applied this method by using a nonparametric spline-based procedure of curve-fitting to estimate each curve. Then based on (1.1.1), the expected response under additivity was estimated and compared to the observed response. A chi-square test was used to determine if the additive response and the observed response differed. Gennings and Carter (1995) placed a prediction interval about the derived response under additivity. If the observed response is not contained in the resulting interval then a deviation from additivity is suggested. It should be noted that the example cited in Gennings' work involves ten agents demonstrating this method can, in fact, be applied to studies that involve a large number of agents.

Another group of authors has considered functional forms that can be used to model an isobol. Based on (1.1.1), properties of the model can then be determined that satisfy additivity. For example, Lam, Pym and Campling, 1991, suggest a model given by

$$\frac{x_1}{ED_1(\pi)} + \frac{x_2}{ED_2(\pi)} + \kappa \frac{x_1 x_2}{(ED_1(\pi)ED_2(\pi))^{1/2}} = 1.$$

where the values for  $ED_i(\pi)$ ,  $i=1,2$  can be estimated by separately modeling each agent's individual dose-response curve. It then follows, for a fixed dose combination  $(x_1, x_2)$  that, if  $\kappa=0$  additivity is indicated, and if  $\kappa$  is greater (less) than 0 synergism (antagonism) is suggested.

Machado and Robinson (1994) have also considered modeling the isobol and then generalizing it to describe the dose-response surface. While several possible forms of this model are described, one example is given by

$$\left(\frac{x_1}{ED_1(\pi)}\right)^\eta + \left(\frac{x_2}{ED_2(\pi)}\right)^\eta = 1$$

where  $\eta = 1$  implies additivity. Assuming each individual dose-response curve is given by  $H_i(X_i; \theta)$ ,  $i=1,2$  where  $\theta$  are the unknown parameters, the effective doses for each agent are given by  $H_i^{-1}(\pi)$ . Then by letting  $\pi$  vary, an expression that describes the entire dose-response relationship is obtained.

Another group of authors has considered models that directly describe the dose-response surface. Once it can be determined that the model adequately describes the data, isobols can be examined by plotting contours from the fitted model at fixed value of  $p$ . Carter, et al., in 1988, described a dose-response model for a quantal response that is given by

$$P(X_1, X_2; \beta) = \frac{1}{1 + \exp[-(\beta_0 + \beta_1 X_1 + \beta_2 X_2 + \beta_{12} X_1 X_2)]}. \quad (1.1.3)$$

This expression was used to model the dose-response surface for the combination of chloral hydrate and ethanol. By applying the interaction index given in (1.1.2), Carter, et al. derived properties of this model that can be used to describe the types of interactions between the agents, i.e.  $\beta_{12} = 0$  indicates additivity and  $\beta_{12}$  greater (less) than 0 suggests synergism (antagonism). A statistical test was applied to determine if  $\beta_{12}$  was, in fact, significantly different from 0. It was determined, in agreement with the result of Gessner and Cabanna, that the agents interact synergistically. Gennings, et al. (1990) also illustrated the usefulness of this approach with examples of isobolograms, estimated from a fitted model based on (1.1.3), for combinations that were additive, synergistic and antagonistic. In addition, Gennings, et al. (1990) demonstrated that by plotting the line

of additivity in conjunction with a confidence region about an isobol a statistically significant nonadditive interaction could be detected graphically.

An alternative model for the dose-response surface has been suggested by Greco, Park and Rustum, (1990). Here each individual agent's dose-response curve is modeled according to the Hill model or, equivalently, the median-effect equation of Chou and Talalay (1984), given by

$$E = \frac{E_{\max} \left( \frac{X_i}{ED_i(\text{median})} \right)^{m_i}}{1 + \left( \frac{X_i}{ED_i(\text{median})} \right)^{m_i}} + B$$

where  $X_i$  is the dose of the  $i$ th agent,  $ED_i(\text{median})$  is the dose of the  $i$ th agent to yield the median response,  $E$  is the effect or response,  $E_{\max}$  is the maximum possible response,  $B$  is the background response and  $m_i$  is referred to as the concentration-effect slope for the  $i$ th agent. Greco, et al. (1990) then modeled the dose-response surface according to

$$1 = \frac{X_1}{ED_1(\text{median}) \left[ \frac{E - B}{E_{\max} - E + B} \right]^{1/m_1}} + \frac{X_2}{ED_2(\text{median}) \left[ \frac{E - B}{E_{\max} - E + B} \right]^{1/m_2}} + \frac{\alpha X_1 X_2}{ED_1(\text{median}) ED_2(\text{median}) \left[ \frac{E - B}{E_{\max} - E + B} \right]^{1/2m_1 + 1/2m_2}}$$

where  $\alpha$  is referred to as the synergism-antagonism parameter. Here  $\alpha = 0$  indicates additivity and  $\alpha$  greater (less) than 0 suggests synergism (antagonism).

Hence, without making assumptions about the mechanism of action for each agent, many approaches have been considered for examining the effects of two agents in

combination. Little work has been done, however, in extending these methods to combinations of three or more agents. For some of the methods just discussed, it is not clear how the methodology described can be extended to more than 2 agents. For example, neither Lam et al. nor Greco et al. describe forms of their model for a higher dimensional study. Theoretically, some of the two agent methods just described could be extended to studies of any number of agents. Berenbaum (1978) noted that the interaction index given in (1.1.2) can be applied to studies of any number of agents. Carter et al. (1988) describe how the response-surface approach can be generalized to more than two agents by including the appropriate number of single agent and cross product terms in a dose-response model. Note, however, that as the number of agents increases the number of cross-product terms and, hence, the number of unknown parameters will increase. Therefore, the size of the experiment needed to estimate these terms will become so large that it may be economically infeasible. For example, consider a possible two agent factorial design with 5 levels of each of the two agents with 6 replications at each dose combination. Hence a total of  $6 * 5^2 = 150$  observations would be collected. Extending this factorial design to a study of 4 agents leads to  $6 * 5^4 = 3750$  observations and in a study of 8 agents over two million observations would be needed. Even if a fractional factorial design is considered the size of the experiment will become unreasonable when a large number of agents are studied. In this dissertation two methods have been developed that can be applied to studies of any number of agents. It will be demonstrated that these methods can be applied to much smaller experiments than required in the typical factorial or fraction of a factorial design.

As previously noted, another purpose of this research is to derive graphical methods of examining data in higher dimensions. Graphical techniques play an important role in many statistical analyses. In particular, the 2-dimensional graphical isobologram was the basis for virtually all of the two agent methods previously discussed. Greshwin

and Smith (1973) showed that for three agents the line of additivity generalizes to a 3-dimensional plane of additivity and that dose combinations below and above the plane were indicative of synergism and antagonism, respectively. Berenbaum (1978, p.123) noted, however, that it is "physically impossible to plot isobols for combinations of more than 3 agents".

In this dissertation several graphical displays will be described that will be shown to be useful in statistical analyses based on higher dimensional data. While in Chapters 5 and 7 these methods will be applied to the study of combinations of any number of agents, in Chapter 2 the usefulness of certain higher dimensional plotting techniques in an alternative type of statistical analysis will also be demonstrated, i.e., one not necessarily related to the study of combinations of drug or chemicals. A plotting method that will be applied in all of these chapters involves the use of a parallel axis system. This technique described by Inselberg (1985) will be defined in Chapter 2. Gennings, et al. (1990) demonstrated that properties of higher-dimensional isobols could be visualized in a parallel axis system. It can also be shown that the parallel axis system is useful in visually detecting properties, some of which may be counterintuitive, of other N-dimensional relationships. For example, consider the following scenario. Suppose, in 2-dimensions, four circles of radius one are drawn, centered each at (-1,1), (1,1), (-1,-1) and (1,-1) as shown in Figure 1.3(a). An additional circle is then drawn, centered at the origin, that touches each of the four circles. Clearly the center circle is enclosed in the square that contains the four circles. This construction can now be extended to 3 dimensions so that 8 spheres are drawn which are enclosed in a cube. A center sphere is also drawn that touches each of the 8 circles. Again by Figure 1.3(b) it is clear that the center sphere lies within the 3-dimensional cube. It would seem obvious that in N-dimensions the N-dimensional center sphere would lie within the N-dimensional cube. It can be shown, however that when  $N = 10$  the result is not true. This is because the radius of the central sphere is given by  $\sqrt{N} - 1$ . Hence,

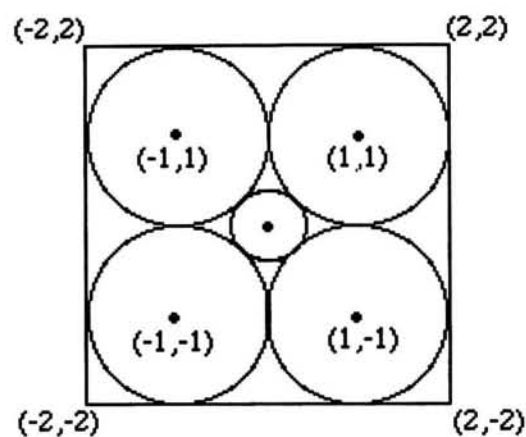


**Figure 1.3(b):** Construction in 2-Dimensions

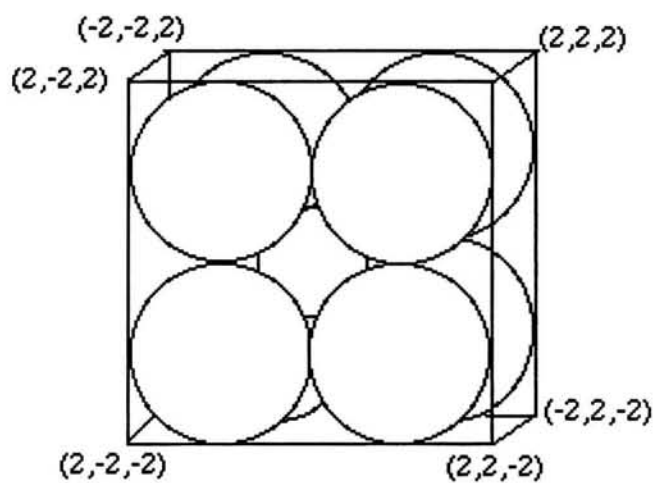


**Figure 1.3(b):** Construction in 3-Dimensions

**Figure 1.3:** "Conjectures based solely on low-dimensional Examples are false in high dimensions", *What's Happening in Mathematics*, p. 25, (1993).

when  $N = 10$  this radius is 2.162. Note however that the distance from the origin to the side of the cube is 2. Therefore, when  $N = 10$  the center sphere is not enclosed in the 10-dimensional cube. While it is not possible to graphically visualize this in the usual Euclidean plane, it can be shown that a plotting algorithm in the parallel axis system demonstrates the result. This algorithm, developed by Inselberg and Dimsdale (1987), graphically determines if a point is inside or outside of a  $N$ -dimensional convex set. The point of interest in this case is a point along the edge of the  $N$ -dimensional cube, i.e., in 3 dimensions this point would be  $(0,0,2)$ . The convex set is the  $N$ -dimensional center sphere. In Figure 1.4 this algorithm is demonstrated for dimensions, 2, 3, 5, 10 and 20. The dark connected line segment in each plot is the parallel axis plot of a point along the edge of the cube. The tangent lines to the pair of curves between each pair of axes represents a boundary on the range of possible values that a coordinate can assume so that the point lies within the sphere. Note that for dimensions 2, 3 and 5 the edge of the cube is outside of the sphere. For dimensions 10 and 20, however, the edge of the cube is inside the sphere.

## 1.2 Prospectus

In Chapter 2 certain higher dimensional plotting techniques are derived and their usefulness illustrated in a repeated measures analysis. Specifically, a mixed modelling approach to this type of analysis is considered, where, in addition to specifying the form of the model, a form for the variance-covariance matrix may be chosen. In this chapter it is demonstrated that in a parallel axis plot of the transformed data certain properties of the variance-covariance matrix can be visualized. An alternative plotting technique, based on the matrix of pairwise plots, or a draftman's display, is also shown to be useful in visually detecting correlation patterns in the data. The analyst can use these plots when initially

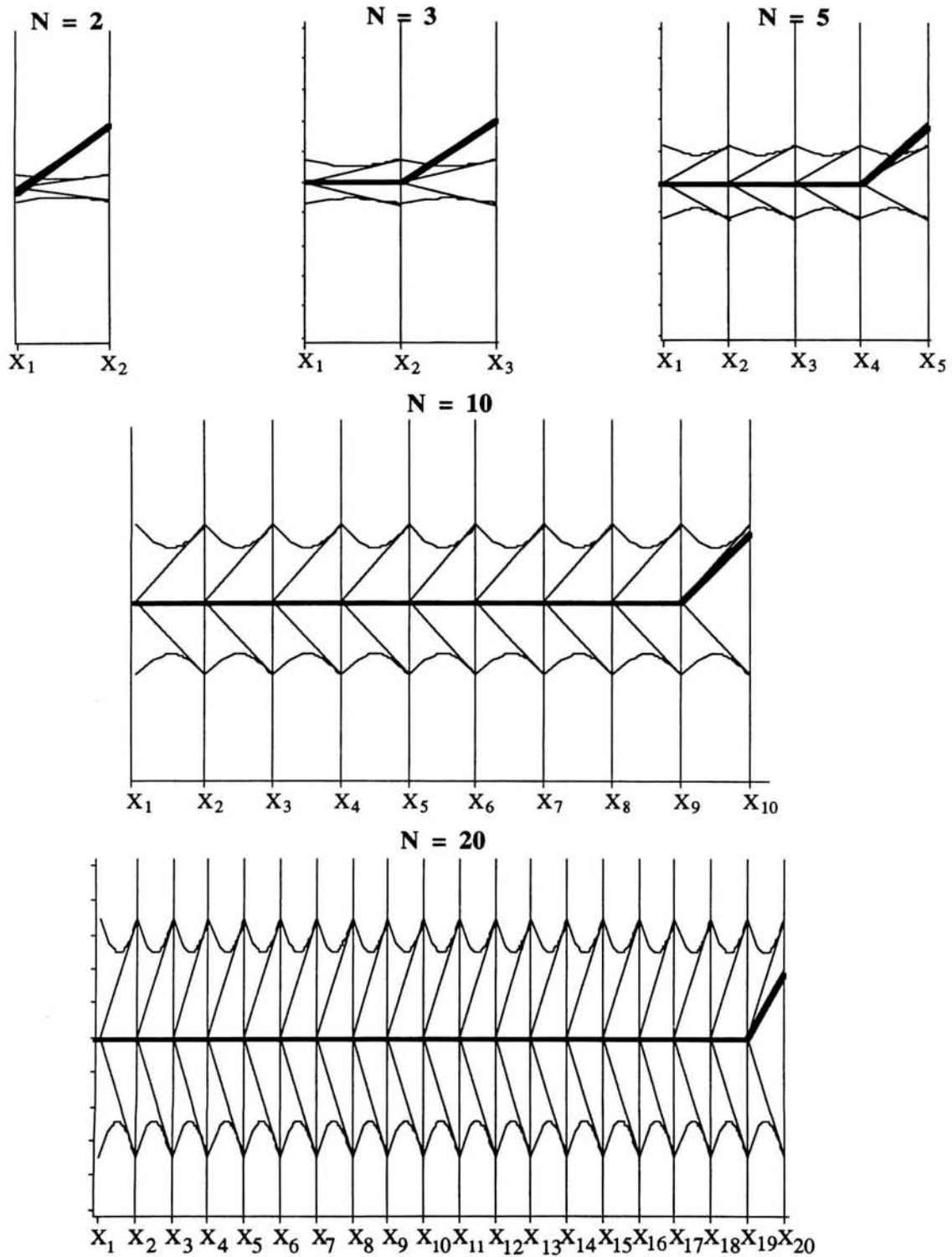


**Figure 1.4:** Parallel Axis N-Dimensional Representation of Point Interior to N-Dimensional Sphere



specifying a form for the variance-covariance matrix. The parallel axis plotting technique as well as the draftman's display will be used again in Chapters 5 and 7.

In Chapters 3 through 7 methods of detecting and characterizing interactions between any number of agents are considered. The focus of this dissertation will be on experiments where the response is quantal. Since the dose-response relationship is often sigmoidal in shape the logistic model was chosen. In Chapter 3, properties of this logistic model are considered. This includes a description of properties of the maximum likelihood estimates of the model parameters and certain useful statistical tests that can be applied in this context. Several definitions and derivations are given in Chapter 4 which formally describe how the agents interact. This chapter concisely summarizes the results and assumptions made in an ad hoc manner and inconsistently throughout the literature. In Chapter 5, the dose-response modeling technique for detecting and characterizing interactions is described. Certain properties of the logistic model are generalized to other types of combinations. It is also shown that a matrix of plots of pairwise isobols is equivalent to the parallel axis display described by Gennings, et al. (1990). It is then shown in Chapter 6 that certain properties of the logistic dose-response surface that were derived in Chapter 5 are not applicable when a model is fit in terms of certain transformations for the doses. A point-wise test to detect deviations from additivity is then derived. In Chapter 7, a method of detecting and characterizing interactions based on dose combinations that satisfy fixed ratios is derived. This method will be shown to be particularly useful in studies of a large number of agents since it can be applied to far fewer observations than needed to fit the parameters in a dose-response model. Lastly, areas of future research will be considered in Chapter 8.

## Chapter 2

### Two Graphical Techniques Useful in Detecting Correlation Structure in Repeated Measures Data with Fixed Effects

#### 2.1 Introduction

In this chapter the usefulness of certain plotting techniques when examining higher dimensional data will be demonstrated in an application not related to dose-response studies. Specifically, fixed effects repeated measures data in which a response is measured on each observational unit on more than one occasion will be considered. The response is assumed to be continuous. This is in contrast to the remainder of this dissertation where quantal responses will be discussed.

Multivariate modeling techniques have been used successfully in the analysis of repeated measures data. Here the  $p$ -vector of observations for the  $i$ th subject,  $\mathbf{y}_i$ , is commonly assumed to be normally distributed with  $p \times 1$  mean vector and  $p \times p$  dispersion matrix. If the number of time points is large however, the number of parameters in this arbitrary dispersion matrix increases and may be poorly estimated (Laird and Ware, 1982).

The mixed model approach to analyzing repeated measures data has been described by several authors including Harville (1977) and Laird and Ware (1982). One advantage of this approach is the ability to model the covariance or correlation structure for the repeated measurements on a subject where positive correlation is expected. This can result in a reduction in the number of parameters in the dispersion matrix to be estimated and can therefore improve the efficiency of inferences and estimates made. This is especially true

when the data are unbalanced and the number of time points is large relative to the number of observations (Ware, 1985).

Assuming no knowledge about the covariance matrix, the analyst could attempt to fit a mixed model with an unspecified structure and use the resulting estimated covariance matrix to suggest a better defined structure. The appropriateness of the more specified model can be evaluated. If, however, the number of subjects and/or time points is large, algorithms used to attain the initial unspecified estimated structure may not converge. In this chapter it will be demonstrated how, without first fitting a model, two different graphical techniques can aid the user in determining an initial form of the covariance matrix.

The two methods considered in the following are the draftman's display and parallel axis plots. The well known draftman's display is a two dimensional array of scatter plots  $X_i \times X_j$ ,  $i=1,2,\dots,p$ ,  $j=1,2,\dots,p$ ,  $i \neq j$ . A  $p$ -dimensional data point  $(x_1, x_2, \dots, x_p)$  can be displayed as a series of points  $(x_i, x_j)$   $i \neq j$  each plotted in the appropriate  $X_i \times X_j$  coordinate system. This technique has been shown to be helpful in detecting clustering and outliers (Chambers, et al 1983).

Plotting in a parallel axis system, as discussed by Inselberg (1985), involves using a set of connected line segments to plot a  $p$ -dimensional point.  $P$  parallel axes are drawn one unit apart corresponding to the variables  $X_1, X_2, \dots, X_p$ . The point  $(x_1, x_2, \dots, x_p)$  is plotted by drawing lines from the values  $x_i$  on the  $X_i$  axis to the value  $x_{i+1}$  on the adjacent  $X_{i+1}$ ,  $i=1,2,\dots,p-1$  axis. The point  $(3,7,5,8,2)$  is shown in Figure 2.1. A complete set of data can be plotted by drawing all of the connected line segments on a common set of axes in a single graph (see Figure 2.4). Gennings, et al (1990) developed analytical results useful in interpreting higher dimensional parallel axis plots of a polynomial model. Wegman (1990) demonstrated the usefulness of this plotting technique in observing structure and clustering in higher dimensional data. With respect to repeated measures data, Weiss and Lazaro (1992) showed by noting trends and patterns in a parallel axis plot

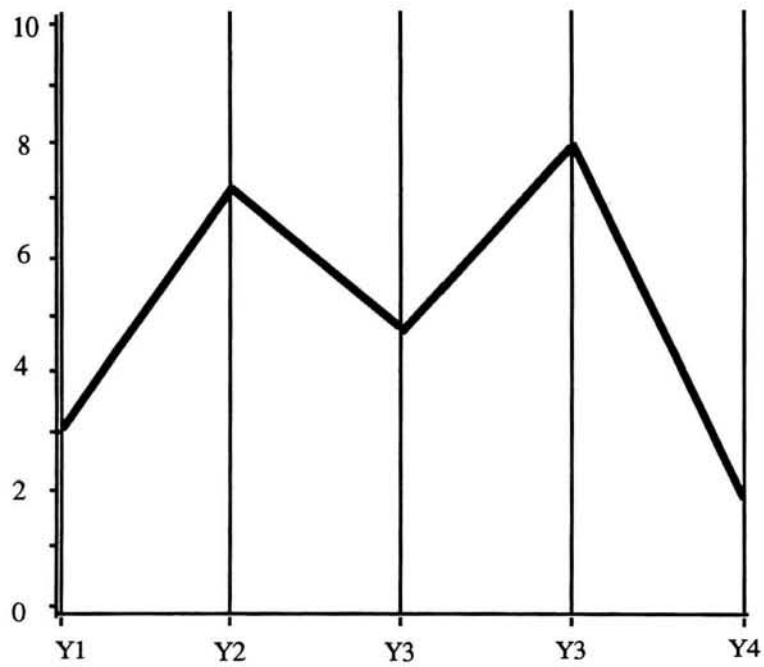


**Figure 2.1:** Five Dimensional Point (3,7,5,8,2) Plotted in a Parallel Coordinate System.

of the observed residuals that the quality of the fitted model can be assessed. In addition unusual observations can be detected. Plots in this system also can be useful in noting distributional properties of the multivariate data (Wilkinson, 1992).

In Section 2.2 a repeated measures model with fixed effects is defined. A centering and scaling technique is described in Section 2.3 that retains certain distributional properties assumed in the statement of the model. By plotting these transformed data a visualization of the dispersion structure can be made without first fitting the model. This information can then be used to specify an actual form for the covariance matrix.

## 2.2 A Linear Repeated Measures Model with Fixed Effects Based on the Mixed Model

Assume there are  $t$  treatment groups with  $n_i$  subjects in each. While it is also assumed that the experiment was designed to take measurements at  $p$  well defined and fixed time points, the actual observed number of observations for the  $j$ th individual in the  $i$ th treatment group is  $p_{ij}$ ,  $0 \leq p_{ij} \leq p$ ,  $j = 1, 2, \dots, n_i$ ;  $i = 1, 2, \dots, t$ . A mixed linear model is given as follows.

$$\mathbf{Y}_{ij} = \mathbf{X}_{ij}\boldsymbol{\beta} + \mathbf{Z}_{ij}\boldsymbol{\nu} + \boldsymbol{\zeta}_{ij}$$

where

$\mathbf{Y}_{ij}$  =  $p_{ij} \times 1$  vector of responses over time for the  $j$ th subject in the  $i$ th treatment group,

$\mathbf{X}_{ij}$  =  $p_{ij} \times q$  design matrix of fixed effects for the  $j$ th subject in the  $i$ th treatment group,

$\boldsymbol{\beta}$  =  $q \times 1$  vector of unknown fixed effect parameters,

- $\mathbf{Z}_{ij}$  =  $p_{ij} \times r$  design matrix of random effects for the  $j$ th subject in the  $i$ th treatment group,
- $\mathbf{G}$  =  $r \times r$  unknown covariance matrix,
- $\mathbf{v}$  =  $r \times 1$  vector of unknown random effect parameters assumed to be iid  $N_r(\mathbf{0}, \mathbf{G})$ ,
- $\mathbf{H}$  =  $p \times p$  unknown covariance matrix,
- $\mathbf{H}_{ij}$  =  $p_{ij} \times p_{ij}$  submatrix of  $\mathbf{H}$  corresponding to the nonmissing times for the  $j$ th subject in the  $i$ th treatment group,
- $\boldsymbol{\zeta}_{ij}$  =  $p_{ij} \times 1$  vector of unobserved random errors assumed to be iid  $N_{p_{ij}}(\mathbf{0}, \mathbf{H}_{ij})$ .

It follows that  $\mathbf{Y}_{ij}$  is  $N_{p_{ij}}(\mathbf{X}_{ij}\boldsymbol{\beta}, \mathbf{Z}_{ij}\mathbf{G}\mathbf{Z}'_{ij} + \mathbf{H}_{ij})$ .

### 2.2.1 A Repeated Measures Model with Fixed Effects

For a repeated measures model which includes just fixed effects, the only random component is associated with the subject. Thus,  $\mathbf{v}$  is an  $n_i \times 1$  vector of random effects due to the  $n_i$  subjects in treatment group  $i$  and is distributed as  $N_{n_i}(\mathbf{0}, \mathbf{G})$ .  $\mathbf{Z}_{ij}$  can be defined as a  $p_{ij} \times n_i$  matrix of zeroes with a  $j$ th column of ones. It follows that  $\mathbf{Z}_{ij}\mathbf{v}$  will be the  $p_{ij} \times 1$  vector  $(v_{ij}, v_{ij}, \dots, v_{ij})' = \mathbf{k}_{ij}$  where  $v_{ij}$  is the scalar random effect due to the  $j$ th subject in the  $i$ th treatment group. If it is assumed, as is commonly the case in repeated measures studies, that the subject effects are independent and identically distributed, then it follows that  $\mathbf{G} = \gamma^2 \mathbf{I}_{n_i}$  where  $\mathbf{I}_{n_i}$  is the  $n_i \times n_i$  identity matrix and  $\mathbf{Z}_{ij}\mathbf{G}\mathbf{Z}'_{ij} = \gamma^2 \mathbf{J}_{p_{ij}}$  where  $\mathbf{J}_{p_{ij}}$  is a  $p_{ij} \times p_{ij}$  matrix of 1's. Letting  $\boldsymbol{\epsilon}_{ij} = \mathbf{k}_{ij} + \boldsymbol{\zeta}_{ij}$  a repeated measures model with fixed effects can be written as

$$\mathbf{Y}_{ij} = \mathbf{X}_{ij}\boldsymbol{\beta} + \boldsymbol{\varepsilon}_{ij} \quad j = 1, 2, \dots, n_i; \quad i = 1, 2, \dots, t$$

where

$$\begin{aligned} \boldsymbol{\Sigma} &= p \times p \text{ unknown covariance matrix,} \\ \boldsymbol{\Sigma}_{ij} &= p_{ij} \times p_{ij} \text{ submatrix of } \boldsymbol{\Sigma} \text{ corresponding to the nonmissing times for} \\ &\quad \text{the } i\text{th subject in the } j\text{th treatment group,} \\ \boldsymbol{\varepsilon}_{ij} &= p_{ij} \times 1 \text{ vector of unobserved random errors assumed to be iid} \\ &\quad N_{p_{ij}}(\mathbf{0}, \boldsymbol{\Sigma}_{ij}). \end{aligned}$$

Furthermore  $\mathbf{Y}_{ij}$  is distributed as  $N_{p_{ij}}(\mathbf{X}_{ij}\boldsymbol{\beta}, \boldsymbol{\Sigma}_{ij})$  where  $\boldsymbol{\Sigma}_{ij} = \mathbf{H}_{ij} + \gamma^2 \mathbf{J}_{p_{ij}}$ .

An implementation of this modeling technique is included in the MIXED procedure of the SAS<sup>®</sup> statistical package. Maximum likelihood or restricted maximum likelihood estimators for  $\boldsymbol{\beta}$  and  $\boldsymbol{\Sigma}$  are found based on algorithms developed by several authors including Harville (1977), Laird, Lange and Stram (1987) and Jennrich and Schluchter (1986). In order to fit the model however, the user must first choose a structure for  $\boldsymbol{\Sigma}$  from a wide range of choices provided in the procedure (examples are provided in Table 2.1). Plots of centered and scaled observations can aid the user in determining an appropriate form for this dispersion structure. Draftman's plots and parallel axis plots are discussed in sections 2.4 and 2.5. Those plots are constructed without first fitting the model thereby avoiding the numerical problems associated with fitting a possibly misspecified or overparameterized model. The next section describes properties of the centered and scaled observations which are useful in a graphical examination of the data.

**Table 2.1**  
Covariance Structures

---

Unequal Diagonal Elements

Unstructured

$$\begin{bmatrix} \sigma_{11}^2 & \sigma_{21} & \sigma_{31} & \sigma_{41} \\ \sigma_{21} & \sigma_{22}^2 & \sigma_{32} & \sigma_{42} \\ \sigma_{31} & \sigma_{32} & \sigma_{33}^2 & \sigma_{431} \\ \sigma_{41} & \sigma_{42} & \sigma_{43} & \sigma_{44}^2 \end{bmatrix}$$

Banded Main Diagonal

$$\begin{bmatrix} \sigma_1^2 & 0 & 0 & 0 \\ 0 & \sigma_2^2 & 0 & 0 \\ 0 & 0 & \sigma_3^2 & 0 \\ 0 & 0 & 0 & \sigma_4^2 \end{bmatrix}$$

---

Equal Diagonal Elements

Simple

$$\begin{bmatrix} \sigma^2 & 0 & 0 & 0 \\ 0 & \sigma^2 & 0 & 0 \\ 0 & 0 & \sigma^2 & 0 \\ 0 & 0 & 0 & \sigma^2 \end{bmatrix}$$

Compound Symmetry

$$\begin{bmatrix} \sigma^2 + \sigma_1^2 & \sigma_1^2 & \sigma_1^2 & \sigma_1^2 \\ \sigma_1^2 & \sigma^2 + \sigma_1^2 & \sigma_1^2 & \sigma_1^2 \\ \sigma_1^2 & \sigma_1^2 & \sigma^2 + \sigma_1^2 & \sigma_1^2 \\ \sigma_1^2 & \sigma_1^2 & \sigma_1^2 & \sigma^2 + \sigma_1^2 \end{bmatrix}$$

First Order Autoregressive

$$\begin{bmatrix} 1 & \rho & \rho^2 & \rho^3 \\ \rho & 1 & \rho & \rho^2 \\ \rho^2 & \rho & 1 & \rho \\ \rho^3 & \rho^2 & \rho & 1 \end{bmatrix}$$

Toeplitz

$$\sigma^2 \begin{bmatrix} 1 & \sigma_1 & \sigma_2 & \sigma_3 \\ \sigma_1 & 1 & \sigma_1 & \sigma_2 \\ \sigma_2 & \sigma_1 & 1 & \sigma_1 \\ \sigma_3 & \sigma_2 & \sigma_1 & 1 \end{bmatrix}$$


---



### 2.3. Properties of the Centered and Scaled Observations

For the  $i$ th treatment group let  $\Sigma_i$  denote the  $p \times p$  covariance matrix with  $k$ th diagonal element  $\sigma_{ik}^2$ . The associated  $p \times p$  correlation matrix is given  $\rho_i = D_{\Sigma_i} \Sigma_i D_{\Sigma_i}$  where  $D_{\Sigma_i}$  denotes the  $p \times p$  diagonal matrix with the  $k$ th diagonal element  $(\sigma_{ik}^2)^{-\frac{1}{2}}$ . This correlation matrix is estimated by the  $p \times p$  sample correlation matrix,  $r_i$ . The  $(st)$  element of  $r_i$  is given by

$$r_{ist} = \frac{\sum_{j=1}^{n_i} (Y_{ijs} - \bar{Y}_{i.s})(Y_{ijt} - \bar{Y}_{i.t})}{\left[ \sum_{j=1}^{n_i} (Y_{ijs} - \bar{Y}_{i.s})^2 (Y_{ijt} - \bar{Y}_{i.t})^2 \right]^{\frac{1}{2}}}$$

where  $n_i$  is the number of subjects in the  $i$ th treatment group and summation is over the nonmissing pairs of observations. Patterns observed in  $r_i$  can suggest the structure of the corresponding correlation matrix.

In order to graphically visualize correlation properties of the observed data it will be useful to first remove the variability in the data associated with differences in the means and variances over time. Let  $n_{ik}$  be the number of nonmissing observations for the  $i$ th treatment group at time  $k$ . For  $i=1,2,\dots,t$ ,  $j = 1,2,\dots,n_{ik}$ ; and  $k = 1,2,\dots,p$ , let

$$\Delta_{ijk} = Y_{ijk} - \bar{Y}_{i.k}$$

and

$$\Delta_{ijk}^* = \frac{\Delta_{ijk}}{s_{i.k}}$$

$$\text{where } \bar{Y}_{i,k} = \frac{\sum_{j=1}^{n_{ik}} Y_{ijk}}{n_{ik}} \text{ and } s_{i,k}^2 = \frac{\sum_{j=1}^{n_{ik}} \Delta_{ijk}^2}{n_{ik} - 1}.$$

Since  $\bar{\Delta}_{i,k}^* = 0$ , the sample correlation matrix based on the centered and scaled values is given by

$$r_{ist}^* = \frac{\sum_{j=1}^{n_i} (\Delta_{ijs}^*) (\Delta_{ijt}^*)}{\left[ \sum_{j=1}^{n_i} (\Delta_{ijs}^*)^2 (\Delta_{ijt}^*)^2 \right]^{\frac{1}{2}}} = \frac{\sum_{j=1}^{n_i} \left( \frac{Y_{ijs} - \bar{Y}_{i,s}}{s_{i,s}} \right) \left( \frac{Y_{ijt} - \bar{Y}_{i,t}}{s_{i,t}} \right)}{\left[ \sum_{j=1}^{n_i} \left( \frac{Y_{ijs} - \bar{Y}_{i,s}}{s_{i,s}} \right)^2 \left( \frac{Y_{ijt} - \bar{Y}_{i,t}}{s_{i,t}} \right)^2 \right]^{\frac{1}{2}}} = r_{ist}.$$

Therefore the sample correlation structure is retained by the centered and scaled observations.

Other distributional properties associated with the univariate marginal distributions at each time point will be shown to be useful in the interpretation of the parallel axis plots of these centered and scaled observations. For ease of notation, consider the case of no missing values so that  $p_{ij} = p$  for all  $i, j$ . Let  $\boldsymbol{\mu}_i$  denote the  $p \times 1$  vector of mean responses for the  $i$ th treatment group. When it has been assumed for  $j = 1, 2, \dots, n_{ik}$  that the  $p \times 1$  vectors  $\mathbf{Y}_{ij}$  are iid  $N_p(\boldsymbol{\mu}_i, \boldsymbol{\Sigma}_i)$ , it follows that at each time point,  $k = 1, 2, \dots, p$ ,  $Y_{ijk}$  is iid  $N(\mu_{ik}, \sigma_{ik}^2)$ . This implies  $E(\Delta_{ijk}) = 0$  and  $E(\Delta_{ijk}^*) = 0$ . Furthermore,

$$\text{Var}(\Delta_{ijk}) = \frac{n_{ik} - 1}{n_{ik}} \sigma_{ik}^2. \text{ Since } s_{i,k}^2 \xrightarrow{p} \sigma_{ik}^2 \text{ and } \bar{Y}_{i,k} \xrightarrow{p} \mu_{ik} \text{ it follows by Slutsky's}$$

$$\text{Theorem that } \Delta_{ijk} = Y_{ijk} - \bar{Y}_{i,k} \xrightarrow{d} Y_{ijk} - \mu_{ik} \text{ and } \Delta_{ijk}^* = \frac{Y_{ijk} - \bar{Y}_{i,k}}{s_{i,k}} \xrightarrow{d} \frac{Y_{ijk} - \mu_{ik}}{\sigma_{ik}}.$$

Hence, when the number of observations in the  $i$ th treatment group at the  $k$ th time is large,  $\Delta_{ijk}$  converges to  $N(0, \sigma_{ik}^2)$  and  $\Delta_{ijk}^*$  converges to  $N(0, 1)$ . While, in general, the number of these observations at each time point within each treatment group may be *limited*, these

properties still may be useful in the examination of the plots of these centered and scaled data.

The following describes two graphical techniques that can be used to display distributional patterns in the centered and scaled data.

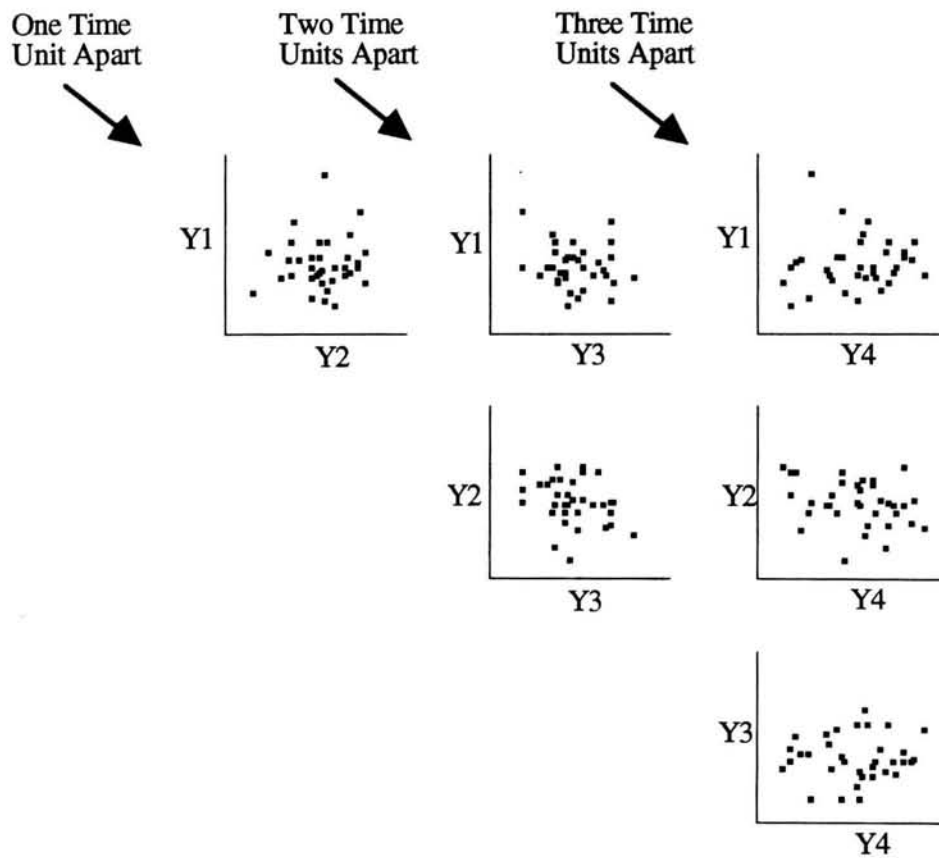
#### 2.4. Draftman's Display

Assuming there are  $p$  time points,  $\frac{p(p-1)}{2}$  pairwise plots of the  $(\Delta_{ijr}^*, \Delta_{ijs}^*)$ ,  $r, s = 1, 2, \dots, p$ ,  $r \neq s$  values at all nonmissing distinct combinations of time points can be used to view the sample correlation structure. This array of plots given in Figure 2.2 can be arranged in a manner similar to the correlation matrix. The diagonal plots correspond to the scaled data a fixed time unit apart. The upper left hand plot corresponds to the first and second time points and the upper right hand corner plot corresponds to the first and last time points. Varying degrees of linearity in each of the plots will be associated with the degree of correlation between the corresponding pairs of variables.

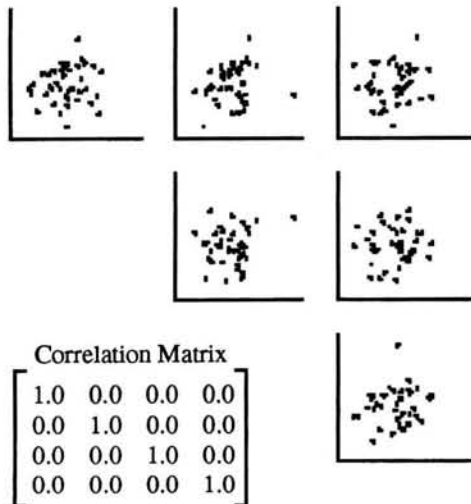
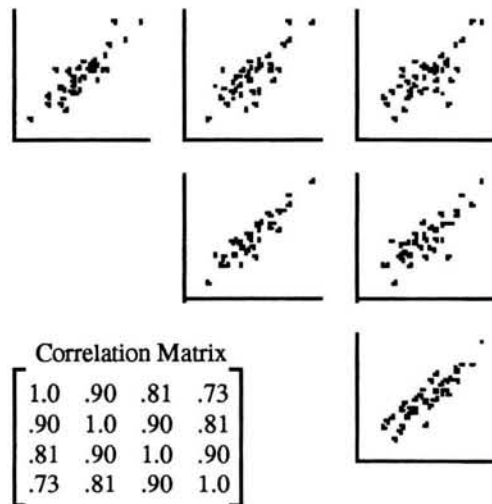
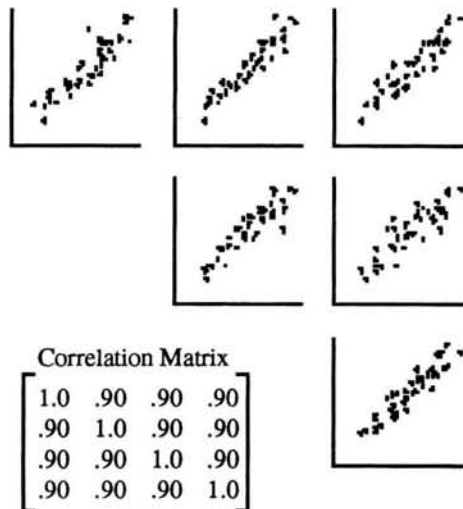
Figure 2.3 shows simulated 4-dimensional normally distributed data sets with differing correlation structures. In Figure 2.3(a) the within-subject observations are independent which is indicated by the absence of a linear trend in any of the pairwise plots. Autoregression is indicated in Figure 2.3(b) by the decrease in correlation as the time interval between measurements increases as well as consistency in the correlation for plots associated with fixed differences in time. The similarity of the pairwise plots of Figure 2.3(c) suggests compound symmetry.

#### 2.5. Parallel Axis Display

In a parallel axis display properties of the  $p$  univariate distributions can be visualized in addition to the correlation structure. In plots of  $\Delta_{ijk}$  and  $\Delta_{ijk}^*$ , the patterns



**Figure 2.2:** Ordering of Scatter Plots in a Draftman's Display to View Correlation Structure.

**Figure 2.3(a): Independence****Figure 2.3(b): Autoregression****Figure 2.3(c): Compound Symmetry****Figure 2.3:** Simulated Four Dimensional Normal Data with Various Correlation Structures Plotted in a Draftman's Display.

formed by the intersections of the line segments with each axis allows graphical assessment of the observed univariate sample distributions at each time point. In the plot of the centered and scaled  $\Delta_{ijk}^*$  values the patterns of the line segments between the axis allow visualization of the observed correlation between the corresponding pairs of variables.

If the normality assumption is correct, then  $E(\Delta_{ijk}) = 0$  and  $\text{Var}(\Delta_{ijk}) = \frac{n_{ik} - 1}{n_{ik}} \sigma_{ik}^2$ .

This implies when  $n_{ik}$  is constant,  $k=1,2,\dots,p$ , a visual comparison of the  $\sigma_{ik}^2$  values can be made in a parallel axis plot of the  $\Delta_{ijk}$  values by examining the distribution of the intersection points of the line segments with the associated parallel axis. In Figure 2.4(a) data simulated from a normal distribution with a nonconstant  $\sigma_{ik}^2$ ,  $k=1,2,3,4$  are plotted. The larger variability associated with the second and fourth measurements is indicated by the wider spread in the distribution of the intersection points with these axes. In contrast in Figure 2.4(b) where data were simulated from a normal distribution with  $\sigma_{ik}^2=1$ ,  $k=1,2,3,4$ , constant variability is suggested. Of course, in cases when  $n_{ik}$  is not constant for all  $k$ , the variability in the plots associated with the nonconstant sample sizes must be taken into account.

Similarly when  $n_{ik}$  is large, the distribution of the centered and scaled  $\Delta_{ijk}^*$  approximates  $N(0,1)$ . Hence in a plot of these values the intersection points along each of the axes should be consistently centered at 0 and virtually all between -3 and 3 (Figure 2.4(b)). Deviations in this pattern when  $n_{ik}$  is not large may not necessarily indicate nonnormality but may warrant further examination.

In plots of  $\Delta_{ijk}^*$  the patterns of the line segments between the axes are associated with the correlation structure. Positive correlation in a parallel axis plot is indicated by a pattern of parallel line segments between the axes. In addition if the positively correlated data are jointly centered about 0, the slopes of the line segments will be close to zero. As the degree of positive correlation diminishes the lines will tend to intersect more often and

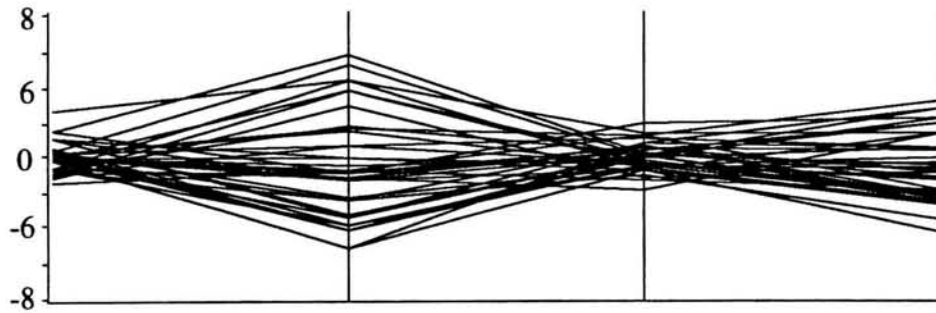


**Figure 2.4 (a):** Nonconstant Diagonal Elements

$$\text{Covariance Matrix} \begin{bmatrix} 1.0 & 0.0 & 0.0 & 0.0 \\ 0.0 & 3.0 & 0.0 & 0.0 \\ 0.0 & 0.0 & 0.8 & 0.0 \\ 0.0 & 0.0 & 0.0 & 2.0 \end{bmatrix}$$

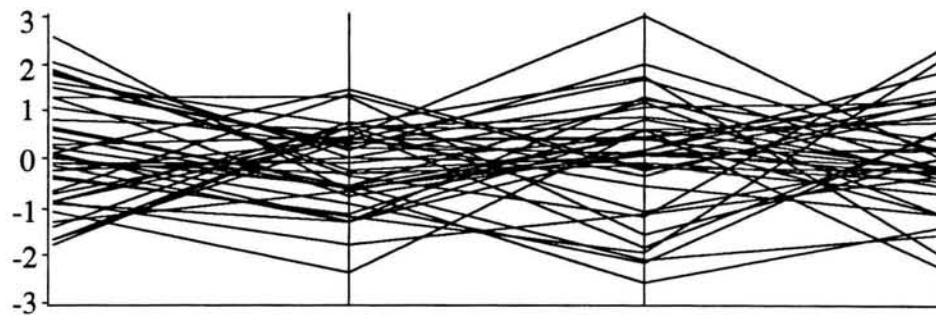


**Figure 2.4 (b):** Nonconstant Diagonal Elements

$$\text{Covariance Matrix} \begin{bmatrix} 1.0 & 0.0 & 0.0 & 0.0 \\ 0.0 & 1.0 & 0.0 & 0.0 \\ 0.0 & 0.0 & 1.0 & 0.0 \\ 0.0 & 0.0 & 0.0 & 1.0 \end{bmatrix}$$

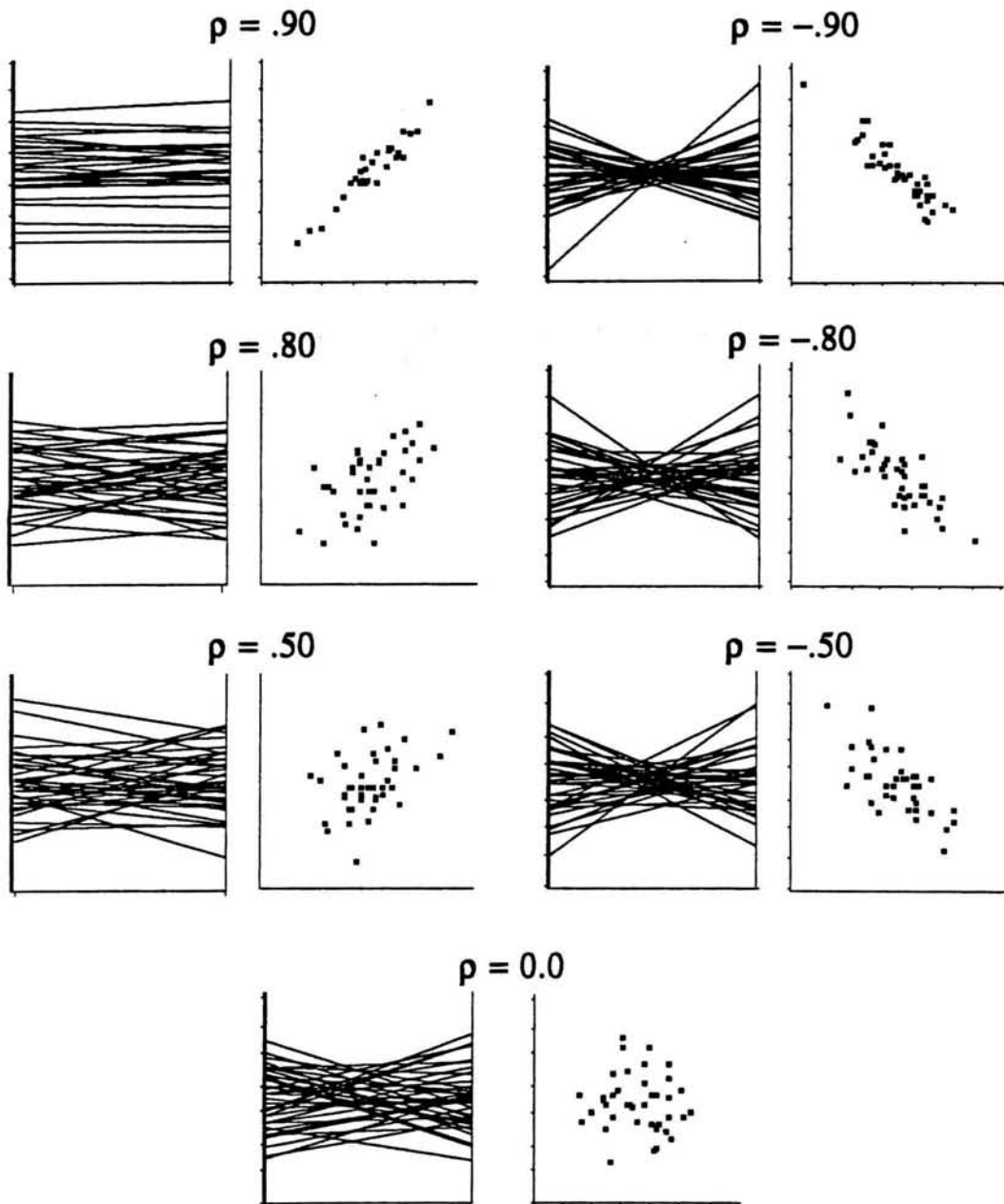
**Figure 2.4:** Comparing the Diagonal Elements of the Covariance Matrix in a Parallel Axis System using Simulated Four Dimensional Normal Data with Different Correlation Structures.

the variability in slopes will increase. In contrast, as negative correlation approaches -1.0 the line segments intersect in a smaller and smaller region. In fact, if there is perfect negative correlation the lines all intersect at a single point (Inselberg, 1985). As the degree of negative correlation diminishes the common intersection region widens. Figure 2.5 shows simulated data for various values of both positive and negative  $\rho$  respectively.

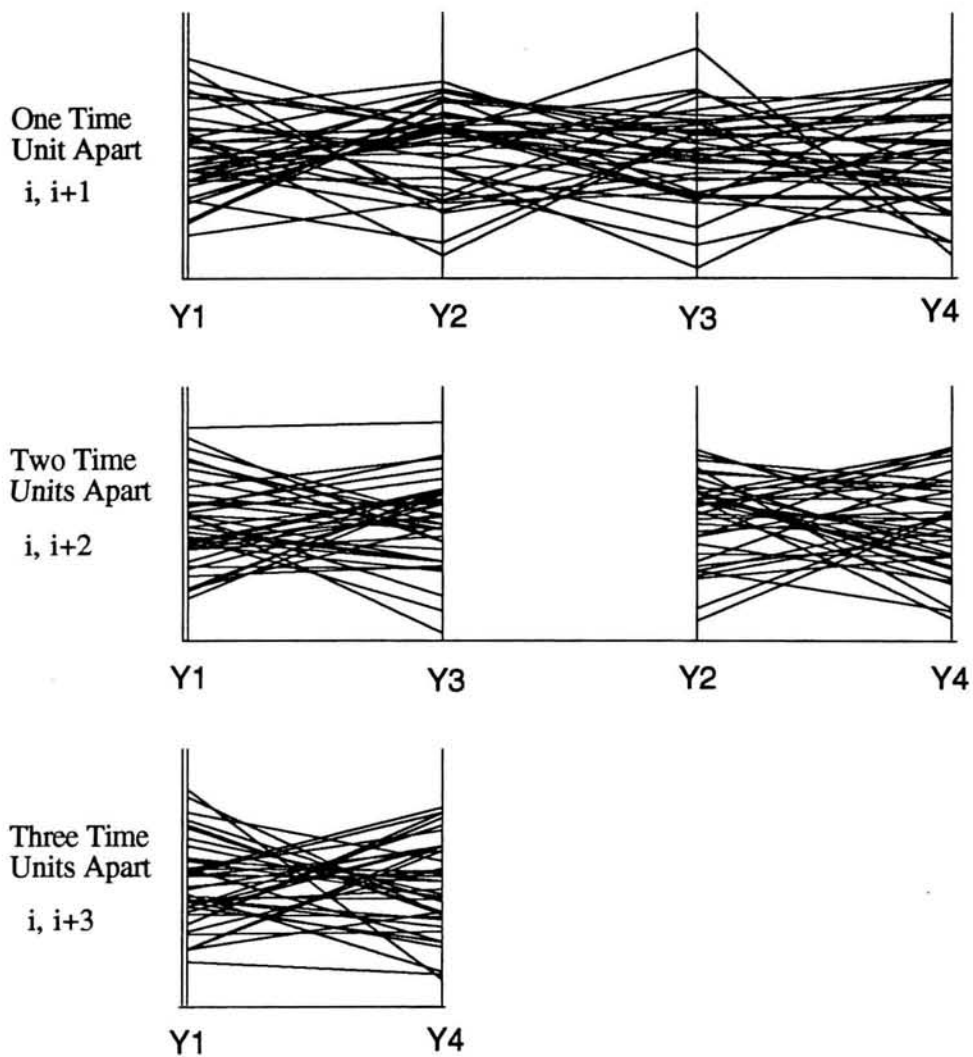
In order to observe correlation patterns between all possible pairs of variables a set of parallel axis plots will be needed. Rather than considering  $\frac{p(p-1)}{2}$  pairwise parallel plots, plotting several dimensions on a single set of axes is convenient. Wegman (1990) has shown that for  $p$  variables a minimal number of parallel plots to show all possible pairwise combinations is  $\frac{p+1}{2}$ . The permutation of the axes using this method results in an ordering of the axes that does not reflect the natural order of the measurements by time. A more convenient ordering of the axes for this type of data using  $(p-1)$  plots is suggested. This is illustrated for 4-dimensional simulated normally distributed data with the 3 plots in Figure 2.6. Here, the first parallel plot orders the variables naturally so that correlation between measurements one time unit apart can be observed. In addition, the user can simultaneously observe the centered and scaled observations through time. The second parallel plot orders the axes so that correlations between measurement taken two time units apart can be observed. Note in this plot the line segments between the axes representing times 3 and 2 are not connected since this comparison is not considered in this plot. The third graph considers values taken 3 time units apart.

Figure 2.7 illustrates this technique for the four data sets previously plotted in the Draftman's Display (Figure 2.3). In Figure 2.7(a), there is no indication of positive correlation due to the absence of parallel lines between any of the axes. In addition, since the regions formed by the intersection of lines between the axes are wide, negative correlation is not indicated. Independence is therefore suggested in Figure 2.7(a). A



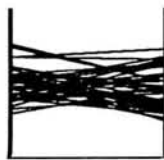
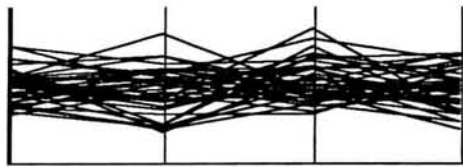


**Figure 2.5:** Simulated Bivariate Normal Data with Various Correlation Coefficients plotted in both a Parallel Axis System and a Scatter Plot



**Figure 2.6:** Ordering of the Parallel Axis Plots to View Correlation Structure. The  $i, j$ th position of the correlation matrix is represented in each plot.

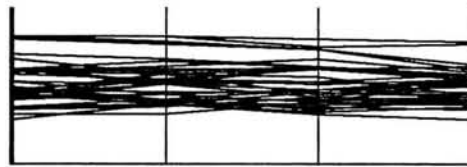
**Figure 2.7 (a): Independence**



Correlation Matrix

$$\begin{bmatrix} 1.0 & 0.0 & 0.0 & 0.0 \\ 0.0 & 1.0 & 0.0 & 0.0 \\ 0.0 & 0.0 & 1.0 & 0.0 \\ 0.0 & 0.0 & 0.0 & 1.0 \end{bmatrix}$$

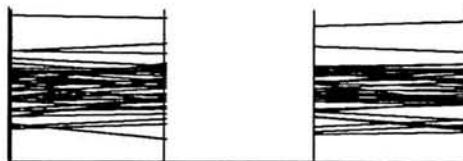
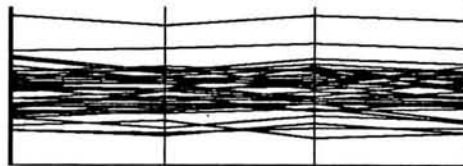
**Figure 2.7 (b): Autoregression**



Correlation Matrix

$$\begin{bmatrix} 1.0 & .90 & .81 & .73 \\ .90 & 1.0 & .90 & .81 \\ .81 & .90 & 1.0 & .90 \\ .73 & .81 & .90 & 1.0 \end{bmatrix}$$

**Figure 2.7 (c): Compound Symmetry**



Correlation Matrix

$$\begin{bmatrix} 1.0 & .90 & .90 & .90 \\ .90 & 1.0 & .90 & .90 \\ .90 & .90 & 1.0 & .90 \\ .90 & .90 & .90 & 1.0 \end{bmatrix}$$

**Figure 2.7:** Simulated 4-Dimensional Normal Data with Various Correlation Structure Plotted in a Parallel Axis System

decrease in positive correlation associated with autoregression is indicated in Figure 2.7(b) by the weakening in the pattern of parallel lines as the differences in time between measurements increases. Compound symmetry is suggested in Figure 2.7(c) since the line patterns between all pairs of variables seems constant.

The following example illustrates the usefulness of both the parallel axis plots and the draftman's display at certain stages of a repeated measures analysis. In particular these plots will be used, without first fitting a model, to suggest the structure of the dispersion matrix.

## 2.6. Example

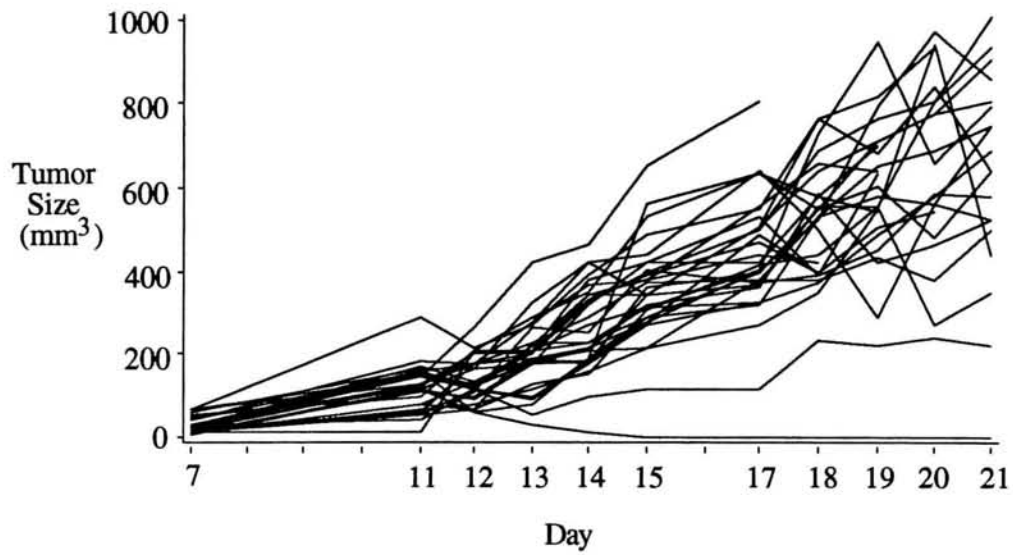
Koziol and Maxwell (Biometrics, 1981) report a study that was conducted to test the efficacy of 3 therapies against colon carcinomas in mice. Thirty mice injected with mouse colon carcinoma cells were randomly divided into the 3 treatment groups. The size of the resulting tumor was recorded on 11 different occasions, days 7,11,12,13,14,15,17,18,19,20 and 21. Nine mice died before the end of the experiment so that measurements at later time points for these mice are missing. The data appear in Table 2.2. A plot of the observed data (Figure 2.8) indicates an increase in tumor size over time. The sixth mouse in group 3 is clearly unusual and was eliminated from the remainder of this analysis.

At this point the analyst could examine the estimated dispersion matrix after fitting a linear repeated measures model with an unstructured covariance matrix. An attempt to perform such an analysis using Proc Mixed in SAS<sup>®</sup> failed to converge. The graphical techniques previously discussed can now be used to provide valuable information which will permit the analyst to proceed.

In order to compare the diagonal elements of the covariance matrix graphically, the centered data using the observed means for each of the 3 treatment groups at each of the 11

**Table 2.2**Tumor Size (mm<sup>3</sup>) over course of the Experiment (Koziol)

|    | Day  |       |       |       |       |       |       |       |       |       |       |
|----|------|-------|-------|-------|-------|-------|-------|-------|-------|-------|-------|
|    | 7    | 11    | 12    | 13    | 14    | 15    | 17    | 18    | 19    | 20    | 21    |
| 1  | 35.3 | 157.1 | 122.5 | 217.6 | 340.3 | 379.0 | 556.6 | 661.3 | 634.8 |       |       |
| 2  | 19.6 | 152.2 | 129.6 | 176.6 | 213.9 | 317.9 | 356.4 | 580.0 | 415.2 | 460.0 | 520.1 |
| 3  | 27.0 | 122.4 | 196.1 | 196.1 | 332.2 | 388.9 | 469.3 | 397.1 | 505.4 | 541.5 |       |
| 4  | 55.0 | 95.0  | 205.9 | 205.9 | 270.0 | 307.3 | 405.1 | 726.0 | 950.4 | 661.5 | 798.6 |
| 5  | 24.6 | 68.8  | 135.3 | 196.0 | 340.2 | 340.4 | 507.3 | 767.2 | 820.0 | 937.5 |       |
| 6  | 12.6 | 85.0  | 70.1  | 225.1 | 225.1 | 289.0 | 317.9 | 529.1 | 653.4 | 687.7 | 750.2 |
| 7  | 35.2 | 129.8 | 180.0 | 274.7 | 420.1 | 340.3 | 507.2 | 634.8 | 714.3 | 777.6 | 912.6 |
| 8  | 29.8 | 157.0 | 126.8 | 202.5 | 225.0 | 307.2 | 320.1 |       |       |       |       |
| 9  | 70.0 | 129.7 | 196.0 | 205.8 | 375.7 | 419.1 | 421.2 | 573.4 | 701.8 |       |       |
| 10 | 29.5 | 156.9 | 176.7 | 225.0 | 289.0 | 372.6 | 379.2 | 529.2 | 573.3 | 560.1 | 520.0 |
| 11 | 48.6 | 115.3 | 90.8  | 176.5 | 317.9 | 421.2 | 529.2 | 388.8 | 629.0 |       |       |
| 12 | 66.7 | 289.0 | 215.6 | 268.8 | 388.8 | 487.4 | 551.3 | 767.1 | 677.6 | 846.4 | 634.9 |
| 13 | 24.5 | 143.7 | 115.0 | 90.7  | 194.3 | 559.6 | 629.3 | 573.3 | 540.0 |       |       |
| 14 | 14.4 | 84.7  | 135.2 | 191.2 | 176.4 | 356.4 | 397.1 | 551.4 | 605.0 | 480.0 | 634.8 |
| 15 | 10.8 | 70.0  | 80.0  | 118.3 | 156.8 | 215.6 | 268.8 | 346.8 | 551.3 | 946.4 | 440.0 |
| 16 | 11.3 | 15.0  | 205.8 | 289.0 | 346.8 | 529.2 | 629.2 | 551.3 | 714.2 | 772.6 | 806.4 |
| 17 | 18.0 | 56.7  | 115.3 | 96.8  | 177.5 | 268.8 | 320.0 | 372.6 | 487.4 | 573.3 | 683.6 |
| 18 | 60.0 | 166.6 | 166.7 | 324.0 | 420.0 | 440.0 | 634.8 | 500.0 | 289.0 | 560.0 | 748.8 |
| 19 | 29.4 | 152.1 | 122.4 | 186.3 | 186.3 | 274.7 | 485.1 | 397.0 |       |       |       |
| 20 | 41.1 | 186.2 | 176.6 | 274.6 | 361.0 | 379.1 | 440.0 | 415.2 |       |       |       |
| 21 | 12.5 | 108.0 | 96.8  | 186.2 | 202.5 | 213.8 | 379.1 | 379.0 | 433.2 | 379.0 | 500.0 |
| 22 | 23.4 | 129.6 | 176.5 | 196.6 | 320.0 | 397.1 | 500.0 | 687.7 | 767.1 | 806.4 | 937.5 |
| 23 | 22.2 | 65.0  | 176.4 | 191.3 | 213.8 | 274.6 | 405.0 | 520.0 | 796.6 | 978.7 | 864.0 |
| 24 | 11.2 | 52.9  | 70.0  | 129.6 | 152.1 | 303.5 | 415.0 | 440.0 | 556.7 | 812.5 | 1014  |
| 25 | 66.6 | 147.0 | 260.1 | 420.0 | 460.0 | 653.4 | 806.4 |       |       |       |       |
| 26 | 11.4 | 115.2 | 65.1  | 32.0  | 10.8  | 3.2   | 1.4   | 0.0   | 0.0   | 0.0   | 0.0   |
| 27 | 22.1 | 55.0  | 115.2 | 55.0  | 93.6  | 118.8 | 118.3 | 230.4 | 217.6 | 243.2 | 217.6 |
| 28 | 40.5 | 156.8 | 65.0  | 84.7  | 191.2 | 291.5 | 400.0 |       |       |       |       |
| 29 | 32.0 | 44.6  | 108.9 | 258.8 | 247.5 | 405.0 | 372.6 | 388.0 | 451.3 | 580.0 | 573.3 |
| 30 | 10.0 | 118.3 | 166.6 | 176.4 | 186.2 | 340.2 | 361.0 | 556.6 | 556.6 | 268.8 | 346.8 |

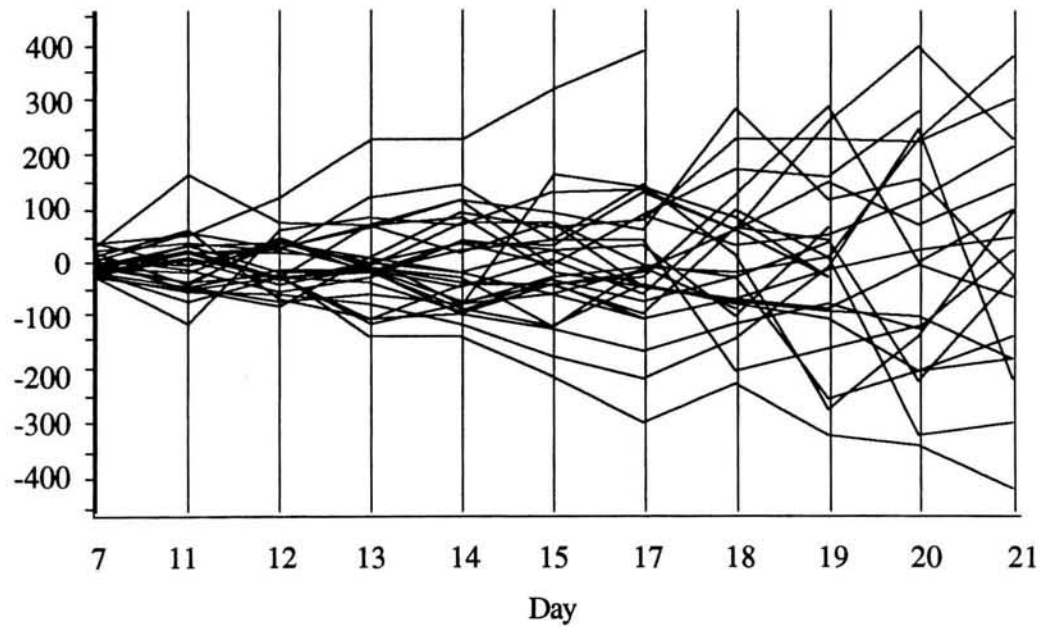
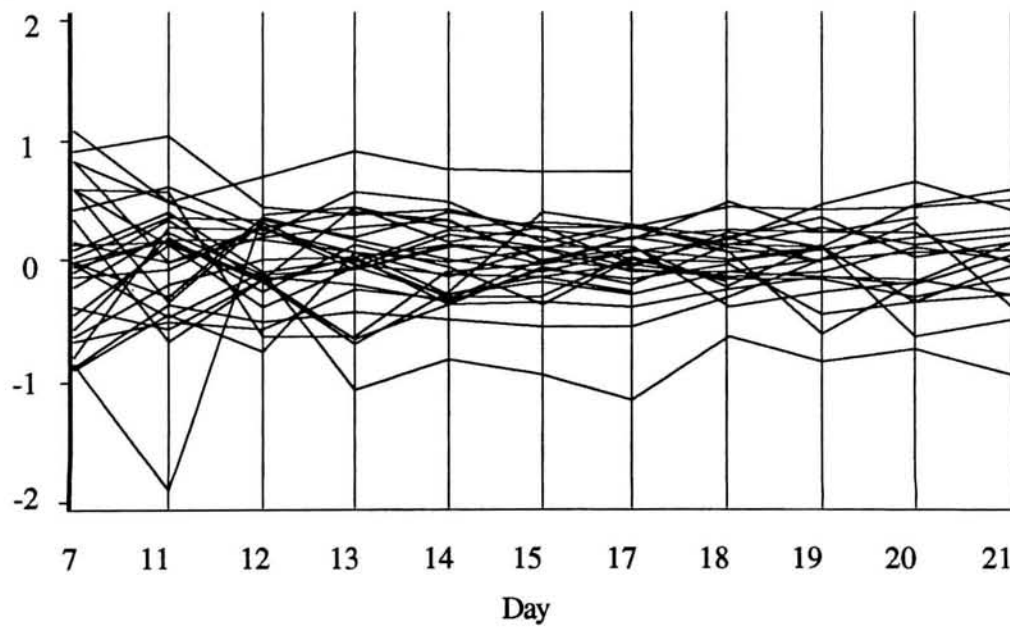


**Figure 2.8:** Observed Koziol Data Plotted Over Time

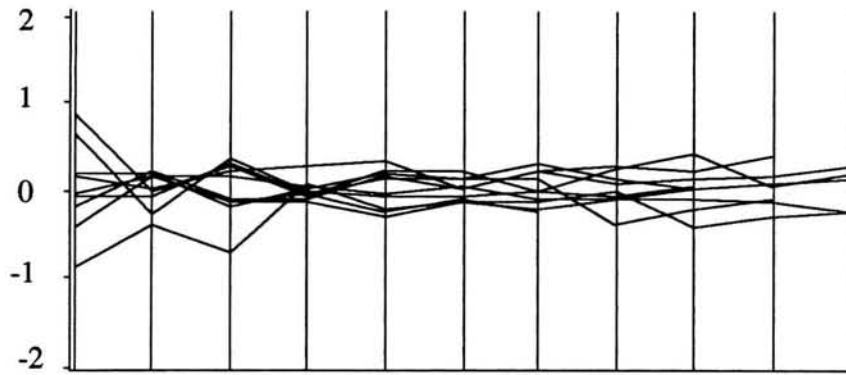
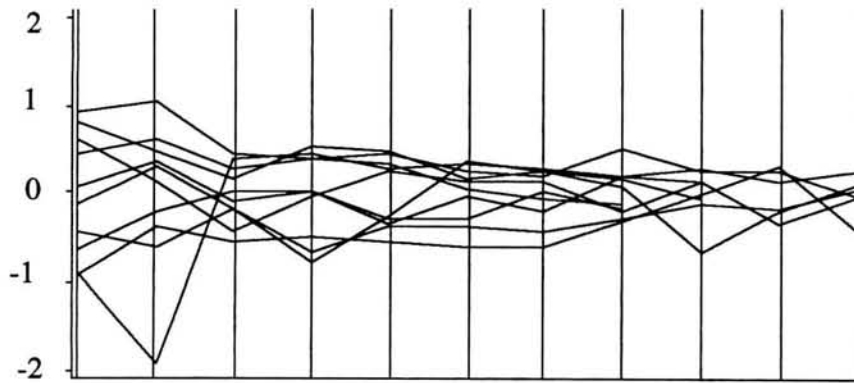
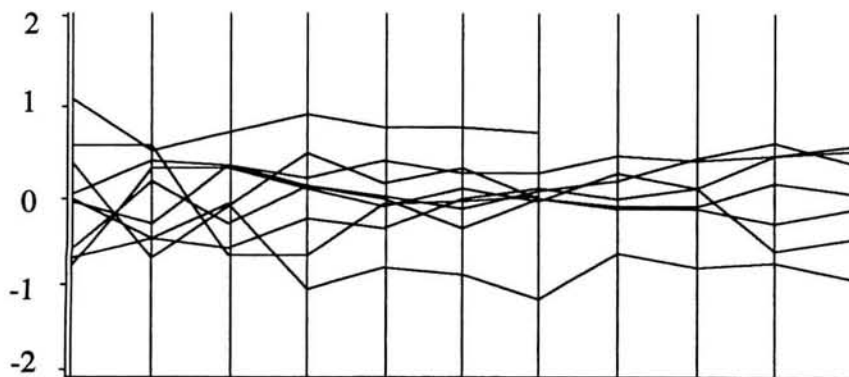
time points are plotted in Figure 2.9(a). An increase in variability is indicated by the widening distribution of the intersections of the line segments with each axis. Since covariance structures associated with constant diagonal elements have fewer parameters to estimate, a transformation to stabilize this variability is suggested and was considered. A plot of the centered  $\ln$  transformed data (Figure 2.9(b)) suggest constant diagonal elements of the covariance matrix associated with these transformed data. Consequently, the  $\ln$  transformation was employed for the remainder of this analysis.

To assess the consistency of the form of the covariance structure by treatment group, the centered  $\ln$  data by treatment group (Figure 2.10) are plotted. Group 3 appears to exhibit a slightly larger degree of variability at each time point and groups 1 and 2 show a possible decrease in variability over time. Bartlett's test for the homogeneity of the covariance matrix (Morrison, p.252) can be applied once it has been determined that there is no indication of nonnormality. Mardia's tests for multivariate normality (Mardia, p. 310) fail to detect a deviation from normality (skewness:  $p=0.5836$ , kurtosis:  $p=0.9122$ ) and significant heterogeneity is not indicated ( $p=1.000$ ). Homogeneity of the covariance matrix by group was therefore concluded.

Since it has been concluded that the diagonal elements of the covariance matrix are likely not different, further refinement of the dispersion structure can be made by considering plots of the centered and scaled data. Using the parallel axis system (Figure 2.11) some positive correlation is indicated especially in the top left plot associated with the  $(i,i+1), i=1,2,\dots,10$  positions of the sample correlation matrix. This indication of positive correlation is not as apparent in the remaining plots. In the draftman's display (Figure 2.12) the similarity of the scatter plots in the top rows support compound symmetry. Along the remaining rows a first order autoregressive pattern with a weakening degree of positive correlation is suggested. By examining the scatter plots along the diagonals, correlation between measurements at constant differences in time appear equal. Both

**Figure 2.9(a): Centered Observed Data****Figure 2.9(b): Centered Ln Data****Figure 2.9:** Centered Observed and Transformed Koziol Data Plotted in a Parallel Axis System.



**Figure 2.10(a): Group 1****Figure 2.10(b): Group 2****Figure 2.10(c): Group 3****Figure 2.10:** Centered Ln Transformed Koziol Data by Group.

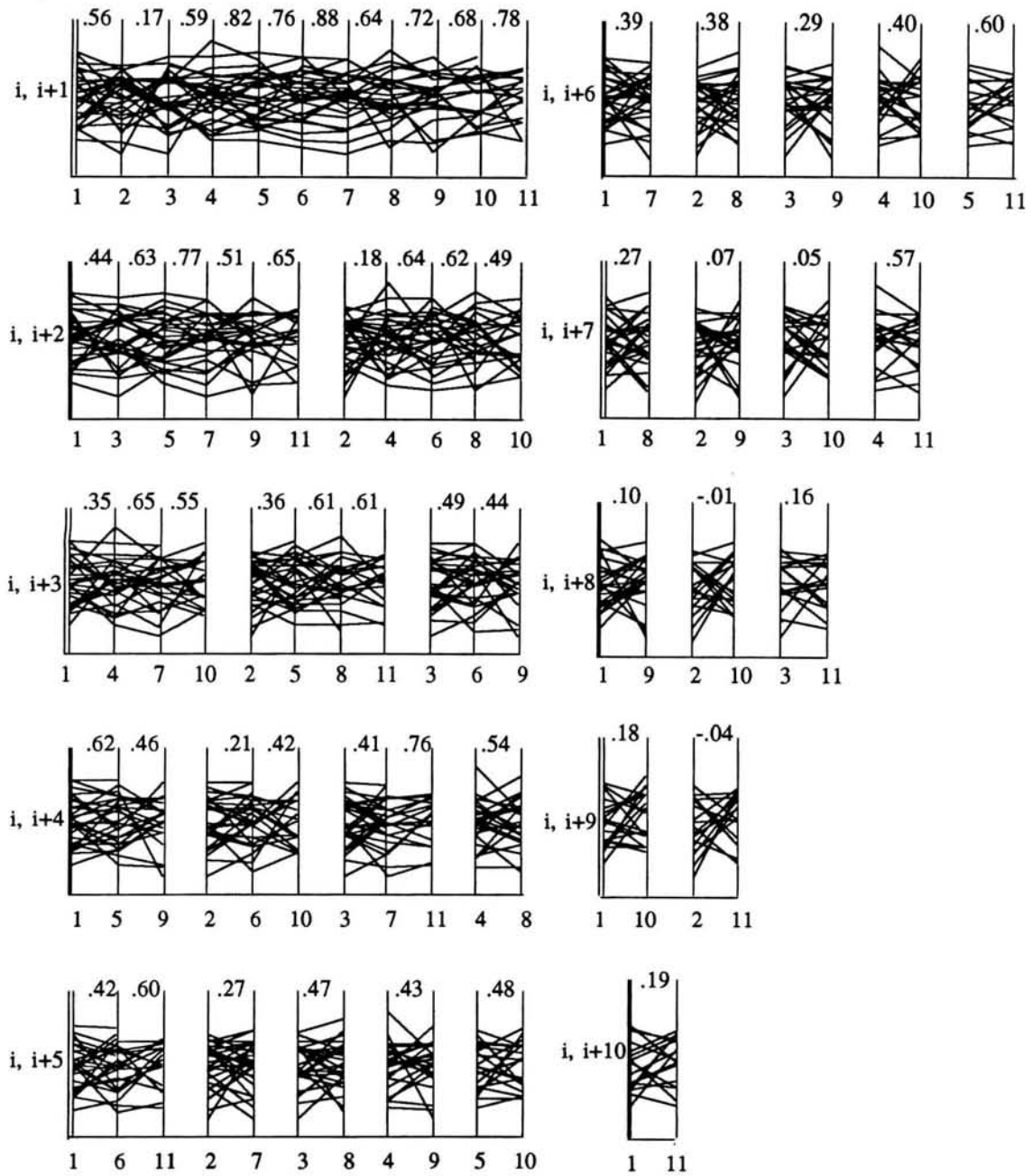


**Figure 2.11:** Centered and Scaled Ln Transformed Koziol Data in a Parallel Axis System. The  $(i,j)$ th position of the correlation matrix is represented in each plot. The sample correlation is shown between each parallel axis.

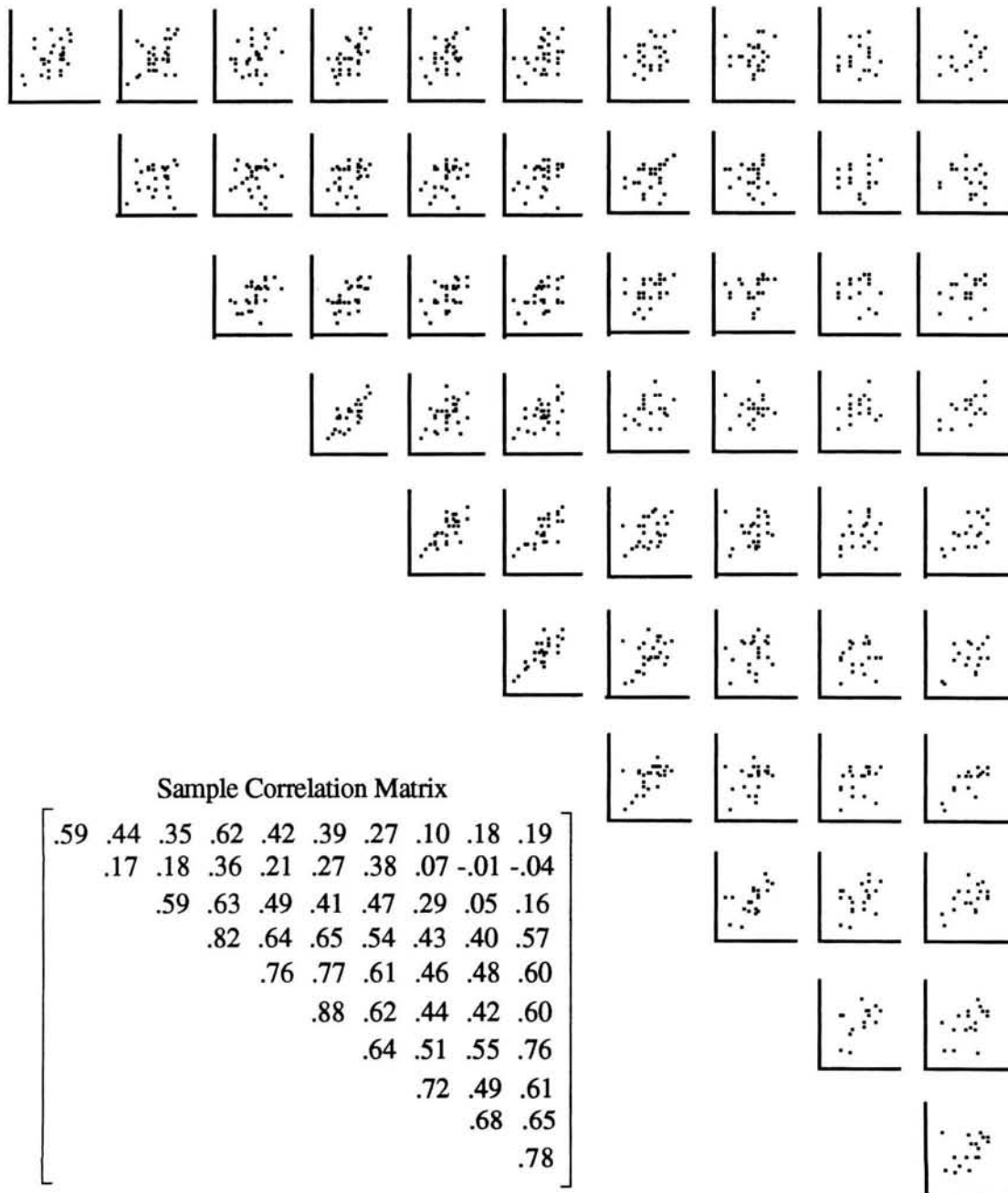


**Figure 2.12:** Centered and Scaled Ln Transformed Koziol Data in a Draftman's Display

graphical presentations and the sample correlation matrix shown in Figure 2.12 indicate compound symmetry or first order autoregression can be considered as possible forms for the covariance structure in the model fitting procedure.

A plot of the observed ln transformed data indicates a possible curvilinear increase over time (Figure 2.13). This implies a linear repeated measures model with a quadratic term may be appropriate. The following defines the initial model considered for the ln data.

$$Y_{ij} = \beta_{0i} + \beta_{1i}t + \beta_{2i}t^2 + \varepsilon_{ij} \quad i=1,2,3 \quad j=1,2,\dots,n_i \quad t=0,1,\dots,10$$

Table 2.3 summarizes the results of fitting this model using SAS<sup>®</sup> Proc Mixed and assuming compound symmetry and autoregression. A simple model assuming independence of the observations within a subject was also run for comparison. In all three cases the iterative procedure successfully converged to parameter estimates. A test comparing the treatment groups however, results in differing p-values with the simple case actually suggesting a difference between the groups. In order to compare the models, the Akaike Information Criterion and Schwartz's Bayesian Criteria can be examined. These statistics can be used as guidelines when comparing models with the same fixed effects but with varying covariance structure (SAS<sup>®</sup>, p.326). Larger values of these statistics suggest more appropriate covariance structure. Thus, at this stage of the analysis the first order autoregressive structure appears to be the most appropriate for this data set.

It has therefore been demonstrated that the parallel axis and a draftman's display of pair-wise plots can be useful in suggesting an appropriate form for the dispersion matrix for a repeated measure experiment with fixed effects. In particular, a centering and scaling technique was described so that properties of the covariance structure were retained in the scaled data. By plotting these scaled data, properties of the covariance matrix could be

**Table 2.3**

Preliminary Analysis Results Using Proc Mixed in SAS®

|                           | Covariance Structure |                   |                 |
|---------------------------|----------------------|-------------------|-----------------|
|                           | Simple               | Compound Symmetry | Auto-regressive |
| Akaike Statistic*         | -179.94              | -141.48           | -127.64         |
| Schwartz Statistic*       | -181.76              | -145.12           | -131.28         |
| p-value group differences | .0652                | .1333             | .9680           |
| parameter estimates       |                      |                   |                 |
| $\beta_{01}$              | 3.42                 | 3.42              | 3.40            |
| $\beta_{02}$              | 3.23                 | 3.24              | 3.31            |
| $\beta_{03}$              | 3.07                 | 3.08              | 3.13            |
| $\beta_{11}$              | 0.40                 | 0.40              | 0.41            |
| $\beta_{12}$              | 0.42                 | 0.41              | 0.40            |
| $\beta_{13}$              | 0.42                 | 0.42              | 0.41            |
| $\beta_{21}$              | -0.013               | -0.012            | -0.014          |
| $\beta_{22}$              | -0.013               | -0.013            | -0.012          |
| $\beta_{23}$              | -0.014               | -0.012            | -0.013          |

\* Higher values are associated with models deemed best.

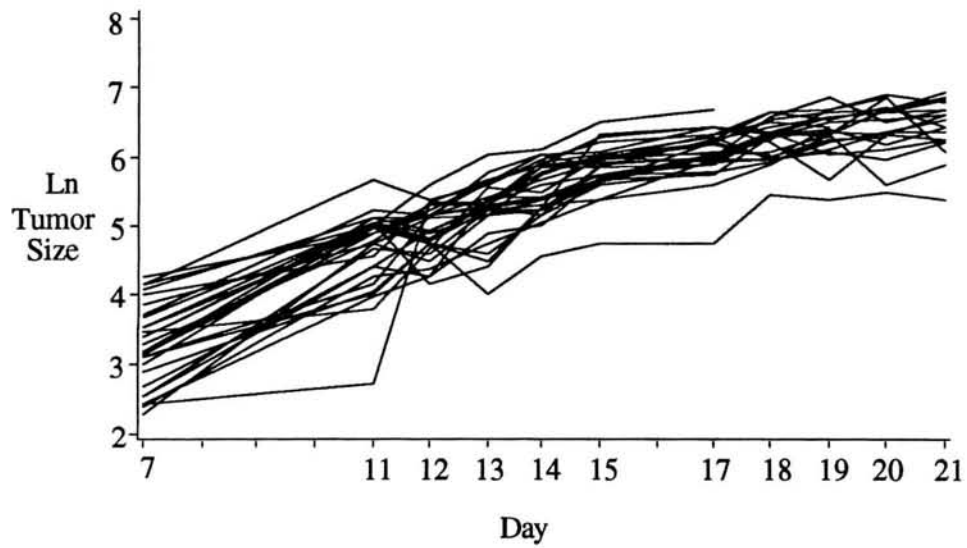


**Figure 2.13:** Ln Transformed Koziol Data Plotted Over Time

visualized. In Chapters 5 and 7 both plotting techniques described in this chapter will be applied to studies of combinations of a large number of chemicals.

## Chapter 3

### The Logistic Model

#### 3.1 Introduction

As described in Chapter 1 the experiments we are considering are those where the response can be classified into one of two possible values; success ( $Z=1$ ) or failure ( $Z=0$ ). Logistic modeling has been shown to be useful in analyzing these data. A general overview of this methodology will now be given. Emphasis will be placed on those results that will be useful in the statistical analyses considered in this dissertation. An example will be given to illustrate the technique. In the next section the notation to be used will be described. Certain distributional and modeling assumptions will also be made.

#### 3.2 Notation and Model Assumptions

The experimental design used for the experiment defines  $G$  distinct design points. At each of these points  $n_i \geq 0$ ,  $i=1,2,\dots,G$ , replications of the experiment will be conducted and the response observed. Let

$\mathbf{x}_i$  = 1 x (p+1) vector of explanatory variables at the  $i$ th observational point =  
 $\begin{bmatrix} 1 & x_{i1} & x_{i2} & \dots & x_{ip} \end{bmatrix}$

$\mathbf{X}$  =  $G$  x (p+1) full rank matrix of explanatory variables with rows  $\mathbf{x}_i$

$Z_{ij}$  =  $j$ th response at the  $i$ th point of observation;  $Z_{ij} \in \{0,1\}$ ;  $j=1,2,\dots,n_i$



$$Y_i = \sum_{j=1}^{n_i} Z_{ij}$$

$$\mathbf{Y} = [Y_1 \ Y_2 \ \dots \ Y_G]'$$

It is assumed for all  $i=1,2,\dots,G$  and  $j=1,2,\dots,n_i$  that  $Z_{ij}$  are independently distributed as Bernoulli random variables with unknown parameter  $\pi_i$ . It therefore follows that the  $Y_i$ ,  $i=1,2,\dots,G$  are independent and distributed as Binomial random variables with known parameter  $n_i$  and unknown parameter  $\pi_i$ . This distribution is denoted by  $\text{Bin}(n_i, \pi_i)$  and its probability distribution function given by

$$f_{Y_i}(y_i; \pi_i, n_i) = \binom{n_i}{y_i} \pi_i^{y_i} (1 - \pi_i)^{n_i - y_i}; \quad 0 \leq \pi_i \leq 1. \quad (3.2.1)$$

Recall that the exponential family of distributions is given by

$$f(y_i; \pi_i) = d(y_i) \exp[a(y_i)b(\pi_i) + c(\pi_i)]$$

where  $b(\pi_i)$  is the natural parameter. By rewriting (3.2.1) as

$$f_{Y_i}(y_i; \pi_i, n_i) = \binom{n_i}{y_i} \exp\left\{y_i \log\left(\frac{\pi_i}{1 - \pi_i}\right) + n_i \log(1 - \pi_i)\right\} \quad (3.2.2)$$

it can be shown that the binomial distribution is a member of this family with natural parameter

$$b(\pi_i) = \log\left(\frac{\pi_i}{1 - \pi_i}\right) = \text{logit}(\pi_i).$$

It is assumed that these natural parameters can be modeled as linear functions of the explanatory variables in the following way. Let

$$\text{logit}(\pi_i) = \log\left(\frac{\pi_i}{1 - \pi_i}\right) = \mathbf{x}_i\boldsymbol{\beta}; \quad i=1,2,\dots,G, \quad (3.2.3)$$

where  $\boldsymbol{\beta}$  is a  $(p+1) \times 1$  vector of unknown parameters. It follows from (3.2.3) that

$$\pi_i = \frac{1}{1 + \exp(-\mathbf{x}_i\boldsymbol{\beta})} = \frac{\exp(\mathbf{x}_i\boldsymbol{\beta})}{1 + \exp(\mathbf{x}_i\boldsymbol{\beta})}. \quad (3.2.4)$$

An overall model can also be written as

$$\boldsymbol{\pi} = \frac{1}{1 + \exp(-\mathbf{X}\boldsymbol{\beta})}, \quad (3.2.5)$$

where  $\boldsymbol{\pi} = (\pi_1 \ \pi_2 \ \dots \ \pi_G)'$  and  $\mathbf{X}$  is the  $G \times (p+1)$  matrix with rows  $\mathbf{x}_i$ . Hence, in this modeling procedure the response, or dependent variable, is the  $\text{logit}(\pi_i)$ , where  $\pi_i$  is the unknown parameter from the assumed binomial distribution. Based on the distributional assumptions made,

$$E(Y_i) = n_i\pi_i = \frac{n_i}{1 + \exp(-\mathbf{x}_i\boldsymbol{\beta})}, \quad (3.2.6)$$

$$\text{Var}(Y_i) = n_i\pi_i(1 - \pi_i) = \frac{n_i \exp(-\mathbf{x}_i\boldsymbol{\beta})}{(1 + \exp(-\mathbf{x}_i\boldsymbol{\beta}))^2}. \quad (3.2.7)$$

One advantage of modeling the natural parameter, or  $\text{logit}(\pi_i)$ , is that the associated transformed parameter space is unrestricted, i.e., while  $\pi_i \in [0,1]$ ,  $\text{logit}(\pi_i) \in \mathbf{R}$ . Since there are no restrictions on  $\text{logit}(\pi_i)$ , it can be assumed, in general, that no restrictions need be placed on the vector  $\boldsymbol{\beta}$ . Hence  $\boldsymbol{\beta} \in \mathbf{R}^{p+1}$ .

However, if  $\pi_i = 0$  or  $1$ , the resulting distribution is degenerate. This means all possible values of  $Y_i$  will be concentrated at the single point  $n_i$  when  $\pi_i = 1$ , or at  $0$  when  $\pi_i = 0$ . By examining (3.2.3), it is also apparent that when  $\pi_i = 0$  or  $1$ ,  $\boldsymbol{\beta}$  will contain one or more infinite values. Therefore while the distribution itself is well defined when  $\pi_i = 1$  or  $0$ , it can not be written in the form (3.2.2). In the context of an actual analysis it can be assumed that the dose ranges studied are such that  $\pi_i \neq 0$  and  $\pi_i \neq 1$ . If  $\pi_i$  is near one of these values, however, the associated  $\boldsymbol{\beta}$  vector will contain values tending towards  $\pm\infty$ . This property should be noted since it may cause convergence problems in the estimation procedure discussed in the next section.

It is also useful at this point to examine the  $(p+1) \times 1$  vector  $\boldsymbol{\beta}$  more closely. Since  $\mathbf{x}_i = (1 \ x_{i1} \ x_{i2} \ \dots \ x_{ip})$ ,  $\mathbf{x}_i \boldsymbol{\beta}$  can be written as  $\beta_0 + \beta_1 x_{i1} + \beta_2 x_{i2} + \dots + \beta_p x_{ip}$ . Therefore,  $p$  of the parameters are associated with the explanatory variables. A model containing only the intercept parameter is given by  $\pi_i = \frac{1}{1 + \exp(-\beta_0)}$ ,  $i=1,2,\dots,G$ , and is referred to as an "intercept only" model.

In the next section the estimation of the elements of  $\boldsymbol{\beta}$  is described. These estimated values can then be used to help evaluate the relationship between the explanatory variables,  $\mathbf{x}_i$ , and the unknown  $\pi_i$ ,  $i=1,2,\dots,G$ .

### 3.3 Estimation

Maximum likelihood methods will be used to estimate  $\boldsymbol{\beta}$ . Let  $\mathbf{y}$  denote a  $G \times 1$  vector of observed values for  $\mathbf{Y}$ . For this fixed sample,  $\mathbf{y}$ , the likelihood which is a function of  $\boldsymbol{\pi}$ , is given by

$$L(\boldsymbol{\pi}; \mathbf{y}) = \prod_{i=1}^G \binom{n_i}{y_i} \pi_i^{y_i} (1 - \pi_i)^{n_i - y_i} \quad (3.3.1)$$

$$= \left\{ \prod_{i=1}^G \binom{n_i}{y_i} \right\} \exp \left\{ \sum_{i=1}^G y_i \ln \left( \frac{\pi_i}{1 - \pi_i} \right) + n_i \ln(1 - \pi_i) \right\}. \quad (3.3.2)$$

Based on (3.2.3) the likelihood (3.3.2) can be written in terms of  $\boldsymbol{\beta}$  as

$$L(\boldsymbol{\beta}; \mathbf{y}) = \left\{ \prod_{i=1}^G \binom{n_i}{y_i} \right\} \exp \left\{ \sum_{i=1}^G y_i \mathbf{x}_i \boldsymbol{\beta} - n_i \ln \{ 1 + \exp(\mathbf{x}_i \boldsymbol{\beta}) \} \right\}. \quad (3.3.3)$$

The goal is to find  $\hat{\boldsymbol{\beta}}$ , the value of  $\boldsymbol{\beta}$  that maximizes the likelihood given in (3.3.3). Since the function  $y = \ln(x)$  is a monotonically increasing function, maximizing  $L(\boldsymbol{\beta}; \mathbf{y})$  is equivalent to maximizing the  $\ln$  of  $L(\boldsymbol{\beta}; \mathbf{y})$  given by

$$l(\boldsymbol{\beta}; \mathbf{y}) = \ln(L(\boldsymbol{\beta}; \mathbf{y})) = \ln \sum_{i=1}^G \binom{n_i}{y_i} + \left[ \sum_{i=1}^G y_i \mathbf{x}_i \boldsymbol{\beta} - n_i \ln \{ 1 + \exp(\mathbf{x}_i \boldsymbol{\beta}) \} \right]. \quad (3.3.4)$$

The usual method of maximization involves setting the first derivatives of (3.3.4) equal to 0, solving for the parameters of interest and then insuring that the values determined are, in fact, associated with the maximum values of  $l(\boldsymbol{\beta}; \mathbf{y})$ . Here, the first derivatives, which are defined as the Scores, are given by

$$U_j(\boldsymbol{\beta}) = \frac{\partial l(\boldsymbol{\beta}; \mathbf{y})}{\partial \beta_j} = \sum_{i=1}^G y_i x_{ij} - \sum_{i=1}^G \frac{n_i x_{ij}}{1 + \exp(-\mathbf{x}_i \boldsymbol{\beta})}; \quad j = 0, 1, 2, \dots, p. \quad (3.3.5)$$

Recall that the underlying distributional assumptions made were that the response variable,  $Y_i$ , is distributed Binomial( $n_i, \pi_i$ ) and that the unknown parameter  $\pi_i$  could be modeled by  $\pi_i = \frac{1}{1 + \exp(-\mathbf{x}_i \boldsymbol{\beta})}$ . Wedderburn (1976, p.31) showed that under these assumptions and assuming  $\pi_i \in (0, 1)$  the maximum likelihood estimate of  $\boldsymbol{\beta}$ ,  $\hat{\boldsymbol{\beta}}$ , exists, is finite and unique.

In order to actually solve for  $\hat{\boldsymbol{\beta}}$  iterative procedures must be used. For purposes of this dissertation an iteratively reweighted least square algorithm (IRLS) will be used to solve the systems of equations given by  $\frac{\partial l(\boldsymbol{\beta}; \mathbf{y})}{\partial \beta_j} = 0$ ;  $j = 0, 1, 2, \dots, p$ . This procedure is described in McCullagh and Nelder (1989, p.40). In general this method may fail to converge if one or more components of  $\hat{\boldsymbol{\beta}}$  is infinite. One way this could occur is when there is little or no variability in the responses observed over particular values of the explanatory variables. For example, consider a drug combination study where all observed responses are constant over the full range of doses for one of the agents alone. The parameter estimate associated with that agent will tend toward positive or negative infinity if the responses are identically 1 or 0, respectively. An adjustment to the  $\mathbf{X}$  matrix and the experiment may be necessary in these cases. This could include increasing the size of the experiment by extending dose combinations in a predetermined fashion. Necessary adjustments to the analysis may then be needed to account for this change in the experimental design. For the remainder of this dissertation, however, it will be assumed that no adjustments will be made to the set of observations considered.

The following section presents a discussion of the statistical properties of these estimators.

### 3.4 Distributional Properties

When the total sample size,  $\sum_{i=1}^G n_i$ , is large certain properties of the maximum likelihood estimators  $\hat{\boldsymbol{\beta}}$  and the scores  $\mathbf{U}(\boldsymbol{\beta}) = [U_0(\boldsymbol{\beta}) \ U_1(\boldsymbol{\beta}) \ \dots \ U_p(\boldsymbol{\beta})]'$  have been derived. A complete discussion of these properties is given in several sources including Serfling (1980) and Rao (1973).

Many of these results involve the  $(p+1) \times (p+1)$  Fisher Information Matrix,  $\mathbf{I}(\boldsymbol{\beta})$ . The  $jk^{\text{th}}$  element of this matrix is given by

$$I_{jk}(\boldsymbol{\beta}) = E[U_j(\boldsymbol{\beta})U_k(\boldsymbol{\beta})'] \quad j,k=0,1,2,\dots,p. \quad (3.4.1)$$

It can be shown that under the distributional assumptions made

$$I_{jk}(\boldsymbol{\beta}) = -E\left(\frac{\partial^2 l(\boldsymbol{\beta}; \mathbf{y})}{\partial \beta_j \partial \beta_k}\right) = \sum_{i=1}^G \frac{n_i x_{ij} x_{ik} \exp(-\mathbf{x}_i \boldsymbol{\beta})}{(1 + \exp(-\mathbf{x}_i \boldsymbol{\beta}))^2} \quad j,k=0,1,2,\dots,p. \quad (3.4.2)$$

where  $x_{i0} = 1$ ,  $i=1,2,\dots,G$ .  $\mathbf{I}(\boldsymbol{\beta})$  can be consistently estimated by evaluating (3.4.2) with  $\boldsymbol{\beta} = \hat{\boldsymbol{\beta}}$ . This estimate is denoted by  $\mathbf{I}(\hat{\boldsymbol{\beta}})$ .

Let  $N_{p+1}$  denote the  $p+1$  dimensional multivariate normal distribution. Two well known approximate distributions are given by

$$\mathbf{U}(\boldsymbol{\beta}) \sim N_{p+1}(\mathbf{0}, \mathbf{I}(\boldsymbol{\beta})) \quad (3.4.3)$$

$$\hat{\boldsymbol{\beta}} \sim N_{p+1}(\boldsymbol{\beta}, \mathbf{I}(\boldsymbol{\beta})^{-1}). \quad (3.4.4)$$

Note that (3.4.4) implies the maximum likelihood estimate,  $\hat{\beta}$ , is an approximate unbiased estimate of the true parameter,  $\beta$ . The covariance matrix for the parameter estimates,  $\hat{\beta}$ , is  $I(\beta)^{-1}$  which can be consistently estimated by taking the inverse of  $I(\hat{\beta})$  and is denoted by  $I(\hat{\beta})^{-1}$ .

Using properties of the multivariate normal distribution it follows from (3.4.3) and (3.4.4) that

$$U(\beta)'I(\beta)^{-1}U(\beta) \sim \chi_{p+1} \quad (3.4.5)$$

$$(\beta - \hat{\beta})'I(\beta)(\beta - \hat{\beta}) \sim \chi_{p+1}. \quad (3.4.6)$$

In addition, based on (3.4.4), the approximate distribution of the individual maximum likelihood estimators can be derived. Let  $\sigma^2(\beta_j)$  denote the  $j^{\text{th}}$  diagonal element of  $I(\beta)^{-1}$ .

Then for  $j=0,1,2,\dots,p$  it follows that

$$\hat{\beta}_j \sim N(\beta_j, \sigma^2(\beta_j)) \quad (3.4.7)$$

or equivalently

$$\frac{(\beta_j - \hat{\beta}_j)^2}{\sigma^2(\beta_j)} \sim \chi_1^2. \quad (3.4.8)$$

An estimate for  $\sigma^2(\beta_j)$  is given by the  $j^{\text{th}}$  diagonal element of  $I(\hat{\beta})^{-1}$  and is denoted by  $\sigma^2(\hat{\beta}_j)$

Lastly, an approximate distribution involving the ln likelihood is given by

$$2\left(l(\hat{\boldsymbol{\beta}}; \mathbf{y}) - l(\boldsymbol{\beta}; \mathbf{y})\right) \sim \chi_{p+1}^2. \quad (3.4.9)$$

These approximate distributions can be used to develop various useful tests of hypotheses involving the parameters  $\boldsymbol{\beta}$ . One important group of tests that is often applied is goodness of fit tests. These will be discussed in the next section. Tests for more general hypotheses then follow.

### 3.5 Goodness-of-Fit Tests

In any model fitting procedure an overall measure of the goodness-of-fit is very useful. Here the null hypothesis is that the defined model of interest adequately describes the data. A small p-value associated with this test implies that the investigator should reexamine the model assumptions.

Pearson's  $C^2$  statistic (Hosmer and Lemeshow, 1989, p. 138) is often used to test this type of hypothesis. This statistic is defined as

$$C^2 = \sum_{i=1}^G \frac{(y_i - n_i \hat{\pi}_i)^2}{n_i \hat{\pi}_i (1 - \hat{\pi}_i)} \quad (3.5.1)$$

where  $\hat{\pi}_i = \frac{1}{1 + \exp(-\mathbf{x}_i \hat{\boldsymbol{\beta}})}$ ,  $i=1,2,\dots,G$ .

Another goodness-of-fit test that has been cited in this context is based on the difference of the ln likelihoods evaluated at two particular estimates of the parameters. Before defining this statistic it is useful to reexamine the maximum of the ln likelihood. Recall that one goal of these studies is to examine the relationship between the explanatory variables and the response values. Therefore, when using the principles of maximum likelihood, the value of  $\boldsymbol{\beta}$  that maximized the ln likelihood was found. Based on this



maximum likelihood estimate,  $\hat{\beta}$ , the predicted response is given as  $\hat{\pi}_i = \frac{1}{1 + \exp(-\mathbf{x}_i \hat{\beta})}$ ;

$i=1,2,\dots,G$ . In general, however, it can be shown that the ln likelihood is maximized in terms of  $\pi_i$  by  $\tilde{\pi}_i = \frac{y_i}{n_i}$ ;  $i=1,2,\dots,G$ . Hence it will follow that  $l(\hat{\pi}; \mathbf{y}) \leq l(\tilde{\pi}; \mathbf{y})$ . The fitted

model based on  $\tilde{\pi}$  is referred to as the maximal model with the number of parameters equal to the number of observational points. In general, these estimators are not useful to the investigator since they do not relate the values of the explanatory variables to the response. The ln likelihood evaluated at  $\tilde{\pi}$  can be used as a standard, however, for comparing alternative fitted models. If the estimated model in terms of  $\hat{\beta}$  fits well, the difference of ln likelihoods evaluated at  $\hat{\beta}$  and  $\tilde{\pi}$  should be small. This difference, defined as the deviance (Hosmer and Lemeshow, 1989, p. 14), is given by

$$D = -2\{l(\hat{\beta}; \mathbf{y}) - l(\tilde{\pi}; \mathbf{y})\}. \quad (3.5.2)$$

Depending on the way the sample size becomes large,  $C^2$  and  $D$  have been shown to converge in distribution to the  $\chi_{G-p-1}^2$  distribution. For the studies considered in this dissertation, the sample size can become large in two ways. One way assumes the number of unique observational points,  $G$ , is fixed and  $n_i$ , the number of replications at each point is large. The other assumes  $n_i$  will be small but  $G$  will be large. The asymptotic results in Section 3.4 hold in both cases. When  $G$  is large but the data are sparse, i.e.,  $n_i$  is small, the use of the  $\chi_{G-p-1}^2$  distribution as an approximation of the distribution of  $C^2$  and  $D$  has been shown to be problematic (McCullagh and Nelder, 1989, p.121). Therefore, before applying these statistics as global measures of goodness of fit, the investigator should insure that the experiment conforms to the asymptotic assumptions made.

Based on the possible problems associated with the use of  $D$  and  $C^2$ , some alternative approaches have been considered. Pregibon (1981) has advocated the use of the individual components of  $D$  and  $C^2$  as indicators of observations poorly accounted for by the fitted model. These individual components, for  $i=1,2,\dots,G$  are given by

$$C_i = \frac{(y_i - n_i \hat{\pi}_i)}{\sqrt{n_i \hat{\pi}_i (1 - \hat{\pi}_i)}} \quad (3.5.3)$$

and

$$d_i = \begin{cases} \sqrt{2} \{l(\tilde{\pi}; y_i) - l(\hat{\beta}; y_i)\}^{1/2}; & \text{if } y_i \neq 0 \text{ and } y_i \neq n_i \text{ and } \tilde{\pi}_i \geq \hat{\pi}_i \\ -\sqrt{2} \{l(\tilde{\pi}; y_i) - l(\hat{\beta}; y_i)\}^{1/2}; & \text{if } y_i \neq 0 \text{ and } y_i \neq n_i \text{ and } \tilde{\pi}_i < \hat{\pi}_i \\ (-2n_i \log(1 - \hat{\pi}_i))^{1/2}; & \text{if } y_i = 0 \\ (-2n_i \log(\hat{\pi}_i))^{1/2}; & \text{if } y_i = n_i. \end{cases} \quad (3.5.4)$$

A large  $C_i$  is indicative of an observation with a large difference between the observed and fitted values or a predicted value close to 0 or 1. A large  $d_i$  implies there is a relatively large disagreement in the maximum of the ln likelihoods evaluated at  $\hat{\beta}$  and  $\tilde{\pi}$ . Hence at the observation in question there is less evidence in support of the maximum likelihood estimate,  $\hat{\beta}$ . Therefore, large values of the individual statistics  $C_i$  that are not associated with predicted  $\hat{\pi}_i$  near 0 or 1, or large  $d_i$  may be associated with observations where the fit of the model may be poor. The analyst can investigate those observations in the usual way for problems in data collection or with the study protocol. In some cases the overall model assumptions may also have to be reconsidered.

McCullagh and Nelder (1989, p.122) have also derived an asymptotically normal distribution for  $C^2$  given in (3.5.1) conditional on the value of  $\hat{\beta}$ . This conditional

asymptotic distribution is not dependent on the manner the sample size becomes large.

Hence

$$C^2|\hat{\beta} \xrightarrow{d} N(\mu_{X^2|\hat{\beta}}, \sigma_{X^2|\hat{\beta}}^2) \quad (3.5.5)$$

where

$$\begin{aligned} \mu_{C^2|\hat{\beta}} = E(C^2|\hat{\beta}) &\approx G - (p+1) - \frac{1}{2} \sum_{i=1}^G \{1 - 6\hat{\pi}_i(1 - \hat{\pi}_i)\} \hat{v}_{ii} + \\ &\frac{1}{2} \sum_{j=1}^G \sum_{i=1}^G n_i \hat{\pi}_i (1 - \hat{\pi}_i) (1 - 2\hat{\pi}_i) \hat{v}_{ii} \hat{v}_{ij} (1 - 2\hat{\pi}_j), \end{aligned}$$

$$\sigma_{C^2|\hat{\beta}}^2 = \text{Var}(C^2|\hat{\beta}) \approx \left(1 - \frac{p+1}{G}\right) 2 \left\{ \sum_{i=1}^G \frac{n_i - 1}{n_i} + \sum_{j=1}^G \sum_{i=1}^G (1 - 2\hat{\pi}_i)(1 - 2\hat{\pi}_j) \hat{v}_{ij} \right\}$$

and  $\hat{v}_{ij}$  is the  $ij$ th element of  $\hat{V} = \mathbf{X}\mathbf{I}(\hat{\beta})^{-1}\mathbf{X}'$ . A goodness-of-fit test based on this approximate distribution can be applied when  $G$  is large and  $n_i$  is small but greater than 1.

For the studies considered in this dissertation it is assumed that in general,  $n_i$ , the number of replications of the experiment at each observation point, will be small but  $G$ , the number of observation points, will be large. Therefore, a goodness of fit test based on  $X^2$  and the approximate normal distribution defined in (3.5.5) will be used. An examination of the individual components of  $X^2$  and  $D$  will also be made. This will be particularly helpful if the overall goodness-of-fit null hypothesis is rejected. When large values of the of  $X_i$  or  $d_i$  are identified the data will be examined to determine if there are problems with data coding or the study protocol at these points. If no problems are found then an adjustment to the model may also be examined. In general, the elimination of these problem points will not be considered.

Once the investigator is satisfied that the fit of the model is adequate, and depending on the questions of interest, one or more of the hypothesis test procedures described in the next section can be applied.

### 3.6 Inference

Based on the asymptotic results given in Section 3.4 several statistical testing procedures can be developed. One important group of hypotheses are of the form

$$\begin{aligned} H_0 : \boldsymbol{\beta} &= \boldsymbol{\gamma}_0 \\ H_a : \boldsymbol{\beta} &\neq \boldsymbol{\gamma}_0 \end{aligned} \quad (3.6.1)$$

where  $\boldsymbol{\gamma}_0$  is a  $(p+1) \times 1$  vector of constants. Let  $I(\boldsymbol{\gamma}_0)$  denote the Information matrix (3.4.1) evaluated at  $\boldsymbol{\gamma}_0$ . The following three test statistics can be used to test (3.6.1).

$$\text{Wald test statistic} \quad (\boldsymbol{\gamma}_0 - \hat{\boldsymbol{\beta}})' I(\hat{\boldsymbol{\beta}}) (\boldsymbol{\gamma}_0 - \hat{\boldsymbol{\beta}}) \quad (3.6.2)$$

$$\text{Score test statistic} \quad \mathbf{U}(\boldsymbol{\gamma}_0)' I(\boldsymbol{\gamma}_0)^{-1} \mathbf{U}(\boldsymbol{\gamma}_0) \quad (3.6.3)$$

$$\text{Likelihood ratio test statistic} \quad 2 \left( l(\hat{\boldsymbol{\beta}}; \mathbf{y}) - l(\boldsymbol{\gamma}_0; \mathbf{y}) \right). \quad (3.6.4)$$

In all three cases, assuming the null hypothesis is true, and based on the results (3.4.5), (3.4.6) and (3.4.9), the asymptotic distribution of these statistics is  $\chi_{p+1}^2$ . Extreme values of the test statistic lead to rejection of the null hypothesis at the appropriate level of significance. Alternatively, the associated observed p-value can be determined using the  $\chi_{p+1}^2$  distribution. If the null hypothesis is rejected the investigator can conclude at least one  $\beta_j \neq \gamma_{0j}$ ,  $j=0,1,2,\dots,p+1$ .

Asymptotically the tests are equivalent since under the null hypothesis, all three test statistics converge to the  $\chi^2_{p+1}$  distribution. Studies comparing the use of these three tests under various finite sample sizes have shown that none of the three tests is uniformly superior to the others (Madansky, 1989). Hauck and Donner (1977) have demonstrated however, that the Wald test has some undesirable characteristics, particularly when at least one parameter estimate,  $\hat{\beta}_j$  is large. In addition, it has been shown that the Wald test is not invariant under transformations of the parameters (Cox and Oates, 1984). The score statistic has a computational advantage since it does not require calculation of the maximum likelihood estimates. If the maximum likelihood estimates are readily available the likelihood ratio statistic is often recommended (Mantel, 1987, Cox and Oates, 1984). McCullagh and Nelder (1989, p.473) have stated that the asymptotic distribution associated with the likelihood ratio statistic is "quite accurate for small values of n even when Normal approximations for parameter estimates are unsatisfactory".

An example of a useful hypothesis that can be expressed in the form (3.6.1) involves testing the dependence of the response variable on at least one of the explanatory variables. This test will be referred to as the intercept-only test. Here  $\boldsymbol{\gamma}_0 = (\hat{\gamma}_{00} \ 0 \ 0 \ \dots \ 0)'$  where  $\hat{\gamma}_{00}$  denotes the maximum likelihood estimate of the single parameter in an intercept-only model. This value, shown below, can be determined in a straight forward way by maximizing the ln likelihood for the intercept-only model with respect to  $\gamma_{00}$ .

$$\hat{\gamma}_{00} = \ln \left( \frac{\sum_{i=1}^G y_i / \sum_{i=1}^G n_i}{1 - \left( \sum_{i=1}^G y_i / \sum_{i=1}^G n_i \right)} \right)$$

This result implies that under the assumption of an intercept only model, the maximum

likelihood estimate of the constant response is given by  $\frac{1}{1 + \exp(-\hat{\gamma}_{00})} = \frac{\sum_{i=1}^G y_i}{\sum_{i=1}^G n_i}$ . The null

hypotheses can therefore be written as  $H_0 : \boldsymbol{\beta} = (\hat{\gamma}_{00} \ 0 \ 0 \ \dots \ 0)'$ . Once  $\hat{\gamma}_0 = (\hat{\gamma}_{00} \ 0 \ 0 \ \dots \ 0)'$  is determined, all three test statistics given in (3.6.2), (3.6.3) and (3.6.4) can be calculated.

Note that in the hypothesis given in (3.6.1) the entire vector of parameters is specified. Another useful group of hypotheses involves specifying that only a subset of the parameters is equal to zero. Let  $\boldsymbol{\beta} = \begin{pmatrix} \boldsymbol{\beta}_{(1)} \\ \boldsymbol{\beta}_{(2)} \end{pmatrix}$  where  $\boldsymbol{\beta}_{(1)}$  is  $r \times 1$  and  $\boldsymbol{\beta}_{(2)}$  is  $s \times 1$  and  $r + s =$

$p+1$ . The hypotheses are given by

$$\begin{aligned} H_0 : \boldsymbol{\beta}_{(2)} &= \mathbf{0} \\ H_a : \boldsymbol{\beta}_{(2)} &\neq \mathbf{0}. \end{aligned} \tag{3.6.5}$$

Under the null hypothesis, a reduced or restricted model with  $r$  parameters is defined. Let  $\hat{\boldsymbol{\psi}}$  denote the  $r \times 1$  vector of maximum likelihood estimates under  $H_0$ . In contrast, under  $H_a$ , the full or unrestricted model is considered with maximum likelihood estimates  $\hat{\boldsymbol{\beta}}$ . A test statistic that can be used to test these hypotheses is based on the deviance (3.5.1).

Expressions for the deviances under the respective hypotheses are given by

$$D_0 = -2\{l(\hat{\boldsymbol{\psi}}; \mathbf{y}) - l(\tilde{\boldsymbol{\pi}}; \mathbf{y})\}$$

$$D_a = -2\{l(\hat{\boldsymbol{\beta}}; \mathbf{y}) - l(\tilde{\boldsymbol{\pi}}; \mathbf{y})\}.$$

The difference in these deviances is the basis for this Full Model versus Restricted Model

Likelihood Ratio test and is given by

$$D_{\Delta} = D_a - D_0 = -2\{l(\hat{\beta}; y) - l(\hat{\psi}; y)\}. \quad (3.6.6)$$

In section 3.5 it was noted that the asymptotic distributions associated with the deviances were dependent on the manner the sample size increased. Dobson (1990, p.62) states however, that the asymptotic distribution of  $D_{\Delta}$  in (3.6.6) is adequately approximated by  $\chi_s^2$ . Note that the degrees of freedom for this test are equal to the dimension of the vector  $\beta_{(2)}$ . This is equivalent to the difference in the number of parameters in the full model  $(p+1)$  and the reduced model, i.e.,  $(p+1)-r = s$ . Note, for this testing procedure, in order to determine  $\hat{\beta}$  and  $\hat{\psi}$  two executions of the IRLS estimating procedure are needed.

Another application of the test defined by (3.6.5) involves testing the significance of only one parameter. If the parameter of interest is  $\beta_j$  then the hypothesis can be written as

$$\begin{aligned} H_0 : \beta_j &= 0 \\ H_a : \beta_j &\neq 0 \end{aligned} \quad (3.6.7)$$

In terms of (3.6.5)  $\beta_{(2)} = (\beta_j)$  and  $\beta_{(1)}$  is the  $p \times 1$  vector of the remaining parameters.

Now, under the null hypothesis, the maximum likelihood estimates are the  $p \times 1$  vector  $\hat{\psi}$ . As usual,  $D_{\Delta}$  is calculated. A p-value based on the  $\chi_1^2$  distribution then can be determined.

This same hypothesis (3.6.7) is also commonly tested using a Wald Statistic and is based on the asymptotic result given in (3.4.8). Since under  $H_0$ ,  $\beta_j = 0$ , the test statistic is given by

$$\text{Wald test statistic} \quad \frac{\hat{\beta}_j^2}{\sigma^2(\hat{\beta}_j)} \quad (3.6.8)$$

where  $\sigma^2(\hat{\beta}_j)$  is the  $j$ th diagonal element of the estimated covariance matrix,  $I(\hat{\beta})^{-1}$ . Using the observed value of (3.6.8) a p-value based on the  $\chi_1^2$  can be determined.

If a large number of these individual tests defined by (3.6.7) are applied the investigator must consider the problems associated with multiple testing. When a large number of individual tests are conducted the overall probability of falsely rejecting at least one null hypothesis becomes quite large. This will be addressed in more detail in Chapter 6.

Another useful statistical tool is the confidence region. In the next section confidence regions about the response and about the individual parameters will be discussed.

### 3.7 Confidence Regions

The result given in (3.4.7) can be applied in a straightforward manner to estimate the endpoints of a confidence region about a given parameter. A  $100(1-\alpha)\%$  confidence region about  $\beta_j$  is given by

$$[\hat{\beta}_j^L, \hat{\beta}_j^U] = \hat{\beta}_j \pm t_{1-\alpha/2; G-p-1} \sigma(\hat{\beta}_j) \quad (3.7.1)$$

where  $t_{1-\alpha/2; G-p-1}$  is the upper  $(1-\alpha/2)$  percentage point from student t distribution with  $G-p-1$  degrees of freedom and  $\sigma^2(\hat{\beta}_j)$  is the  $j$ th diagonal element of the estimated covariance matrix,  $I(\hat{\beta})^{-1}$ .

A confidence region about the response at a single fixed value of the explanatory variables,  $\mathbf{x}_i$ , can be determined using (3.7.1) as follows,



$$[\hat{\pi}_i^L, \hat{\pi}_i^U] = \left[ \frac{1}{1 + \exp(-\mathbf{x}_i \hat{\boldsymbol{\beta}}_i^L)}, \frac{1}{1 + \exp(-\mathbf{x}_i \hat{\boldsymbol{\beta}}_i^U)} \right]$$

In general, however, an examination of the confidence regions about the response at several levels of the explanatory variables will be considered. Recall the coverage probability,  $1 - \alpha$ , associated with a confidence interval is the probability the interval covers the true parameter. If the methodology just described is applied repeatedly the overall confidence probability will become small. For example, if ten confidence intervals with individual coverage probability .95 are constructed based on ten independent samples, the overall coverage probability will be  $.95^{10} = .5987$ . The construction of a simultaneous confidence region can be used, however, to insure an overall coverage probability of at least .95.

Hauck (1983) developed a conservative simultaneous  $100(1 - \alpha)\%$  confidence region about the response. Using (3.4.6), a  $100(1 - \alpha)\%$  confidence ellipsoid about the parameters,  $\boldsymbol{\beta}$ , is based on

$$P \left[ (\hat{\boldsymbol{\beta}} - \boldsymbol{\beta})' \mathbf{I}(\hat{\boldsymbol{\beta}}) (\hat{\boldsymbol{\beta}} - \boldsymbol{\beta}) \leq \chi_{p+1, 1-\alpha}^2 \right] = 1 - \alpha \quad (3.7.2)$$

where  $\chi_{p+1, 1-\alpha}^2$  is the upper  $1 - \alpha$  percentage point of the  $\chi_{p+1}^2$  distribution and  $\mathbf{I}(\hat{\boldsymbol{\beta}})$  is a consistent estimator of  $\mathbf{I}(\boldsymbol{\beta})$ . Let  $\mathbf{w}$  be an arbitrary  $1 \times (p+1)$  vector of independent variables. Applying a form of the Cauchy-Schwartz inequality given by

$$\frac{(\mathbf{w}(\hat{\boldsymbol{\beta}} - \boldsymbol{\beta}))^2}{\mathbf{w} \mathbf{I}(\hat{\boldsymbol{\beta}})^{-1} \mathbf{w}} \leq (\hat{\boldsymbol{\beta}} - \boldsymbol{\beta})' \mathbf{I}(\hat{\boldsymbol{\beta}}) (\hat{\boldsymbol{\beta}} - \boldsymbol{\beta}) \text{ for any } \mathbf{w}, \quad (3.7.3)$$

(3.7.2) can be rewritten as

$$P \left[ \frac{\left( \mathbf{w}(\hat{\boldsymbol{\beta}} - \boldsymbol{\beta}) \right)' \right)^2}{\mathbf{w} \mathbf{I}(\hat{\boldsymbol{\beta}})^{-1} \mathbf{w}'} \leq \chi_{p+1, \alpha}^2, \forall \mathbf{w} \right] \geq 1 - \alpha. \quad (3.7.4)$$

Simplifying (3.7.4) gives

$$P \left[ \mathbf{w} \hat{\boldsymbol{\beta}} - \left( \chi_{p+1, \alpha}^2 \mathbf{w} \mathbf{I}(\hat{\boldsymbol{\beta}})^{-1} \mathbf{w}' \right)^{1/2} \leq \mathbf{w} \boldsymbol{\beta} \leq \mathbf{w} \hat{\boldsymbol{\beta}} + \left( \chi_{p+1, \alpha}^2 \mathbf{w} \mathbf{I}(\hat{\boldsymbol{\beta}})^{-1} \mathbf{w}' \right)^{1/2}, \forall \mathbf{w} \right] \geq 1 - \alpha. \quad (3.7.5)$$

Note that (3.7.5) applies to all values of  $\mathbf{w}$ . For a specific value of  $\mathbf{w}$ , say  $\mathbf{x}_i$ , the corresponding probability statement is given by

$$P \left[ \mathbf{x}_i \hat{\boldsymbol{\beta}} - \left( \chi_{p+1, \alpha}^2 \mathbf{x}_i \mathbf{I}(\hat{\boldsymbol{\beta}})^{-1} \mathbf{x}_i' \right)^{1/2} \leq \mathbf{x}_i \boldsymbol{\beta} \leq \mathbf{x}_i \hat{\boldsymbol{\beta}} + \left( \chi_{p+1, \alpha}^2 \mathbf{x}_i \mathbf{I}(\hat{\boldsymbol{\beta}})^{-1} \mathbf{x}_i' \right)^{1/2} \right] \geq 1 - \alpha. \quad (3.7.6)$$

A conservative simultaneous confidence interval about  $\mathbf{x}_i \boldsymbol{\beta}$  is therefore given by the interval

$$[\lambda_L(\mathbf{x}_i), \lambda_U(\mathbf{x}_i)] = \mathbf{x}_i \hat{\boldsymbol{\beta}} \pm \left( \chi_{p+1, \alpha}^2 \mathbf{x}_i \mathbf{I}(\hat{\boldsymbol{\beta}})^{-1} \mathbf{x}_i' \right)^{1/2}. \quad (3.7.7)$$

Using (3.2.4), upper and lower bounds on the response at  $\mathbf{x}_i$  can be determined and are given by

$$[\hat{\pi}_i^L, \hat{\pi}_i^U] = \left[ \frac{1}{1 + \exp(-\lambda_L(\mathbf{x}_i))}, \frac{1}{1 + \exp(-\lambda_U(\mathbf{x}_i))} \right]. \quad (3.7.8)$$

This interval is considered conservative since the probability statement upon which it is based given in (3.7.6) is greater than or equal to  $1 - \alpha$  rather than equal to it. Note also that if this procedure is repeated for several values of  $\mathbf{x}_i$ , there is no reduction in the overall coverage probability, which will consistently be at least  $1 - \alpha$ . This follows since (3.7.3) is true for any  $\mathbf{w}$ .

The following section provides an example of an analysis that uses many of the results described in this chapter.

### 3.8 Example

Carter, et al. (1988) described in detail a two agent experiment involving thirty-eight dose combinations of the chemicals chloral hydrate and ethanol. Six mice were tested at each of these 38 combinations. A drug combination was administered and after 30 minutes the mouse was evaluated for loss of righting reflex (yes or no). The dose levels and the results are summarized in Table 3.1.

For reasons that will be described in Chapter 5, the model of interest at the  $i$ th dose combination is given by

$$\pi_i = \frac{1}{1 + \exp(-\mathbf{x}_i \boldsymbol{\beta})}; \quad i=1,2,\dots,38$$

where

$$\mathbf{x}_i = [1 \quad x_{i1} \quad x_{i2} \quad x_{i1}x_{i2}]$$

$$\boldsymbol{\beta} = [\beta_0 \quad \beta_1 \quad \beta_2 \quad \beta_{12}]'$$

$x_{i1}$  = dose of chloral hydrate

$x_{i2}$  = dose of ethanol.

An overall model can be written as

$$\boldsymbol{\pi} = \frac{1}{1 + \exp(-\mathbf{X}\boldsymbol{\beta})}$$

where

$$\boldsymbol{\pi} = (\pi_1 \pi_2 \dots \pi_{38})'$$

$$\mathbf{X} = 38 \times 4 \text{ matrix of explanatory variables} = \begin{bmatrix} 1 & X_{11} & X_{12} & X_{11}X_{12} \\ 1 & X_{21} & X_{22} & X_{21}X_{22} \\ \vdots & \vdots & \vdots & \vdots \\ 1 & X_{38,1} & X_{38,2} & X_{38,1}X_{38,2} \end{bmatrix}.$$

The fitted parameters and the various test statistics are listed in Table 3.2. The Goodness-of-Fit (3.5.5) p-value of 0.3737 suggests that the model adequately represents the data. In Table 3.1 the individual goodness of fit statistics  $X_i$  and  $d_i$  are listed. Three observations have large  $X_i$  values: (900,250), (900,300) and (1600,250). Only the first two of these observations also have relatively large values of  $d_i$ . Since no problems were identified with the coding or collecting of the data in this study and since the fit of the model is adequate, it is reasonable to proceed with the analysis of the complete dataset.

Both the score and likelihood versions of the intercept-only tests show that at least one of the nonintercept terms is significantly different from zero. This implies that at least one of the two chemicals has a significant effect on the response.

In Chapter 5 it will be shown that a test of the hypotheses given by

$$H_0 : \beta_{12} = 0$$

$$H_a : \beta_{12} \neq 0$$

**Table 3.1**

Chloral Hydrate and Ethanol Study: Loss of Righting Reflex in Mice

Data and Goodness of Fit Statistics

| Dose Levels |                 | $y_i/n_i$ | Responses                 |                            | Goodness of Fit |        |
|-------------|-----------------|-----------|---------------------------|----------------------------|-----------------|--------|
| Ethanol     | Chloral Hydrate |           | Observed<br>$\bar{\pi}_i$ | Predicted<br>$\hat{\pi}_i$ | $\chi_i$        | $d_i$  |
| 0           | 300             | 0/6       | .000                      | .120                       | -.903           | -1.236 |
| 0           | 325             | 2/6       | .333                      | .350                       | -.086           | -.086  |
| 0           | 350             | 4/6       | .666                      | .681                       | -.076           | -.076  |
| 0           | 375             | 5/6       | .833                      | .895                       | -.487           | -.454  |
| 0           | 400             | 6/6       | .667                      | .971                       | .423            | .593   |
| 0           | 425             | 6/6       | .667                      | .994                       | .212            | .299   |
| 200         | 100             | 0/6       | .000                      | .000                       | -.006           | -.008  |
| 200         | 150             | 0/6       | .000                      | .000                       | -.024           | -.034  |
| 200         | 200             | 0/6       | .000                      | .002                       | -.096           | -.136  |
| 200         | 250             | 0/6       | .000                      | .023                       | -.388           | -.546  |
| 200         | 300             | 3/6       | .500                      | .290                       | 1.133           | 1.078  |
| 900         | 100             | 0/6       | .000                      | .000                       | -.032           | -.045  |
| 900         | 150             | 0/6       | .000                      | .003                       | -.137           | -.194  |
| 900         | 200             | 0/6       | .000                      | .054                       | -.588           | -.820  |
| 900         | 250             | 6/6       | 1.00                      | .513                       | 2.385           | 2.829  |
| 900         | 300             | 4/6       | .667                      | .951                       | -3.218          | -2.194 |
| 1600        | 100             | 0/6       | .000                      | .005                       | -.174           | -.246  |
| 1600        | 150             | 0/6       | .000                      | .094                       | -.791           | -1.090 |
| 1600        | 200             | 5/6       | .833                      | .682                       | .794            | .842   |
| 1600        | 250             | 5/6       | .833                      | .978                       | -2.411          | -1.563 |
| 1600        | 300             | 6/6       | 1.00                      | .999                       | .081            | .115   |
| 2300        | 100             | 0/6       | .000                      | .130                       | -.095           | -1.290 |
| 2300        | 150             | 4/6       | .667                      | .775                       | -.638           | -.609  |
| 2300        | 200             | 6/6       | 1.00                      | .988                       | .274            | .386   |
| 2300        | 250             | 6/6       | 1.00                      | .999                       | .057            | .080   |
| 2300        | 300             | 6/6       | 1.00                      | .999                       | .012            | .017   |
| 3000        | 100             | 6/6       | 1.00                      | .814                       | 1.171           | 1.571  |
| 3000        | 150             | 6/6       | 1.00                      | .991                       | .229            | .323   |
| 3000        | 200             | 6/6       | 1.00                      | .999                       | .045            | .063   |
| 3000        | 250             | 6/6       | 1.00                      | .999                       | .009            | .012   |
| 3000        | 300             | 6/6       | 1.00                      | 1.000                      | .002            | .002   |
| 4000        | 0               | 2/6       | .333                      | .365                       | -.159           | -.160  |
| 4050        | 0               | 2/6       | .333                      | .418                       | -.421           | -.426  |
| 4100        | 0               | 2/6       | .333                      | .474                       | -.688           | -.696  |
| 4150        | 0               | 3/6       | .500                      | .530                       | -.145           | -.145  |
| 4200        | 0               | 4/6       | .667                      | .585                       | .406            | .411   |
| 4250        | 0               | 5/6       | .833                      | .638                       | .994            | 1.057  |
| 4300        | 0               | 4/6       | .667                      | .528                       | -.115           | -.114  |

**Table 3.2**

Chloral Hydrate and Ethanol Study: Loss of Righting Reflex in Mice  
Analysis Results

---

| Parameter Estimates |              |                        |                |         |
|---------------------|--------------|------------------------|----------------|---------|
| Parameter           |              | Estimate               | Wald Statistic | p-value |
| Intercept           | $\beta_0$    | -18.5314               | 33.9322        | .0001   |
| Chloral Hydrate     | $\beta_1$    | .00449                 | 33.9340        | .0001   |
| Ethanol             | $\beta_2$    | .0551                  | 33.0552        | .0001   |
| Interaction         | $\beta_{12}$ | $3.382 \times 10^{-6}$ | 4.1261         | .0422   |

---

Estimated Variance-Covariance Matrix:  $I(\hat{\beta})^{-1}$

|              | $\beta_0$ | $\beta_1$              | $\beta_2$              | $\beta_{12}$            |
|--------------|-----------|------------------------|------------------------|-------------------------|
| $\beta_0$    | 10.1206   | -.00244                | -.03022                | $-8.410 \times 10^{-7}$ |
| $\beta_1$    |           | $5.951 \times 10^{-7}$ | $7.296 \times 10^{-6}$ | $1.651 \times 10^{-10}$ |
| $\beta_2$    |           |                        | $9.190 \times 10^{-5}$ | $1.427 \times 10^{-9}$  |
| $\beta_{12}$ |           |                        |                        | $2.773 \times 10^{-12}$ |

---

Overall Goodness of Fit test (3.5.5)

$$\chi^2 = 30.9093 \quad E(\chi^2 | \hat{\beta}) = 22.87485 \quad V(\chi^2 | \hat{\beta}) = 622.1356 \quad \text{p-value} = .3737$$

Intercept Only Tests (3 degrees of freedom)

Score Test statistic = 108.702      p-value = .0001

Likelihood Test statistic = 178.151      p-value = .0001

---

is particularly interesting. Since the p-value associated with the Wald test applied to this single parameter is .0422 it can be concluded that  $\beta_{12} \neq 0$ . This analysis will be referred to and elaborated on throughout the remaining chapters of this dissertation.

Throughout the next several chapters the logistic modeling technique and the results described in this chapter will also be applied to studies involving an arbitrary number of agents. The interpretation of the parameters in the fitted model in the context of this type of study will be considered in detail.

## Chapter 4

# Additivity, Deviations from Additivity, and Isobolograms

### 4.1 Introduction

In the last chapter the logistic modeling technique was described. This model will later be used to study the dose response relationship between two or more agents. Specifically in the next chapter, it will be shown that properties of the model may be used to describe how the agents interact. Before these properties can be derived, however, it is necessary to first formally define the types of interactions that can be observed. In general the approach that has been adopted for this dissertation has been described by Berenbaum (e.g. 1981 and 1989). Assuming the dose-response relationship for each agent is known, a set of basic definitions is given that can be used to characterize the single agent dose-response relationships. Definitions and properties associated with the combination of two agents are then considered. The use of an isobologram is also described. These results are then generalized to combinations of any number of agents.

The definitions and derivations presented in this chapter are a synthesis of materials found in the following sources: Loewe (1953), Berenbaum (1977, 1978, 1981, 1985, 1989), Hewlett and Plackett (1979), Tallarida (1979), Wessinger (1986), Brunden (1988), and Calabrese (1991). However, as described in Chapter 1, the literature has not been consistent in its use of terminology. When inconsistencies were found, the approach taken here was to choose the most commonly used version, or, alternatively, the approach used by Berenbaum.



## 4.2 Types of Dose-Response Relationships

Initially, assume that all single agent dose-response curves are monotone. Non-monotone dose-response curves will be considered in Section 4.4 . Furthermore, assume that the background response, at zero doses of all of the agents, is a constant. Let  $\pi$  denote a fixed response,  $X$  the dose of an agent, and  $P(X)$  the dose-response curve.

Examples of single agent dose-response curves defined in this section are illustrated in Figure 4.1. Combinations of two agents are shown in Figure 4.2. In each of the plots the dose levels are plotted on the X-axis and the response is plotted in the Y-axis. For two agent combinations the dose-response curves for both agents are simultaneously plotted in the same set of axes. Note that while sigmodal curves are illustrated, the definitions are generalizable to any continuous dose-response curve.

The following definitions describe the dose-response curve of each agent alone relative to the background rate.

- Definition 4.2.1:**
- i) If the dose-response curve is constant for all dose levels, the agent is inert.
  - ii) An agent is active if the dose-response curve is nonconstant over the dose levels considered.

It follows that the dose-response curve for an inert agent is simply a horizontal line through the background response.

The dose-response curve associated with a single agent can also be described relative to  $\pi$ , a fixed response of interest.

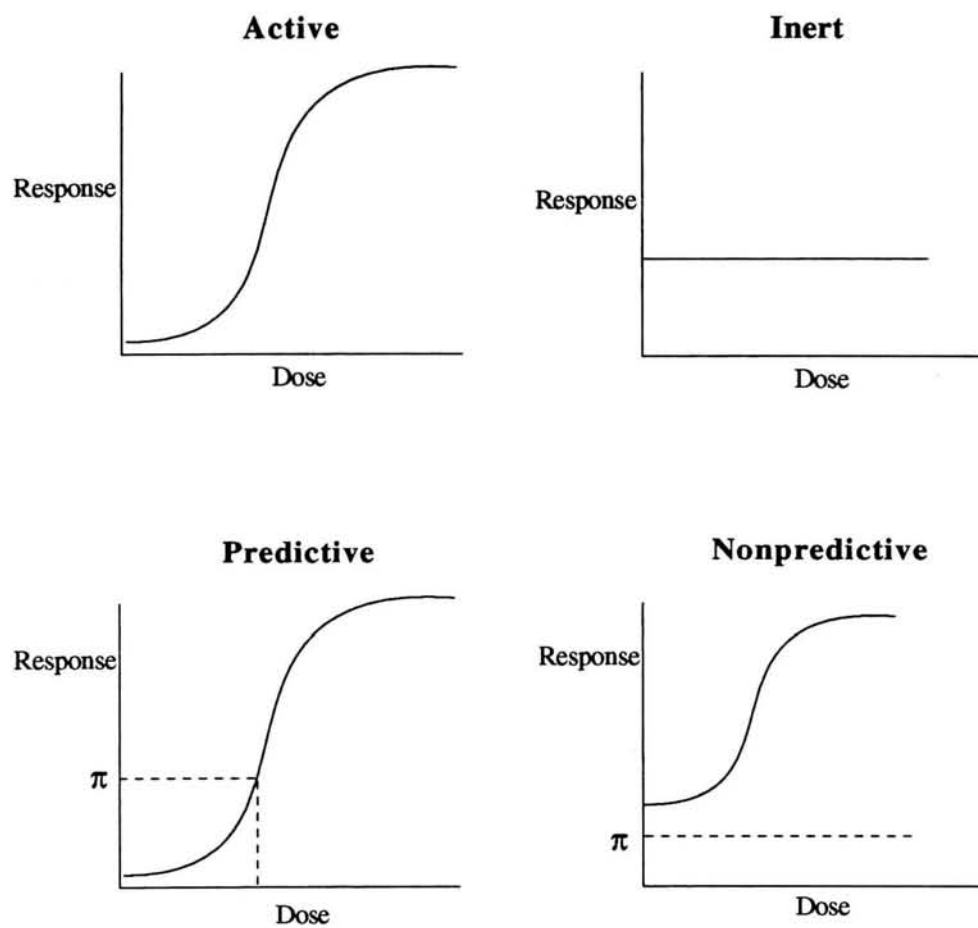


**Figure 4.1:** Single Agent Dose-Response Curves

**Definition 4.2.2:** Let  $\pi$  be a fixed level of response.

- i) If a finite, nonzero dose of the agent exists which yields  $\pi$ , the agent is predictive.
- ii) If no dose of the agent yields the response  $\pi$  the agent is nonpredictive.

In general an inert agent is nonpredictive.

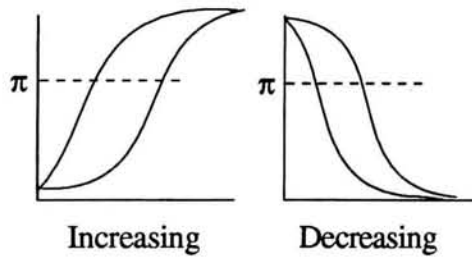
Certain useful definitions can also be made about the combination of two agents.

- Definition 4.2.3:**
- i) Two active, predictive agents form a homergic combination.
  - ii) A heterergic combination involves a predictive agent and nonpredictive agent.
  - iii) Two nonpredictive agents form a coalitive combination.

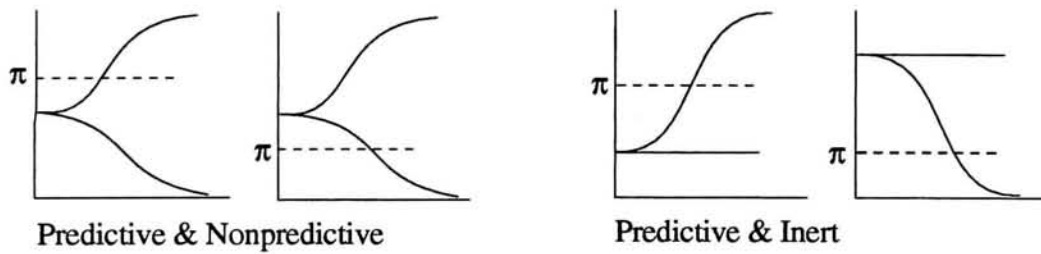
Certain properties of these combinations can be noted by examining Figure 4.2. Heterergic combinations can include the combination of a predictive and nonpredictive agent or the combination of a predictive and an inert agent. Coalitive combinations include the combinations of two nonpredictive agents, a nonpredictive agent and an inert agent, and two inert agents. Consider now a homergic combination such that the dose-response curves associated with both agents are monotone. Since the background response is constant it follows that the dose-response curves for both agents must be monotonically increasing or both must be monotonically decreasing.

Definitions will now be given that describe the type of interactions that can be observed when agents are given in combination.

### Homergic Two Agent Combinations



### Heterergic Two Agent Combinations



### Coalitive Two Agent Combinations

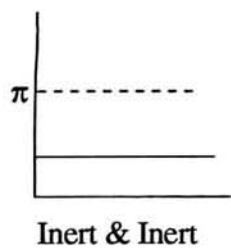
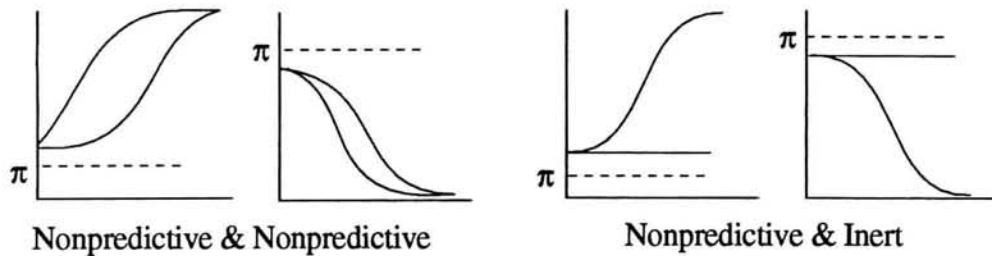


**Figure 4.2:** Types of Two Agent Combinations

### 4.3 Types of Interactions

First, a general definition which characterizes the types of interactions between two agents is given. This definition forms the basis for the derivation of more specific definitions and results. Let  $X_1$  and  $X_2$  denote the continuous doses of the two agents considered. Further, let  $(x_1, x_2)$  denote an observed dose combination of the two agents, and  $\pi$  the associated observed response.

**Definition 4.3.1:** Assume a dose combination is administered and the response observed. Additivity implies the observed response is identical to the expected response .

**Definition 4.3.2:** Assume a dose combination is administered and the response,  $\pi$ , observed. Assume all dose-response curves are monotonically increasing or all are monotonically decreasing. Let  $\pi^A$  denote the response expected under additivity. The type of interaction between the agents is given by

|   |               |               |
|---|---------------|---------------|
| Single Agent<br>Dose-Response<br>Curves | $\pi > \pi^A$ | $\pi < \pi^A$ |
| Increasing                              | Synergism     | Antagonism    |
| Decreasing                              | Antagonism    | Synergism     |

Note that Definition 4.3.2 is dependent on the determination of  $\pi^A$ , an expected or additive response. In order to derive this expected response under additivity it will be useful to first consider homergic combinations. These results are then generalized to the other combinations.

### 4.3.1 Homergic Combinations

Assuming the dose-response curves for each single agent is known, two strategies are derived for characterizing the types of interactions in a homergic combination of agents. To begin, an expression is derived which holds when the agents interact in an additive manner. Note that while these derivations are dependent on knowing each single agent's dose-response curve, they are not dependent on a specific form for any of these curves.

A general formulation for describing additivity at a fixed response can be derived by considering a "sham" combination of two agents that clearly will not interact, i.e. a combination of an agent with a dilution of itself. The goal is to determine dose combinations of these two agents that yield a fixed response, say  $\pi = 0.50$ . Suppose 10 mg of agent A yields a 50% response. Let agent B be a 40% dilution of agent A so that a dose of 25 mg of B will also yield the 50% response. Because these agents do not interact, a dose combination of 5 mg of A and 12.5 mg of B will also yield the response of interest. Note that the sum of the ratios of these doses equals 1, i.e.  $\frac{5}{10} + \frac{12.5}{25} = 1$ . If  $(x_1, x_2)$  denotes any dose combination of A and B that yields a response of 50% then  $\frac{x_1}{10} + \frac{x_2}{25} = 1$ .

This idea can now be generalized as follows.

**Result 4.3.1:** Let  $\pi$  denote the response observed at the dose combination  $(x_1, x_2)$ . Let  $ED_i(\pi)$ ,  $i=1,2$  denote the effective dose of each agent alone that yields  $\pi$ .

At the dose combination considered the interaction between the two agents is additive if  $\frac{x_1}{ED_1(\pi)} + \frac{x_2}{ED_2(\pi)} = 1$ .

Implicit in this derivation is the ability to determine the effective dose of each agent alone, i.e., the dose of each agent that yields the fixed response of interest. Since the single agent dose-response curves are monotone, unique values for these effective doses can be determined. For example, assume for illustrative purposes that each single agent's dose response curve is given by

$$P(X_i; \beta_0, \beta_i) = \frac{1}{1 + \exp[-(\beta_0 + \beta_i X_i)]}, \quad i = 1, 2. \quad (4.3.1)$$

Then, for a fixed value of the response,  $\pi$ , the effective doses are

$$ED_i(X_i) = \frac{\text{logit}(\pi) - \beta_0}{\beta_i}, \quad i = 1, 2.$$

If  $x_1$  and  $x_2$  were allowed to vary in the additive equation given in Result 4.3.1, an equation of a straight line is defined.

**Definition 4.3.3:** Let  $\pi$  denote a fixed response and  $ED_i(\pi)$ ,  $i=1,2$  the effective dose of the  $i$ th agent alone that yields  $\pi$ . The line of additivity is given by

$$\left\{ (x_1, x_2) : \frac{x_1}{ED_1(\pi)} + \frac{x_2}{ED_2(\pi)} = 1; \quad x_1, x_2 \geq 0 \right\}.$$

The additive equation given in Result 4.3.1 can also be used at a fixed dose combination  $(x_1, x_2)$  to determine the response expected under additivity.

**Definition 4.3.4:** Let  $(x_1, x_2)$  be a homergic dose combination. The expected response under additivity,  $\pi^A$ , is given by

$$\left\{ \pi^A : \frac{x_1}{ED_1(\pi^A)} + \frac{x_2}{ED_2(\pi^A)} = 1; 0 \leq \pi^A \leq 1 \right\}.$$

For example, assuming the dose-response curves for each agent are given by (4.3.1), the expected response under additivity is given by

$$\frac{\beta_1 x_1}{\text{logit}(\pi^A) - \beta_0} + \frac{\beta_2 x_2}{\text{logit}(\pi^A) - \beta_0} = 1$$

or

$$\pi^A = \frac{1}{1 + \exp[-(\beta_0 + \beta_1 x_1 + \beta_2 x_2)]}.$$

Assume now that  $\pi^A$  is specified. Based on Definition 4.3.2, by comparing  $\pi^A$  to the observed response  $\pi$ , the type of interaction between the agents at  $(x_1, x_2)$  can be characterized. This approach will be referred to as the Comparison Method of characterizing interaction and is summarized in Table 4.1. For example, assuming the single agent dose-response curves are increasing, if  $\pi > \pi^A$  then the agents are interacting synergistically at  $(x_1, x_2)$ .

Another technique for characterizing the interactions between two agents can also be derived after first noting the following property.



**Table 4.1**

Comparison Method Applied to Homergic Combinations

Types of Interactions Detected by Comparing the  
Expected Response Under Additivity ( $\pi^A$ ) to the Observed Response ( $\pi$ )

|               | Single Agent Dose-Response Curves |            |
|---------------|-----------------------------------|------------|
|               | Increasing                        | Decreasing |
| $\pi = \pi^A$ | Additivity                        | Additivity |
| $\pi > \pi^A$ | Synergism                         | Antagonism |
| $\pi < \pi^A$ | Antagonism                        | Synergism  |

**Result 4.3.2:** Assume both single agent dose-response curves are monotone. Let  $\pi^A$  denote the response expected under additivity and  $\pi$  the observed response. Furthermore, let  $ED_i(\pi)$  and  $ED_i(\pi^A)$  denote the effective doses of the  $i$ th agent associated with each response,  $i = 1, 2$ . Then

| Type of Interaction |                                  |
|---------------------|----------------------------------|
| Synergism           | $ED_i(\pi) > ED_i(\pi^A), i=1,2$ |
| Antagonism          | $ED_i(\pi) < ED_i(\pi^A), i=1,2$ |

**Proof:**

Assume monotonically increasing dose-response curves. If the agents interact synergistically, by Definition 4.3.2,  $\pi > \pi^A$ . Since each dose-response curve is monotonically increasing it follows  $ED_i(\pi) > ED_i(\pi^A), i = 1, 2$ . If the agents interact antagonistically, by Definition 4.3.2,  $\pi < \pi^A$ . Since each dose-response curve is monotonically increasing it follows  $ED_i(\pi) < ED_i(\pi^A), i = 1, 2$ .

The proof for monotonically decreasing dose-response curves is similar.

Assume now, at a given dose combination  $(x_1, x_2)$ , with observed response  $\pi$ , a synergism is observed. Therefore, by Result 4.3.2,  $ED_i(\pi) > ED_i(\pi^A) > 0, i=1,2$ . Now since, by Definition 4.3.4,  $\frac{x_1}{ED_1(\pi^A)} + \frac{x_2}{ED_2(\pi^A)} = 1$ , it follows that

$$\frac{x_1}{ED_1(\pi)} + \frac{x_2}{ED_2(\pi)} < 1. \text{ Similarly when an antagonism is observed,}$$

$$ED_i(\pi^A) > ED_i(\pi) > 0, i = 1, 2 \text{ and } \frac{x_1}{ED_1(\pi)} + \frac{x_2}{ED_2(\pi)} > 1.$$

These results can be summarized as follows.

**Definition 4.3.5:** Let  $(x_1, x_2)$  denote a dose combination and  $\pi$  the observed response.

$$\text{The Interaction Index is given by } II(x_1, x_2, \pi) = \frac{x_1}{ED_1(\pi)} + \frac{x_2}{ED_2(\pi)}.$$

**Result 4.3.3:** Let  $(x_1, x_2)$  denote the dose combination of two homergic agents and  $\pi$  the observed response. The type of interaction between the agents at this dose combination is characterized by

$$\begin{aligned} < 1 &\Rightarrow \text{synergism} \\ II(x_1, x_2, \pi) = 1 &\Rightarrow \text{additivity} . \\ > 1 &\Rightarrow \text{antagonism} \end{aligned}$$

For homergic combinations it has been shown that, given the dose-response curves for each single agent, two approaches can be taken to describe the interaction between the agents at a given dose combination. The first approach, the Comparison Method, is based on determining the expected response under additivity and then comparing it to the observed response. This method, summarized in Table 4.1, requires calculation of the expected response under additivity. The second approach is based on the Interaction Index. This technique, based on Result 4.3.3, does not require the expected response under additivity. Rather, the effective doses of each agent alone are used.

### 4.3.2 Heterergic Combinations: Predictive & Inert

Both the Comparison Method and the Interaction Index can be applied to these combinations. In order to apply the Comparison Method the expected response under additivity,  $\pi^A$ , must be derived. Let  $x_1$  denote a dose of the predictive agent and  $x_2$  a dose of the inert agent. Assume that at the combination  $(x_1, x_2)$  the response  $\pi$  was observed. Since the inert agent alone has no effect on the response, the expected response under additivity is determined from the dose response curve of the active agent only. Hence  $\pi^A$

is equal to the response predicted at a dose of  $x_1$  alone. By then comparing  $\pi$  to  $\pi^A$  the type of interaction can be determined based on Definition 4.3.1.

In order to apply the Interaction Index technique it can be noted that since  $\pi^A$  is equal to the response at the dose of  $x_1$  alone,  $ED_1(\pi^A) = x_1$  or  $\frac{x_1}{ED_1(\pi^A)} = 1$ . Now if the two agents interact in an additive manner, the response will equal the additive response, i.e.  $\pi^A = \pi$ , so that  $\frac{x_1}{ED_1(\pi)} = 1$ . If a synergism is observed, by Result 4.3.2,  $ED_1(\pi) > ED_1(\pi^A)$ . Therefore  $\frac{x_1}{ED_1(\pi)} < 1$ . In a similar way it can be shown that if an antagonism is observed  $\frac{x_1}{ED_1(\pi)} > 1$ .

Note now that if it is assumed that the effective dose for the inert agent is infinite then  $\frac{x_1}{E_1(\pi)} = \frac{x_1}{E_1(\pi)} + \frac{x_2}{\infty} = \frac{x_1}{E_1(\pi)} + \frac{x_2}{E_2(\pi)} = II(x_1, x_2, \pi)$ . Therefore Result 4.3.3 can be generalized as follows.

**Result 4.3.4:** Let  $(x_1, x_2)$  denote a homergic combination or a heterergic combination of a predictive and inert agent where the effective dose of the inert agent is infinite. Let  $\pi$  be the observed response and  $II(x_1, x_2, \pi)$  denote the interaction at this combination and response. The type of interaction between the agents is given by

$$\begin{aligned} < 1 &\Rightarrow \text{synergism} \\ II(x_1, x_2, \pi) &= 1 \Rightarrow \text{additivity} . \\ > 1 &\Rightarrow \text{antagonism} \end{aligned}$$

While it has been shown that the two methods described for homergic combinations for characterizing interactions can be applied to heterergic combinations of predictive and inert agents neither method can be applied for the following combination.

### 4.3.3 Heterergic Combinations: Predictive & Nonpredictive

To apply the Interaction Index method of characterizing interactions the effective doses of each agent must be determined. Note that for a nonpredictive agent no dose exists that yields the fixed response of interest. Furthermore, since the agent is active the response as the dose of this agent approaches infinity is known. Therefore, it can not be assumed, as for an inert agent, that the effective dose is infinite. The effective dose for the active, nonpredictive agent is, therefore, undefined and the Interaction Index can not be applied to these combinations.

In addition, the Comparison Method of characterizing interactions can not be applied for this combination. Recall that the expected response under additivity can sometimes be determined at a fixed dose combination  $(x_1, x_2)$  by solving for  $\pi^A$  in  $\frac{x_1}{ED_1(\pi^A)} + \frac{x_2}{ED_2(\pi^A)} = 1$ . In this type of combination, however, there is no common value of the response that simultaneously satisfies both dose-response curves (see Figure 4.2). Since  $\pi^A$  can not be determined the Comparison Method is not applicable.

Note also that, since the nonpredictive agent is active, it may not be reasonable to assume that the nonpredictive agent does not have an effect on the response, even under the assumption of additivity. This implies that the argument used to derive  $\pi^A$  for the heterergic combination of a predictive agent and an inert agent can not be applied in this case.

Therefore, since neither of the approaches previously developed to characterize interactions can be applied without further assumptions, this combination will not be considered further in this dissertation.

#### 4.3.4 Coalitive Combinations

For coalitive combinations the effective doses for a fixed value of  $\pi$  are undefined or infinite for both agents. It therefore follows that the Interaction Index is undefined for these combinations. The Comparison Method, however, can be applied to all types of coalitive combinations.

Consider first the combination of two inert agents. Since both agents alone are inert,  $\pi^A$  is simply the constant background response at 0 levels of both agents. When  $\pi$  differs from the background response an interaction has been detected. Since neither agent is active, however, the interaction can not be classified as synergistic or antagonistic based on Definition 4.3.2.

Consider now the combination of two active but nonpredictive agents. Now based on  $\frac{x_1}{ED_1(\pi^A)} + \frac{x_2}{ED_2(\pi^A)} = 1$ ,  $\pi^A$ , the response expected under additivity can be determined. The type of interaction between the agents can then be described, based on Definition 4.3.2, by comparing  $\pi$  to  $\pi^A$ .

Lastly the combination of a nonpredictive agent and an inert agent can be considered. Here  $\pi^A$  is determined solely from the dose-response curve for the nonpredictive but active agent. Again, the type of interaction between the agents can then be determined by comparing  $\pi$  to  $\pi^A$ .

#### 4.3.5 Summary

Two approaches were described in this section for characterizing interactions at a given dose combination. Both methods assume each single agent dose-response curve is known. For the Comparison Method, an expected response based on additivity,  $\pi^A$ , is determined using  $\frac{x_1}{ED_1(\pi^A)} + \frac{x_2}{ED_2(\pi^A)} = 1$ . Based on Definition 4.3.1 by comparing  $\pi^A$  to  $\pi$  the type of interaction can then be described. This approach was shown to be

applicable to all types combinations with the exception of the predictive and nonpredictive heterergic combination. The second approach is based on the use of the Interaction Index. By determining the effective doses of each agent alone and then comparing the value of  $II(x_1, x_2, \pi) = \frac{x_1}{ED_1(\pi)} + \frac{x_2}{ED_2(\pi)}$  to 1 the type of interaction between the agents can be determined. This approach was shown to be applicable only to homergic and heterergic combinations of predictive and inert agents.

In the next section non-monotone single agent dose-response curves will be considered.

#### 4.4 Non-monotonic Single Agent Dose-Response Curves

Throughout the last section it was assumed that the dose-response curve for each agent alone was monotone. In general, this assumption is necessary to insure that  $ED_i(\pi)$ ,  $i=1,2$ , can be uniquely determined for a given value of  $\pi$ . Virtually all of the definitions and results of Section 4.3 were dependent on these values. For example, based on Result 4.3.3, an interaction is characterized by examining the value of the Interaction Index. If one or both of the effective doses,  $ED_i(\pi)$ ,  $i=1,2$ , are not uniquely determined, the resulting value of the Interaction Index, and hence the type of interaction at a given dose combination, may vary. Alternatively, the Comparison Method of describing interactions is dependent on the determination of the response expected under additivity based on  $\frac{x_1}{ED_1(\pi^A)} + \frac{x_2}{ED_2(\pi^A)} = 1$ . Again if one or more of  $ED_i(\pi^A)$ ,  $i=1,2$ , are not unique the value of this additive response, and hence the type of interaction at a given dose combination may vary.

Since it is not possible, without further assumptions, to apply the definitions and results given in Section 4.3 to studies that include agents with non-monotone dose-

response curves, only monotone single agent dose-response curves will be considered for the remainder of this dissertation.

#### 4.5 Isobolograms

For a two agent study the dose-response relationship is 3-dimensional. A 2-dimensional tool that has been shown to be useful in characterizing interactions graphically is the isobologram. An isobologram is a plot of the isobol or set of dose combinations that yield a fixed response of interest. When applicable these plots also include the line of additivity.

Consider first a homergic combination of agents. The line of additivity for a homergic combination was given in Definition 4.3.3 as

$\left\{ (x_1, x_2) : \frac{x_1}{ED_1(\pi)} + \frac{x_2}{ED_2(\pi)} = 1; \quad x_1, x_2 \geq 0 \right\}$ . This line intersects each axis at the

corresponding effective dose for each agent alone. Each point on the line represents a dose combination that satisfies the assumption of additivity at the fixed response of interest.

In general the line of additivity divides the  $X_1 \times X_2$  plane into two regions. A point  $(x_1, x_2)$  that lies below the line satisfies  $\frac{x_1}{ED_1(\pi)} + \frac{x_2}{ED_2(\pi)} < 1$  and a point that lies above the line satisfies  $\frac{x_1}{ED_1(\pi)} + \frac{x_2}{ED_2(\pi)} > 1$ . Therefore based on Result 4.3.4 if the point

associated with a dose combination lies below the line of additivity a synergism is indicated. A point that lies above the line of additivity indicates an antagonism. This is illustrated in Figure 4.3. By plotting the dose combinations that yield a fixed response of interest in conjunction with the line of additivity the types of interactions between the agents at those dose combinations can be graphically assessed.

Consider now a heterergic combination of a predictive agent and inert agent.

Assume  $X_2$  denotes the dose associated with the inert agent and  $\pi$  is the fixed response of



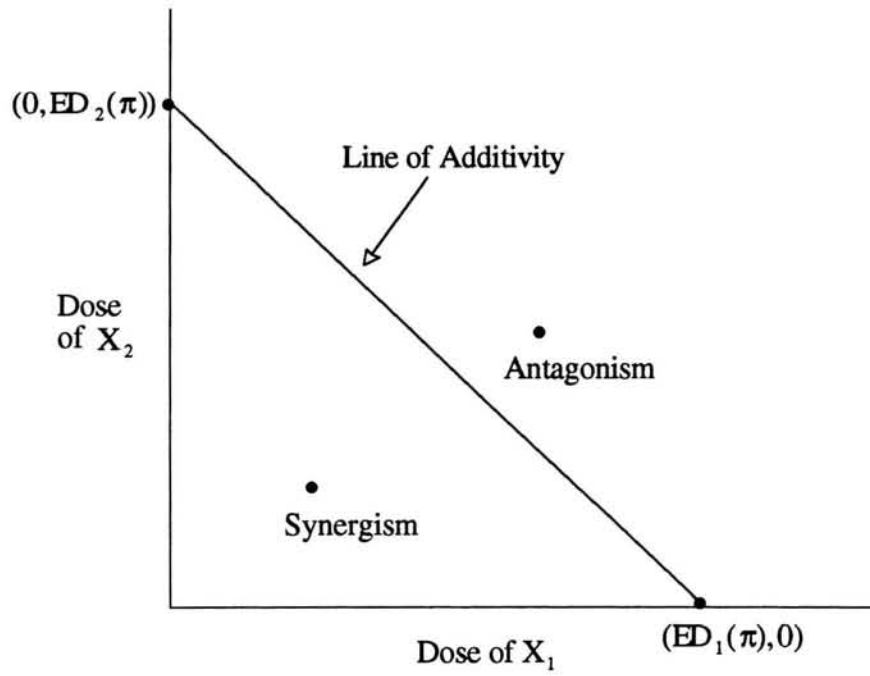


**Figure 4.3:** Isobologram for a Two Agent Study

interest. Recall that for the inert agent  $ED_2(\pi) = \infty$ . The line of additivity in this case is therefore the vertical straight line through  $(ED_1(\pi), 0)$ . Based on Result 4.3.4, a synergism at this dose combination implies  $\frac{x_1}{ED_1(\pi)} < 1$  or equivalently  $x_1 < ED_1(\pi)$ .

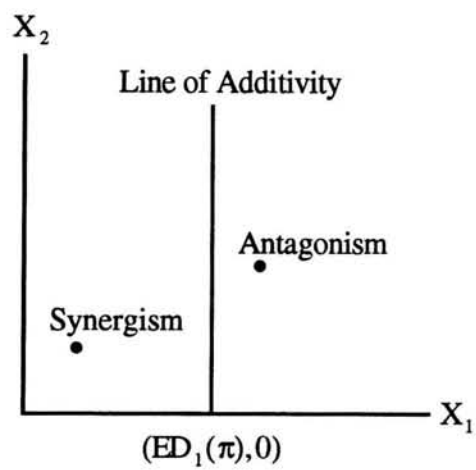
Similarly, an antagonism implies  $x_1 > ED_1(\pi)$ . Hence, if the point associated with the dose combination lies to the left of the line of additivity, a synergism is found. If the point is to the right of the line of additivity, an antagonism is found. A similar derivation can be made for this type of combination when  $X_1$  denotes the inert agent. Here the synergistic and antagonistic points will lie above or below respectively the line of additivity. (See Figure 4.4).

Recall now for coalitive combinations the effective doses for both agents are undefined. This implies the line of additivity does not exist. Therefore, while plots of the observed dose combinations that yield a fixed response may be useful, an isobologram can not be used to graphically characterize interactions for these combinations.

For isobolograms that include the line of additivity the magnitude of the deviations from additivity can be described using the potentiation coefficient (Gessner and Cabana, 1970).

**Definition 4.5.1:** Consider a vector that intersects the origin and the point associated with the dose combination  $(x_1, x_2)$ . Let R be the point of intersection of the vector with  $(x_1, x_2)$  and S be the point of intersection of the vector with the line of additivity. In addition, let RS denote the distance from R to S and OS the distance from the origin to S. The potentiation coefficient is given by  $PC(\pi, x_1, x_2) = \frac{RS}{OS}$ .

**$X_1$  Predictive &  $X_2$  Inert**



**$X_2$  Predictive &  $X_1$  Inert**

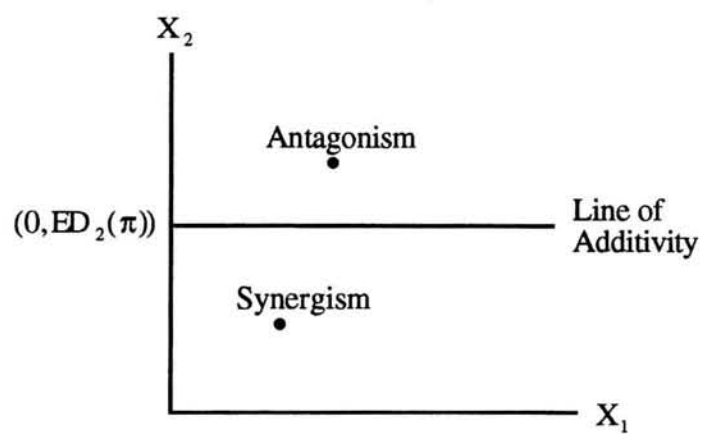


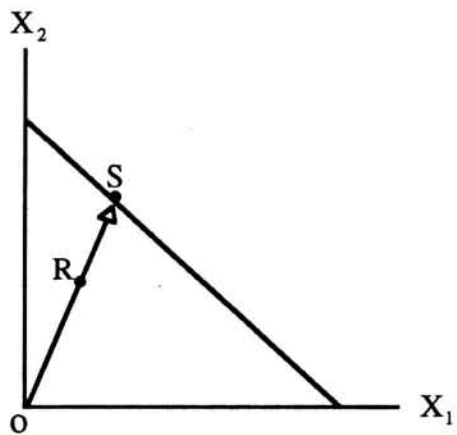
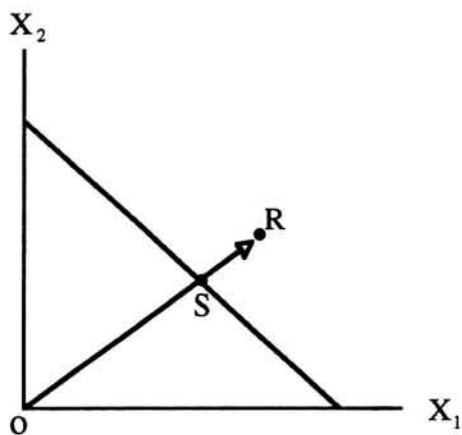
**Figure 4.4:** Isobolograms for the Heterergic Combination of a Predictive Agent and an Inert Agent

By examining Figure 4.5 it is clear that synergism implies  $RS > 0$  and  $OS > 0$  so that  $PC(\pi, x_1, x_2) > 0$ . In contrast, for antagonism,  $RS < 0$  so that  $PC(\pi, x_1, x_2) < 0$ . Assume now two dose combinations  $(x_{11}, x_{21})$  and  $(x_{12}, x_{22})$  are found that yield  $\pi$ , the fixed response of interest. The values of  $PC(\pi, x_{11}, x_{21})$  and  $PC(\pi, x_{12}, x_{22})$  can be used to describe the relative magnitudes of the interactions, i.e. if  $0 < PC(\pi, x_{11}, x_{21}) < PC(\pi, x_{12}, x_{22})$  a larger degree of synergism is evident at  $(x_{12}, x_{22})$  than at  $(x_{11}, x_{21})$ .

The joint action ratio described by Hewlett (1969) is closely related to the potentiation coefficient. Referring to Figure 4.5, the joint action ratio is defined to be  $JA(\pi, x_1, x_2) = \frac{OS}{OR}$  and will be less than 1, equal to 1 or greater than 1 if antagonism, additivity or synergism respectively is indicated.

Using the vector that intersects the dose combination,  $(x_1, x_2)$ , and the line of additivity another property of synergism and antagonism can be derived. Note, first, that dose-combinations along this vector satisfy  $x_2 = \alpha x_1$  where  $\alpha > 0$ . In addition, the total of the doses at this combination is given by  $x_1 + x_2 = (\alpha + 1)x_1 = t$ . Let  $(z_1, z_2)$  denote the point of intersection of the vector and the line of additivity. Clearly  $z_2 = \alpha z_1$  and the total of these doses is  $z_1 + z_2 = (\alpha + 1)z_1 = t^A$ . By now inspecting Figure 4.6, it follows that under synergism  $x_1 < z_1$  which implies  $t < t^A$ . This implies the total dose at the combination considered is less than the total dose under additivity. Hence less of the agents in combination are needed to yield the fixed response of interest under synergism than expected under additivity. In a similar way it can be argued that when an antagonism is observed more of the agents in combination are needed to yield the fixed response than expected under additivity.

Before generalizing the definitions and results discussed in the last two sections to studies of more than two agents it will be useful to first examine alternative definitions of additivity.

**Synergism****Antagonism**

**Figure 4.5:** The Use of the Potentiation Coefficient

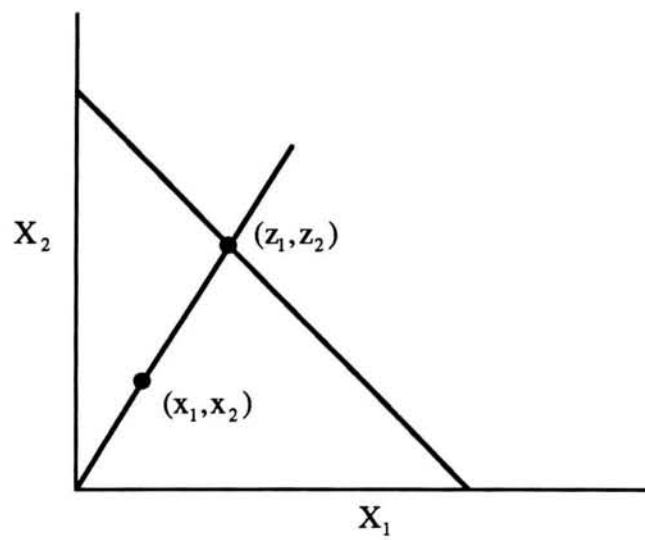


**Figure 4.6:** Comparison of Total of Doses at  $(x_1, x_2)$  and  $(z_1, z_2)$

#### 4.6 Alternative Definitions of Additivity

In this section alternative definitions for additivity will be briefly described. It will be shown that under certain constraints these definitions are equivalent to the definitions of additivity previously assumed. In general, however, these definitions will be shown to be problematic.

In this chapter the overall approach to characterizing interactions has been to, first, define the response expected under additivity, and then compare the observed response to this additive response. No assumptions were made about the mechanism of action of the agents considered. In addition, while the results were dependent on knowing the dose-response curves for each agent, the particular form for these curves was not specified.

Virtually all of the results developed in this chapter were dependent on the notation that an additive interaction at the dose combination  $(x_1, x_2)$  with response  $\pi$  satisfies

$$\frac{x_1}{ED_1(\pi)} + \frac{x_2}{ED_2(\pi)} = 1. \quad (4.6.1)$$

Recall that this expression was derived by determining dose levels of two additive agents that in combination yield  $\pi$ , a fixed response of interest. Because the process involves combining doses to yield a specified effect, this technique for describing additivity has been referred to as dose-addition. Since it was shown that this definition holds for the sham combination of an agent with a dilution of itself, it has an intuitive basis.

Let  $P_i(x_i)$ ,  $i=1,2$  denote the response at dose  $x_i$  of each agent alone and  $P(x_1, x_2)$  the response at the combination. The first alternative definition of additivity is referred to as effect-addition. Here the response expected under additivity is given by

$$P(x_1, x_2) = P_1(x_1) + P_2(x_2). \quad (4.6.2)$$

When the response is bounded, as is the case with proportions or probabilities, this definition can result in nonsensical results. For example, if the response is a probability and  $P_1(x_1) = 0.6$  and  $P_2(x_2) = 0.7$  the response expected under additivity would be 1.3.

Berenbaum (1989) showed however, that for studies with linear dose-response curves in the region of interest, i.e.  $P_i(X_i) = \alpha_i X_i$ , that (4.6.2) and (4.6.1) are in agreement. In fact, it can be shown that effect-addition holds for a broader set of single agent dose-response curves. Suppose that a transformation of the response can be found so that  $\eta_i(X_i) = g[p_i(X_i)] = \alpha_i X_i$ ,  $i=1,2$  where  $g^{-1}$  exists. An example of the type of transformation is given by  $g[p_i(X_i)] = \log\left(\frac{p_i(X_i)}{1-p_i(X_i)}\right) - \beta_0 = \text{logit}(p_i(X_i)) - \beta_0$ . Let  $\eta(X_1, X_2)$  denote the transformed response observed when the agents are given in combination. In terms of this transformed effect, effect-addition may be written as

$$\eta(X_1, X_2) = \eta_1(X_1) + \eta_2(X_2). \quad (4.6.3)$$

Under these constraints effect-addition and (4.6.1) are in agreement. For example, by

(4.6.3)  $\eta(X_1, X_2) = \alpha_1 X_1 + \alpha_2 X_2$ . Alternatively, based on (4.6.1)

$$\frac{X_1}{\eta(X_1, X_2)/\alpha_1} + \frac{X_2}{\eta(X_1, X_2)/\alpha_2} = 1, \text{ which simplifies to } \eta(X_1, X_2) = \alpha_1 X_1 + \alpha_2 X_2. \text{ From a}$$

statistical perspective this result is appealing since, under the assumption of no interaction between the agents, the transformed response can be written as the sum of the effects of each agent, a form commonly assumed in statistical modeling.

Another definition for additivity based on the probability notation of independence is referred to as multiplication of effects. Here



$$P(X_1, X_2) = P_1(X_1) + P_2(X_2) - P_1(X_1)P_2(X_2). \quad (4.6.4)$$

where  $0 \leq P_i(X) \leq 1$ ,  $i = 1, 2$ . An alternative form for this expression can also be derived by letting  $Q_i(X_i) = 1 - P_i(X_i)$ ,  $i=1, 2$  and  $Q(X_1, X_2) = 1 - P(X_1, X_2)$ . This implies (4.6.4) can be rewritten as

$$\begin{aligned} Q(X_1, X_2) &= 1 - P(X_1, X_2) = 1 - P_1(X_1) - P_2(X_2) + P_1(X_1)P_2(X_2) \\ &= 1 - (1 - Q_1(X_1)) - (1 - Q_2(X_2)) + (1 - Q_1(X_1))(1 - Q_2(X_2)) \\ &= Q_1(X_1)Q_2(X_2). \end{aligned} \quad (4.6.5)$$

It can be shown that, in general, this definition of additivity fails for the sham combination. For example, consider, the combination of an agent with itself such that  $P(d) = 0.4$  and  $P(2d) = 0.9$ . Based on (4.6.4) the predicted dose of combination consisting of  $d + d$  is given by  $.4 + .4 - (.4)^2 = .64$ . Since this does not equal  $P(2d) = .9$  this multiplication of effects approach to defining additivity does not hold for this sham combination.

Berenbaum (1989) showed, however, that when both single agent dose response curves are in the form  $Q_i(X_i) = e^{-\alpha_i X_i}$ ,  $i=1, 2$  multiplication of effects and dose-addition are equivalent. For example, by (4.6.5) it follows that  $Q(X_1, X_2) = e^{-\alpha_1 X_1 - \alpha_2 X_2}$ . Alternatively by (4.6.1)  $\frac{X_1}{-\ln[1 - Q(X_1, X_2)]/\alpha_1} + \frac{X_2}{-\ln[1 - Q(X_1, X_2)]/\alpha_2} = 1$  which can be simplified to

$$Q(X_1, X_2) = e^{-\alpha_1 X_1 - \alpha_2 X_2}.$$

Other methods that have been introduced to define additivity include the modeling technique described by Chou and Talalay (1991). Here the model for each agent is given by

$$\frac{P_i(X_i)}{1 - P_i(X_i)} = \left( \frac{X_i}{ED_i(0.5)} \right)^{m_i} \quad (4.6.6)$$

where  $0 \leq P_i(X) \leq 1$ ,  $i = 1, 2$ . Equation (4.6.6) is referred to as the median-effect equation.

Since (4.6.6) can be rewritten as  $\logit(P_i(X_i)) = m_i \log_e(X_i) - m_i \log_e(ED_i(0.5))$  a transformation of the response can be written as a linear function of the log of the dose.

This is in contrast to the logistic dose-response curve given in (4.3.1) where the transformed response, given by  $\logit(P_i(X_i)) = \beta_0 + \beta_i X_i$ , is a linear function of dose.

The expression for additivity that Chou and Talalay derived is given by

$$\frac{X_1}{ED_1(\pi)} + \frac{X_2}{ED_2(\pi)} + \alpha \frac{X_1 X_2}{ED_1(\pi) ED_2(\pi)} = 1 \quad (4.6.7)$$

where  $\alpha = 0$  or  $1$  depending on the mechanisms of action of each agent. If the agents are mutually exclusive, i.e. "they share the same binding sites and the occupation of one site by one agent excludes its occupation by another" (Berenbaum, 1989, p.109),  $\alpha = 0$ . For mutually non-exclusive agents which have different binding sites  $\alpha = 1$ . In contrast to (4.6.1) which is based solely on knowledge of each agent's dose-response curve this definition of additivity is dependent on knowledge of each agent's mechanism of action. Since this information may not be available for all of the agents studied this approach may be difficult to apply without further assumptions.

One last approach to examining additivity that will be described here involves the construction of an additivity envelope (Steel and Peckham, 1979). Here, based on the dose-response curves for both agents alone, the authors derive dose combinations that yield a fixed value of  $\pi$ . Two methods, Mode I and Mode II, are used to achieve this so that two sets of dose combinations were determined. Both methods assume first that a dose, say

$x_1$ , of the first agent is given and that based on the dose-response curve for this agent the response associated with that dose is  $\pi_1$ . For Mode I, the dose of the second agent is determined by  $ED_2(\pi - \pi_1)$ . For Mode II the dose of the second agent is given by  $ED_2(\pi) - ED_2(\pi_1)$ . In addition, based on dose-addition given in (4.6.1), the dose of the second agent that satisfies additivity is given by  $x_2 = ED_2(\pi) - \frac{ED_2(\pi)}{ED_1(\pi)} x_1$ . Since in general  $ED_2(\pi - \pi_1) \neq ED_2(\pi) - ED_2(\pi_1) \neq ED_2(\pi) - \frac{ED_2(\pi)}{ED_1(\pi)} x_1$  the calculated dose of the second agent can vary for all of these methods. Even for the sham combination of an agent with itself, i.e. where  $ED_2(\pi) = ED_1(\pi)$ , the dose of the second agent by Mode I,  $ED_2(\pi - \pi_1)$ , will still differ from the other methods. In addition, while it is also assumed the agents are given simultaneously and only examined sequentially in this context, the combinations determined by Mode I and Mode II methods may vary by the order that the agents were considered. It can be shown, however, that under the constraint that a transformation of the response can be found so that

$$\eta_i(x_i) = g[p_i(x_i)] = \alpha_i x_i, \quad i=1,2$$

where  $g^{-1}$  exists, then the dose combinations determined by Modes I and II as well as by dose-addition agree and that the order that the agents are considered does not effect the result.

Under certain conditions it has been shown that these alternative approaches to describing additivity are in agreement with the approach adopted for this dissertation given in (4.6.1). It has also been shown that problems are associated with each of these alternatives including the inability in some cases to describe the sham combination of an agent with itself. The approach adapted in this dissertation is free from assumptions concerning the form of the individual dose-response curves, does not depend on knowing

the mechanism of action of the agents, and adequately describes the additive sham combination. In the next section the definitions and results will be generalized to experiments that involve any number of agents.

#### **4.7 Additivity and Deviations from Additivity for Combinations of Any Number of Agents**

Certain definitions, given in Section 4.2, which classified two agent combinations can be generalized to studies of  $N$  agents as follows. As before each single agent dose-response curve is assumed to be monotone.

- Definition 4.7.1:** i)  $N$  active, predictive agents form an  $N$ -dimensional homergic combination.
- ii) An  $N$ -dimensional heterergic combination involves  $N_1 > 0$  predictive agents and  $N_2 > 0$  nonpredictive agents where  $N_1 + N_2 = N$ .
- iii)  $N$  nonpredictive agents form a  $N$ -dimensional coalitive combination.

In Section 4.3 general definitions of additivity, synergism and antagonism were given which did not depend on the number of agents studied. These can therefore be applied to combinations of  $N$  agents. All of the remaining definitions and results given in Section 4.3 are easily generalizable and are summarized as follows.

**Result 4.7.1:** Consider an  $N$ -dimensional homergic combination or an  $N$ -dimensional heterergic combination of predictive and inert agent. Let  $\pi$  denote the response observed at the dose combination  $(x_1, x_2, \dots, x_N)$ . Let  $ED_i(\pi)$ ,  $i=1,2,\dots,N$  denote the dose of the  $i$ th agent alone that yields the response  $\pi$ . Assume that the effective dose for each of the inert agents is infinite. The

interaction between the  $N$  agents at the dose combination considered is additive if  $\sum_{i=1}^N \frac{x_i}{ED_i(\pi)} = 1$ .

Based on this result an  $N$ -dimensional hyperplane of additivity can be defined.

**Definition 4.7.2:** Consider an  $N$ -dimensional homergic combination or an  $N$ -dimensional heterergic combination of predictive and inert agents. Let  $\pi$  denote the response observed at the dose combination  $(x_1, x_2, \dots, x_N)$ . Let  $ED_i(\pi)$ ,  $i=1,2,\dots,N$  denote the dose of the  $i$ th active agent alone that yields a response  $\pi$ . Assume that the effective dose for each of the inert agents is infinite. The hyperplane of additivity is given by

$$\left\{ (x_1, x_2, \dots, x_N) : \sum_{i=1}^N \frac{x_i}{ED_i(\pi)} = 1; \quad x_1, x_2, \dots, x_N \geq 0 \right\}.$$

The additive response can also be derived in this setting.

**Definition 4.7.3:** Let  $(x_1, x_2, \dots, x_N)$  be an  $N$ -dimensional homergic combination, or an  $N$ -dimensional heterergic combination of predictive and inert agents, or an  $N$ -dimensional coalitive combination. The additive response,  $\pi^A$ , is given by

$$\left\{ \pi^A : \sum_{i=1}^N \frac{x_i}{ED_i(\pi^A)} = 1; \quad \pi^A \geq 0 \right\}.$$

Hence  $\pi^A$  can be determined and then compared to  $\pi$ . By Definitions 4.3.1 and 4.3.2, the type of interaction between the agents at the dose combination considered can be determined. This implies the Comparison Method of characterizing interactions can be

generalized to N agent studies. In addition, the Interaction Index approach can be extended as follows.

Consider n-dimensional homergic combinations and N-dimensional heterergic combinations of predictive and inert agents. As in the two agent case, it can be assumed that all of the active agent dose-response curves are monotonically increasing or all are monotonically decreasing. Note that Result 4.3.2 still holds for each of the active agents considered. An N-dimensional Interaction Index can therefore be defined as follows.

**Definition 4.7.4:** Let  $(x_1, x_2, \dots, x_N)$  denote an N-dimensional dose combination and  $\pi$

the observed response. The Interaction Index is given by

$$II(x_1, x_2, \dots, x_n, \pi) = \sum_{i=1}^N \frac{x_i}{ED_i(\pi)}.$$

The Interaction Index can now be used to classify the types of interactions according to the following.

**Result 4.7.3:** Let  $(x_1, x_2, \dots, x_N)$  be an N-dimensional homergic combination, or an N-dimensional heterergic combination of predictive and inert agents where the effective doses of the inert agents are infinite. The type of interaction between the agents at this dose combination is characterized by

$$\begin{aligned} < 1 &\Rightarrow \text{synergism} \\ II(\mathbf{x}, \pi) = 1 &\Rightarrow \text{additivity} . \\ > 1 &\Rightarrow \text{antagonism} \end{aligned}$$

Therefore, as before, for certain N-agent combinations two methods are available for describing the types of interactions. By generalizing the methods described in Section 4.3 to the combination of N agents it can be seen that the Comparison Method can be applied to

all types of combinations with the exception of the N-dimensional heterergic combination of predictive agents with active nonpredictive agents. The Interaction Index Method can be applied to N-dimensional homergic combinations and N-dimensional heterergic combinations of predictive and inert agents.

In Section 4.4 the Isobologram was defined and shown to be useful in graphically describing the interactions between two agents at a fixed level of the response. For three agents a 3-dimensional hyperplane of additivity can be plotted in conjunction with points associated with dose combinations that yield the fixed response of interest. As argued for the two-agent study, if a point is below or above the plane of additivity it is indicative of synergism or antagonism, respectively. As demonstrated in Figure 4.7, however, this plot may be difficult to interpret since the position of a point relative to the hyperplane of additivity may be unclear. In addition, since this method is graphical, it is not possible to extend the technique, as defined in the Euclidean plane, to studies that involve more than 3 agents. In later chapters alternative plots will be shown to be useful in graphically assessing the interactions in these higher dimensional studies.

In the next chapter the definitions and results derived will be applied in a statistical modeling setting. There the variability in the responses will also be considered. Hypothesis testing procedures will be developed to determine if the interactions are statistically different from random fluctuations in the data.

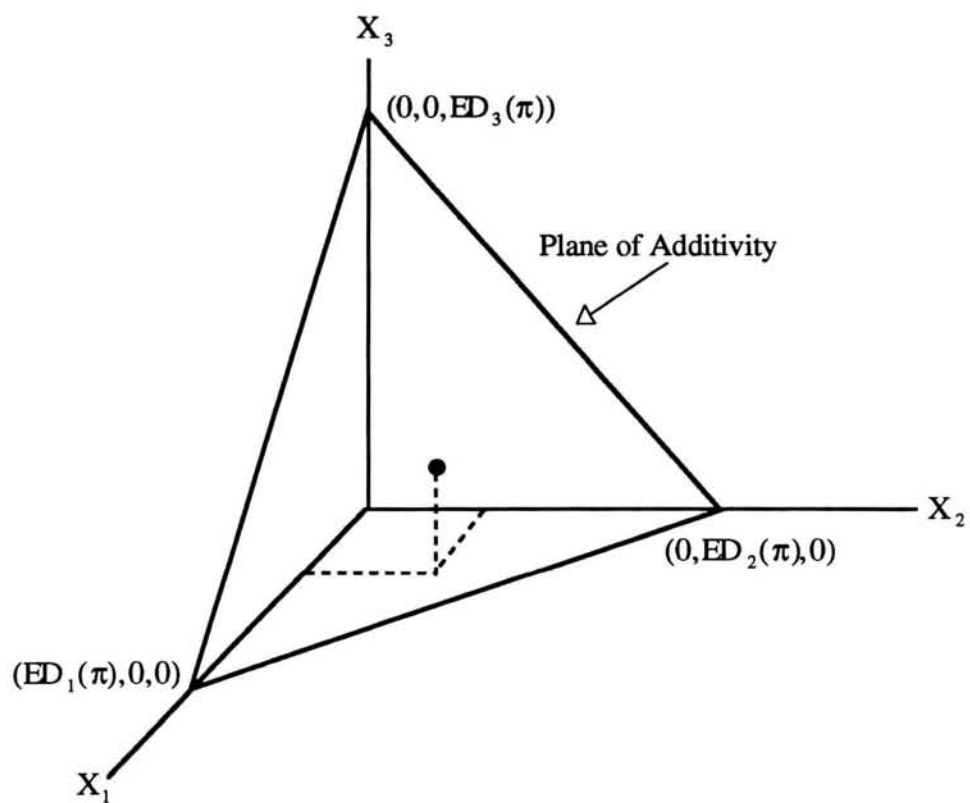


**Figure 4.7:** Three Agent Isobologram



## Chapter 5

# The Dose-Response Surface Approach to Characterizing and Detecting Interactions

### 5.1 Introduction

In the previous chapter two methods for characterizing, in a point-wise fashion, the interactions between two or more agents in a combination study were described. There the dose-response curve for each agent was assumed to be known. In this chapter, based on experimental data, a model that describes a dose-response surface will be estimated. This response-surface approach, using a logistic dose-response model, was described by Carter, et al. in 1988. Based on the properties of the Interaction Index, given in Result 4.3.3, Carter et al. derived properties of the logistic model that can be used to characterize the types of interactions estimated from the experimental data. In contrast to the point-wise results described in the last chapter, these results apply to a range of dose combinations. While this approach can be applied to studies that involve any number of agents, it will be shown that the applicability of this technique is limited when a large number of agents is being considered.

In this chapter the usefulness of isobolograms in this context will also be discussed. Because this graphical tool can not be used for studies that include more than two agents, new graphical techniques will be shown to be useful in studies that include an arbitrarily large number of agents. Before examining the properties of the dose-response models the single agent logistic dose-response curve will be briefly discussed.

## 5.2 A Single Agent Dose-Response Curve

Let  $x_i$  denote a fixed value of  $X_i$ , the dose level for the  $i$ th agent, and  $\pi$  a fixed level of the response. For purposes of this dissertation the logistic function will be used to model the dose-response curve as

$$P(X_i; \beta_0, \beta_i) = \frac{1}{1 + e^{-(\beta_0 + \beta_i X_i)}} \quad (5.2.1)$$

where  $\beta_0$  and  $\beta_i$  are the unknown parameters. Equivalently (5.2.1) can be written as

$$\logit[P(X_i; \beta_0, \beta_i)] = \ln\left(\frac{P(X_i; \beta_0, \beta_i)}{1 - P(X_i; \beta_0, \beta_i)}\right) = \beta_0 + \beta_i X_i. \quad (5.2.2)$$

The baseline response rate associated with a dose of  $X_i = 0$  is given by

$$P(0; \beta_0) = \frac{1}{1 + e^{-\beta_0}} \quad (5.2.3)$$

which implies  $\beta_0$  is the logit of  $P(0; \beta_0)$ .  $\beta_i$  is referred to as the slope parameter associated with the dose-response curve for the  $i$ th agent. For an inert agent  $\beta_i = 0$ . Certain properties of these parameters are listed in the following result.

**Result 5.2.1** Let the single agent dose response curve be given by (5.2.1) where  $\beta_0$  is the logit of the baseline response and  $\beta_i$  is the slope parameter.

- i) If  $P(0; \beta_0) < .5$  then  $\beta_0 < 0$
- If  $P(0; \beta_0) = .5$  then  $\beta_0 = 0$

If  $P(0; \beta_0) > .5$  then  $\beta_0 > 0$ .

ii) If the dose-response curve is monotonically increasing then  $\beta_1 > 0$ .

If the dose-response curve is constant then  $\beta_1 = 0$ .

If the dose-response curve is monotonically decreasing then  $\beta_1 < 0$ .

Three examples are plotted in Figure 5.1.

It will now be shown that the logistic model is symmetric about  $\pi = 0.5$ .

**Result 5.2.2:** Let  $\beta_0$  and  $\beta_1$  be any real constants. The function

$$P(X; \beta_0, \beta_1) = \frac{1}{1 + e^{-(\beta_0 + \beta_1 X)}}; -\infty \leq X \leq \infty$$

is symmetric about  $\pi = 0.5$ .

**Proof:**

Let  $\xi$  be such that  $P(\xi; \beta_0, \beta_1) = 0.5$ . Therefore  $e^{-(\beta_0 + \beta_1 \xi)} = 1$ .

Let  $\varepsilon > 0$ . Then

$$P(\xi + \varepsilon; \beta_0, \beta_1) = \frac{1}{1 + e^{-(\beta_0 + \beta_1 \xi + \beta_1 \varepsilon)}} = \frac{1}{1 + e^{-(\beta_0 + \beta_1 \xi)} e^{-\beta_1 \varepsilon}} = \frac{1}{1 + e^{-\beta_1 \varepsilon}}$$

$$P(\xi - \varepsilon; \beta_0, \beta_1) = \frac{1}{1 + e^{-(\beta_0 + \beta_1 \xi - \beta_1 \varepsilon)}} = \frac{1}{1 + e^{-(\beta_0 + \beta_1 \xi)} e^{\beta_1 \varepsilon}} = \frac{1}{1 + e^{\beta_1 \varepsilon}}$$

Let  $\Delta_1 = |P(\xi; \beta_0, \beta_1) - P(\xi - \varepsilon; \beta_0, \beta_1)|$  and  $\Delta_2 = |P(\xi + \varepsilon; \beta_0, \beta_1) - P(\xi; \beta_0, \beta_1)|$ . Then

$$\Delta_1 = \left| \frac{1}{2} - P(\xi - \varepsilon; \beta_0, \beta_1) \right| = \left| \frac{1}{2} - \frac{1}{1 + e^{\beta_1 \varepsilon}} \right| = \left| \frac{e^{-\beta_1 \varepsilon} - 1}{2(1 + e^{-\beta_1 \varepsilon})} \right| = \left| \frac{1 - e^{\beta_1 \varepsilon}}{2(1 + e^{\beta_1 \varepsilon})} \right|$$

$$\Delta_2 = \left| P(\xi + \varepsilon; \beta_0, \beta_1) - \frac{1}{2} \right| = \left| \frac{1}{1 + e^{-\beta_1 \varepsilon}} - \frac{1}{2} \right| = \left| \frac{1 - e^{\beta_1 \varepsilon}}{2(1 + e^{\beta_1 \varepsilon})} \right|.$$

Since  $\Delta_1 = \Delta_2$  it follows that  $P(X; \beta_0, \beta_1)$  is symmetric about  $\pi = 0.5$ .

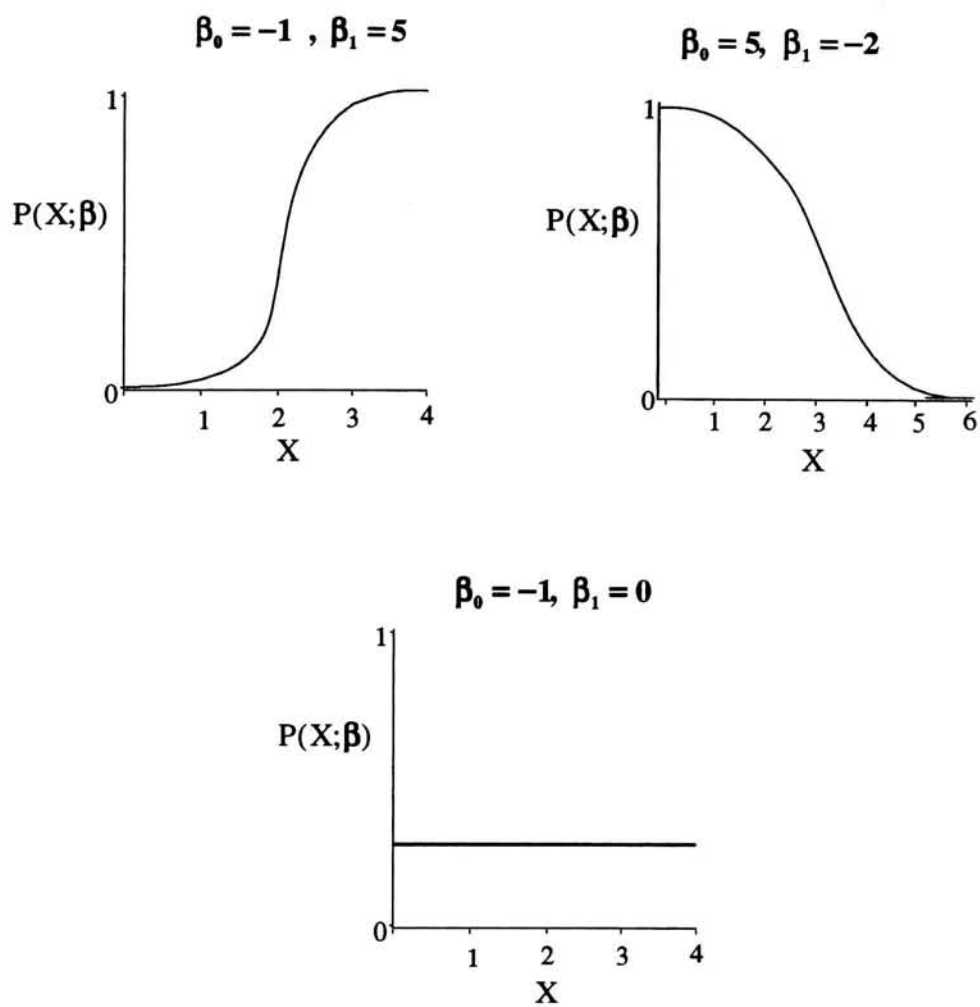


**Figure 5.1:** Examples of Single Agent Logistic Dose-Response Curves

$$P(X; \beta) = \frac{1}{1 + \exp[-(\beta_0 + \beta_1 X)]}$$

For studies that involve a single agent, where the model is assumed to be (5.2.1), the unknown parameters,  $\beta_0$  and  $\beta_1$ , can be estimated using the maximum likelihood methods described in Chapter 3. Likelihood ratio, Score, Wald and goodness-of-fit tests can be applied to the fitted model to assess the adequacy of the fit. In the next section properties of the model associated with a two agent study will be considered.

### 5.3 Two Agent Model with Single Interaction Term

Assume the active agents dose-response curves are monotonic. For combinations that contain two active agents, the dose-response curves for both agents will either be increasing or decreasing. Assume the dose-response curve for each agent is given by

$$\logit[P(X_i; \beta_0, \beta_i)] = \beta_0 + \beta_i X_i, \quad i=1,2 \quad (5.3.1)$$

where  $\beta_i \in (-\infty, \infty)$ . A common background response is assumed and is given by (5.2.3).

A logistic two agent model with a single first order cross product term is given by

$$P(X_1, X_2; \boldsymbol{\beta}) = \frac{1}{1 + e^{-(\mathbf{X}\boldsymbol{\beta})}} = \frac{1}{1 + e^{-(\beta_0 + \beta_1 X_1 + \beta_2 X_2 + \beta_{12} X_1 X_2)}} \quad (5.3.2)$$

with  $\mathbf{X} = (1 \quad X_1 \quad X_2 \quad X_1 X_2)$  and unknown parameters  $\boldsymbol{\beta} = (\beta_0 \quad \beta_1 \quad \beta_2 \quad \beta_{12})'$ .

Equivalently (5.3.2) can be written as

$$\logit[P(X_1, X_2; \boldsymbol{\beta})] = \beta_0 + \beta_1 X_1 + \beta_2 X_2 + \beta_{12} X_1 X_2. \quad (5.3.3)$$

This model describes a 3-dimensional dose-response surface. Two examples are plotted in Figures 5.2.

It can be shown that this two agent model agrees with each of the single agent dose-response curves. For example, when say  $X_1 = 0$ , the dose-response curve for  $X_2$  alone is given. This implies the 3-dimensional dose-response surface intersects the 2-dimensional  $X_2 \times P$  plane along the dose-response curve for  $X_2$ . Similarly, when  $X_2 = 0$ , the surface intersects the 2-dimensional  $X_1 \times P$  plane along the dose-response curve for  $X_1$ . In addition, when  $X_1 = 0$  and  $X_2 = 0$  the response predicted is the common background response given by (5.2.3).

Linking the interaction index with the logistic dose-response model, Carter, et al. (1988) showed that for homergic combinations the type of interaction between the two agents can be characterized by examining the sign of the cross-product parameter,  $\beta_{12}$ . This result is generalized to all combinations in the following result.

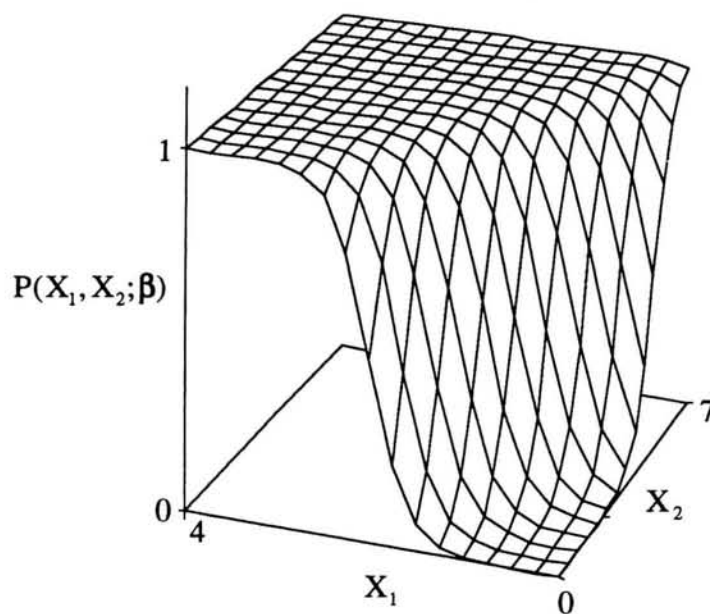
**Result 5.3.1:** Assume a two agent dose-response relationship is given by (5.3.3).

Furthermore, assume that the dose-response curves associated with each active agent alone are monotonic. Then for any dose combination the type of interaction between the two agents is determined by the sign of  $\beta_{12}$  as shown.

| Combination | Single Agent Dose          | $\beta_{12} = 0$ | $\beta_{12} > 0$ | $\beta_{12} < 0$ |
|-------------|----------------------------|------------------|------------------|------------------|
|             | Response Curves            |                  |                  |                  |
| Homergic    | $\beta_i > 0, i = 1, 2$    | Additivity       | Synergism        | Antagonism       |
|             | $\beta_i < 0, i = 1, 2$    | Additivity       | Antagonism       | Synergism        |
| Heterergic  | $\beta_i > 0, \beta_j = 0$ | Additivity       | Synergism        | Antagonism       |
|             | $\beta_i < 0, \beta_j = 0$ | Additivity       | Antagonism       | Synergism        |

### Increasing Single Agent Dose-Response Curves

$$\beta_0 = -10, \beta_1 = 5, \beta_2 = 2, \beta_{12} = 0.5$$



### Decreasing Single Agent Dose-Response Curves

$$\beta_0 = 10, \beta_1 = -4, \beta_2 = -2.5, \beta_{12} = -1$$

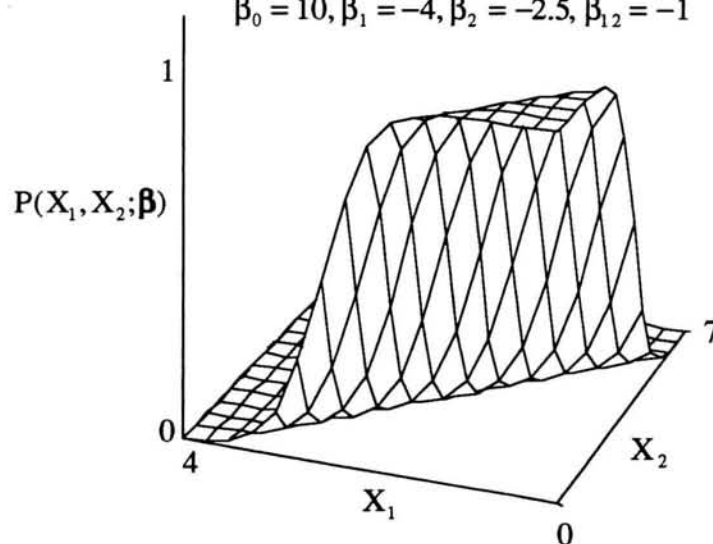


**Figure 5.2:** Examples of Two Agent Logistic Dose-Response Surfaces

$$P(X_1, X_2; \beta) = \frac{1}{1 + \exp[-(\beta_0 + \beta_1 X_1 + \beta_2 X_2 + \beta_{12} X_1 X_2)]}$$

|           |                            |            |               |               |
|-----------|----------------------------|------------|---------------|---------------|
| Coalitive | $\beta_i > 0, \beta_j = 0$ | Additivity | Synergism     | Antagonism    |
|           | $\beta_i < 0, \beta_j = 0$ | Additivity | Antagonism    | Synergism     |
|           | $\beta_i = 0, \beta_j = 0$ | Additivity | Nonadditivity | Nonadditivity |

**Proof:**

Assume each active single agent dose-response curve is monotonically increasing.

The proof for monotonically decreasing single-dose response curves is similar.

**Case i:** Homnergic or heternergic combination of a predictive agent and an inert agent.

Let  $(x_1, x_2)$  denote a fixed dose combination with response

$$\pi = P(x_1, x_2; \beta) = \frac{1}{1 + e^{-(\beta_0 + \beta_1 x_1 + \beta_2 x_2 + \beta_{12} x_1 x_2)}}.$$

For the combinations considered in this case at least one agent is predictive. Since each single agent dose-response curve is monotonically increasing it follows that  $\pi > P(0; \beta_0)$  where  $P(0; \beta_0)$  is given in (5.2.3). Hence  $\text{logit}(\pi) > \beta_0$  or  $\text{logit}(\pi) - \beta_0 > 0$ .

Based on definition (4.3.4) the interaction index is given by

$$II(\pi, x_1, x_2) = \frac{x_1}{ED_1(\pi)} + \frac{x_2}{ED_2(\pi)}.$$

Using (5.3.1)  $ED_i(\pi) = \frac{\text{logit}(\pi) - \beta_0}{\beta_i}$ ,  $i=1,2$ .

$$\text{Therefore } II(\pi, x_1, x_2) = \frac{\beta_1 x_1}{\text{logit}(\pi) - \beta_0} + \frac{\beta_2 x_2}{\text{logit}(\pi) - \beta_0}. \quad (5.3.4)$$

The model in (5.3.3) can also be written as

$$\frac{\beta_1 x_1}{\text{logit}(\pi) - \beta_0} + \frac{\beta_2 x_2}{\text{logit}(\pi) - \beta_0} = 1 - \frac{\beta_{12} x_1 x_2}{\text{logit}(\pi) - \beta_0}. \quad (5.3.5)$$



The left side of (5.3.4) is identical to  $II(\pi, x_1, x_2)$  given in (5.3.4). Therefore, since  $x_i > 0$ ,  $i = 1, 2$ , and  $\text{logit}(\pi) - \beta_0 > 0$ , if  $\beta_{12} > 0$  then  $II(\pi, x_1, x_2) < 1$  which by Result 4.7.3 indicates synergism. Similarly, if  $\beta_{12} < 0$  then  $II(\pi, x_1, x_2) > 1$ , indicating antagonism and if  $\beta_{12} = 0$  additivity is indicated.

**Case ii:** Coalitive Combination of an inert and active, nonpredictive agent.

In this case the Comparison Method, described in Section 4.3, can be used to compare the response by the full model and the response expected under additivity.

Let  $x_1$  denote the fixed dose level associated with the active, nonpredictive agent.

The expected response under additivity,  $\pi^A$ , is determined solely by the dose-response curve associated with the active agent, i.e.,

$$\text{logit}(\pi^A) = \beta_0 + \beta_1 x_1. \quad (5.3.6)$$

The response under the full model is given by

$$\text{logit}(\pi) = \beta_0 + \beta_1 x_1 + \beta_{12} x_1 x_2. \quad (5.3.7)$$

By comparing (5.3.6) to (5.3.7), when  $\beta_{12} > 0$ ,  $\text{logit}(\pi) > \text{logit}(\pi^A)$ , which by Definition 4.3.2 indicates a synergism. Similarly when  $\beta_{12} < 0$ , an antagonism is suggested. When  $\beta_{12} = 0$  additivity is indicated.

**Case iii:** Coalitive Combination of two inert agents.

The approach in this case will be similar to Case ii. The response expected under additivity is simply the background response, i.e.

$$\text{logit}(\pi^A) = \beta_0. \quad (5.3.8)$$

The response determined by the full model is given by

$$\text{logit}(\pi) = \beta_0 + \beta_{12} x_1 x_2. \quad (5.3.9)$$

By comparing (5.3.8) to (5.3.9), when  $\beta_{12} \neq 0$  then  $\text{logit}(\pi) \neq \text{logit}(\pi^A)$  which indicates a nonadditive interaction. In this case, however, since both single agent dose-response curves are inert, the character of the interaction will be study dependent.

Therefore, when the two agent dose-response relationship is given by (5.3.3) the type of interaction between the agents can be determined by simply examining the sign of  $\beta_{12}$ . Because the result was dependent on the doses only through the constraint that  $x_i \geq 0$ ,  $i = 1, 2$ , the result holds for all dose combinations in the dose-space studied.

Using this result, when  $\beta_{12} = 0$ , a response expected under additivity,  $P^A(X_1, X_2; \beta)$ , can be written as

$$\text{logit}[P^A(X_1, X_2; \beta)] = \beta_0 + \beta_1 X_1 + \beta_2 X_2. \quad (5.3.10)$$

Note now, that for these types of studies, monotonically decreasing curves can be transformed into monotonically increasing curves by redefining the response as  $Q = 1 - P$ . Hence, for the remainder of this chapter, only monotonically increasing single agent dose response curves will be considered. It will be shown, however, that this does not imply that the associated dose-response surface will be uniformly increasing.

Using the experimental data and the maximum likelihood methods described in Chapter 3, the unknown parameters for this model (5.3.3) can be estimated. The goodness-of-fit procedures described in Section 3.5 can be used to assess the adequacy of the fit. A Wald Test, defined in Section 3.6, can also be used to test  $H_0 : \beta_{12} = 0$ . This Hypothesis of Additivity is equivalent to testing if the data supports a significant

nonadditive interaction. When the null hypothesis is rejected the sign of  $\hat{\beta}_{12}$  can be used to characterize the type of interaction the data supports.

An example of this type of analysis is the chloral hydrate ( $X_1$ ) and ethanol ( $X_2$ ) study previously discussed in Section 3.8. The fitted model, given by

$$\text{logit}(\hat{P}(X_1, X_2; \boldsymbol{\beta})) = -18.53 + .0049X_1 + .0551X_2 + .00000338X_1X_2,$$

was shown to adequately describe the data. A Wald Test was applied to the hypothesis  $H_0 : \beta_{12} = 0$  with a p-value of .0422. Thus, the data suggest that  $\beta_{12} \neq 0$  or equivalently that nonadditivity is indicated. Furthermore, since  $\hat{\beta}_{12} > 0$ , a synergistic interaction between the two agents has been detected for dose combinations in the range  $\{(X_1, X_2) : 0 \leq X_1 \leq 3000, 0 \leq X_2 \leq 300\}$ .

A plot of the fitted dose-response surface for the chloral hydrate and ethanol study is given in Figure 5.3. Also shown, for comparison purposes, is the dose-response curve under the assumption of additivity, i.e., when  $\beta_{12} = 0$ . Note that it is difficult to visualize any differences in these 3-dimensional plots. In the next section, the isobologram will be shown to be useful in visually interpreting the interactions in these two agent studies.

#### **5.4 Isobolograms Based on the Two Agent Model with Single Interaction Term**

Recall that for a fixed value of the response,  $\pi$ , an isobol is a plot of the set of dose combinations that yields  $\pi$ . For a 3-dimensional fitted dose-response surface it follows that, in this context, the isobol is a 2-dimensional contour from the fitted surface. Assume the fitted model is given by

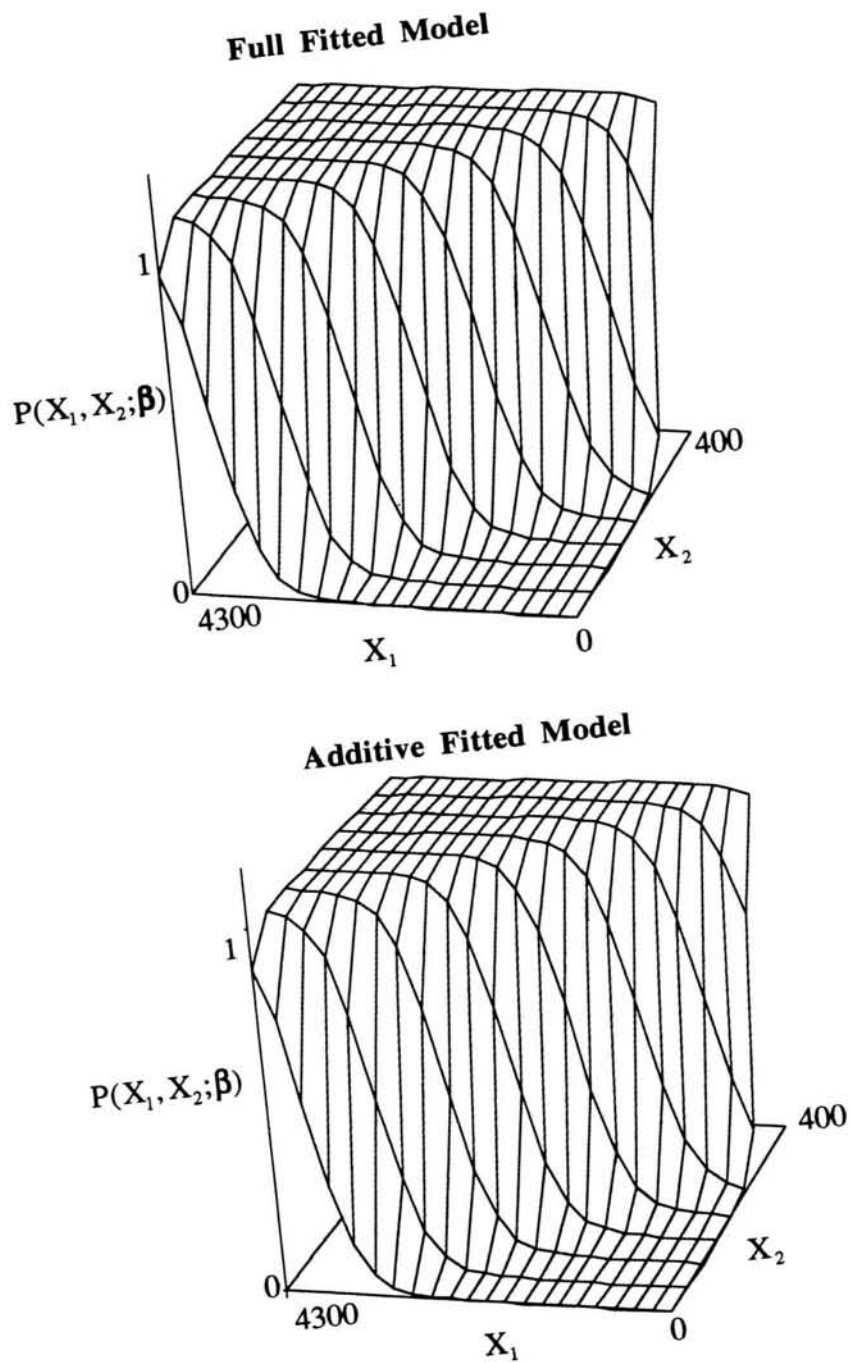


**Figure 5.3:** Chloral Hydrate and Ethanol Dose-Response Surface, Carter (1988): Full Model versus Model Expected Under Additivity

$$\text{logit}[\hat{P}(X_1, X_2; \hat{\beta})] = \hat{\beta}_0 + \hat{\beta}_1 X_1 + \hat{\beta}_2 X_2 + \hat{\beta}_{12} X_1 X_2. \quad (5.4.1)$$

At the fixed response,  $\pi$ , the isobol is given by

$$I_\pi(X_1, X_2; \hat{\beta}) = \{(X_1, X_2) : \text{logit}(\pi) = \hat{\beta}_0 + \hat{\beta}_1 X_1 + \hat{\beta}_2 X_2 + \hat{\beta}_{12} X_1 X_2; X_1, X_2 > 0\}. \quad (5.4.2)$$

The isobologram is a plot of this contour and the line of additivity given by

$$I_\pi^A(X_1, X_2; \hat{\beta}) = \{(X_1, X_2) : \text{logit}(\pi) = \hat{\beta}_0 + \hat{\beta}_1 X_1 + \hat{\beta}_2 X_2; X_1, X_2 > 0\}. \quad (5.4.3)$$

In order to derive properties of the isobologram it will be useful to consider homergic two agent combinations first.

#### 5.4.1 Isobolograms for Homergic Two Agent Combinations

By equating the expression for the line of additivity given in (5.4.3) to that for the isobol given in (5.4.2) it can be shown that the line of additivity and the isobol intersect along each axis at the points  $\left(\frac{\text{logit}(\pi) - \hat{\beta}_0}{\hat{\beta}_1}, 0\right)$  and  $\left(0, \frac{\text{logit}(\pi) - \hat{\beta}_0}{\hat{\beta}_2}\right)$ . Other properties of the isobologram can be noted by rewriting the isobol equation given in (5.4.2) as

$$I_\pi(X_1, X_2; \hat{\beta}) = \left\{ (X_1, X_2) : X_2 = \frac{\text{logit}(\pi) - \hat{\beta}_0 - \hat{\beta}_1 X_1}{\hat{\beta}_2 + \hat{\beta}_{12} X_1}; 0 \leq X_1 \leq \frac{\text{logit}(\pi) - \hat{\beta}_0}{\hat{\beta}_1} \right\}. \quad (5.4.4)$$

Similarly the line of additivity given in (5.4.3) can be rewritten as

$$I_{\pi}^{\wedge}(X_1, X_2; \hat{\beta}) = \left\{ (X_1, X_2) : X_2 = \frac{\text{logit}(\pi) - \hat{\beta}_0 - \hat{\beta}_1 X_1}{\hat{\beta}_2}; 0 \leq X_1 \leq \frac{\text{logit}(\pi) - \hat{\beta}_0}{\hat{\beta}_1} \right\}. \quad (5.4.5)$$

By comparing (5.4.4) and (5.4.5), under synergism, when  $\hat{\beta}_{12} > 0$ , the set of points that satisfy the isobol will lie below the line of additivity. Similarly under antagonism, when  $\hat{\beta}_{12} < 0$ , the isobol is above the line of additivity. This is in agreement with the Figure 4.4 which demonstrated, for a single dose-combination, that points below or above the line of additivity were indicative of synergy or antagonism. Examples of isobols for homergic two agent combinations are shown in Figures 5.4(a)-(c). For illustrative purposes, the dose-response surface associated with each isobol is also shown.

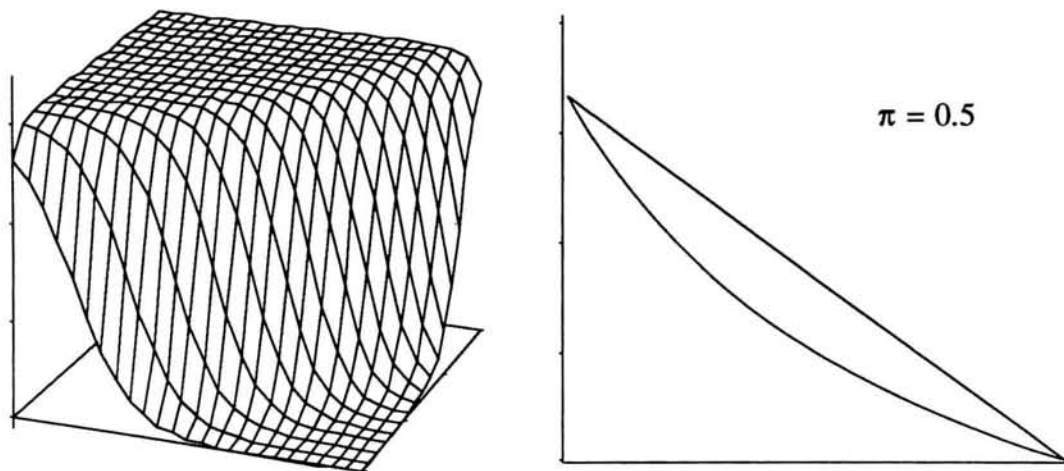
By examining (5.4.4) it can be determined that the isobol is discontinuous when  $X_1 = \frac{-\hat{\beta}_2}{\hat{\beta}_{12}}$  and  $0 < \frac{-\hat{\beta}_2}{\hat{\beta}_{12}} < \frac{\text{logit}(\pi) - \hat{\beta}_0}{\hat{\beta}_{12}}$ . Since  $\hat{\beta}_2 \geq 0$ , it follows that this can only occur when  $\hat{\beta}_{12} < 0$ , or equivalently when there is an antagonistic interaction. An example is illustrated in Figure 5.4(c). There it can be noted that for large values of both agents the dose-response surface begins to decrease so that at a particular fixed level of the response, the surface may fall below that level in the experimental dose-space considered.

By examining the first and second derivatives of the equation of the isobol given in (5.4.4), an additional property of the continuous isobol can be noted. Here

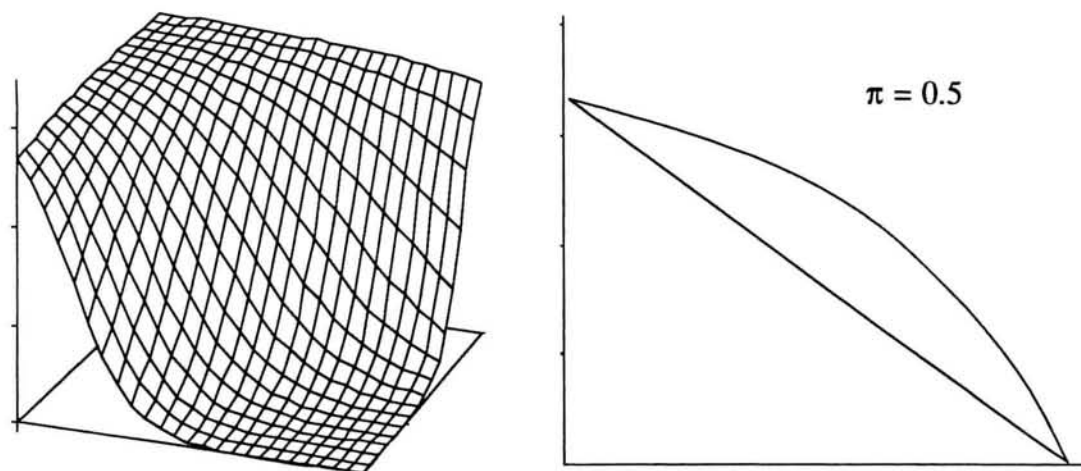
$$\frac{\partial X_2}{\partial X_1} = \frac{-\beta_1 \beta_2 - (\text{logit}(\pi) - \beta_0) \beta_{12}}{(\beta_2 + \beta_{12} X_1)^2} \quad (5.4.6)$$

and

**Figure 5.4 (a): Synergism**  
 $\beta_0 = -10, \beta_1 = 2, \beta_2 = 3, \beta_{12} = 0.8$



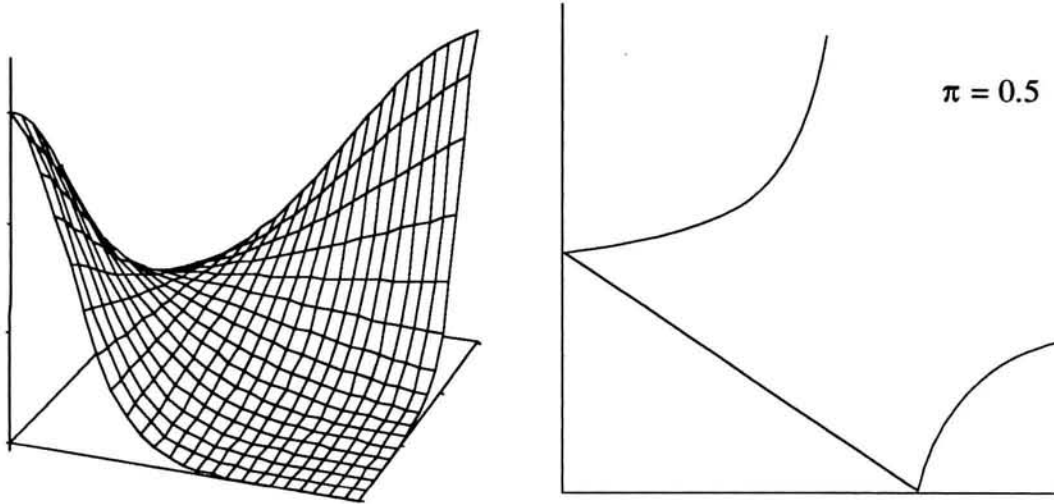
**Figure 5.4 (b): Antagonism**  
 $\beta_0 = -10, \beta_1 = 2, \beta_2 = 3, \beta_{12} = -0.4$



**Figure 5.4:** Homergic Combinations

**Figure 5.4 (c): Discontinuous Antagonism**

$$\beta_0 = -10, \beta_1 = 2, \beta_2 = 3, \beta_{12} = -0.7$$

**Figure 5.4 (continued): Homergic Combinations**



$$\frac{\partial^2 X_2}{\partial X_1^2} = \frac{2\{\beta_1\beta_2 + (\text{logit}(\pi) - \beta_0)\beta_{12}\}\beta_{12}}{(\beta_2 + \beta_{12}X_1)^3}. \quad (5.4.7)$$

Since for  $0 \leq X_1 \leq \frac{\text{logit}(\pi) - \beta_0}{\beta_1}$ , the continuous isobol decreases as  $X_1$  increases it follows by (5.4.6) that  $-\beta_1\beta_2 - (\text{logit}(\pi) - \beta_0)\beta_{12} < 0$ . Applying this inequality now in (5.4.7), it follows that, if  $\beta_{12} > 0$  then  $\frac{\partial^2 X_2}{\partial X_1^2} > 0$  and the continuous isobol will be concave up. Similarly, if  $\beta_{12} < 0$  then  $\frac{\partial^2 X_2}{\partial X_1^2} < 0$  and the continuous isobol will be concave down.

This property is illustrated in Figures 5.4(a) and 5.4(b).

#### 5.4.2 Isobolograms for Heterergic Combination of an Active, Predictive Agent and an Inert Agent

For this combination since the active agent is predictive,  $\pi > P(0; \hat{\beta}_0)$ . This implies  $\text{logit}(\pi) - \hat{\beta}_0 > 0$ . Assume initially that  $X_1$  denotes the doses of the inert agent so that  $\hat{\beta}_1 = 0$ . The isobol and the line of additivity can be written as

$$I_\pi(X_1, X_2, \hat{\beta}) = \left\{ (X_1, X_2) : X_2 = \frac{\text{logit}(\pi) - \hat{\beta}_0}{\hat{\beta}_2 + \hat{\beta}_{12}X_1}; X_1 > 0 \right\} \quad (5.4.8)$$

and

$$I_\pi^A(X_1, X_2, \hat{\beta}) = \left\{ (X_1, X_2) : X_2 = \frac{\text{logit}(\pi) - \hat{\beta}_0}{\hat{\beta}_2}; X_1 > 0 \right\}. \quad (5.4.9)$$

By equating (5.4.8) to (5.4.9) it can be shown that the isobol and line of additivity intersect only on the  $X_2$  axis at  $\left(0, \frac{\text{logit}(\pi) - \hat{\beta}_0}{\hat{\beta}_2}\right)$ . The line of additivity given in (5.4.9) is

a horizontal line. By comparing (5.4.8) and (5.4.9), when  $\hat{\beta}_{12} > 0$  the synergistic isobol is below the horizontal line of additivity. When  $\hat{\beta}_{12} < 0$  the antagonistic isobol is above the line of additivity. As in the homergic case the isobol is discontinuous when  $X_1 = \frac{-\hat{\beta}_2}{\hat{\beta}_{12}}$  and

$$0 < \frac{-\hat{\beta}_2}{\hat{\beta}_{12}} < \frac{\text{logit}(\pi) - \hat{\beta}_0}{\hat{\beta}_{12}}.$$

It can be shown in a similar way that when  $X_2$  is the inert agent, the line of additivity will be a vertical line. Now the isobol will lie to the left (right) of the line of additivity when a synergism (antagonism) is indicated. Examples of these isobols are shown in Figures 5.5(a) - (d).

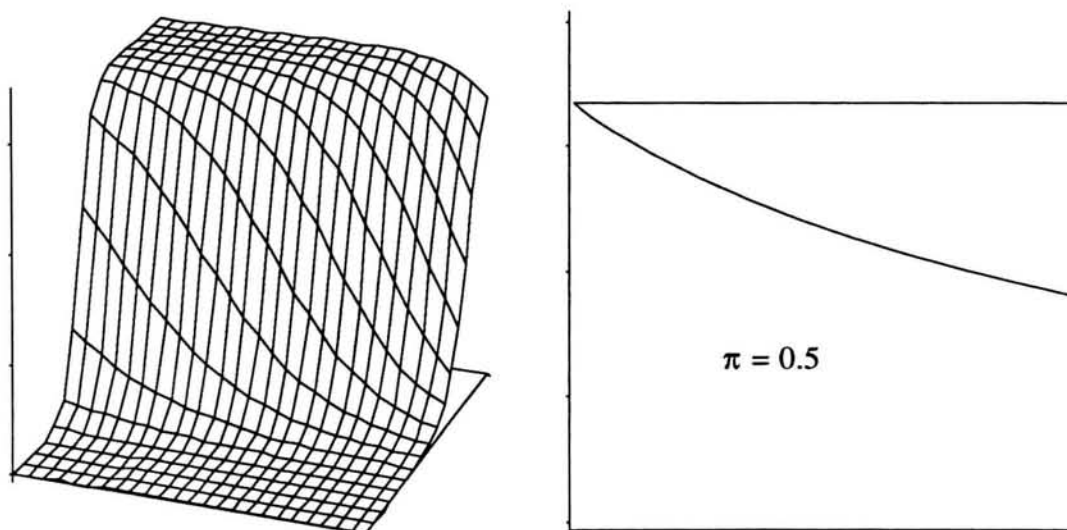
### 5.4.3 Isobolograms for Coalitive Combinations

In this case, since neither agent alone yields the fixed response of interest, the line of additivity given in Definition 4.3.2 does not exist. The isobols, however, can be plotted. Several cases are shown in Figures 5.6(a)-(h). These examples indicate that care must be taken in interpreting the type of interaction from these plots. For example, the isobols in Figure 5.6(a) and Figure 5.6(b) look similar, but one is associated with an antagonism and one is associated with a synergism. Hence, it is not recommended that isobolograms be used to visually interpret the interactions between the agents for coalitive combinations of agents.

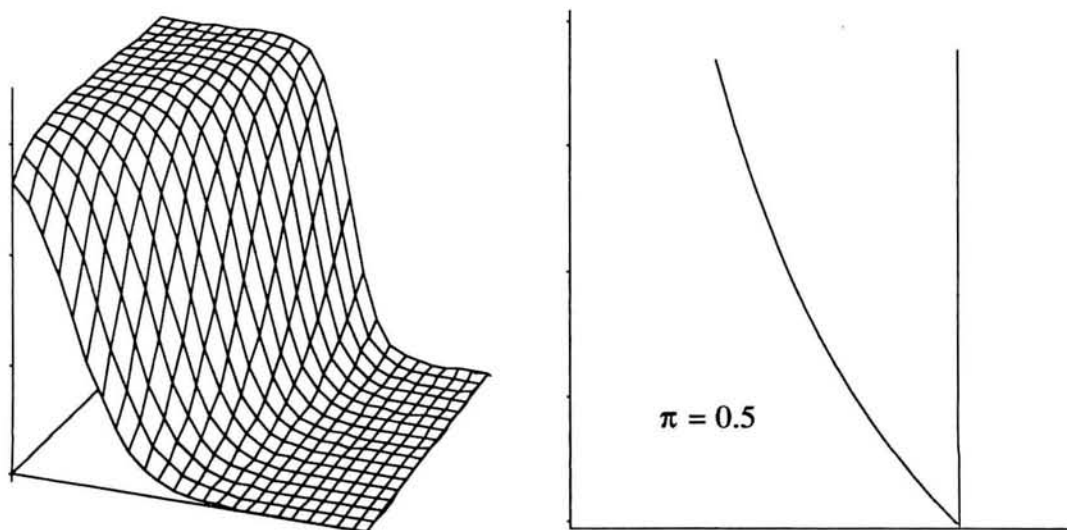
By Result 5.3.1 it was shown that when the model is given by (5.3.3) the type of interaction is determined by examining the sign of  $\beta_{12}$ . This interaction is consistent over all levels of the doses and over all levels of the response. Suppose now a combination of agents is studied which the investigator feels, at a fixed level of the response, can exhibit

**Figure 5.5 (a):** Predictive & Inert - Synergism

$$\beta_0 = -10, \beta_1 = 0, \beta_2 = 3, \beta_{12} = 0.5$$

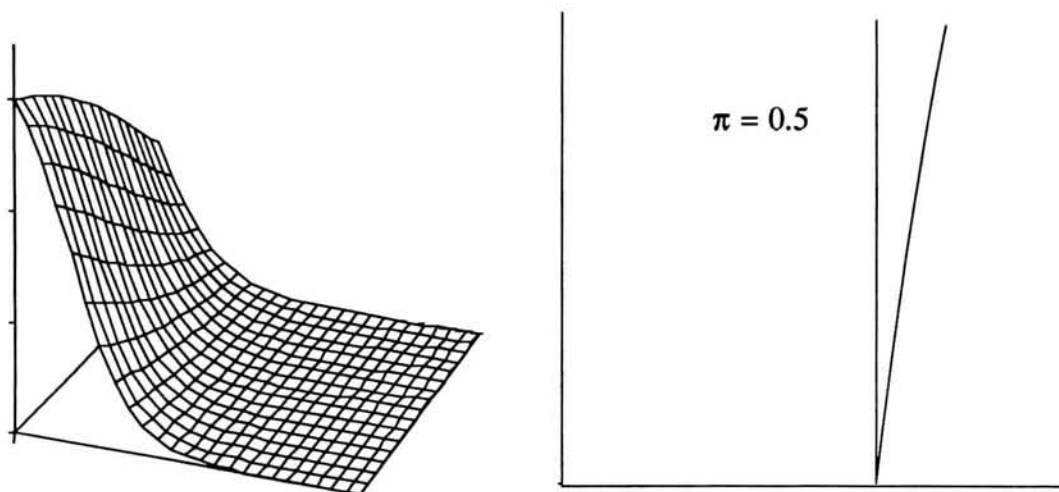
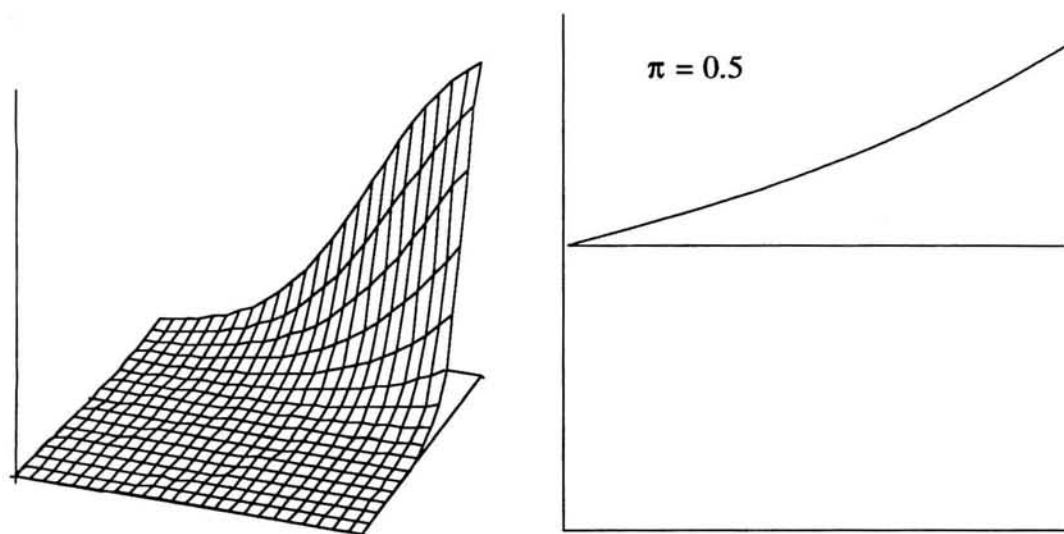
**Figure 5.5 (b):** Predictive & Inert - Antagonism

$$\beta_0 = -10, \beta_1 = 2, \beta_2 = 0, \beta_{12} = 0.5$$

**Figure 5.5:** Heterergic Combinations

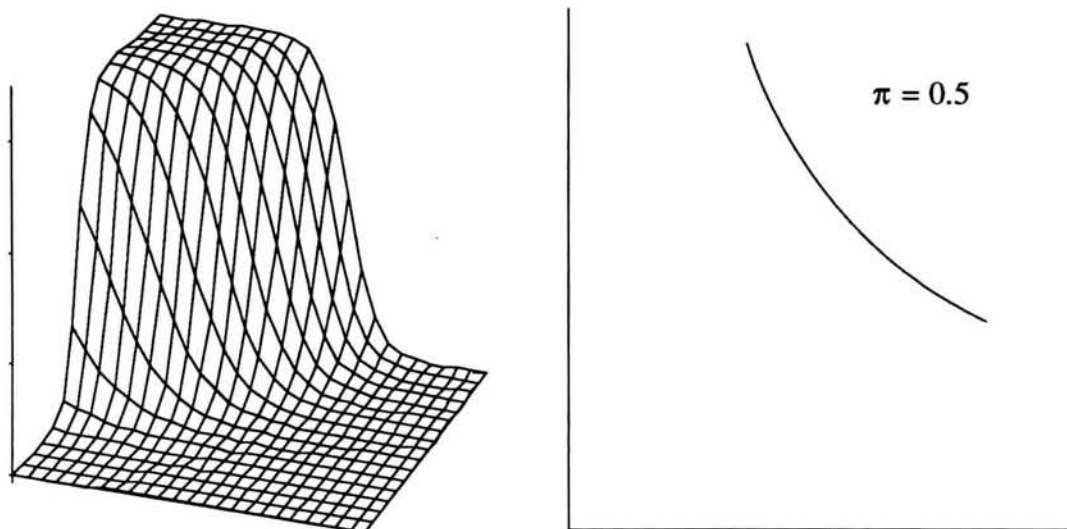
**Figure 5.5 (c):** Predictive & Inert - Antagonism

$$\beta_0 = -10, \beta_1 = 2, \beta_2 = 0, \beta_{12} = -0.1$$

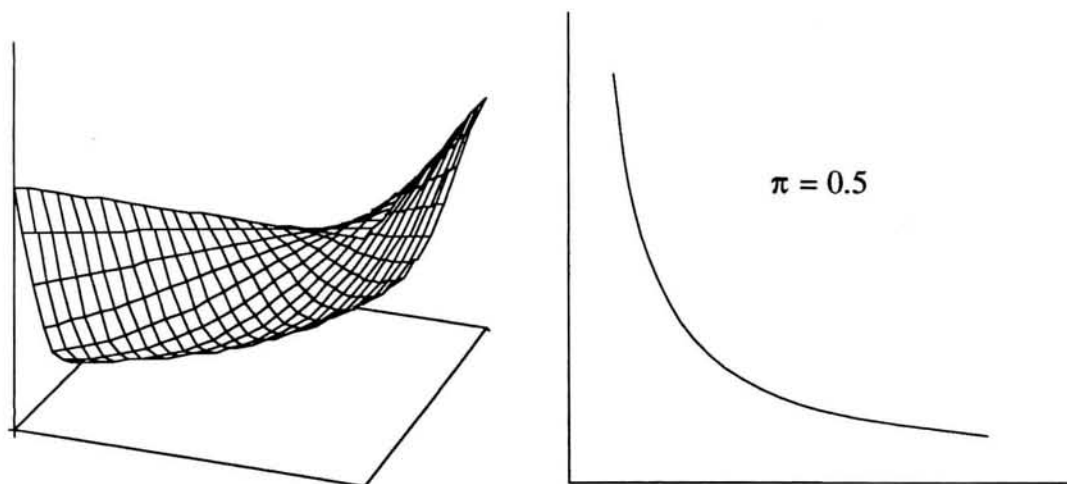
**Figure 5.5 (d):** Predictive & Inert - Antagonism**Figure 5.5 (Continued):** Heterergic Combinations

**Figure 5.6 (a): Inert & Inert - Synergism**

$$\beta_0 = -10, \beta_1 = 0, \beta_2 = 0, \beta_{12} = 1$$

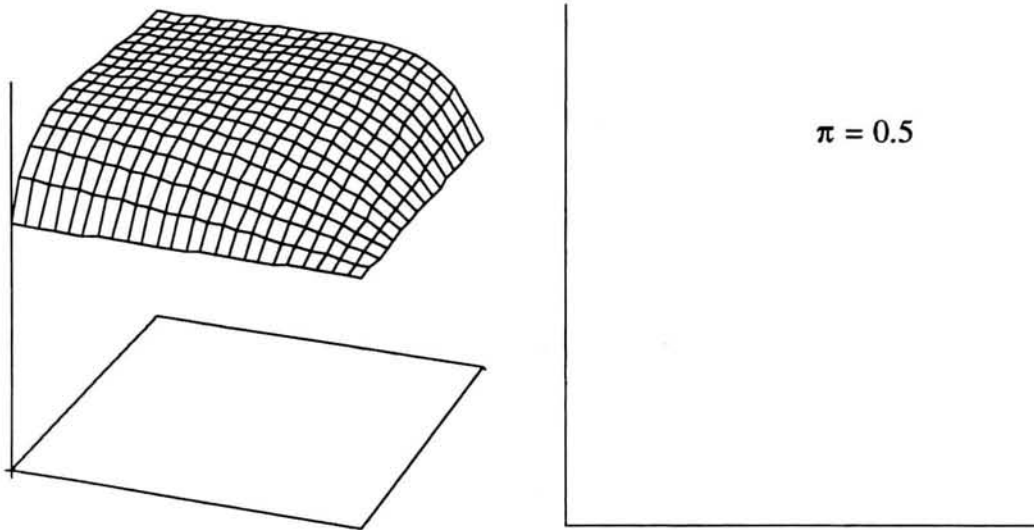
**Figure 5.6 (b): Inert & Inert - Antagonism**

$$\beta_0 = 1, \beta_1 = 0, \beta_2 = 0, \beta_{12} = -0.5$$

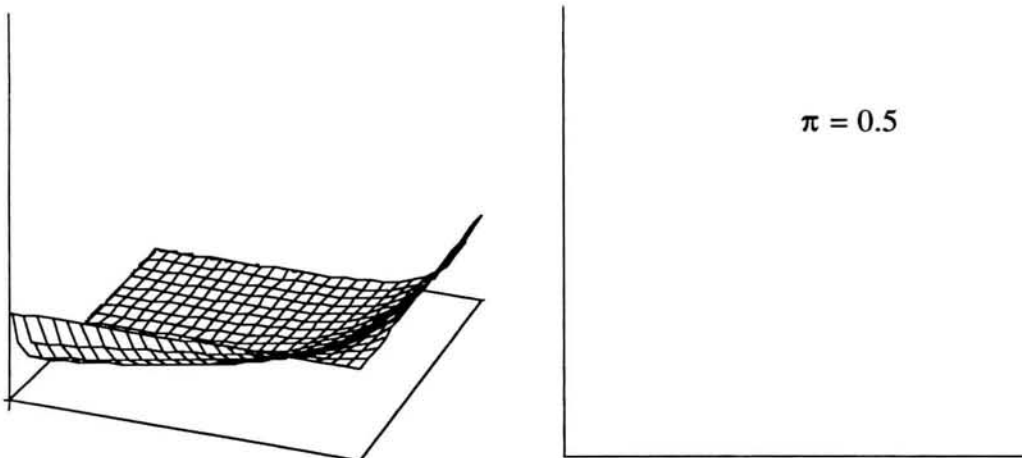
**Figure 5.6: Coalitive Combinations**

**Figure 5.6 (c): Inert & Inert - Synergism**

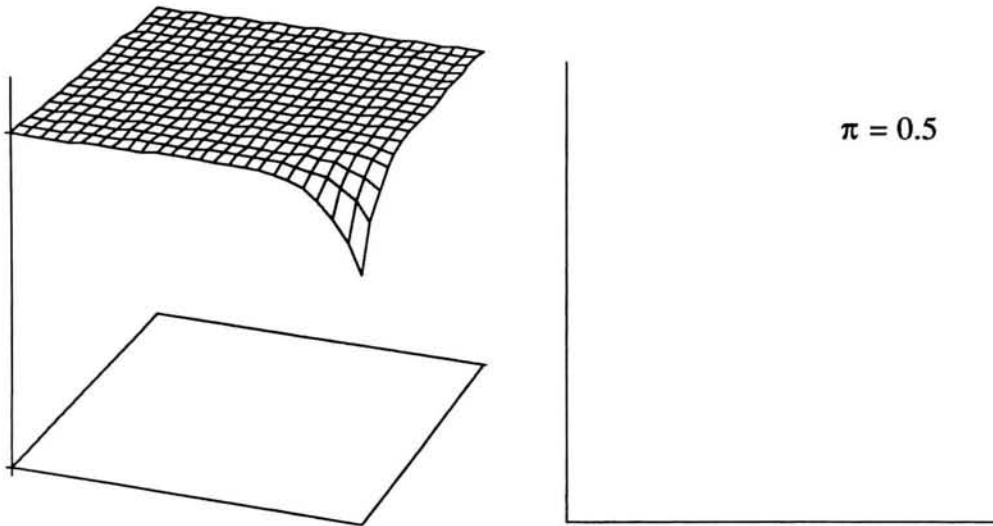
$$\beta_0 = 1, \beta_1 = 0, \beta_2 = 0, \beta_{12} = 0.5$$

**Figure 5.6 (d): Inert & Inert - Antagonism**

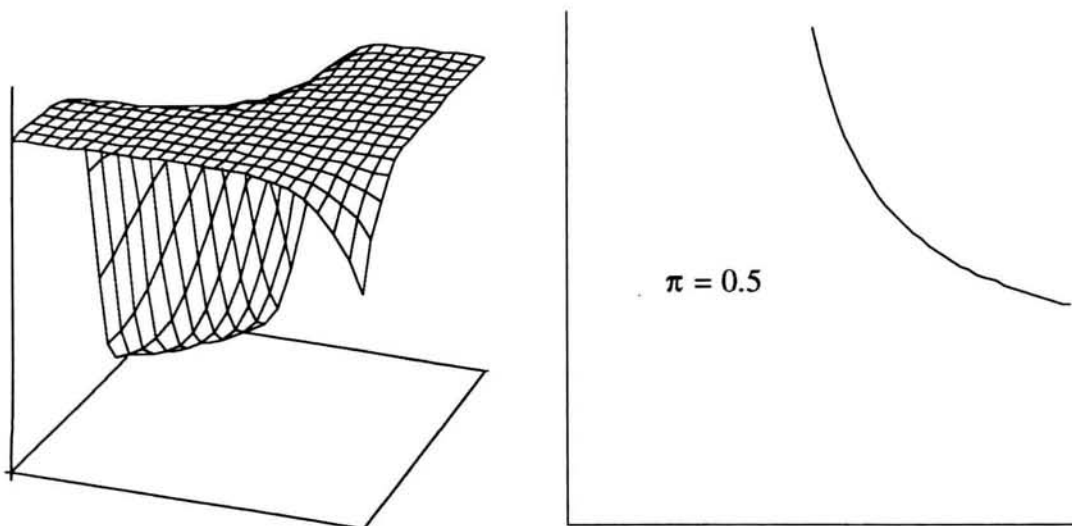
$$\beta_0 = -1, \beta_1 = 0, \beta_2 = 0, \beta_{12} = -0.5$$

**Figure 5.6 (Continued): Coalitive Combinations**

**Figure 5.6 (e):** Nonpredictive & Nonpredictive - Synergism  
 $\beta_0 = 1, \beta_0 = 2 \beta_0 = 3, \beta_{12} = 0.5$



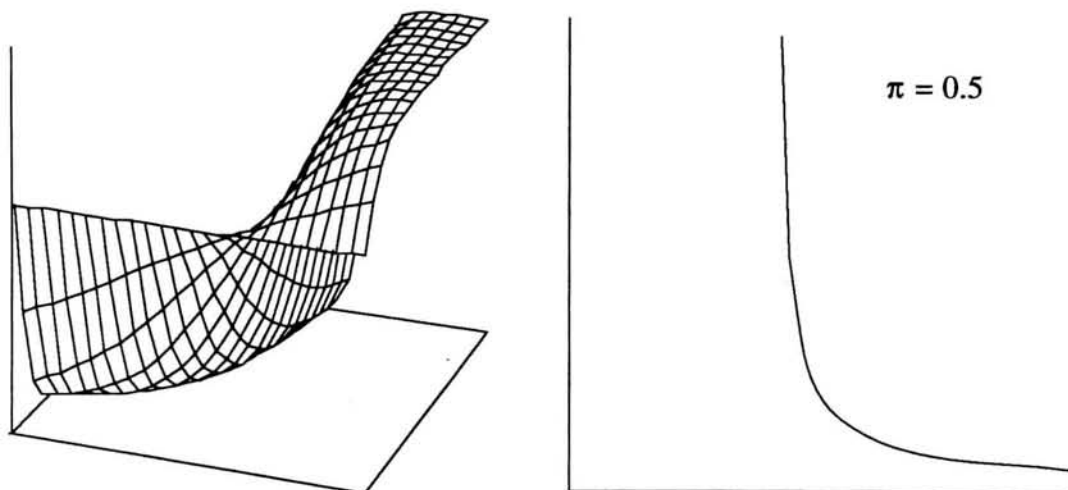
**Figure 5.6 (f):** Nonpredictive & Nonpredictive - Antagonism  
 $\beta_0 = 0.8, \beta_0 = 2 \beta_0 = 3, \beta_{12} = -1.5$



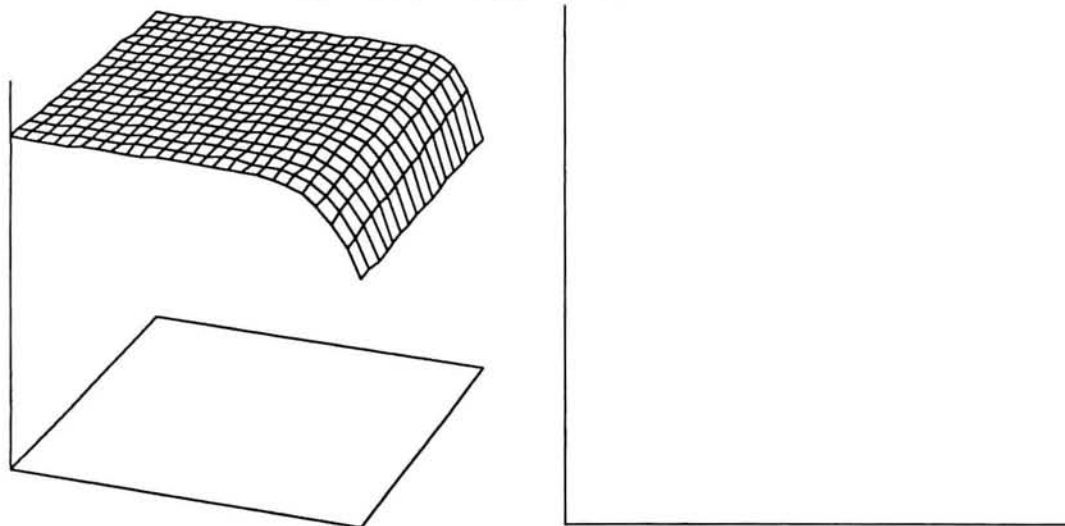
**Figure 5.6 (Continued):** Coalitive Combinations

**Figure 5.6 (g): Inert & Nonpredictive - Antagonism**

$$\beta_0 = .8, \beta_1 = 0, \beta_2 = 3, \beta_{12} = -1.5$$

**Figure 5.6 (h): Inert & Nonpredictive - Antagonism**

$$\beta_0 = 1, \beta_1 = 2, \beta_2 = 0, \beta_{12} = 0.5$$

**Figure 5.6 (Continued): Coalitive Combinations**



synergism, antagonism, and additivity in the dose-space studied. In the next section an example of a model that can exhibit this pattern of interactions will be given.

### 5.5 Two Agent Model with More Than One Interaction Term

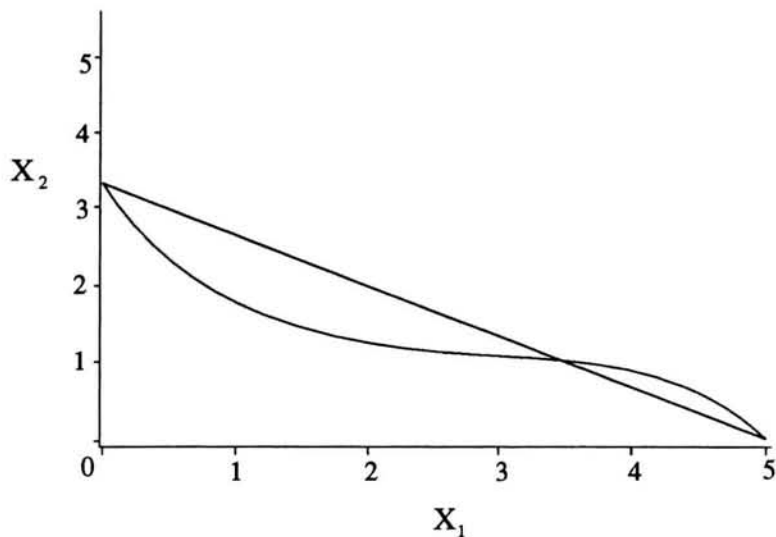
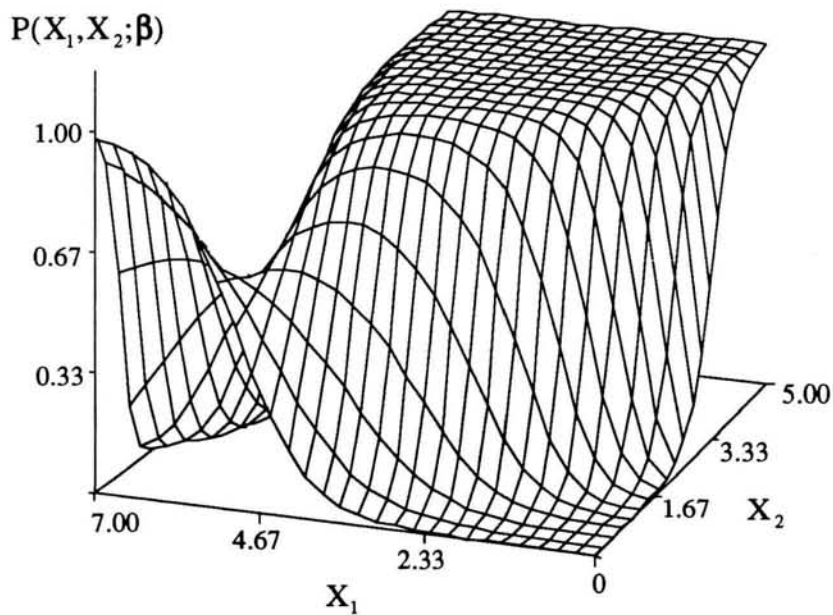
Suppose, for some fixed value of the response, a model is needed for a homergic combination that can yield the isobologram given by Figure 5.7. Note that the isobol and line of additivity now intersect at three points. As before, assume each single agent dose-response curve is monotonically increasing. For the fitted model given in (5.4.1), at a fixed value of  $\pi$ , it was shown the isobol and the line of additivity intersect at two points, one on each axis. Hence the form of the model assumed in (5.4.1) can not describe the isobol shown in Figure 5.7. While several alternative models have isobols that allow regions of synergism and antagonism one example is given by

$$\begin{aligned} \text{logit}[P(X_1, X_2; \boldsymbol{\beta})] &= \beta_0 + \beta_1 X_1 + \beta_2 X_2 + \beta_{12} X_1 X_2 + \beta_{112} X_1^2 X_2; \\ 0 \leq X_1 \leq 7, 0 \leq X_2 \leq 5. \end{aligned} \quad (5.5.1)$$

Note that this model is consistent with each single agent dose response curve given in (5.3.1) and with the common background response given in (5.2.3). The response surface associated with this fitted model is shown in Figure 5.7(b). By rewriting this model as

$$\frac{\beta_1 X_1}{\text{logit}(\pi) - \beta_0} + \frac{\beta_2 X_2}{\text{logit}(\pi) - \beta_0} = 1 - \left( \frac{\beta_{12} X_1 X_2}{\text{logit}(\pi) - \beta_0} + \frac{\beta_{112} X_1^2 X_2}{\text{logit}(\pi) - \beta_0} \right) \quad (5.5.2)$$

the types of interactions can be described using the interaction index and Result 4.7.3. If  $\beta_{12} = \beta_{112} = 0$ , additivity is indicated. Alternatively, synergism is found if  $\beta_{12}, \beta_{112} > 0$  and antagonism is indicated if  $\beta_{12}, \beta_{112} < 0$ . However, if the signs of  $\beta_{12}$  and  $\beta_{112}$  differ, the

**Figure 5.7(a):** Isobologram -  $\pi = 0.5$ **Figure 5.7(b):** Dose-Response Surface**Figure 5.7:** Isobologram and Associated Dose-Response Surface with Regions of Synergism and Antagonism

type of interaction will depend on the levels of the doses considered and can vary as the dose levels and the response vary.

To show that this model can yield the isobologram given in Figure 5.7(a) note that the isobol and the line of additivity for this model are given by

$$I_{\pi}(x_1, x_2, \boldsymbol{\beta}) = \{(x_1, x_2) : \log \text{it}(\pi) = \beta_0 + \beta_1 x_1 + \beta_2 x_2 + \beta_{12} x_1 x_2 + \beta_{112} x_1^2 x_2; x_1, x_2 > 0\} \quad (5.5.3)$$

and

$$I_{\pi}^{\wedge}(x_1, x_2, \boldsymbol{\beta}) = \{(x_1, x_2) : \log \text{it}(\pi) = \beta_0 + \beta_1 x_1 + \beta_2 x_2; x_1, x_2 > 0\}. \quad (5.5.4)$$

By equating (5.5.3) and (5.5.4) it can be shown the line of additivity and the isobol intersect along the axes at  $\left(0, \frac{\log \text{it}(\pi) - \beta_0}{\beta_1}\right)$ ,  $\left(\frac{\log \text{it}(\pi) - \beta_0}{\beta_2}, 0\right)$  and also at the nonaxis

point  $\left(\frac{-\beta_{12}}{\beta_{112}}, \frac{\log \text{it}(\pi) - \beta_0 + \frac{\beta_{12}\beta_1}{\beta_{112}}}{\beta_2 + \left(\frac{\beta_{11}\beta_{12}}{\beta_{112}}\right)^2}\right)$ . Therefore, if  $0 \leq \frac{-\beta_{12}}{\beta_{112}} \leq \frac{\log \text{it}(\pi) - \beta_0}{\beta_1}$ , the isobol

will exhibit the pattern shown in Figure 5.7(a).

In the next section the results discussed thus far in this chapter will be extended to studies that include any number of agents.

## 5.6 Logistic Dose-Response Models for N Agent Studies

An N agent logistic model which contains first order interactions can be written as

$$\begin{aligned} \text{logit}[P(\mathbf{X}, \boldsymbol{\beta})] = & \beta_0 + \sum_{i=1}^N \beta_i X_i + \sum_{i=1}^{N-1} \sum_{j=i+1}^N \beta_{ij} X_i X_j + \sum_{i=1}^{N-2} \sum_{j=i+1}^{N-1} \sum_{k=j+1}^N \beta_{ijk} X_i X_j X_k + \\ & \dots + \beta_{123\dots N} X_1 X_2 \dots X_N. \end{aligned} \quad (5.6.1)$$

At a fixed value of the response,  $\pi$ , this model also can be written as

$$\begin{aligned} \sum_{i=1}^N \frac{\beta_i X_i}{\text{logit}(\pi) - \beta_0} = \\ 1 - \frac{\left( \sum_{i=1}^{N-1} \sum_{j=i+1}^N \beta_{ij} X_i X_j + \sum_{i=1}^{N-2} \sum_{j=i+1}^{N-1} \sum_{k=j+1}^N \beta_{ijk} X_i X_j X_k + \dots + \beta_{12\dots N} X_1 X_2 \dots X_N \right)}{\text{logit}(\pi) - \beta_0}. \end{aligned} \quad (5.6.2)$$

The left side of (5.6.2) is the Interaction Index as given in Definition 4.7.4. For an N-dimensional homergic combinations or an N-dimensional heterergic combination of predictive and inert agents, Result 4.7.3 can be applied to determine the types of interactions that the model describes. For example, if all of the cross product parameters are zero,  $\sum_{i=1}^N \frac{\beta_i X_i}{\text{logit}(\pi) - \beta_0} = 1$ . Hence, additivity is indicated for all dose levels and all levels of the response. If all of the nonzero cross product parameters have the same sign, the type of interaction can also be determined; positive parameters will indicate synergism and negative parameters antagonism. If, however, the signs of the cross product terms vary, the type of interaction will depend on the values of the dose combinations and the value of the fixed level of response considered.

As in the two agent case, the parameters for this model can be estimated using the maximum likelihood methods described in Chapter 3. The goodness-of-fit procedures given in Section 3.5 can be applied to assess the adequacy of the fit. In addition, a likelihood ratio test can be used to test the Additivity Hypothesis given by

$$H_0 : \beta_{12} = \beta_{13} = \cdots \beta_{123} = \beta_{124} = \cdots = \beta_{123 \dots N} = 0.$$

If this hypothesis is rejected nonadditivity is indicated. It has been shown, however, that the type of interaction may depend on the dose levels of the agents considered as well as on the response. It will now be demonstrated that several approaches can be taken to examine more closely the interactions between the N-agents. For each approach, graphical techniques will be shown to be useful in visually characterizing the interactions between the agents.

Assume for the following that the fitted model, based on (5.6.1), is given by

$$\begin{aligned} \log \text{it}[\hat{P}(\mathbf{X}, \hat{\boldsymbol{\beta}})] = & \hat{\beta}_0 + \sum_{i=1}^N \hat{\beta}_i X_i + \sum_{i=1}^{N-1} \sum_{j=i+1}^N \hat{\beta}_{ij} X_i X_j + \sum_{i=1}^{N-2} \sum_{j=i+1}^{N-1} \sum_{k=j+1}^N \hat{\beta}_{ijk} X_i X_j X_k + \\ & \cdots + \hat{\beta}_{123 \dots N} X_1 X_2 \cdots X_N. \end{aligned} \quad (5.6.3)$$

A fitted model under additivity is also given by

$$\log \text{it}[\hat{P}^A(\mathbf{X}, \hat{\boldsymbol{\beta}})] = \hat{\beta}_0 + \sum_{i=1}^N \hat{\beta}_i X_i \quad (5.6.4)$$

### 5.6.1 Point-Wise Interpretation of the Interactions in an N Agent Model

Based on the Comparison Method described in Section 4.3, the interactions in this N agent model can be described in a point wise fashion. Let  $\mathbf{x} = (x_1, x_2, \dots, x_N)$  denote a fixed dose combination. At this fixed dose combination, the response predicted by the full model  $\hat{P}(\mathbf{x}, \hat{\boldsymbol{\beta}})$  can be compared to the response expected under the assumption of additivity,  $\hat{P}^A(\mathbf{x}, \hat{\boldsymbol{\beta}})$ . Since it has been assumed each single agent dose-response curve is monotonically increasing, based on Definition 4.3.2, if  $\hat{P}(\mathbf{x}, \hat{\boldsymbol{\beta}}) > \hat{P}^A(\mathbf{x}, \hat{\boldsymbol{\beta}})$ , synergism is

suggested, and if  $\hat{P}(\mathbf{x}, \hat{\boldsymbol{\beta}}) < \hat{P}^A(\mathbf{x}, \hat{\boldsymbol{\beta}})$ , there is evidence of an antagonism. Of course the differences between  $\hat{P}(\mathbf{x}, \hat{\boldsymbol{\beta}})$  and  $\hat{P}^A(\mathbf{x}, \hat{\boldsymbol{\beta}})$  may be due to random fluctuations. In the next chapter a testing procedure will be introduced that can be applied in a point-wise fashion to detect significant differences from additivity. Here a graphical procedure will be introduced that can be used to determine regions of the N-dimensional dose space where synergism, antagonism and additivity are suggested. This graphical technique uses the parallel axis system defined in Section 2.5.

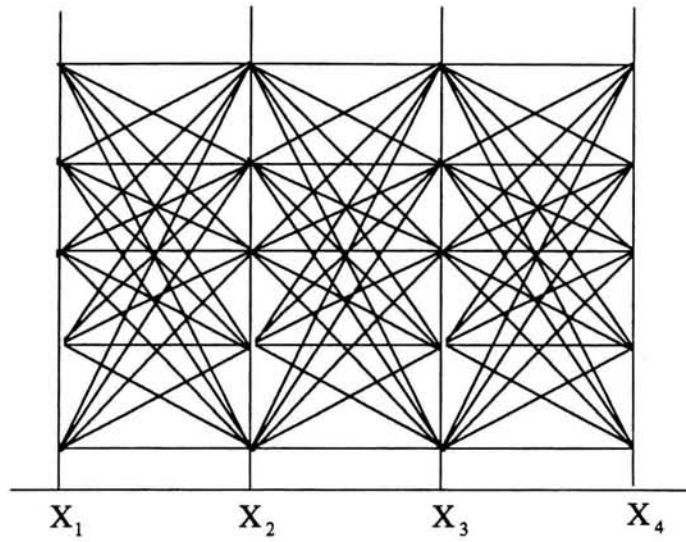
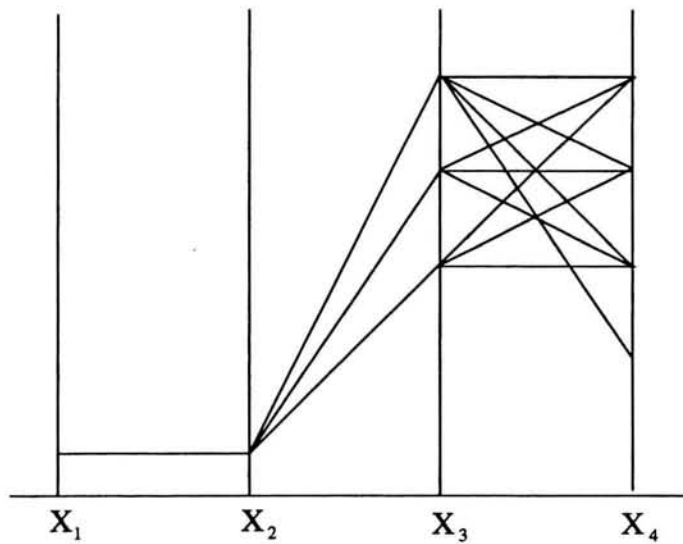
For illustrative purposes assume the 4-dimensional fitted model is given by

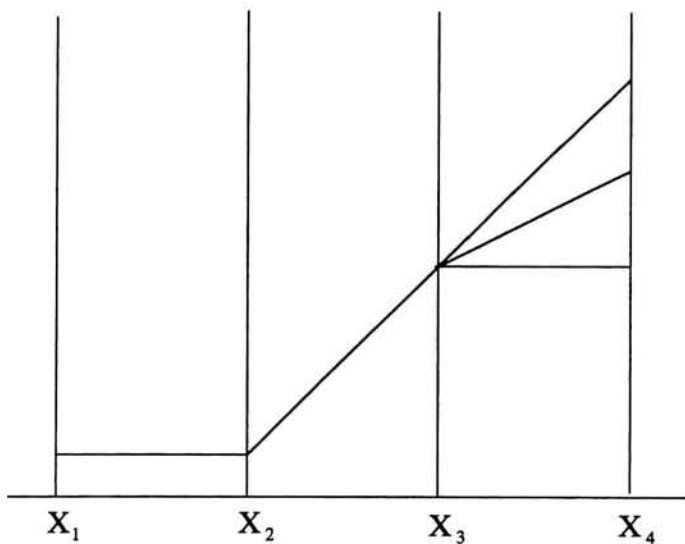
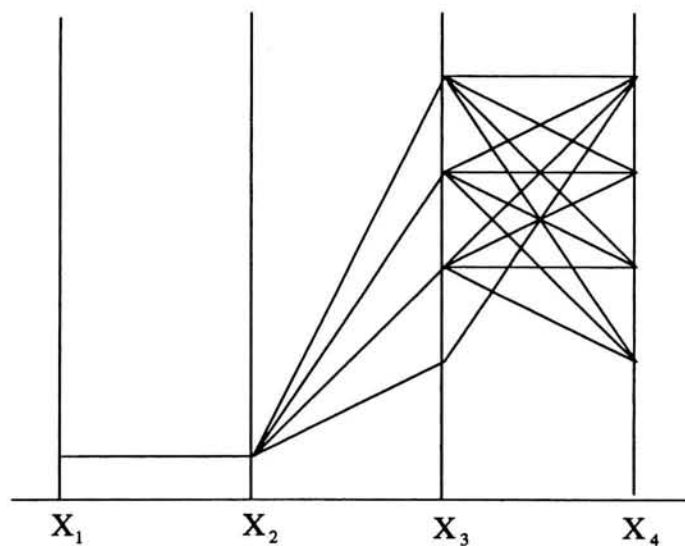
$$\begin{aligned} \logit[P(\mathbf{X}; \hat{\boldsymbol{\beta}})] = & -20 + 2X_1 + 5X_2 + 7X_3 + 4X_4 + .75X_1X_2 + .8X_1X_3 \\ & + .65X_1X_4 - .3X_2X_3 + .6X_2X_4 - .5X_3X_4 + .5X_1X_2X_3 \\ & + .55X_1X_2X_4 - .4X_1X_3X_4 + .45X_2X_3X_4 + .85X_1X_2X_3X_4 \end{aligned} \quad (5.6.5)$$

where  $0 \leq X_i \leq 3.0$ ,  $i=1,2,3,4$ . The fitted model under additivity is given by

$$\logit[P^A(\mathbf{X}; \hat{\boldsymbol{\beta}})] = -20 + 2X_1 + 5X_2 + 7X_3 + 4X_4 \quad (5.6.6)$$

Two parallel axis plots can be used to determine regions in this dose-space that are suggestive of departures from additivity.  $\hat{P}(\mathbf{x}, \hat{\boldsymbol{\beta}})$  and  $\hat{P}^A(\mathbf{x}, \hat{\boldsymbol{\beta}})$  are calculated at points that satisfy a grid-like pattern in the dose-range. In Figure 5.8(a) the set of points suggesting synergism, i.e., where  $\hat{P}(\mathbf{x}, \hat{\boldsymbol{\beta}}) > \hat{P}^A(\mathbf{x}, \hat{\boldsymbol{\beta}})$ , are plotted. No distinct regions in the dose space are identified in this case. Alternatively in Figure 5.8(b) the antagonistic points are plotted. From this figure a region of antagonism can be identified for low doses of  $X_1$  and  $X_2$  in combination with high doses of  $X_3$  and  $X_4$ . This is verified in Figure 5.9 where only doses in that region were considered. This type of plotting technique can also be used

**Figure 5.8(a): Synergism****Figure 5.8(b): Antagonism****Figure 5.8:** Regions of Synergism and Antagonism for Model Given in (5.6.5) and  $X_i = 0.5, 1.0, 1.5, 2.0, 2.5; i = 1, 2, 3, 4$

**Figure 5.9(a): Synergism****Figure 5.9(b): Antagonism**

**Figure 5.9:** Regions of Synergism and Antagonism for Model Given in (5.6.5) and  $X_1 = 0.25$ ,  $X_2 = 0.25$ ,  $X_3, X_4 = 1, 1.5, 2, 2.5$



to examine combinations associated with a range of predicted responses, i.e.,  $0.4 < \hat{P}(\mathbf{x}, \hat{\boldsymbol{\beta}}) < 0.6$ . In either application the investigator may be able to isolate regions of the higher dimensional dose-space where synergism and antagonism are suggested. These regions in the dose-space may then be studied in more detail in future experiments.

### 5.6.2 Interactions in an N Agent Model at Varying Doses of a Single Agent

This approach to describing the interactions can be considered an extension to the point-wise approach just described. In an N agent study, the dose-response relationship for a single agent can be examined at fixed levels of the remaining (N - 1) agents. For example, in a 4-agent fitted model based on (5.6.3), suppose  $X_1$  was allowed to vary when the remaining agents are fixed at  $X_i = a_i, i = 2, 3, 4$ , where  $a_i$  is in the experiment dose space for the  $i$ th agent. Hence, the fitted model and the model under additivity can be written as

$$\begin{aligned} \logit[P(X_1, \hat{\boldsymbol{\beta}})] = & \hat{\beta}_0 + \hat{\beta}_2 a_2 + \hat{\beta}_3 a_3 + \hat{\beta}_4 a_4 + \hat{\beta}_{23} a_2 a_3 + \hat{\beta}_{24} a_2 a_4 + \hat{\beta}_{234} a_2 a_3 a_4 \\ & + (\hat{\beta}_1 + \hat{\beta}_{12} a_2 + \hat{\beta}_{13} a_3 + \hat{\beta}_{14} a_4 + \hat{\beta}_{123} a_2 a_3 + \hat{\beta}_{124} a_2 a_4 + \hat{\beta}_{1234} a_2 a_3 a_4) X_1. \end{aligned} \quad (5.6.7)$$

and

$$\logit[P^A(X_1, \hat{\boldsymbol{\beta}})] = (\hat{\beta}_0 + \hat{\beta}_2 a_2 + \hat{\beta}_3 a_3 + \hat{\beta}_4 a_4) + \hat{\beta}_1 X_1. \quad (5.6.8)$$

The type of interaction between the agents when  $X_i = a_i, i = 2, 3, 4$ , as  $X_1$  increases, can be assessed by comparing  $P^A(X_1, \hat{\boldsymbol{\beta}})$  to  $P(X_1, \hat{\boldsymbol{\beta}})$ . By examining (5.6.7) and (5.6.8) it is apparent that the type of interaction may change as  $X_1$  varies.

In order to graphically summarize this,  $P^A(X_1, \hat{\beta})$  and  $P(X_1, \hat{\beta})$  can be jointly plotted over levels of  $X_1$ . For example, in Figure 5.10(a),  $X_2 = X_3 = X_4 = 1$  in the fitted model given in (5.6.5). There synergism is suggested over all levels of  $X_1$ . Alternatively in Figure 5.10(b), where  $X_2 = 0.1$ ,  $X_3 = 2$ , and  $X_4 = 1$ , the type of interaction changes from antagonism to synergism. Hence, using these plots, the effects of increasing levels of a single agent, at fixed levels of the other agents, can be visually summarized. This may be particularly useful in applications where the goal is to examine the effect of various levels of a new agent in combination with another compound.

### 5.6.3 Pair-Wise Interactions in an N Agent Model

Another approach to describing the interactions between the agents in the N agent model given in (5.6.3) is in a pair-wise manner. Assume the investigator is interested in determining how  $X_i$  and  $X_j$  interact at various fixed levels of the  $N - 2$  remaining agents. Let  $X_k = a_k$ ,  $k = 1, 2, \dots, N$ ;  $k \neq i, j$  where  $a_k$  is at fixed dose level in the experimental dose-range for the  $k$ th agent. The fitted model in (5.6.3) can then be simplified into an expression that involves only  $X_i$  and  $X_j$  and is given by

$$\log \text{it}[\hat{P}(X_i, X_j, \hat{C})] = \hat{C}_0 + \hat{C}_i X_i + \hat{C}_j X_j + \hat{C}_{ij} X_i X_j \quad (5.6.9)$$

where

$$\hat{C}_0 = \hat{\beta}_0 + \sum_{\substack{k=1 \\ k \neq i, j}}^N \hat{\beta}_k a_k$$

$$\hat{C}_i = \hat{\beta}_i + \sum_{\substack{j=1 \\ k \neq i}}^N \hat{\beta}_{ik} a_k + \sum_{\substack{l=k+1 \\ l \neq i, j}}^N \sum_{\substack{k=1 \\ k \neq i, j}}^{N-1} \hat{\beta}_{ijk} a_j a_k + \dots$$

**Figure 5.10(a):**  $0 \leq X_1 \leq 3, X_2 = X_3 = X_4 = 1$

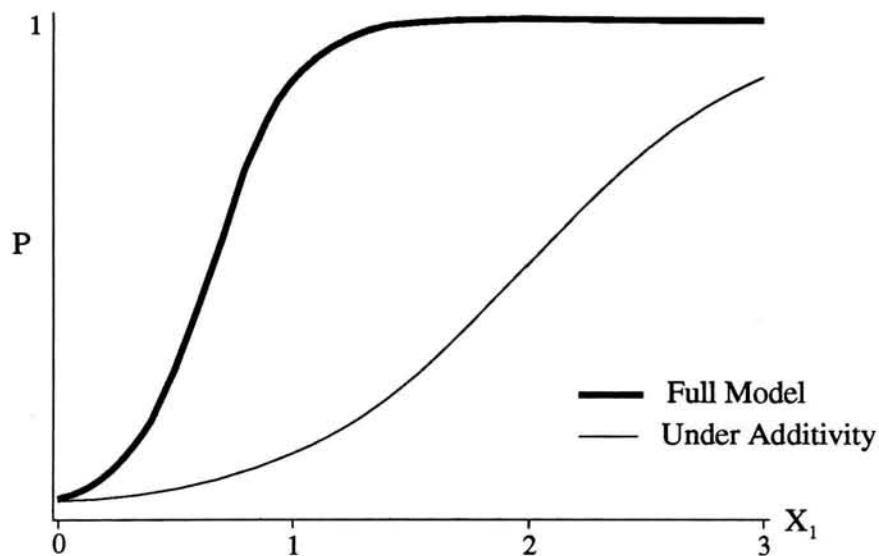


**Figure 5.10(b):**  $0 \leq X_1 \leq 3, X_2 = 0.1, X_3 = 2, X_4 = 1$

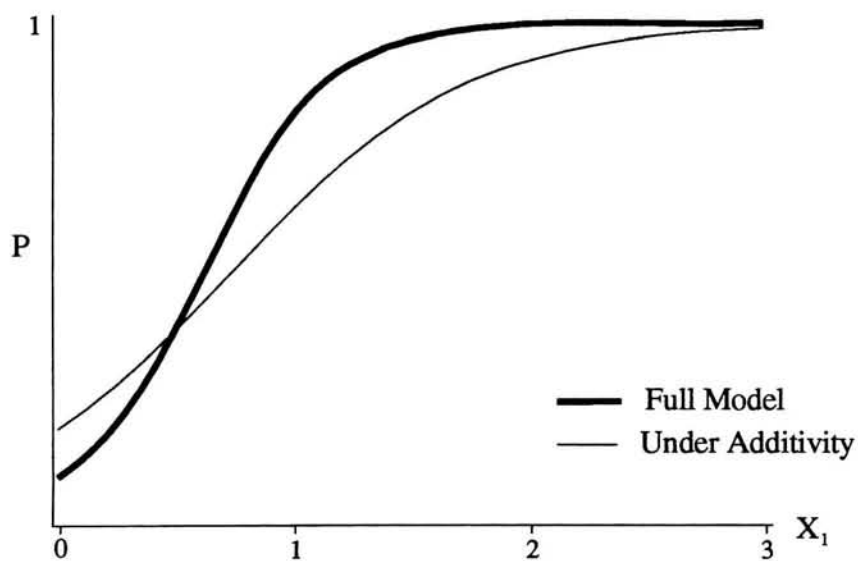


**Figure 5.10:** Full Model Versus Model Under Additivity Over Levels of  $X_1$  at Fixed Levels  $X_2, X_3,$  and  $X_4$  - Model Given in (5.6.5)

$$\hat{C}_j = \hat{\beta}_j + \sum_{\substack{k=1 \\ k \neq i}}^N \hat{\beta}_{jk} a_k + \sum_{\substack{l=k+1 \\ l \neq i, j}}^N \sum_{\substack{k=1 \\ k \neq i, j}}^{N-1} \hat{\beta}_{jkl} a_k a_l + \dots$$

$$\hat{C}_{ij} = \hat{\beta}_{ij} + \sum_{\substack{k=1 \\ k \neq i, j}}^N \hat{\beta}_{ijk} a_k + \sum_{\substack{l=k+1 \\ l \neq i, j}}^N \sum_{\substack{k=1 \\ k \neq i, j}}^{N-1} \hat{\beta}_{ijkl} a_k a_l + \dots$$

Note that (5.6.9) describes a two agent fitted model. Therefore the interactions between  $X_i$  and  $X_j$  at the fixed levels of the other agents can be made based on an examination of the sign of  $\hat{C}_{ij}$ . An isobologram can also be used to visually characterize the deviation from additivity between  $X_i$  and  $X_j$  when  $X_k = a_k$ ,  $k = 1, 2, \dots, N$ ;  $k \neq i, j$

By allowing the levels of the other agents to vary and simultaneously plotting the resulting  $X_i$ ,  $X_j$  isobols on the same set of axes the pair-wise interaction can be summarized graphically over various levels of these other agents. In general, the fixed levels of the other agents are chosen to adequately cover the dose space of interest. To summarize the interactions described by the entire model, the technique described for the  $X_i$ ,  $X_j$  pair of agents can be repeated for all unique pairs of agents. The isobolograms can be displayed in the array of pair-wise plots.

To simplify these plots the lines of additivity are eliminated. Note, however, that for homergic combinations the types of interactions between  $X_i$  and  $X_j$  at the fixed levels of the remaining agents can still be described by examining only the isobol. As demonstrated in Section 5.4.1 a linear isobol indicates additivity, an isobol that intersects each axis and is concave up (down) indicates synergism (antagonism). A discontinuous isobol indicates an antagonism.

In Figure 5.11 this technique is illustrated for the 4-agent fitted model given in (5.6.5). Since this fitted model includes both positive and negative interaction terms, the

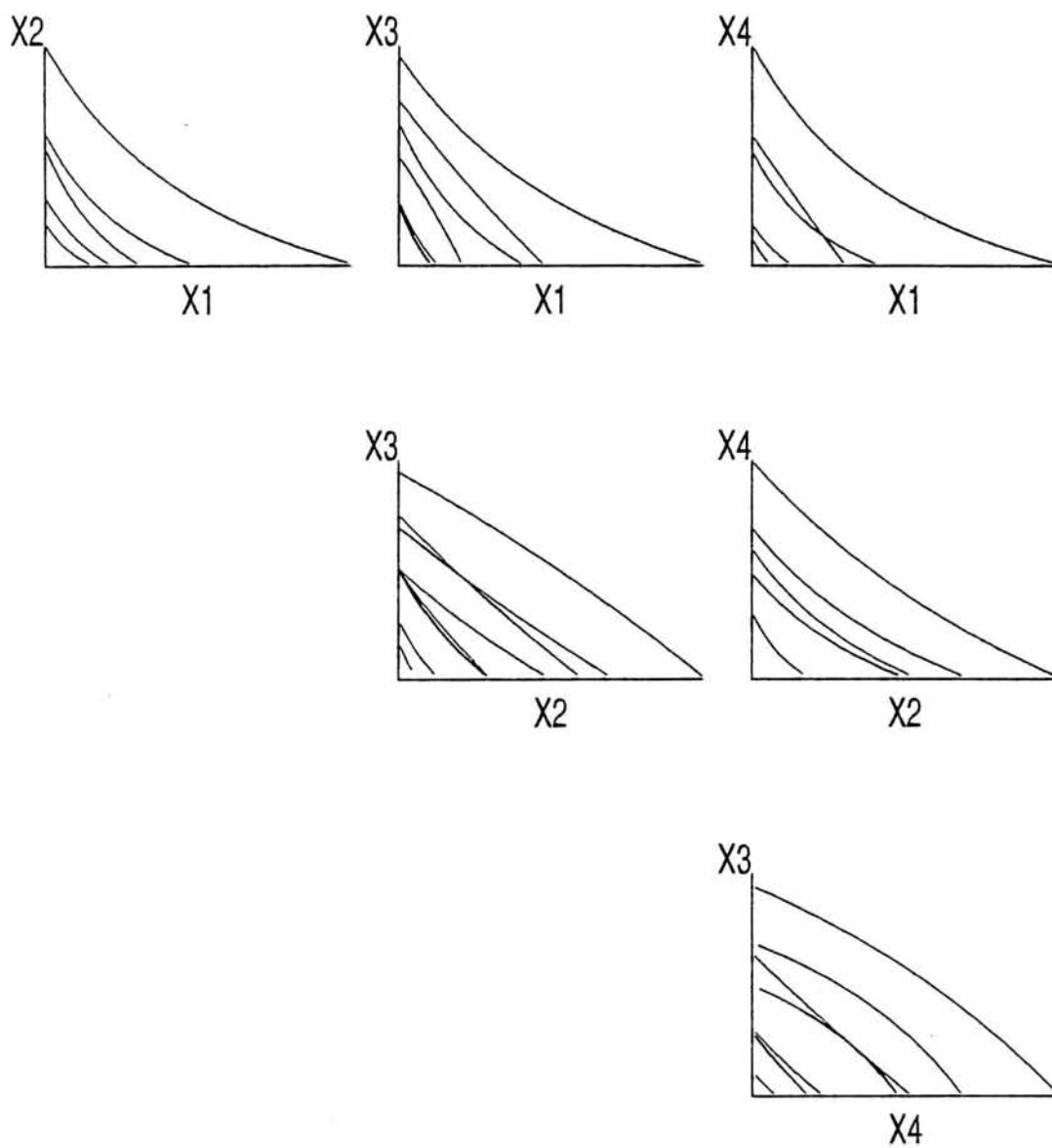


**Figure 5.11:** Draftman's Display of Pairwise Isobols ( $\pi = 0.5$ )  
Model Given in (5.6.5)

character of the interaction between pairs of agents may change over fixed levels of the remaining two agents. By examining the array of plots, it appears that synergism exists between  $X_1$  and  $X_2$  at all levels of  $X_3$  and  $X_4$  considered. This is in contrast to the interactions between  $X_3$  and  $X_4$ , which at certain levels of  $X_1$  and  $X_2$  may be synergistic or antagonistic.

Note that if the original model contained cross product terms that included powers of  $X_i$  and/or  $X_j$  the resulting simplified expression, analogous to (5.6.9), will include terms in the form  $X_i^k$ . In Chapter 4 it was shown that the type of interactions between the agents could not be described when non-monotonic single agent dose-response curves were considered. The inclusion of the term  $X_i^k$  in the resulting model implies the resulting single agent dose-response under the constraints described may not be monotonic. Hence this pair-wise approach to describing interactions will be most useful in cases when the model contains strictly first-order cross product terms.

This array of pair-wise plots can also be shown to be equivalent to a parallel axis plotting technique described by Gennings et al. (1990). Here it was shown that the isobol from an N-agent logistic model with first-order cross product terms can be represented in a parallel axis system by a set of curves. Assume a parallel axis system is embedded in a X-Y Cartesian coordinate system. Hence, a point in the parallel axis system can be referenced by the appropriate coordinates (x,y). This set of curves is defined as follows. For a fixed value of the response,  $\pi$ , the relationship between  $X_i$  and  $X_j$  for fixed levels of the other agents given in (5.6.9) can be written as

$$X_j = f_i(X_i) = \frac{\text{logit}(\pi) - \hat{C}_0 - \hat{C}_i X_i}{\hat{C}_j + \hat{C}_{ij} X_i} \quad (5.6.10)$$

where  $X_i \in \left(0, \frac{\text{logit}(\pi) - \hat{C}_0}{\hat{C}_i}\right)$ . For  $X_i$  in this interval,  $f_i(X_i)$  is discontinuous at one point if  $\frac{-\hat{C}_j}{\hat{C}_{ij}} \in \left(0, \frac{\text{logit}(\pi) - \hat{C}_0}{\hat{C}_i}\right)$ . Assume, for now, that  $\frac{-\hat{C}_j}{\hat{C}_{ij}} \notin \left(0, \frac{\text{logit}(\pi) - \hat{C}_0}{\hat{C}_i}\right)$  so that  $f_i$  is continuous in this interval. Assuming the  $X_i$  and  $X_j$  parallel axes are adjacent and plotted in the  $X$ - $Y$  plane as vertical lines at  $X = k$  and  $X = k+1$  a parallel axis representation of  $f_i$  is given by the curve defined by

$$S(X, Y; C) = \left\{ (X, Y) : X = \frac{1}{1 - f'_i(X_i)} + k, Y = \frac{f_i(X_i) - X_i f'_i(X_i)}{1 - f'_i(X_i)}, X_i \in \left(0, \frac{\text{logit}(\pi) - \hat{C}_0}{\hat{C}_i}\right) \right\}.$$

Since

$$f'_i(X_i) = \frac{\partial f_i(X_i)}{\partial X_i} = \frac{-\hat{C}_i \hat{C}_j - (\text{logit}(\pi) - \hat{C}_0) \hat{C}_{ij}}{(\hat{C}_j + \hat{C}_{ij} X_i)^2} = \frac{-\hat{C}_i - \hat{C}_{ij} X_j}{\hat{C}_j + \hat{C}_{ij} X_i}$$

it follows that

$$S(X, Y; C) = \left\{ \begin{array}{l} (X, Y) : X = \frac{\hat{C}_j + \hat{C}_{ij} X_i}{\hat{C}_i + \hat{C}_j + \hat{C}_{ij} (X_i + X_j)} + k, Y = \frac{\text{logit}(\pi) - \hat{C}_0 + \hat{C}_{ij} X_i X_j}{\hat{C}_i + \hat{C}_j + \hat{C}_{ij} (X_i + X_j)}; \\ 0 \leq X_i \leq \frac{\text{logit}(\pi) - \hat{C}_0}{\hat{C}_i}, X_j = \frac{\text{logit}(\pi) - \hat{C}_0 - \hat{C}_i X_i}{\hat{C}_j + \hat{C}_{ij} X_i} \end{array} \right\}.$$

In the case that  $\frac{-\hat{C}_j}{\hat{C}_{ij}} \in \left(0, \frac{\text{logit}(\pi) - \hat{C}_0}{\hat{C}_i}\right)$  the parallel axis representation,  $S(X, Y; \hat{C})$ , will consist of  $S(X, Y; \hat{C}) = S_1(X, Y; \hat{C}) \cup S_2(X, Y; \hat{C})$  where  $S_1(X, Y; \hat{C})$  is the curve derived as

above for  $X_i \in \left(0, \frac{-\hat{C}_j}{\hat{C}_{ij}}\right)$  and  $S_2(X, Y; \hat{C})$  for  $X_i \in \left(\frac{-\hat{C}_j}{\hat{C}_{ij}}, \frac{\text{logit}(\pi) - \hat{C}_0}{\hat{C}_i}\right)$ . This resulting

pair of curves is similar to a plot of a discontinuous isobol in the usual Cartesian plane (see Figure 5.4(c)). Note, however, that  $S(X, Y; \hat{C})$  does not exist when  $f_i'(X_i)=1$ .

Therefore, for a fixed value of the response and when  $X_k = a_k$ ,

$k = 1, 2, \dots, N; k \neq i, j$ , the resulting pair-wise isobol between  $X_i$  and  $X_j$  can be graphically represented in both the  $X_i \times X_j$  Cartesian plane and in a parallel axis system relative to the  $X_i, X_j$  adjacent pairs of axes.

It was also shown by Gennings, et al. (1990) that properties of  $S(X, Y; \hat{C})$  are associated with the sign of the  $\hat{C}_{ij}$  term and hence from deviations from additivity. These results are summarized in Table 5.1. For example, if a concave up curve appears between the  $X_i$  and  $X_j$  parallel axes, an antagonism exists between  $X_i$  and  $X_j$  when  $X_k = a_k$ ,

$k = 1, 2, \dots, N; k \neq i, j$ .

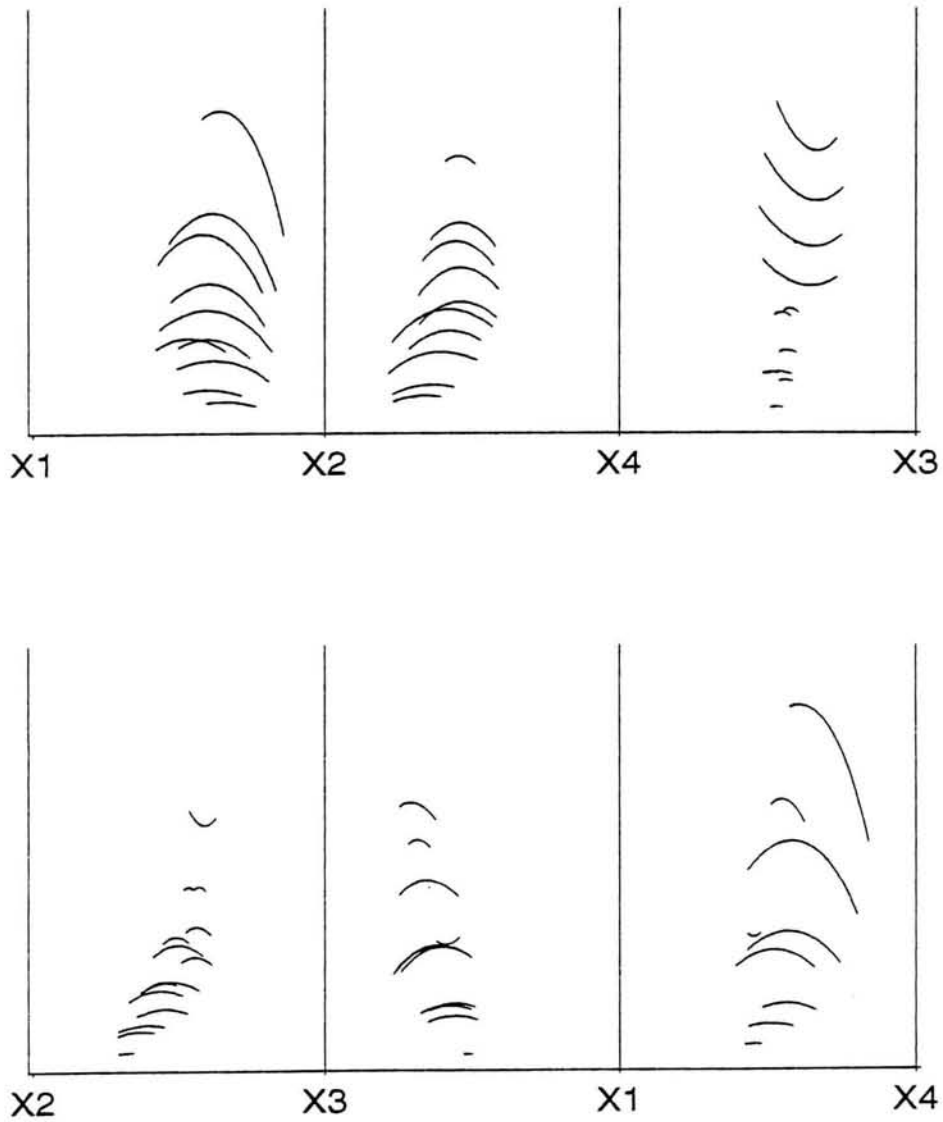
In a manner similar to the pair-wise array of plots all pairs of agents can now be considered at various fixed levels of the other agents. A set of curves will be constructed for each pair-wise relationship  $X_j = f_i(X_i)$ . An example of this method is shown in Figure 5.12 for the fitted 4 agent model given in (5.6.5). So that all pair-wise combinations of agents can be viewed using a minimal set of axes, the axes are ordered in two parallel plots according to an algorithm by Wegman (1990). Since all of the curves between the  $X_1$  and  $X_3$  axes are concave down, a synergism is indicated between these agents at all fixed level of  $X_2$  and  $X_4$  considered. In contrast, the concavity of the curves between the  $X_2$  and  $X_3$  axis changes, so that synergism and antagonism is indicated at various fixed levels of  $X_1$  and  $X_4$ .



Table 5.1

Parallel Axis Representation of  $X_i$   $X_j$  Isobol

| $f'_i(X_i)$            | Horizontal Position in Parallel System   | $\hat{\beta}_{ij}$     | Concavity in parallel system | Type Interaction |
|------------------------|--|------------------------|------------------------------|------------------|
| $f'_i(X_i) \leq 0$     | Between the two parallel axes<br>( $f'_i(X_i) < 0$ ) or<br>coincident with the $X_j$<br>axis ( $f'_i(X_i) = 0$ ) | $\hat{\beta}_{ij} > 0$ | Concave down                 | Synergism        |
|                        |  | $\hat{\beta}_{ij} < 0$ | Concave up                   | Antagonism       |
| $0 \leq f'_i(X_i) < 1$ | To the right of<br>( $f'_i(X_i) \neq 0$ ) or<br>coincident with<br>( $f'_i(X_i) = 0$ ) the $X_j$ axis            | $\hat{\beta}_{ij} < 0$ | Concave down                 | Synergism        |
|                        |  | $\hat{\beta}_{ij} > 0$ | Concave up                   | Antagonism       |
| $f'_i(X_i) = 1$        | S does not exist   |                        |                              |                  |
| $f'_i(X_i) > 1$        | To the left of $X_j$ parallel<br>axis  | $\hat{\beta}_{ij} < 0$ | Concave up                   | Antagonism       |
|                        |  | $\hat{\beta}_{ij} > 0$ | Concave down                 | Synergism        |



**Figure 5.12:** Parallel Axis Display of Pairwise Isobols ( $\pi = 0.5$ )  
Model Given in (5.6.5)

It can now be shown that with the exception of the points of discontinuity, a 1-1 correspondence exists between the points on the parallel axis representation,  $S$ , and points in the usual Cartesian pair-wise plot of the isobol.

**Result 5.3.1:** Assume the fitted model for an  $N$  agent study is given by (5.6.9) where  $X_k = a_k$ ,  $k = 1, 2, \dots, N$ ;  $k \neq i, j$ . For  $\pi$  a fixed response, let  $I_\pi(X_i, X_j; \hat{C})$  denote the set of points that satisfy the  $X_i, X_j$  isobol,

$$I_\pi(X_i, X_j; \hat{C}) = \left\{ (X_i, X_j) : X_j = \frac{\text{logit}(\pi) - \hat{C}_0 - \hat{C}_i X_i}{\hat{C}_j + \hat{C}_{ij} X_i}, 0 < X_i < \frac{\text{logit}(\pi) - \hat{C}_0}{\hat{C}_i} \right\}.$$

Let  $S(X, Y; \hat{C})$  be the set of points in the parallel axis system corresponding the  $X_i, X_j$  isobol,

$$S(X, Y; \hat{C}) = \left\{ \begin{array}{l} (X, Y) : X = \frac{\hat{C}_j + \hat{C}_{ij} X_i}{\hat{C}_i + \hat{C}_j + \hat{C}_{ij}(X_i + X_j)} + k, \\ Y = \frac{\text{logit}(\pi) - \hat{C}_0 + \hat{C}_{ij} X_i X_j}{\hat{C}_i + \hat{C}_j + \hat{C}_{ij}(X_i + X_j)}; \\ 0 \leq X_i \leq \frac{\text{logit}(\pi) - \hat{C}_0}{\hat{C}_i}, X_j = \frac{\text{logit}(\pi) - \hat{C}_0 - \hat{C}_i X_i}{\hat{C}_j + \hat{C}_{ij} X_i} \end{array} \right\}. \quad (5.6.11)$$

A 1-1 correspondence exists between a continuous point  $(X, Y) \in S(X, Y; \hat{C})$  and a continuous point  $(X_i, X_j) \in I_\pi(X_i, X_j; \hat{C})$ .

**Proof:**

Let  $(X_i, X_j) \in I_{\pi}(X_i, X_j; \hat{C})$ . Then by definition (5.6.11) a unique point

$(X, Y) \in S(X, Y; \hat{C})$  is determined.

Let  $(X, Y) \in S(X, Y; \hat{C})$ . By definition, (5.6.11)  $X$  and  $Y$  are uniquely determined

from values  $(X_i, X_j)$  such that  $(X_i, X_j) \in I_{\pi}(X_i, X_j; \hat{C})$ .

One advantage of using the array of Cartesian coordinate plots is the interpretability of the points in this plotting system; a point in these plots represents the dose combination of  $X_i$  and  $X_j$  which together with the fixed levels of the other agents yields the response of interest. In the parallel axis system these dose levels are not apparent from the plot, even in cases when all of the agents are measured on the same scale. It can be argued, however, that the type of deviation from additivity is more apparent in the parallel axis plots. For example, in the array of pair-wise plots a small degree of curvature in an isobol could be misinterpreted as linear. In the parallel plot the antagonism is clearly indicated.

In this chapter it has been shown that response-surface techniques are useful in detecting and characterizing the interactions between the agents considered. For the two agent study it was shown that when the model contained only a single interaction term the type of interaction between the agents could be characterized by examining the sign of the estimated cross-product parameter,  $\hat{\beta}_{12}$ . In addition, the isobologram was shown to be useful for graphically interpreting these models. When  $N$  agents are considered the interpretation of the model becomes more difficult, i.e., when the signs of the parameters associated with the cross-product terms vary, the type of interaction that the model suggests depends on the level of response and the dose combinations considered. Several graphical techniques were shown to be useful in characterizing the interactions that the fitted model describes. When applying these techniques to studies that involve a large number of agents, however, the number of possible cross product terms increases. It follows that in

order to estimate these parameters adequately the number of dose combinations considered must increase. In fact, in Chapter 1 it was noted that the size of the experiments in these type of studies can become economically unfeasible when a large number of agents is considered. In Chapter 7 a technique will be introduced that allows the detection and characterization of interactions between a large number of agents but with far fewer observations.

## Chapter 6

### A Point-Wise Test to Detect Interactions

#### 6.1 Introduction

In the last chapter response-surface techniques were used to examine the interactions that might exist among the agents in a combination. There the model,

$$P(\mathbf{X};\boldsymbol{\beta}) = \frac{1}{1 + \exp(-\mathbf{X}\boldsymbol{\beta})},$$

was fit to the data where  $\mathbf{X}$  is a vector of doses and cross-product terms involving the doses, and  $\boldsymbol{\beta}$  was the vector of unknown parameters. For the two agent logistic model, with a single cross product term, it was shown that the type of interaction could be determined by simply examining the sign of the estimated parameter associated with the cross-product term, i.e.,  $\hat{\beta}_{12}$ . Nonadditivity was also indicated for the N-agent experiment when one or more cross-product terms were included in the fitted model.

It will now be shown that this interpretation of the logistic response-surface model does not generalize to the case when the model is fit in terms of an arbitrary transformation of the doses. A point-wise testing procedure is therefore developed in this chapter which can be used to detect significant nonadditivity.

## 6.2 Characterizing the Interactions When the Response-Surface Model is Based on a Transformation of the Doses

It will be useful to briefly review the arguments applied in the last chapter for a two agent homergic combination. Assume the following response-surface model which is a function of the doses of both agents:

$$\text{logit}[P(X_1, X_2; \boldsymbol{\beta})] = \beta_0 + \beta_1 X_1 + \beta_2 X_2 + \beta_{12} X_1 X_2. \quad (6.2.1)$$

For a fixed level of the response,  $\pi$ , the interaction index is given by

$$II(X_1, X_2, \pi; \boldsymbol{\beta}) = \frac{\beta_1 X_1}{\text{logit}(\pi) - \beta_0} + \frac{\beta_2 X_2}{\text{logit}(\pi) - \beta_0}. \quad (6.2.2)$$

At the same fixed level of the response,  $\pi$ , the model given in (6.2.1) can also be rewritten as

$$\frac{\beta_1 X_1}{\text{logit}(\pi) - \beta_0} + \frac{\beta_2 X_2}{\text{logit}(\pi) - \beta_0} = 1 - \frac{\beta_{12} X_1 X_2}{\text{logit}(\pi) - \beta_0}. \quad (6.2.3)$$

By comparing (6.2.2) and (6.2.3) and then applying Result 4.3.4 the type of interaction can be determined by examining the sign of  $\beta_{12}$ .

Suppose, now, that, based on a goodness-of-fit procedure, it is determined that the model given in (6.2.1) does not adequately fit the data. An alternative approach could be to write the model in terms of a transformation of the doses, e.g.,  $Z_i = \ln(X_i + 1)$ . In general, assume  $Z_i = g(X_i)$  where  $g^{-1}$  exists. Now, analogously to (6.2.3), the model can be written as

$$\frac{\beta_1 g(X_1)}{\text{logit}(\pi) - \beta_0} + \frac{\beta_2 g(X_2)}{\text{logit}(\pi) - \beta_0} = 1 - \frac{\beta_{12} g(X_1) g(X_2)}{\text{logit}(\pi) - \beta_0} \quad (6.2.4)$$

The interaction index, which is defined in terms of doses, can also be written as

$$II(\mathbf{X}, \pi; \boldsymbol{\beta}) = \frac{X_1}{g^{-1}\left(\frac{\text{logit}(\pi) - \beta_0}{\beta_1}\right)} + \frac{X_2}{g^{-1}\left(\frac{\text{logit}(\pi) - \beta_0}{\beta_2}\right)}. \quad (6.2.5)$$

If  $g^{-1}$  is a linear function, the expressions given in (6.2.4) and (6.2.5) can be simplified, so as before, the type of interaction can be characterized by examining the the sign of  $\beta_{12}$ . In general, however, the expressions given in (6.2.4) and (6.2.5) can not be simplified in this manner. Hence, the sign of the cross product parameter can not be used in this case to detect and characterize a nonadditive interaction between the agents.

As a specific example assume that  $Z_i = g(X_i) = \ln(X_i + 1)$  so that  $X_i = g^{-1}(Z_i) = e^{Z_i} - 1$ . The model and the interaction index can be written by

$$\frac{\beta_1 \ln(x_1 + 1)}{\text{logit}(\pi) - \beta_0} + \frac{\beta_2 \ln(x_2 + 1)}{\text{logit}(\pi) - \beta_0} = 1 - \frac{\beta_{12} \ln(x_1 + 1) \ln(x_2 + 1)}{\text{logit}(\pi) - \beta_0}. \quad (6.2.6)$$

$$II(\mathbf{X}, \pi; \boldsymbol{\beta}) = \frac{X_1}{\exp\left(\frac{\text{logit}(\pi) - \beta_0}{\beta_1}\right) - 1} + \frac{X_2}{\exp\left(\frac{\text{logit}(\pi) - \beta_0}{\beta_2}\right) - 1}. \quad (6.2.7)$$

Here, it is not possible to simplify these expressions so that the the model in (6.2.6) can be written in terms of the interaction index in (6.2.7).

An alternative approach is to examine, in a point-wise fashion, the value of the interaction index. Let  $\mathbf{x}$  denote a fixed dose combination. Let  $\pi_{\text{obs}}$  denote the associated



observed response at  $\mathbf{x}$ . Then, by Result 4.3.4, if the interaction index does not equal 1, a nonadditive interaction is suggested, with values greater (less) than 1 indicating synergism (antagonism). To determine if the difference from 1 is not due to random fluctuations in the data, a testing procedure will be developed in the next section.

### 6.3 The Interaction Index Test

Consider now an N-dimensional homergic combination or a N-dimensional heterergic combination of predictive and inert agents. Since the interaction index is undefined for coalitive combinations, this approach can not be applied to those combinations. Let  $\mathbf{x} = (x_1, x_2, \dots, x_N)$  denote a dose combination and  $\pi_{\text{obs}}$  the observed response at that combination. Let  $Z_i = g(X_i)$  so that  $X_i = g^{-1}(Z_i)$ . In general, the interaction index can be written by

$$II(\mathbf{x}, \pi_{\text{obs}}) = \sum_{i=1}^N \frac{x_i}{ED_i(\pi_{\text{obs}})} \quad (6.3.1)$$

where  $ED_i(\pi_{\text{obs}})$  is the effective dose of the  $i$ th agent associated with  $\pi_{\text{obs}}$ . To estimate the effective doses for the agents, the following model, which relies on data for each agent alone, can be used. Assuming a common baseline parameter,  $\beta_0$ , this model simultaneously estimates each single agent's dose response curve. Let

$$\text{logit}[P(\mathbf{Z};\boldsymbol{\beta})] = \mathbf{Z}\boldsymbol{\beta} \quad (6.3.2)$$

where

$$\mathbf{Z} = \begin{bmatrix} 1 & z_{11} & 0 & \cdots & 0 \\ 1 & z_{12} & 0 & \cdots & 0 \\ \vdots & \vdots & \vdots & \vdots & \vdots \\ 1 & z_{1m_1} & 0 & 0 & 0 \\ 1 & 0 & z_{21} & 0 & 0 \\ 1 & 0 & z_{22} & 0 & 0 \\ \vdots & \vdots & \vdots & \vdots & \vdots \\ 1 & 0 & z_{2m_2} & \cdots & 0 \\ \vdots & \vdots & \vdots & \vdots & \vdots \\ 1 & 0 & 0 & \cdots & z_{N1} \\ 1 & 0 & 0 & \cdots & z_{N2} \\ \vdots & \vdots & \vdots & \vdots & \vdots \\ 1 & 0 & 0 & \cdots & z_{Nm_N} \end{bmatrix}, \quad \boldsymbol{\beta} = (\beta_0 \beta_1 \beta_2 \cdots \beta_N)'$$

and  $m_i, i=1,2,\dots,N$ , is the number of nonzero observations for the  $i$ th agent alone.

Alternatively, this model can be written as

$$\text{logit}[P(Z_i;\boldsymbol{\beta})] = \beta_0 + \beta_i Z_i; \quad Z_i \geq 0, \quad i = 1,2,\dots,N; \quad Z_j = 0, \quad j = 1,2,\dots,N, \quad j \neq i.$$

Using this model, the effective doses and the interaction index can now be derived and are given by

$$ED_i(\pi_{\text{obs}}) = g^{-1}\left(\frac{\text{logit}(\pi_{\text{obs}}) - \beta_0}{\beta_i}\right) \quad (6.3.3)$$

$$II(\mathbf{x}, \pi_{\text{obs}}, \boldsymbol{\beta}) = \sum_{i=1}^N \frac{x_i}{g^{-1}\left(\frac{\text{logit}(\pi_{\text{obs}}) - \beta_0}{\beta_i}\right)}. \quad (6.3.4)$$

Note assuming the  $i$ th agent is inert,  $\beta_i = 0$  and  $ED_i(\pi_{\text{obs}}) = \infty$ . As described in Chapter 3 the unknown parameters,  $\boldsymbol{\beta}$ , can be estimated using maximum likelihood methods and the adequacy of the fit of the model can be assessed using a goodness-of-fit test. The estimated values of the effective doses and the interaction index can then be determined based on  $\hat{\boldsymbol{\beta}}$ .

To determine if there is a significant nonadditive interaction at  $\mathbf{x}$ , conditional on  $\pi_{\text{obs}}$ , the following hypothesis can be tested

$$H_0 : II(\mathbf{x}, \pi_{\text{obs}}; \boldsymbol{\beta}) = 1$$

$$H_A : II(\mathbf{x}, \pi_{\text{obs}}; \boldsymbol{\beta}) \neq 1$$

By use of the properties of the maximum likelihood estimates described in Chapter 3, it can be shown that  $\hat{\boldsymbol{\beta}}$  is approximately distributed as

$$\hat{\boldsymbol{\beta}} \sim N_{N+1}(\boldsymbol{\beta}, I^{-1}(\boldsymbol{\beta}))$$

where  $I^{-1}(\boldsymbol{\beta})$  is the inverse of the  $(N + 1) \times (N + 1)$  Fisher Information Matrix. Using the Delta Method (Agresti, 1990, p. 419), an approximate distribution of  $II(\mathbf{x}, \pi_{\text{obs}}; \hat{\boldsymbol{\beta}})$  is given

by

$$II(\mathbf{x}, \pi_{\text{obs}}; \hat{\boldsymbol{\beta}}) \sim N(II(\mathbf{x}, \pi_{\text{obs}}; \boldsymbol{\beta}), \boldsymbol{\Phi}' I^{-1}(\boldsymbol{\beta}) \boldsymbol{\Phi})$$

where

$$\Phi = (\Phi_0(\beta) \Phi_1(\beta) \cdots \Phi_N(\beta))', \quad \Phi_i(\beta) = \frac{\partial I(x, \pi_{\text{obs}}; \beta)}{\partial \beta_i}; \quad i=0,1,2,\dots,N.$$

The value of  $\Phi_i(\beta)$  is estimated by  $\Phi_i(\hat{\beta})$  and the value of  $\Gamma^{-1}(\beta)$  is estimated by  $\Gamma^{-1}(\hat{\beta})$ .

Based on the Wald Test described in Section 3.6, the following test statistic, can be used to test  $H_0 : II(x, \pi_{\text{obs}}; \beta) = 1$ .

$$W_{11} = \frac{(1 - II(x, \pi_{\text{obs}}; \hat{\beta}))^2}{\Phi(\hat{\beta}) \Gamma^{-1}(\hat{\beta}) \Phi(\hat{\beta})} \sim \chi_1^2. \quad (6.3.5)$$

When  $W_{11} > \chi_{1,1-\alpha}^2$ ,  $H_0$  should be rejected. When  $H_0$  is rejected, the values of  $II(x, \pi_{\text{obs}}; \hat{\beta})$  can be used to characterize the interaction;  $II(x, \pi_{\text{obs}}; \hat{\beta}) < 1$  indicates synergism and  $II(x, \pi_{\text{obs}}; \hat{\beta}) > 1$  indicates antagonism.

This method can now be applied to a set of dose combinations. Let  $K$  be the total number of dose combinations considered. Because the Interaction Index Test is repeated at each of the  $K$  dose combinations, the overall probability of incorrectly rejecting the null hypothesis will become large. A multiple testing procedure can therefore be applied to insure the overall probability of falsely rejecting a null hypothesis for the group of  $K$  tests is at most  $\alpha$ . The Bonferroni Correction is used frequently in such situations. Here, the  $p$ -value associated with the  $i$ th test is determined by  $p\text{-value}_i = P(W_{11} > \chi_{1,1-\alpha}^2)$ ;  $i=1,2,\dots,K$ . If  $p\text{-value}_i < \alpha/K$  then rejection of the associated  $i$ th hypothesis is appropriate. While it has been shown that the overall probability of falsely rejecting any of the  $K$  hypotheses is at most  $\alpha$  it has also been shown that this procedure may be

conservative, i.e., it may fail to reject a particular hypothesis when it is false (Weller, 1992).

For our applications, a procedure described by Hochberg (1988) will be employed. This technique has been shown to be less conservative than the Bonferroni procedure while still insuring the overall probability of type I error be at most  $\alpha$ . Here the p-values associated with each of the K tests are ordered from largest to smallest. These ordered p-values are denoted by  $p\text{-value}_{(i)}$ ,  $i=1,2,\dots,K$  so that  $p\text{-value}_{(1)}$  denotes the largest value and  $p\text{-value}_{(K)}$  the smallest. The associated hypotheses are denoted by  $H_{(i)}$ ,  $i=1,2,\dots,K$ . Starting with the largest p-value, if  $p\text{-value}_{(1)} < \alpha/K$  then all K hypotheses are rejected. If  $p\text{-value}_{(1)} > \alpha/K$  then  $H_{(1)}$  is not rejected and  $p\text{-value}_{(2)}$  is examined. Now if  $p\text{-value}_{(2)} < \frac{\alpha}{k-1}$  then  $H_{(2)}, H_{(3)}, \dots, H_{(k)}$  are rejected. If  $p\text{-value}_{(2)} > \frac{\alpha}{k-1}$  this procedure continues so that, in general, if  $p\text{-value}_{(i)} < \frac{\alpha}{k-i+1}$  then  $H_{(i)}, H_{(i+1)}, \dots, H_{(k)}$  are rejected. This procedure will be illustrated in the next section.

#### 6.4 Example

Data from a simulated two agent experiment are shown in Table 6.1. The model given in (6.2.1) was initially fit to all 20 observations of this data. The results of this analysis are shown in Table 6.2. Since  $\hat{\beta}_{12} > 0$  there is evidence of a synergism. The p-value associated with the goodness of fit test,  $p = 1.4 \times 10^{-5}$ , indicates, however, that the model does not adequately fit the data.

Alternatively the transformation,  $Z_i = \log_{10}(X_i + 1)$ , where  $X_i$ ,  $i = 1, 2$ , is the dose of the  $i$ th agent was considered. For illustrative purposes, the model, given in (6.2.1) was fit in terms of the transformed doses. In that case  $\hat{\beta}_{12} < 0$ . Hence, if the estimated value of this cross product parameter was inappropriately examined to characterize an interaction, an antagonism would have been indicated.

**Table 6.1**

Simulated Two Agent Dose-Response Study Data

 $X_i$  = Dose of  $i$ th agent,  $i=1,2$  $y/n$  = number responding/number replications

| $X_1$ | $X_2$ | $y/n$ | $X_1$ | $X_2$ | $y/n$ | $X_1$ | $X_2$ | $y/n$ | $X_1$ | $X_2$ | $y/n$ |
|-------|-------|-------|-------|-------|-------|-------|-------|-------|-------|-------|-------|
| 0     | 0     | 0/30  | 5     | 0     | 1/10  | 0     | 5     | 0/10  | 10    | 285   | 5/10  |
|       |       |       | 10    | 0     | 2/10  | 0     | 25    | 0/10  | 35    | 260   | 5/10  |
|       |       |       | 25    | 0     | 3/10  | 0     | 55    | 4/10  | 50    | 215   | 4/10  |
|       |       |       | 130   | 0     | 4/10  | 0     | 280   | 4/10  | 70    | 175   | 3/10  |
|       |       |       | 265   | 0     | 7/10  | 0     | 565   | 4/10  | 90    | 130   | 9/10  |
|       |       |       | 670   | 0     | 9/10  | 0     | 1420  | 7/10  | 110   | 85    | 6/10  |
|       |       |       |       |       |       |       |       |       | 125   | 40    | 7/10  |

**Table 6.2**

## Simulated Two Agent Dose-Response Study

## Analysis Results for Model

$$\log \text{it}[P(\mathbf{X}, \boldsymbol{\beta})] = \beta_0 + \beta_1 X_1 + \beta_2 X_2 + \beta_{12} X_1 X_2$$

---

| Parameter Estimates |          |                |         |
|---------------------|----------|----------------|---------|
| Parameter           | Estimate | Wald Statistic | p-value |
| $\beta_0$           | -1.7227  | 44.0508        | .0001   |
| $\beta_1$           | .00862   | 17.1761        | .0001   |
| $\beta_2$           | .00204   | 14.4638        | .0001   |
| $\beta_{12}$        | .000096  | 8.3448         | .0039   |

---

Overall Goodness of Fit test (3.5.5)

$$\chi^2 = 32.1332 \quad E(\chi^2 | \hat{\boldsymbol{\beta}}) = 7.5854 \quad V(\chi^2 | \hat{\boldsymbol{\beta}}) = 34.5157 \quad \text{p-value} = 1.4 \times 10^{-5}$$


---

To apply the Interaction Index Test the model defined in (6.3.2) was fit to the 13 observations taken only along each axis. The transformation  $Z_i = \log_{10}(X_i + 1)$  was used. The results of this analysis are shown in Table 6.3. Since the fit appears adequate (goodness-of-fit p-value = .2331) the Interaction Index Test can now be derived and then applied to each of the 7 dose combinations where nonzero doses of both agents were given. The Interaction Index Test Statistic,  $W_{II}$  is given by (6.3.5) where

$$II(\mathbf{x}, \pi_{\text{obs}}; \hat{\boldsymbol{\beta}}) = \frac{x_1}{10^{\frac{\log_{10}(\pi_{\text{obs}}) - \hat{\beta}_0}{\hat{\beta}_1}} - 1} + \frac{x_2}{10^{\frac{\log_{10}(\pi_{\text{obs}}) - \hat{\beta}_0}{\hat{\beta}_2}} - 1}$$

and

$$\phi_0(\boldsymbol{\beta}) = \frac{\partial II(\mathbf{x}, \pi_{\text{obs}}; \boldsymbol{\beta})}{\partial \beta_0} = \frac{10^{\left(\frac{\log_{10}(\pi_{\text{obs}}) - \beta_0}{\beta_1}\right)} x_1 \ln(10)}{\beta_1 \left(10^{\left(\frac{\log_{10}(\pi_{\text{obs}}) - \beta_0}{\beta_1}\right)} - 1\right)^2} + \frac{10^{\left(\frac{\log_{10}(\pi_{\text{obs}}) - \beta_0}{\beta_2}\right)} x_2 \ln(10)}{\beta_2 \left(10^{\left(\frac{\log_{10}(\pi_{\text{obs}}) - \beta_0}{\beta_2}\right)} - 1\right)^2}$$

$$\phi_i(\boldsymbol{\beta}) = \frac{\partial II(\mathbf{x}, \pi_{\text{obs}}; \boldsymbol{\beta})}{\partial \beta_i} = \frac{\ln(10) 10^{\left(\frac{\log_{10}(\pi_{\text{obs}}) - \beta_0}{\beta_i}\right)} x_i \log_{10}(x_i + 1)}{\beta_i \left(10^{\left(\frac{\log_{10}(\pi_{\text{obs}}) - \beta_0}{\beta_i}\right)} - 1\right)^2}; i=1,2.$$

$\phi_0(\boldsymbol{\beta})$  and  $\phi_i(\boldsymbol{\beta})$ ,  $i=1,2$ , are estimated by  $\phi_0(\hat{\boldsymbol{\beta}})$  and  $\phi_i(\hat{\boldsymbol{\beta}})$ ,  $i=1,2$  respectively. For each of the 7 dose combinations considered, the values of this test statistic and each associated p-value are shown in Table 6.4. There, two dose combinations were found to have values of the interaction index that were different from 1. In each case a synergism was detected.

For illustrative purposes,  $\hat{\pi}^A$ , the estimated response under additivity for each of the combinations, are also shown in Table 6.4. Based on Definition 4.3.3, these values were determined for each  $(x_1, x_2)$  by solving for  $\log_{10}(\hat{\pi}^A)$  in the following expression.



**Table 6.3**

## Simulated Two Agent Dose-Response Study

## Analysis Results for Model

$$\text{logit}[P(\mathbf{X}, \boldsymbol{\beta})] = \beta_0 + \beta_1 \log_{10}(X_1 + 1) + \beta_2 \log_{10}(X_2 + 1)$$

---

| Parameter Estimates |          |                |         |
|---------------------|----------|----------------|---------|
| Parameter           | Estimate | Wald Statistic | p-value |
| $\beta_0$           | -4.1640  | 36.3844        | .0001   |
| $\beta_1$           | 2.0802   | 33.4339        | .0001   |
| $\beta_2$           | 1.5298   | 26.6632        | .0001   |

---

Estimated Variance-Covariance Matrix:  $I(\hat{\boldsymbol{\beta}})^{-1}$ 

|           | $\beta_0$ | $\beta_1$ | $\beta_2$ |
|-----------|-----------|-----------|-----------|
| $\beta_0$ | 0.47654   | -.22213   | -.18496   |
| $\beta_1$ |           | .12943    | .08622    |
| $\beta_2$ |           |           | .08777    |

---

Overall Goodness of Fit test (3.5.5)

$$\chi^2 = 8.2897 \quad E(\chi^2 | \hat{\boldsymbol{\beta}}) = 4.7255 \quad V(\chi^2 | \hat{\boldsymbol{\beta}}) = 23.9305 \quad \text{p-value} = .2331$$

**Table 6.4**

Simulated Two Agent Dose-Response Study  
Interaction Test Results

| $x_1$ | $x_2$ | $\pi_{\text{obs}}$ | $\hat{\pi}^A$ | $\Pi(x, \pi_{\text{obs}}, \hat{\beta})$ | Wald Test |         | Critical p* | Type of Interaction |
|-------|-------|--------------------|---------------|---|-----------|---------|-------------|---------------------|
|       |       |                    |               |   | Statistic | p-value |             |                     |
| 35    | 260   | 0.5                | .4679         | .8463                                   | 0.32      | .5691   | .0071       |                     |
| 110   | 85    | 0.6                | .5493         | .7917                                   | 0.62      | .4310   | .0083       |                     |
| 50    | 215   | 0.4                | .4808         | 1.5460                                  | 1.40      | .2362   | .0100       |                     |
| 10    | 285   | 0.5                | .4235         | 0.6422                                  | 1.85      | .1734   | .0125       |                     |
| 70    | 175   | 0.3                | .5058         | 3.0243                                  | 5.29      | .0215   | .0167       |                     |
| 125   | 40    | 0.7                | .5613         | .5106                                   | 7.03      | .0080   | .0250       | Synergism           |
| 90    | 130   | 0.9                | .5280         | .0879                                   | 1015.90   | .0000   |             | Synergism           |

\* Based on Multiple Testing Procedure of Hochberg (1988) Critical  $p = \frac{\alpha}{K - i + 1}$ ;

$i=1,2,\dots,K$  where  $\alpha = 0.5$  and  $K = 7$ .

$$\frac{x_1}{10^{\frac{\log \text{it}(\pi^A) - \hat{\beta}_0}{\hat{\beta}_1}} - 1} + \frac{x_2}{10^{\frac{\log \text{it}(\hat{\pi}^A) - \hat{\beta}_0}{\hat{\beta}_2}} - 1} = 1. \quad (6.3.6)$$

Since the equation given in (6.3.6) can not be solved explicitly, a root finding procedure (Mathematica, 1991) was used to find each value. As expected by Definition 4.3.1, when a significant synergism was indicated,  $\pi_{\text{obs}} > \hat{\pi}^A$ .

It has been shown that the Interaction Index Test can be used, in a point-wise fashion, to detect deviations from additivity. This was particularly useful when a dose-response model, in terms of the doses, could not be adequately fit to the data. Another advantage of the Interaction Index Test is that it can be applied in a N-agent study to a smaller set of observations than needed to fit the entire (N+1)-dimensional dose-response surface. While data are needed along each axis to estimate adequately each single agent's dose-response curve, as few as one nonaxis combination can be examined for nonadditivity. However, since the method is based on a point-wise test, a disadvantage of this technique is that the conclusions drawn apply only to the specific dose combinations considered. In contrast, the results determined using a dose-response approach apply to a range of dose combinations. Another disadvantage of this approach is that the conclusion drawn is conditional on the assumption that the response is fixed at the value of  $\pi_{\text{obs}}$ . In the next chapter another approach to detecting and characterizing deviations from additivity will be described. It will be demonstrated that this approach requires less data than needed for fitting the dose-response surface but provides more global results than the point-wise approach described in this chapter.

## **Chapter 7**

### **Detecting and Characterizing Interactions Based on a Ray Designed Experiment**

#### **7.1 Introduction**

In Chapter 5 the response surface modelling approach to the study of drug interactions was discussed. Several problems associated with this technique were found. For example, the size of the experiment needed to adequately model a response can be unrealistically large. Even if a fraction of a factorial design is used, the cost of the experiment may become prohibitive. It was also shown that as the number of agents increased, the number of significant interaction terms in the model can also become large. When the goal is to characterize interactions among the agents, the interpretation of the model may therefore become difficult.

In this chapter it will be demonstrated that an analysis based on data collected along rays, or at several levels of a fixed ratio, offers several advantages compared with the response surface technique. When examining dose combinations along rays, the dimensionality of the study is reduced. In an  $N$  agent study the fitted model based on a response surface approach is an  $(N+1)$ -dimensional surface. In contrast, the fitted model based on a ray design, defines a set of 2-dimensional dose response curves.

In the following sections, the model based on a ray design will be defined and an example will be presented. A simultaneous test for assessing deviations from additivity will be developed. In cases where a nonadditive interaction is detected, techniques will be

developed which characterize the types of interactions, i.e., synergism or antagonism. An examination of the isobols estimated from this type of experiment will also be made. Graphical techniques will be introduced that will be shown to be useful in the interpretation of the fitted model.

## 7.2 The Model

In order to insure that the definitions of additivity derived in Chapter 4 hold it will be assumed that all active single agent dose-response curves will monotonically increasing or all monotonically decreasing. Under this constraint, all the combinations defined in Chapter 4, with the exception of the heterergic combination of a predictive agent and a nonpredictive agent, can be studied using the methods derived in this chapter.

For this analysis data are collected along rays. A ray can be thought of as a straight line originating at the origin. It can be shown that dose combinations that lie along a ray satisfy a fixed ratio. For example, consider the ray in 2-dimensional Euclidean space through the point (2,4). Dose combinations taken along that 2-dimensional line, or ray, satisfy the fixed ratio 1:2.

Let  $N$  denote the number of agents considered in the study. Let  $M > N$  denote the total number of rays along which dose combinations will be taken. Assume a ray is included along each of the  $N$  axes. These  $N$  rays will be referred to as axis rays. There are  $M - N$  non-axis rays. The following definitions describe the drug combinations and the observed responses for a ray design experiment. In addition to the observations taken along each ray, assume observations are also taken at the origin. As in previous chapters,  $s \geq 1$  replications of the experiment are conducted at each dose combination and the dichotomous response is given by success ( $Z = 1$ ) or failure ( $Z = 0$ ). Let

$m_r$  = number of nonzero dose combinations on the  $r$ th ray;  $r=1,2,\dots,M$

$G$  = total number of distinct dose combinations including the origin;

$$G = 1 + \sum_{r=1}^M m_r$$

$n_0$  = number of replications at the origin

$Z_{0s}$  = response for the  $s$ th replication at the origin;  $s=1,2,\dots,n_0$

$$Y_0 = \sum_{s=1}^{n_0} Z_{0s}$$

$n_{rk}$  = number of replications at the  $k$ th combination on the  $r$ th ray

$Z_{rks}$  = response for the  $s$ th replication at the  $k$ th combination on the  $r$ th ray;

$$s=1,2,\dots,n_{rk}$$

$$Y_{rk} = \sum_{s=1}^{n_{rk}} Z_{rks} = \text{number of responses observed at the } k\text{th combination of the}$$

$r$ th ray

$Y_r$  =  $1 \times m_r$  vector given by  $(Y_{r1} \ Y_{r2} \ \dots \ Y_{rm_r})$ ,  $r=1,2,\dots,M$ ;  $k=1,2,\dots,m_r$ .

In order to uniquely identify each of the  $M$  rays we can use the property noted earlier that the rays are line segments originating at the origin in  $N$ -dimensional space. The set of  $N$ -dimensional points that lie along a given ray satisfy a fixed set of ratios. While these ratios can be defined in several ways, for this dissertation, a unique set of ratios for the  $r$ th ray are given by  $a_{r1} : a_{r2} : \dots : a_{rN}$  where  $\sum_{i=1}^N a_{ri} = 1$  and  $0 \leq a_{ri} \leq 1$ . For example, the ratios (0.25, 0.0, 0.75) identify the ray through the point (1, 0, 3).

In general, let the  $1 \times N$  vector  $\mathbf{a}_r = (a_{r1} \ a_{r2} \ \dots \ a_{rN})$  denote the ratios for the  $r$ th ray,  $r=1,2,\dots,M$ . Let  $A$  be the  $M \times N$  matrix with rows  $\mathbf{a}_r$ . Assume rays  $1,2,\dots,N$  correspond to the  $N$  axes. For these axis rays the elements of  $\mathbf{a}_r$ ,  $r=1,2,\dots,N$  are identically 0 with the exception of a 1 in the  $i$ th position, i.e., for the  $X_1$  axis  $\mathbf{a}_1 = (1,0,\dots,0)$ .

For a given dose combination along a fixed ray, a well defined relationship exists between the doses of the  $N$  agents and the total of the doses. Consider the  $r$ th ray with ratio vector  $\mathbf{a}_r$ . Let  $\mathbf{x}_{rk} = (x_{rk1} \ x_{rk2} \ \dots \ x_{rkN})$  denote the  $1 \times N$  vector of dose levels for the  $N$  agents at the  $k$ th combination on the  $r$ th ray,  $r = 1, 2, \dots, M$ ;  $k = 1, 2, \dots, m_r$ . The total of the  $N$  individual doses is given by

$$t_{rk} = \sum_{j=1}^N x_{rkj} = \mathbf{x}_{rk} \mathbf{1}_N \quad (7.2.1)$$

where  $\mathbf{1}_N$  is the  $N \times 1$  vector of 1's. Conversely, given the total dose,  $t_{rk}$ , the individual doses of the  $N$  agents at the  $k$ th observation on the  $r$ th ray is given by

$$\mathbf{x}_{rk} = t_{rk} \mathbf{a}_r. \quad (7.2.2)$$

Therefore, for observations along the  $r$ th ray uniquely identified by  $\mathbf{a}_r$ , no information about the doses of the individual agents,  $\mathbf{x}_{rk}$ ,  $k=1, 2, \dots, m_r$ , is lost by examining only the total doses,  $t_{rk}$ .

It is assumed that the responses  $Z_{rks}$ ,  $s=1, 2, \dots, n_{rk}$ , are independent and identically distributed as Bernoulli random variables with unknown parameter  $\pi_{rk}$  for all  $r = 1, 2, \dots, M$  and  $k=1, 2, \dots, m_r$ . A similar assumption is made for the observations taken at the origin, i.e.,  $Z_{0s}$ ,  $s=1, 2, \dots, n_0$  are independent and identically distributed Bernoulli random variables with unknown parameter  $\pi_0$ . It follows that  $Y_{rk}$  and  $Y_0$  are independently distributed as  $\text{Bin}(n_{rk}, \pi_{rk})$  and  $\text{Bin}(n_0, \pi_0)$  random variables, respectively.

Since no information is lost by considering the total of the doses at each combination, the unknown parameters can be modeled as functions of the total doses. Let

$$\text{logit}(\pi_0) = \ln\left(\frac{\pi_0}{1-\pi_0}\right) = \beta_0 \quad (7.2.3)$$

and

$$\text{logit}(\pi_{rk}) = \ln\left(\frac{\pi_{rk}}{1-\pi_{rk}}\right) = \beta_0 + \beta_r t_{rk}; \quad k=1,2,\dots,m_r; \quad r = 1,2,\dots,M. \quad (7.2.4)$$

These expressions can be rewritten as

$$\pi_0 = \frac{1}{1 + \exp(-\beta_0)} \quad (7.2.5)$$

and

$$\pi_{rk} = \frac{1}{1 + \exp\{-(\beta_0 + \beta_r t_{rk})\}} \quad k=1,2,\dots,m_r; \quad r = 1,2,\dots,M. \quad (7.2.6)$$

A common intercept parameter for all  $M$  rays is given by  $\beta_0$ . The slope parameter for the  $r$ th ray is  $\beta_r$ ,  $r=1,2,\dots,M$ .

An overall model is written as

$$\boldsymbol{\pi} = \frac{1}{1 + \exp\{-\mathbf{T}\boldsymbol{\beta}\}} \quad (7.2.7)$$

where  $\boldsymbol{\pi}$  is the  $G \times 1$  vector,  $\mathbf{T}$  is the  $G \times (M+1)$  design matrix in terms of  $t_{rk}$  and  $\boldsymbol{\beta}$  is the  $(M+1) \times 1$  vector given below.



$$\boldsymbol{\pi}' = [\pi_0 \ \pi_{11} \ \pi_{12} \ \cdots \ \pi_{1m_1} \ \pi_{21} \ \pi_{22} \ \cdots \ \pi_{2m_2} \ \cdots \ \pi_{M1} \ \pi_{M2} \ \cdots \ \pi_{Mm_M}]$$

$$\mathbf{T}' = \begin{bmatrix} 1 & 1 & 1 & \cdots & 1 & 1 & 1 & \cdots & 1 & \cdots & 1 & 1 & \cdots & 1 \\ 0 & t_{11} & t_{12} & \cdots & t_{1m_1} & 0 & 0 & \cdots & 0 & \cdots & 0 & 0 & \cdots & 0 \\ 0 & 0 & 0 & \cdots & 0 & t_{21} & t_{22} & \cdots & t_{2m_2} & \cdots & 0 & 0 & \cdots & 0 \\ \vdots & \vdots & \vdots & \cdots & \vdots & \vdots & \vdots & \cdots & \vdots & \cdots & \vdots & \vdots & \cdots & \vdots \\ 0 & 0 & 0 & \cdots & 0 & 0 & 0 & \cdots & 0 & \cdots & t_{M1} & t_{M2} & \cdots & t_{Mm_M} \end{bmatrix}$$

$$\boldsymbol{\beta}' = [\beta_0 \ \beta_1 \ \beta_2 \ \cdots \ \beta_M].$$

The maximum likelihood methods described in Chapter 3 can be applied to this model to simultaneously estimate  $\boldsymbol{\beta}$ , the  $(M+1) \times 1$  vector of unknown parameters. The likelihood and log-likelihood are given by

$$L(\boldsymbol{\pi}; \mathbf{y}) = \binom{n_0}{y_0} \exp \left\{ y_0 \ln \left( \frac{\pi_0}{1 - \pi_0} \right) + n_0 \ln(1 - \pi_0) \right\}^* \\ \left\{ \prod_{r=1}^M \prod_{k=1}^{m_r} \binom{n_{rk}}{y_{rk}} \right\} \exp \left\{ \sum_{r=1}^M \sum_{k=1}^{m_r} y_{rk} \ln \left( \frac{\pi_{rk}}{1 - \pi_{rk}} \right) + n_{rk} \ln(1 - \pi_{rk}) \right\} \quad (7.2.8)$$

$$l(\boldsymbol{\pi}; \mathbf{y}) = \ln \binom{n_0}{y_0} + y_0 \ln \left( \frac{\pi_0}{1 - \pi_0} \right) + n_0 \ln(1 - \pi_0) + \\ \sum_{r=1}^M \sum_{k=1}^{m_r} \left\{ \ln \binom{n_{rk}}{y_{rk}} + y_{rk} \ln \left( \frac{\pi_{rk}}{1 - \pi_{rk}} \right) + n_{rk} \ln(1 - \pi_{rk}) \right\}. \quad (7.2.9)$$

Based on (7.2.3) and (7.2.4) the log-likelihood can also be written as

$$l(\boldsymbol{\beta}; \mathbf{y}) = \ln \binom{n_0}{y_0} + y_0 \beta_0 - n_0 \ln(1 + \exp(\beta_0)) + \sum_{r=1}^M \sum_{k=1}^{m_r} \left\{ \ln \binom{n_{rk}}{y_{rk}} + y_{rk} (\beta_0 + \beta_r t_{rk}) - n_{rk} \ln(1 + \exp(\beta_0 + \beta_r t_{rk})) \right\}. \quad (7.2.10)$$

The elements of the  $(M+1) \times 1$  vector of scores,  $\mathbf{U}(\boldsymbol{\beta})$ , are given by

$$\begin{aligned} U_0(\boldsymbol{\beta}) &= \frac{\partial l(\boldsymbol{\beta}; \mathbf{y})}{\partial \beta_0} = y_0 - \frac{n_0}{1 + \exp(-\beta_0)} + \sum_{r=1}^M \sum_{k=1}^{m_r} \left\{ y_{rk} - \frac{n_{rk}}{1 + \exp(-(\beta_0 + \beta_r t_{rk}))} \right\} \\ &= y_0 - \frac{n_0}{1 + \exp(-\beta_0)} + \sum_{r=1}^M \sum_{k=1}^{m_r} \{ y_{rk} - n_{rk} \pi_{rk} \} \\ U_j(\boldsymbol{\beta}) &= \frac{\partial l(\boldsymbol{\beta}; \mathbf{y})}{\partial \beta_j} = \sum_{k=1}^{m_j} \left\{ y_{jk} t_{jk} - \frac{n_{jk} t_{jk}}{1 + \exp(-(\beta_0 + \beta_j t_{jk}))} \right\} \\ &= \sum_{k=1}^{m_j} \{ y_{jk} t_{jk} - n_{jk} t_{jk} \pi_{jk} \}; \quad j=1, 2, \dots, M. \end{aligned} \quad (7.2.11)$$

The  $M \times M$  elements of Fisher's Information Matrix,  $\mathbf{I}(\boldsymbol{\beta})$ , are defined by

$$\begin{aligned} I_{00}(\boldsymbol{\beta}) &= -E \left( \frac{\partial^2 l(\boldsymbol{\beta}; \mathbf{y})}{\partial \beta_0^2} \right) = \frac{\exp(-\beta_0)}{(1 + \exp(-\beta_0))^2} \quad (7.2.12) \\ I_{0j}(\boldsymbol{\beta}) &= -E \left( \frac{\partial^2 l(\boldsymbol{\beta}; \mathbf{y})}{\partial \beta_0 \partial \beta_j} \right) = \sum_{k=1}^{m_j} \frac{n_{jk} t_{jk} \exp(-(\beta_0 + \beta_j t_{jk}))}{(1 + \exp(-(\beta_0 + \beta_j t_{jk})))^2}; \quad j=1, 2, \dots, M \\ I_{jj}(\boldsymbol{\beta}) &= -E \left( \frac{\partial^2 l(\boldsymbol{\beta}; \mathbf{y})}{\partial^2 \beta_j} \right) = \sum_{k=1}^{m_j} \frac{n_{jk} t_{jk}^2 \exp(-(\beta_0 + \beta_j t_{jk}))}{(1 + \exp(-(\beta_0 + \beta_j t_{jk})))^2}; \quad j=1, 2, \dots, M \\ I_{jw}(\boldsymbol{\beta}) &= -E \left( \frac{\partial^2 l(\boldsymbol{\beta}; \mathbf{y})}{\partial \beta_j \partial \beta_w} \right) = 0; \quad j, w=1, 2, \dots, M; \quad j \neq w. \end{aligned}$$

As usual,  $\hat{\boldsymbol{\beta}}$ , the maximum likelihood estimate for  $\boldsymbol{\beta}$ , found by solving the system of equations that results when (7.2.11) is set equal to zero. An iterative approach can be used to solve this system. As described in Chapter 3, it follows that

$$\hat{\boldsymbol{\beta}} \sim N_{M+1}(\boldsymbol{\beta}, I(\boldsymbol{\beta})^{-1}) \quad (7.2.13)$$

where  $I(\boldsymbol{\beta})^{-1}$  is estimated by  $I(\hat{\boldsymbol{\beta}})^{-1}$ .

It is interesting to note that expression (7.2.12) implies that the off-diagonal elements of  $I(\boldsymbol{\beta})$  are zero with the exception of the first row and first column. This does not imply, however, that the corresponding elements of  $I(\boldsymbol{\beta})^{-1}$  will be zero. Hence, while the  $M$  slope parameters are associated with distinct rays, the maximum likelihood estimates of these slope parameters are correlated. This is due to the presence of the common intercept parameter.

Once a model is fit, various tests described in Chapter 3 assessing the fit of the model can be applied. In the next section a two agent example will be given to illustrate the application of these tests.

### 7.3 Two Agent Example

A two agent data set was generated based on the 2-dimensional dose-response surface given by

$$\log \text{it}(\pi) = -10 + 3X_1 + 2X_2 + 2.2X_1X_2 - .667X_1^2X_2$$

where  $X_1$  and  $X_2$  are the dose levels for the agents considered.

Data were simulated along  $M = 4$  rays at a total of  $G = 19$  distinct dose combinations (Figure 7.1). The 4 rays are defined by

$$\mathbf{A} = \begin{bmatrix} 1 & 0 \\ 0 & 1 \\ .667 & .333 \\ .333 & .667 \end{bmatrix}.$$

It can be assumed a range-finding procedure was used to determine the observed dose levels along each ray. The simulated data are shown in Table 7.1

The model considered for this analysis is given by

$$\begin{aligned} \text{logit}(\pi_0) &= \beta_0; & t_{rk} &= 0, \quad r=1,2,3,4; \quad k=1,2,\dots,m_r \\ \text{logit}(\pi_{rk}) &= \beta_0 + \beta_r t_{rk}; & & r=1,2,3,4; \quad k=1,2,\dots,m_r \end{aligned}$$

or equivalently as

$$\text{logit}(\boldsymbol{\pi}) = \mathbf{T}\boldsymbol{\beta}$$

where

$$\mathbf{T} = \begin{bmatrix} 1 & 1 & 1 & 1 & 1 & 1 & 1 & 1 & 1 & 1 & 1 & 1 & 1 & 1 & 1 & 1 & 1 & 1 \\ 0 & 2 & 3 & 4 & 5 & 0 & 0 & 0 & 0 & 0 & 0 & 0 & 0 & 0 & 0 & 0 & 0 & 0 \\ 0 & 0 & 0 & 0 & 0 & 3 & 4 & 5 & 6 & 7 & 8 & 0 & 0 & 0 & 0 & 0 & 0 & 0 \\ 0 & 0 & 0 & 0 & 0 & 0 & 0 & 0 & 0 & 0 & 0 & 2 & 3 & 4 & 5 & 0 & 0 & 0 \\ 0 & 0 & 0 & 0 & 0 & 0 & 0 & 0 & 0 & 0 & 0 & 0 & 0 & 0 & 2 & 3 & 4 & 5 \end{bmatrix}'$$

and

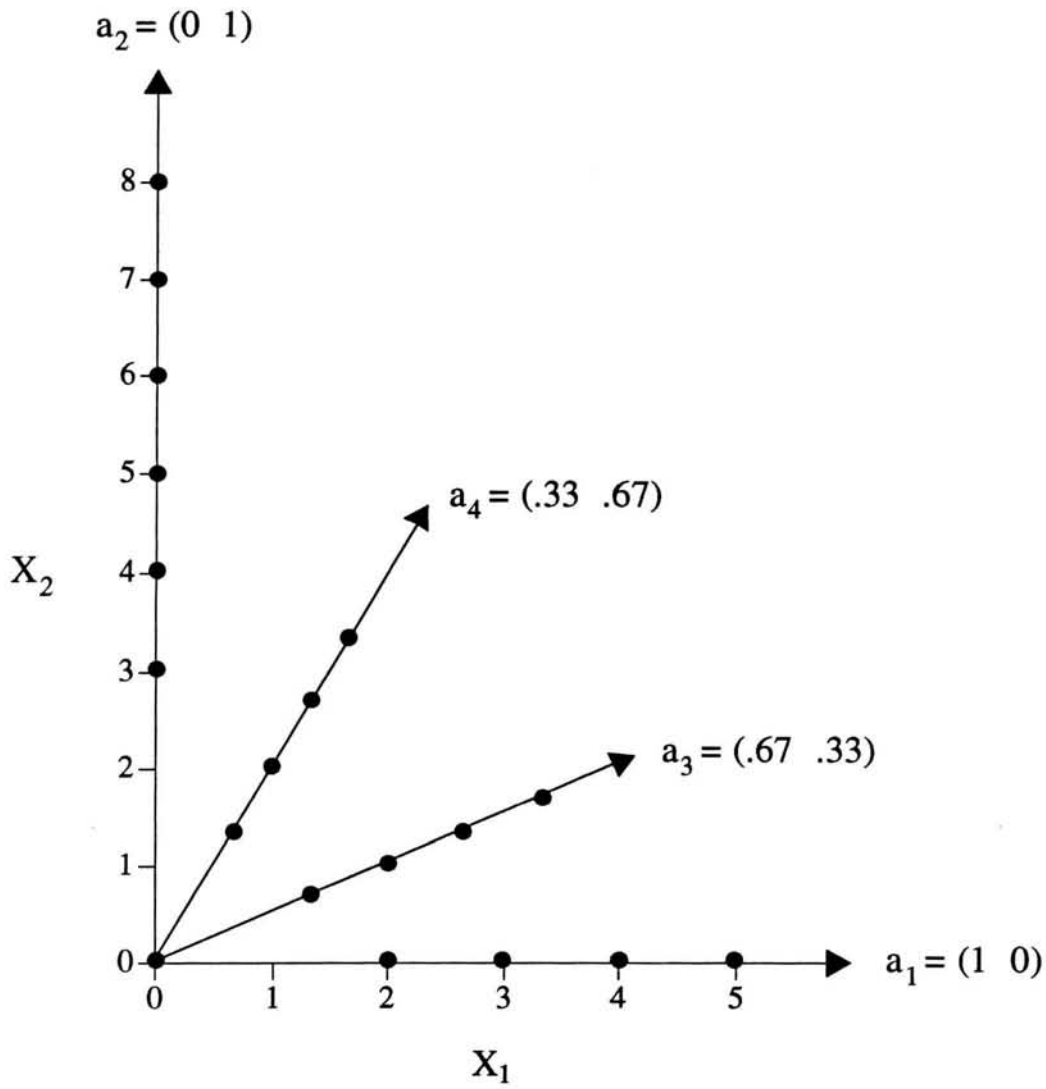


**Figure 7.1:** Experimental Design for Two-Agent Simulated Data

**Table 7.1**

Two Agent Simulated Data  
Number of responses from 5 replications

| Ray    | $\mathbf{a}_r$ | Total Dose |   |   |   |   |   |   |   |   |
|--------|----------------|------------|---|---|---|---|---|---|---|---|
|        |                | 0          | 1 | 2 | 3 | 4 | 5 | 6 | 7 | 8 |
| origin |                | 0          |   |   |   |   |   |   |   |   |
| 1      | (1 0)          |            |   | 0 | 3 | 5 | 5 |   |   |   |
| 2      | (0 1)          |            |   |   | 0 | 0 | 3 | 3 | 4 | 5 |
| 3      | (.67 .33)      |            |   | 0 | 2 | 4 | 5 |   |   |   |
| 4      | (.33 .67)      |            |   | 0 | 4 | 5 | 5 |   |   |   |

$$\boldsymbol{\beta} = [\beta_0 \quad \beta_1 \quad \beta_2 \quad \beta_3 \quad \beta_4]'$$

The results from model fitting are shown in Table 7.2. The intercept only likelihood ratio and score test results ( $p=.0001$ ) both indicate at least one of the slope parameters is nonzero. The result of the overall goodness-of-fit test ( $p=.5651$ ) indicates that this model adequately describes the data. Examination of the individual goodness-of-fit statistics (Table 7.3) shows that none of the observations appear problematic.

In the next section three different simultaneous tests to detect deviations from additivity will be presented. The tests will be applied to this two agent example and to a higher dimensional experiment.

#### 7.4 Statistical Tests for Detecting Deviations from Additivity

Let  $\pi^A$  denote an expected response under additivity. Based on the definition of additivity given in Result 4.3.1 it follows that the additive dose-response relationship at the  $k$ th observation on the  $r$ th ray is given by

$$\frac{X_{rk1}}{ED_1(\pi_{rk}^A)} + \frac{X_{rk2}}{ED_2(\pi_{rk}^A)} + \dots + \frac{X_{rkN}}{ED_N(\pi_{rk}^A)} = 1 \quad (7.4.1)$$

where  $ED_i(\pi_{rk}^A)$  is the effective dose associated with the  $i$ th agent,  $i = 1, 2, \dots, N$ . Recall along the  $i$ th axis,  $i=1, 2, \dots, N$  the total dose is equal to the dose of the  $i$ th agent. Therefore, using (7.2.4) the effective doses for each agent alone are given by

$$ED_r(\pi_{rk}^A) = \frac{\text{logit}(\pi_{rk}^A) - \beta_0}{\beta_r}; r = 1, 2, \dots, M.$$

**Table 7.2**  
Two Agent Simulated Data Analysis Results

---

| Ray    | Parameter | Estimate | Wald Statistic | p-value |
|--------|-----------|----------|----------------|---------|
| origin | $\beta_0$ | -9.5663  | 21.1563        | .0001   |
| 1      | $\beta_1$ | 3.3223   | 19.9926        | .0001   |
| 2      | $\beta_2$ | 1.7262   | 20.7768        | .0001   |
| 3      | $\beta_3$ | 2.8937   | 19.6213        | .0001   |
| 4      | $\beta_4$ | 3.5733   | 20.2762        | .0001   |

---

Estimated Variance-Covariance Matrix:  $I(\hat{\beta})^{-1}$

|           | $\beta_0$ | $\beta_1$ | $\beta_2$ | $\beta_3$ | $\beta_4$ |
|-----------|-----------|-----------|-----------|-----------|-----------|
| $\beta_0$ | 4.3256    | -.14398   | -.7568    | 0.12722   | -1.5200   |
| $\beta_1$ |           | .5521     | .2519     | .4235     | .5059     |
| $\beta_2$ |           |           | .1434     | .2226     | .2659     |
| $\beta_3$ |           |           |           | .4268     | .4470     |
| $\beta_4$ |           |           |           |           | .6297     |

---

Overall Goodness of Fit test (3.5.5)

$\chi^2 = 5.9819$     $E(\chi^2|\hat{\beta}) = 7.5908$     $V(\chi^2|\hat{\beta}) = 96.3564$    p-value = .5651

Intercept Only Tests (4 degrees of freedom)

Score Test statistic                      = 54.253                      p-value = .0001

Likelihood Test statistic                = 81.778                      p-value = .0001

---



**Table 7.3**

## Two Agent Simulated Data

## Observed and Predicted Responses and Goodness-of-Fit Statistics

| Ray    | $\mathbf{a}_r$ | Total Dose | $\tilde{\pi}$<br>observed<br>response | $\hat{\pi}$<br>predicted<br>response | Goodness-<br>of-Fit<br>$C_i$ | Goodness-<br>of-Fit<br>$D_i$ |
|--------|----------------|------------|---------------------------------------|--------------------------------------|------------------------------|------------------------------|
| origin |                | 0          | 0.00                                  | .0001                                | -.01871                      | .02647                       |
| 1      | (1 0)          | 2          | 0.00                                  | .0511                                | -.5189                       | .7242                        |
|        |                | 3          | 0.60                                  | .5989                                | .0053                        | .0053                        |
|        |                | 4          | 1.00                                  | .9764                                | .3476                        | .4886                        |
|        |                | 5          | 1.00                                  | .9991                                | .0660                        | .0933                        |
| 2      | (0 1)          | 3          | 0.00                                  | .0123                                | -.2493                       | .3515                        |
|        |                | 4          | 0.00                                  | .0653                                | -.5910                       | .8217                        |
|        |                | 5          | 0.60                                  | .2819                                | 1.5810                       | 1.4805                       |
|        |                | 6          | 0.60                                  | .6881                                | -.4251                       | -.4159                       |
|        |                | 7          | 0.80                                  | .9254                                | -1.0664                      | -.8980                       |
|        |                | 8          | 1.00                                  | .9859                                | .2679                        | .3776                        |
| 3      | (.67 .33)      | 2          | 0.00                                  | .0222                                | -.3370                       | .4740                        |
|        |                | 3          | 0.40                                  | .2903                                | .5402                        | .5240                        |
|        |                | 4          | 0.80                                  | .8805                                | -.5549                       | -.5128                       |
|        |                | 5          | 1.00                                  | .9925                                | .1941                        | .2740                        |
| 4      | (.33 .67)      | 2          | 0.00                                  | .0811                                | -.6645                       | .9199                        |
|        |                | 3          | 0.80                                  | .7582                                | .2183                        | .2230                        |
|        |                | 4          | 1.00                                  | .9911                                | .2119                        | .2990                        |
|        |                | 5          | 1.00                                  | .9998                                | .0356                        | .0503                        |

Therefore, under additivity

$$\log \text{it}(\pi_{rk}^A) = \beta_0 + \beta_1 X_{rk1} + \beta_2 X_{rk2} + \cdots + \beta_N X_{rkN}. \quad (7.4.2)$$

By applying the relationship between total dose and the doses of the  $N$  agents given in (7.2.2) this expression can also be written as

$$\begin{aligned} \log \text{it}(\pi_{rk}^A) &= \beta_0 + \beta_1 t_{rk} a_{r1} + \beta_2 t_{rk} a_{r2} + \cdots + \beta_N t_{rk} a_{rN} \\ &= \beta_0 + t_{rk} \sum_{i=1}^N \beta_i a_{ri} \\ &= \beta_0 + \beta_r^A t_{rk} \end{aligned} \quad (7.4.3)$$

where  $\beta_r^A = \sum_{i=1}^N \beta_i a_{ri}$ ;  $r = 1, 2, \dots, M$ .

Recall that the elements of  $\mathbf{a}_r$  associated with the  $r$ th axis ray, are identically zero with the exception of the  $r$ th element which is 1. It follows then from (7.4.3) that for the axis rays

$$\begin{aligned} \beta_r^A &= \sum_{i=1}^N \beta_i a_{ri} \\ &= \beta_r; \quad r=1, 2, \dots, N. \end{aligned}$$

Therefore under the assumption of additivity the  $(M+1) \times 1$  parameter vector is given by

$$\boldsymbol{\beta}^A = \left[ \beta_0 \quad \beta_1 \quad \cdots \quad \beta_N \quad \sum_{i=1}^N a_{N+1,i} \beta_i \quad \cdots \quad \sum_{i=1}^N a_{M,i} \beta_i \right]'$$

with only  $(N+1)$  unknown parameters,  $\beta_0, \beta_1, \dots, \beta_N$ . Thus, the hypothesis of interest can be expressed as

$$\begin{aligned} H_0 : \beta &= \beta^A \\ H_a : \beta &\neq \beta^A \end{aligned} \tag{7.4.4}$$

Rejection of  $H_0$  implies at least one  $\beta_j \neq \beta_j^A$ ;  $j=N+1, \dots, M$ , or, equivalently, there is a nonadditive interaction along at least one of the non-axis rays. Likelihood ratio, Wald and Score tests for this hypothesis will now be developed. Asymptotically, all three test statistics converge to the same Chi-square distribution. In general, it has been shown that none of the three testing approaches is consistently superior to the others (Kotz, et. al., Encyclopedia of Statistics, 1988, Vol 8, p. 307). The likelihood ratio test can be considered the most practical since the required likelihood statistics are often incorporated in the commonly used computer software packages that fit these models. For illustrative purposes all three statistics will be reported for the following two examples.

#### 7.4.1 Likelihood Ratio Test for Nonadditivity

In Section 3.6, likelihood ratio tests which compared a restricted and unrestricted model were discussed. There it was assumed the unrestricted model contained  $p$  parameters. The restricted model, defined in the null hypothesis, was constructed by setting  $r < p$  of these parameters equal to 0. Hence  $r$  restrictions were specified. The two models were fit and the log-likelihood evaluated at each set of maximum likelihood estimates. The difference of these log-likelihoods was then determined. A large difference in these log-likelihoods was evidence that the null hypothesis could be rejected.

In order to test  $H_0 : \beta = \beta^A$  a similar approach can be taken. Here, however, rather than restricting a subset of the parameters to equal 0, the restrictions are given by

$$\beta_j = \sum_{i=1}^N a_{ji} \beta_i; \quad j = N+1, N+2, \dots, M.$$

There are  $M - N$  restrictions corresponding the  $M - N$  non-axis rays. Let  $\hat{\beta}$  denote the  $(M+1) \times 1$  vector of maximum likelihood estimates for  $\beta$  in the unrestricted model specified in  $H_a$ . Let  $\hat{\beta}^A$  denote the maximum likelihood estimates for the restricted model under the assumption of additivity. In addition let  $l(\hat{\beta}; y)$  and  $l(\hat{\beta}^A; y)$  denote the log-likelihood evaluated at each of these parameter estimates. Serfling (1980, p.158) has shown that the approximate distribution of

$$\lambda^A = -2\{l(\hat{\beta}; y) - l(\hat{\beta}^A; y)\} \quad (7.4.5)$$

is  $\chi_{M-N}^2$  where the degrees of freedom are associated with the number of restrictions defined in  $H_0$ . Large values of  $\lambda^A$  indicate the null hypothesis, i.e., additivity, can be rejected.

The unrestricted model can be fit as illustrated in Section 7.3. In order to fit the model under additivity recall that the additive model is given by

$$\begin{aligned} \log \text{it}(\pi_{rk}^A) &= \beta_0 + \beta_r^A t_{rk} = \beta_0 + \left( \sum_{i=1}^N a_{ri} \beta_i \right) t_{rk} = \beta_0 + \sum_{i=1}^N \beta_i a_{ri} t_{rk} \\ &= \beta_0 + \sum_{i=1}^N \beta_i X_{rki}. \end{aligned}$$

Hence the restricted model can be fit in a straightforward manner in terms of the doses of the individual agents as opposed to the total doses.

Once the two models are fit the difference in the log-likelihoods can be determined and the hypothesis tested.

#### 7.4.2 Wald Test for Nonadditivity

The Wald statistic,  $W^A$ , for testing for deviations from additivity is based on the approximate distribution of the  $(M+1) \times 1$  vector of maximum likelihood estimates. Recall that under the unrestricted model this approximate distribution is given by

$$\hat{\boldsymbol{\beta}} \sim N_{M+1}(\boldsymbol{\beta}, I(\boldsymbol{\beta})^{-1}) \quad (7.4.6)$$

where  $I(\boldsymbol{\beta})^{-1}$  is the inverse of the information matrix defined in (7.2.12).

In this case it is useful to rewrite the null hypothesis as  $H_0 : \boldsymbol{\beta} - \boldsymbol{\beta}^A = 0$ . This hypothesis can be simplified further by noting

$$\begin{aligned} (\boldsymbol{\beta} - \boldsymbol{\beta}^A) &= [\beta_0 - \beta_0^A \quad \beta_1 - \beta_1^A \quad \cdots \quad \beta_N - \beta_N^A \quad \beta_{N+1} - \beta_{N+1}^A \quad \beta_{N+2} - \beta_{N+2}^A \quad \cdots \quad \beta_M - \beta_M^A]' \\ &= \left[ 0 \quad \cdots \quad 0 \quad \beta_{N+1} - \sum_{i=1}^N a_{N+1,i} \beta_i \quad \beta_{N+2} - \sum_{i=1}^N a_{N+2,i} \beta_i \quad \cdots \quad \beta_M - \sum_{i=1}^N a_{Mi} \beta_i \right]'. \end{aligned}$$

Hence the null hypothesis can be written in terms of only the  $M-N$  nontrivial restrictions as

$H_0 : \boldsymbol{\beta}_j - \sum_{i=1}^N a_{ji} \beta_i = 0; j = N+1, N+2, \dots, M$ . If we now define a  $(M-N) \times (M+1)$  matrix  $C$

as

$$C = \begin{bmatrix} 0 & -a_{N+1,1} & \cdots & -a_{N+1,N} & 1 & 0 & \cdots & 0 \\ 0 & -a_{N+2,1} & \cdots & -a_{N+2,N} & 0 & 1 & \cdots & 0 \\ \vdots & \vdots & \vdots & \vdots & \vdots & \vdots & \vdots & \vdots \\ 0 & -a_{M1} & \cdots & -a_{MN} & 0 & 0 & \cdots & 1 \end{bmatrix} \quad (7.4.7)$$

the null hypothesis can also be written as  $H_0 : \mathbf{C}\boldsymbol{\beta} = \mathbf{0}$ .

Based on the approximate distribution of  $\hat{\boldsymbol{\beta}} - \boldsymbol{\beta}$  given in (7.4.6) it follows that

$$\mathbf{C}\hat{\boldsymbol{\beta}} \sim N_{M-N}(\mathbf{C}\boldsymbol{\beta}, \mathbf{C}\mathbf{I}(\boldsymbol{\beta})^{-1}\mathbf{C}').$$

The Wald Statistic,  $W^A$  and its approximate distribution are therefore given by

$$W^A = (\mathbf{C}\hat{\boldsymbol{\beta}})' (\mathbf{C}\mathbf{I}(\hat{\boldsymbol{\beta}})^{-1}\mathbf{C}')^{-1} \mathbf{C}\hat{\boldsymbol{\beta}} \sim \chi_{M-N}^2. \quad (7.4.8)$$

If the observed value of this statistic is large, nonadditivity is indicated on at least one of the non-axis rays.

### 7.4.3 Score Test for Nonadditivity

Recall that the scores are the partial derivatives of the log-likelihood with respect to  $\boldsymbol{\beta}$ , the unknown parameters. The goal of maximum likelihood estimation is to find  $\hat{\boldsymbol{\beta}}$ , the estimated values of the parameters that maximize this likelihood. This is equivalent to simultaneously setting all of the scores equal to 0 and solving for  $\hat{\boldsymbol{\beta}}$ .

In Chapter 3 the scores were used to test the hypothesis  $H_0: \boldsymbol{\beta} = \boldsymbol{\gamma}_0$  where  $\boldsymbol{\gamma}_0$  is a vector of constants. In general, if the scores evaluated at  $\boldsymbol{\gamma}_0$  are close to 0, it can be concluded that the log-likelihood evaluated at  $\boldsymbol{\gamma}_0$  is close to the maximum. This can be especially useful if a subset of the elements of  $\boldsymbol{\gamma}_0$  are equal to 0. If the hypothesis  $H_0: \boldsymbol{\beta} = \boldsymbol{\gamma}_0$  is not rejected it implies that a subset of the parameters  $\boldsymbol{\beta}$  can be used to model the data.

In a similar way the scores can be used to test for deviations from additivity. Let  $\hat{\beta}^A$  denote the maximum likelihood estimates of the parameters under the assumption of additivity. If  $U(\hat{\beta}^A)$ , the scores evaluated at  $\hat{\beta}^A$  are close to zero, it can be concluded that the assumption of additivity should not be rejected. Conversely, if  $U(\hat{\beta}^A)$  is large, it implies the unrestricted model defined in the alternative hypothesis is the more appropriate model. Rao (1973, p. 419) has shown the following statistic and its approximate distribution can be used to formally test  $H_0 : \beta = \beta^A$ :

$$S^A = U(\hat{\beta}^A)' I(\hat{\beta}^A)^{-1} U(\hat{\beta}^A) \sim \chi_{M-N}^2 \quad (7.4.9)$$

Large values of  $S^A$  indicate the null hypothesis of additivity should be rejected.

Once the null hypothesis of additivity has been rejected the investigator can conclude nonadditivity is indicated along at least one non-axis ray. In the following section techniques are presented to determine the non-axis rays associated with nonadditivity. The nature of the departure from additivity will also be described.

### 7.5 Characterizing and Testing for Deviations from Additivity Along Each Non-axis Ray

Recall that in Definition 4.3.2, definitions of synergism and antagonism were given. For example, assuming each active single agent dose-response curve is increasing, there is evidence of a synergism at the  $r$ th observation along the  $k$ th ray if the predicted response is greater than the response expected under additivity, i.e.,  $\hat{\pi}_{rk} > \hat{\pi}_{rk}^A$ . Conversely an antagonism is indicated if  $\hat{\pi}_{rk} < \hat{\pi}_{rk}^A$ . A similar argument can be made for decreasing dose-response curves. Since  $\logit(\hat{\pi}_{rk}) = \hat{\beta}_0 + \hat{\beta}_r t_{rk}$  and  $\logit(\hat{\pi}_{rk}^A) = \hat{\beta}_0 + \hat{\beta}_r^A t_{rk}$  a

comparison of  $\hat{\beta}_r$  and  $\hat{\beta}_r^A$  is equivalent to comparing  $\hat{\pi}_{rk}$  and  $\hat{\pi}_{rk}^A$ . Thus, for  $r = 1, 2, \dots, M$  the type of interaction suggested by the fitted model is given by the following:

| Active Single Agent<br>Dose-Response<br>Curves | $\hat{\beta}_r = \hat{\beta}_r^A$ | $\hat{\beta}_r > \hat{\beta}_r^A$ | $\hat{\beta}_r < \hat{\beta}_r^A$ |
|--|-----------------------------------|-----------------------------------|-----------------------------------|
| Increasing                                     | Additivity                        | Synergism                         | Antagonism                        |
| Decreasing                                     | Additivity                        | Antagonism                        | Synergism                         |

(7.5.1)

However, for each non-axis ray, it still must be determined if there is a statistically significant difference between  $\hat{\beta}_r$  and  $\hat{\beta}_r^A$ . In Section 7.4.2 a Wald statistic,  $W^A$  was used to simultaneously test for nonadditivity along all of the  $M-N$  non-axis rays. A similar statistic,  $W_r^A$  can now be applied to each of these non-axis rays individually.

For  $r$ th non-axis ray,  $r=N+1, \dots, M$  the hypothesis of interest is  $H_0 : \beta_r = \beta_r^A$  or equivalently

$$H_0 : \beta_r - \sum_{i=1}^N a_{ri} \beta_i = 0. \quad (7.5.2)$$

The expression given in the null hypothesis is the  $(r-N)$ th,  $r = N+1, \dots, M$ , element of the  $(M-N) \times 1$  vector,  $C\hat{\beta}$  where  $C$  is given by (7.4.7). Since  $C\hat{\beta} \sim N_{M-N}(\beta, CI(\beta)^{-1}C')$  the  $r$ th row of the vector  $C\hat{\beta}$  is also approximately normal, i.e.,

$$\hat{\beta}_r - \sum_{i=1}^N a_{ri} \hat{\beta}_i \sim N\left(\beta_r - \sum_{i=1}^N a_{ri} \beta_i, (CI(\beta)^{-1}C')_{r-N, r-N}\right)$$



where  $(\mathbf{CI}(\boldsymbol{\beta})^{-1}\mathbf{C}')_{r-N,r-N}$  is the  $(r-N)$ th diagonal element of  $(\mathbf{CI}(\boldsymbol{\beta})^{-1}\mathbf{C}')$ . The Wald Test Statistic associated with the  $r$ th ray and its approximate distribution are therefore given by

$$W_r^A = \frac{n \left( \hat{\beta}_r - \sum_{i=1}^N a_{ri} \hat{\beta}_i \right)^2}{(\mathbf{CI}(\boldsymbol{\beta})^{-1}\mathbf{C}')_{r-N,r-N}} \sim \chi_1^2; \quad r=N+1, \dots, M. \quad (7.5.3)$$

For studies which include more than one non-axis ray this procedure will be applied  $(M-N)$  times. This implies the probability of incorrectly rejecting additivity along at least one of the rays, or the probability of a type I error, will be greater than  $\alpha$ . In order to insure the overall probability of a Type I error is less than or equal to  $\alpha$  the multiple comparison described in Section 6.3 will be applied. Once an overall additivity test has indicated the existence of nonadditivity along at least one of the non-axis rays, these individual Wald Tests based on  $W_r^A$  can be applied to determine where the deviations occur. For the rays where nonadditivity was found the types of interaction can be distinguished by applying (7.5.1).

To illustrate an application of these tests for deviations from additivity the two agent simulated data discussed in Section 7.3 will be examined. To also demonstrate the technique in higher dimensions, a 4 agent, 19 ray, simulated data set will then be analyzed.

### 7.5.1 Two Agent Example

Consider the two agent simulated data set described in Section 7.3. The results of applying the three overall tests for deviations from additivity are listed in the top of Table 7.4. Clearly there is a significant interaction along at least one of the two non-axis rays. Listed in the bottom of Table 7.4 are the estimated slope parameters under the full and

**Table 7.4**  
Two Agent Simulated Data

Simultaneous Tests for Deviations from Additivity

| Test                  | $\chi^2$ | df | p-value |
|-----------------------|----------|----|---------|
| Likelihood Ratio Test | 18.3300  | 2  | .0001   |
| Wald Test             | 10.0079  | 2  | .0067   |
| Score Test            | 12.5542  | 2  | .0019   |

Test for Deviations from Additivity Along Each Nonaxis ray

| Ray | $\mathbf{a}_r$ |     | $\hat{\beta}$ | $\hat{\beta}^A$ | Wald      |         | Critical p* | Type of Interaction |
|-----|----------------|-----|---------------|-----------------|-----------|---------|-------------|---------------------|
|     |                |     |               |                 | Statistic | p-value |             |                     |
| 3   | .67            | .33 | 2.8937        | 2.7875          | .1359     | .7120   | .0250       |                     |
| 4   | .33            | .67 | 3.5733        | 2.2560          | 10.376    | .0013   | .0500       | Synergism           |

\* Based on Multiple Testing Procedure of Hochberg (1988), Critical  $p = \frac{\alpha}{K - i + 1}$ ;

$i=1,2,\dots,K$  where  $\alpha = 0.05$  and  $K = 2$

additive model as well as the individual Wald additivity test results. A synergism is indicated along ray 4. No deviation from additivity was found for ray 3.

In order to graphically summarize the results of this study the predicted dose response relationships under the full and restricted models can be plotted for each ray (Figure 7.2). The actual observed values can also be included to allow a graphical assessment of the fit of the model. In agreement with the results of the goodness-of-fit test shown in Table 7.2 ( $p=.5651$ ), the fitted model appears to adequately describe the data. The response curves predicted under additivity are plotted for the non-axis rays using a dotted line. Synergism is indicated when the additive dose response curve is below the curve predicted under the unrestricted model. Conversely, when the additive curve is above the curve predicted under the unrestricted model there is evidence of an antagonistic interaction. In Figure 7.2, both plots associated with the non-axis rays indicate a synergism. However, when examining the closeness of the two curves in the plot associated with ray 3, it is not surprising that no deviation from additivity was found for this ray.

It can therefore be concluded from this two agent study that for certain regions of the 2-dimensional dose space, specifically when the doses are in the .33 : .67 or 1:2 ratio, a synergistic interaction occurs between the agents. When the agents are in the .67 : .33 or 2:1 ratio, there is no evidence of deviations from additivity.

### **7.5.2 Four Agent Example**

In order to extend the illustration of these techniques to higher dimensions, a four agent, 15 ray, data set was simulated based on the 4-dimensional dose-response relationship

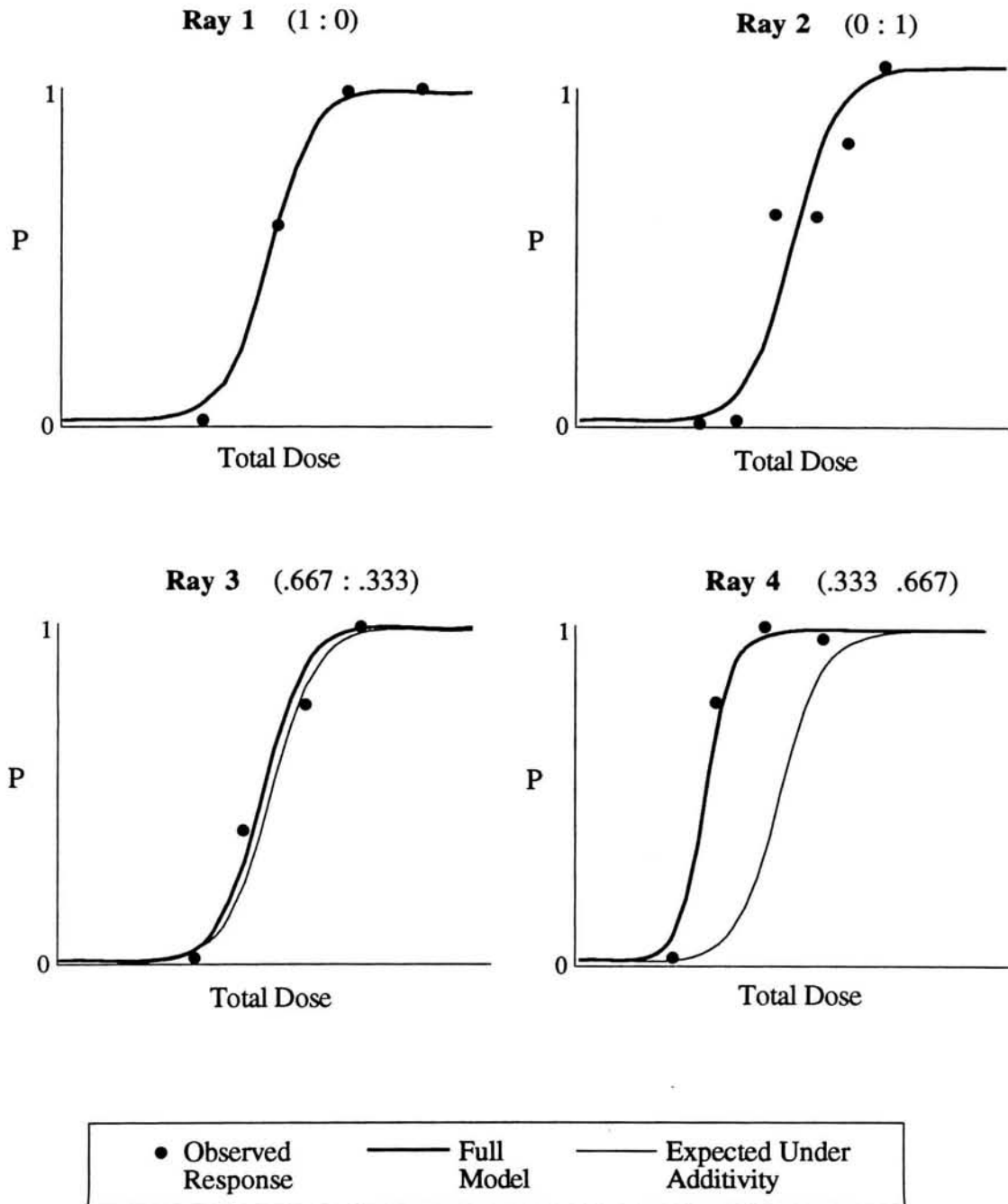


**Figure 7.2:** Two Agent Simulated Data - Full Model versus Expected Under Additivity

$$\begin{aligned} \text{logit}(\pi) = & -20 + 2X_1 + 5X_2 + 7X_3 + 4X_4 + \\ & .75X_1X_2 + .8X_1X_3 + .65X_1X_4 - .3X_2X_3 + .6X_2X_4 - .5X_3X_4 + \\ & .5X_1X_2X_3 + .55X_1X_2X_4 - .4X_1X_3X_4 + .45X_2X_3X_4 + .85X_1X_2X_3X_4. \end{aligned}$$

The simulated data are listed in Table 7.5. The rays run through the center of each of the dose subspaces. For example, the ray given by (.5 .5 0 0) runs through the center of the  $X_1 X_2$  dose space while (.25 .25 .25 .25) runs through the center of the 4 agent space. Assume that a range finding procedure was used to determine the total doses along each of the rays. The estimated parameters and the statistics associated with the fit of the model are shown in Table 7.6. The results of the intercept only tests indicate at least one nonintercept parameter is nonzero. The overall goodness-of-fit test (p-value of .7679) implies the model adequately describes the data.

In the top of Table 7.7 the results of the overall tests for nonadditivity are given. All three of the tests indicate there is a nonadditive interaction along at least one of the non-axis rays. The individual Wald tests are shown in the bottom of Table 7.7. According to the multiple comparison procedure described in Section 6.3, the results are ordered by the size of the observed p-values. Once an observed p-value is less than the adjusted p-value, the comparisons stop and rejection of the null hypothesis is concluded for the remaining rays. There are clearly regions in the dose space where significant nonadditive interactions are found. The type of interaction, however, varies.

A graphical representation of these results is given in Figure 7.3. In each plot the observed responses and predicted response curve are shown. For each non-axis ray the additive dose response relationship is also plotted. By examining these plots the following conclusions about the interactions between the agents can be drawn. Synergistic



Table 7.6

Four Agent Simulated Data  
Analysis Results

| Ray    | $\mathbf{a}_r$    | Parameter    | Estimate | Wald Statistic | p-value |
|--------|-------------------|--------------|----------|----------------|---------|
| origin |                   | $\beta_0$    | -21.9163 | 90.6856        | .0001   |
| 1      | (1 0 0 0)         | $\beta_1$    | 2.2102   | 84.6759        | .0001   |
| 2      | (0 1 0 0)         | $\beta_2$    | 5.2972   | 83.0073        | .0001   |
| 3      | (0 0 1 0)         | $\beta_3$    | 7.6814   | 82.1227        | .0001   |
| 4      | (0 0 0 1)         | $\beta_4$    | 4.6226   | 84.6285        | .0001   |
| 5      | (.5 .5 0 0)       | $\beta_5$    | 4.6123   | 84.6515        | .0001   |
| 6      | (.5 0 .5 0)       | $\beta_6$    | 4.3350   | 84.9695        | .0001   |
| 7      | (.5 0 0 .5)       | $\beta_7$    | 4.0041   | 83.7230        | .0001   |
| 8      | (0 .5 .5 0)       | $\beta_8$    | 6.1888   | 82.0405        | .0001   |
| 9      | (0 .5 0 .5)       | $\beta_9$    | 5.5589   | 83.5148        | .0001   |
| 10     | (0 0 .5 .5)       | $\beta_{10}$ | 4.9324   | 83.3943        | .0001   |
| 11     | (.33 .33 .33 0)   | $\beta_{11}$ | 5.3025   | 83.0073        | .0001   |
| 12     | (.33 .33 0 .33)   | $\beta_{12}$ | 4.7207   | 82.0842        | .0001   |
| 13     | (.33 0 .33 .33)   | $\beta_{13}$ | 3.3830   | 86.3757        | .0001   |
| 14     | (0 .33 .33 .33)   | $\beta_{14}$ | 6.0091   | 81.8450        | .0001   |
| 15     | (.25 .25 .25 .25) | $\beta_{15}$ | 5.5416   | 83.4791        | .0001   |

---

Overall Goodness of Fit test (3.5.5)

$$\chi^2 = 45.7393 \quad E(\chi^2 | \hat{\beta}) = 65.0893 \quad V(\chi^2 | \hat{\beta}) = 699.2338 \quad p\text{-value} = .7679$$

Intercept Only Tests (14 degrees of freedom)

Score Test statistic = 249.715 p-value = .0001

Likelihood Test statistic = 418.540 p-value = .0001

---

**Table 7.7**

## Four Agent Simulated Data

Simultaneous Tests for Deviations from Additivity

| Test                  | $\chi^2$ | df | p-value |
|-----------------------|----------|----|---------|
| Likelihood Ratio Test | 140.474  | 11 | <.0001  |
| Wald Test             | 65.9924  | 11 | <.0001  |
| Score Test            | 111.9763 | 11 | <.0001  |

Test for Deviations from Additivity Along Each Non-axis Ray

| Ray | $\mathbf{a}_r$    | $\hat{\beta}$ | $\hat{\beta}^A$ | Wald<br>Statistic | p-value | Critical p* | Type of<br>Interaction |
|-----|-------------------|---------------|-----------------|-------------------|---------|-------------|------------------------|
| 14  | (0 .33 .33 .33)   | 6.009         | 5.861           | .4360             | .5091   | .0045       |                        |
| 8   | (0 .5 .5 0)       | 6.189         | 6.489           | 1.595             | .2066   | .0050       |                        |
| 11  | (.33 .33 0 .33)   | 5.303         | 5.058           | 1.671             | .1961   | .0056       |                        |
| 9   | (0 .5 0 .5)       | 5.559         | 4.960           | 8.552             | .0035   | .0063       | Synergism              |
| 15  | (.25 .25 .25 .25) | 5.542         | 4.953           | 8.999             | .0027   |             | Synergism              |
| 6   | (.5 0 .5 0)       | 4.335         | 4.9456          | 15.356            | <.0001  |             | Antagonism             |
| 7   | (.5 0 0 .5)       | 4.004         | 3.416           | 16.847            | <.0001  |             | Synergism              |
| 12  | (.33 .33 0 .33)   | 4.721         | 4.039           | 17.206            | <.0001  |             | Synergism              |
| 5   | (.5 .5 0 0)       | 4.612         | 3.754           | 27.606            | <.0001  |             | Synergism              |
| 10  | (0 0 .5 .5)       | 4.932         | 6.152           | 45.766            | <.0001  |             | Antagonism             |
| 13  | (.33 0 .33 .33)   | 3.383         | 4.933           | 111.815           | <.0001  |             | Antagonism             |

\* Based on Multiple Testing Procedure of Hochberg (1988), Critical  $p = \frac{\alpha}{K - i + 1}$ ;

$i=1,2,\dots,K$  where  $\alpha = 0.05$  and  $K = 11$



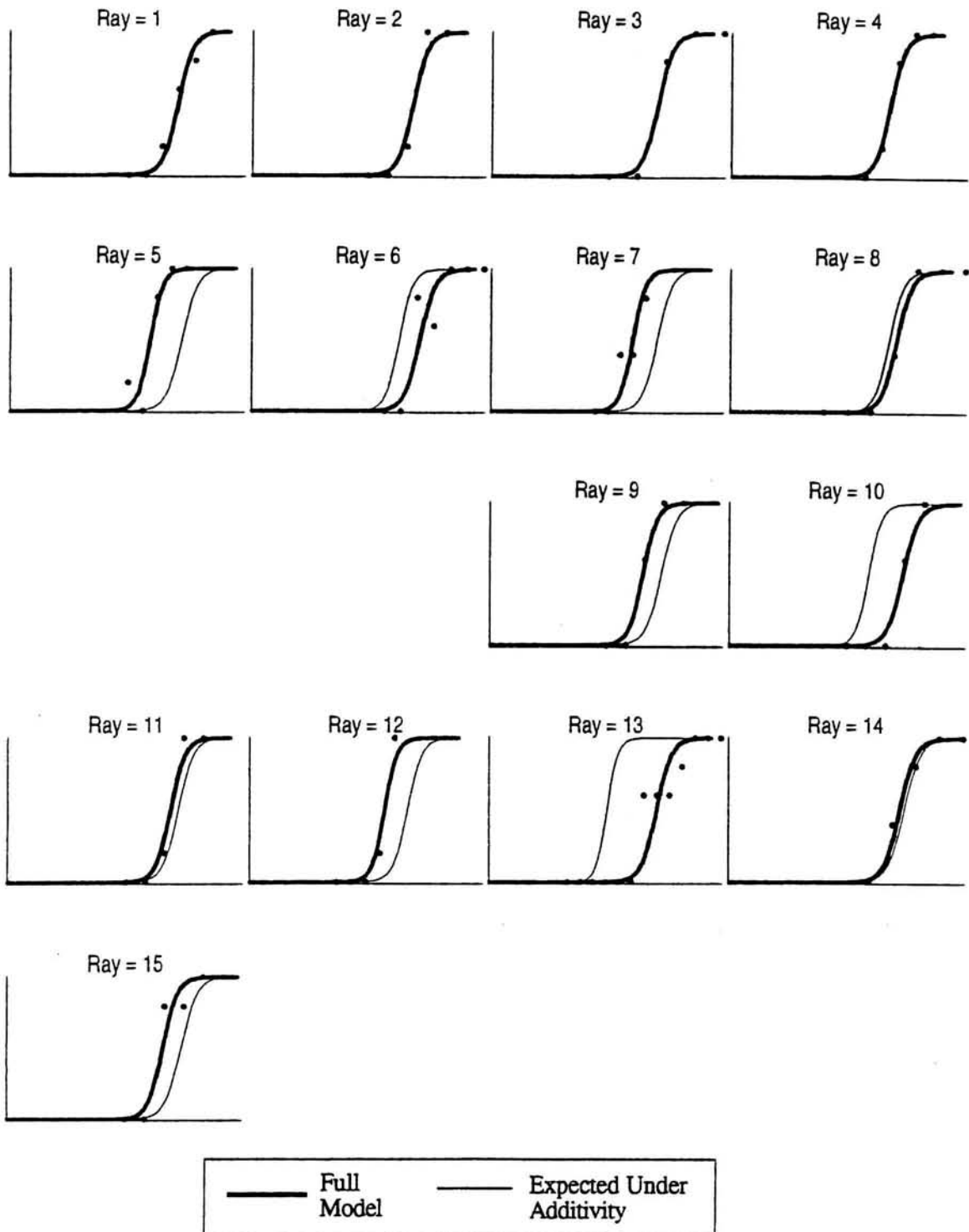


**Figure 7.3:** Four Agent Simulated Data - Full Model versus Expected Under Additivity

interactions are indicated between the pairs  $X_1$  and  $X_2$ ,  $X_1$ , and  $X_4$  and between  $X_2$  and  $X_4$ . In contrast antagonisms are indicated between  $X_1$  and  $X_3$ , and  $X_3$  and  $X_4$ . The synergistic interaction between  $X_1$  and  $X_2$  is no longer present when an equal dose of  $X_3$  is added (ray 11). When  $X_4$  is added to  $X_1$  and  $X_2$ , however, a synergism is still found. The synergistic interaction between  $X_1$  and  $X_4$  is changed to an antagonism when  $X_3$  is added. The antagonisms between  $X_1$  and  $X_3$ , and between  $X_3$  and  $X_4$  are maintained when all three agents are combined. When all four agents are combined, however, the antagonistic interactions disappear and a synergistic interaction is found.

In this 4-dimensional example the rays were chosen to span the entire four agent dose space. In this way, information about the interactions between the agents taken two at a time, three at a time, and then all together could be obtained. A different set of non-axis rays may be more appropriate, however, if the investigator was primarily interested in examining a particular region of the dose space. This example however, clearly illustrates the flexibility of the use of a ray design in determining a variety of nonadditive interactions throughout a dose space.

In earlier chapters it was noted that the focus of many studies of this kind was on a particular fixed level of the response, i.e., isobols at say  $p=0.5$ . In the next section, higher dimensional graphical displays of isobolograms, based on a ray designed experiment will be discussed.

## 7.6 Isobolograms for an N Agent Ray Designed Experiment

Recall the two agent isobologram for a fixed response,  $\pi$ , is a plot of the line of additivity in conjunction with a set of dose combinations that yield the response  $\pi$ . If a dose combination lies below the line of additivity a synergism is indicated. Conversely, if the dose combination lies above the line of additivity there is evidence of an antagonism.

In order to apply this type of plotting technique in a ray designed experiment the effective total doses along the  $r$ th ray, denoted by  $EDT_r(\pi)$ ,  $r = 1, 2, \dots, M$ , can be determined. Based on the model given in (7.2.4) these values are given by

$$EDT_r(\pi) = \frac{\text{logit}(\pi) - \hat{\beta}_0}{\hat{\beta}_r}; \quad r=1, 2, \dots, M. \quad (7.6.1)$$

In a similar way, by applying (7.4.3), the effective total doses under the assumption of additivity,  $EDT_r^A(\pi)$ , can be determined. Using (7.2.2) the dose levels for each agent corresponding to this total dose can be determined.

For the two-agent simulated experiment discussed, in Section 7.3, an isobologram is plotted in the Euclidean plane for  $\pi = 0.5$ . The predicted dose combinations that yield 0.5 are plotted along each ray with dots. As usual, connecting the two effective doses associated with each agent alone gives the line of additivity. The stars represent the dose combinations predicted under additivity. These points are simply the intersections of the rays with the line of additivity. Along both rays synergism is indicated since along each ray the predicted dose combinations are below the line of additivity. Along ray 3, however, the estimated dose combination is relatively close to the line of additivity. This is in agreement with the failure to detect an interaction along this ray.

An alternative representation of this plot, the parallel isobologram, is shown in Figure 7.5. Here each ray is plotted in a parallel fashion. The ratios associated with each ray are listed above the ray to indicate where in the dose-space the ray is located. The estimated total doses that yield the fixed response are plotted using dots. The total dose predicted under the assumption of additivity are plotted using a star. If the unrestricted predicted total dose is below the total dose predicted under additivity, a synergism is indicated. Conversely, if the unrestricted predicted point is above the additive predicted

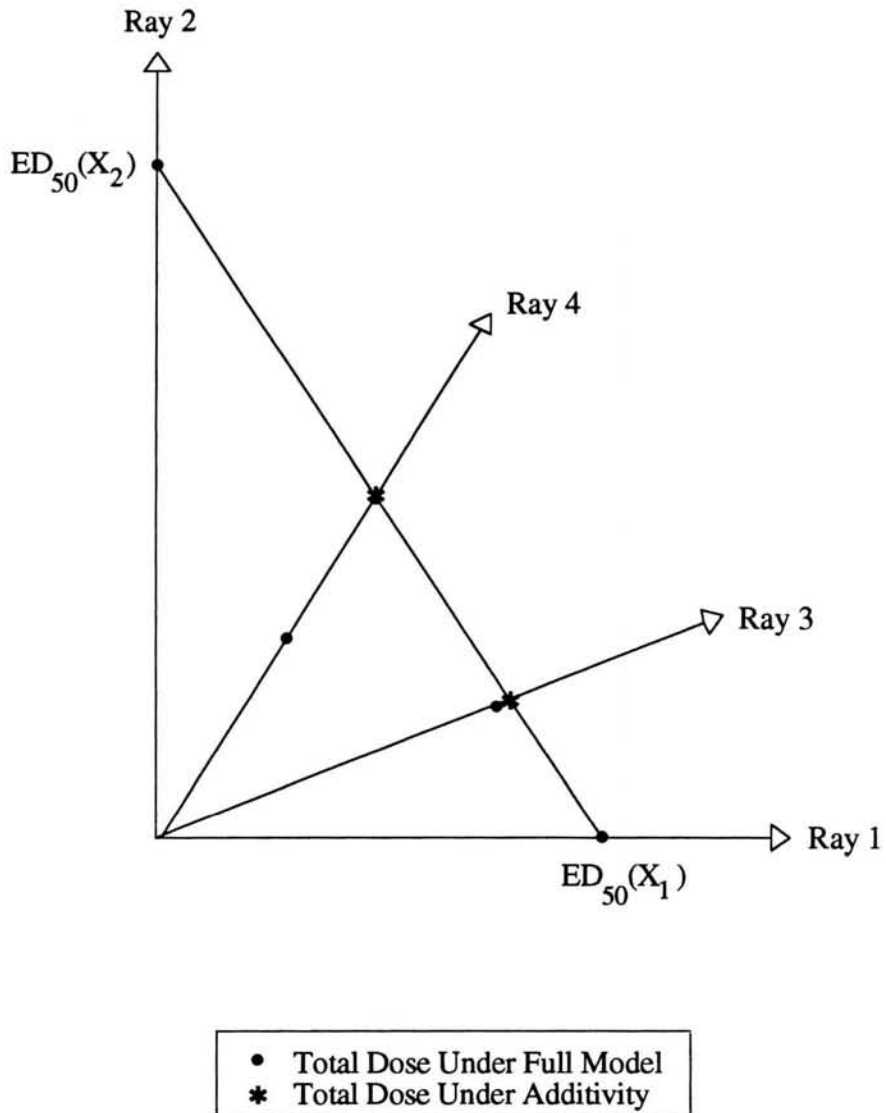


**Figure 7.4:** Isobologram ( $\pi=0.5$ ) for Two Agent Simulated Data

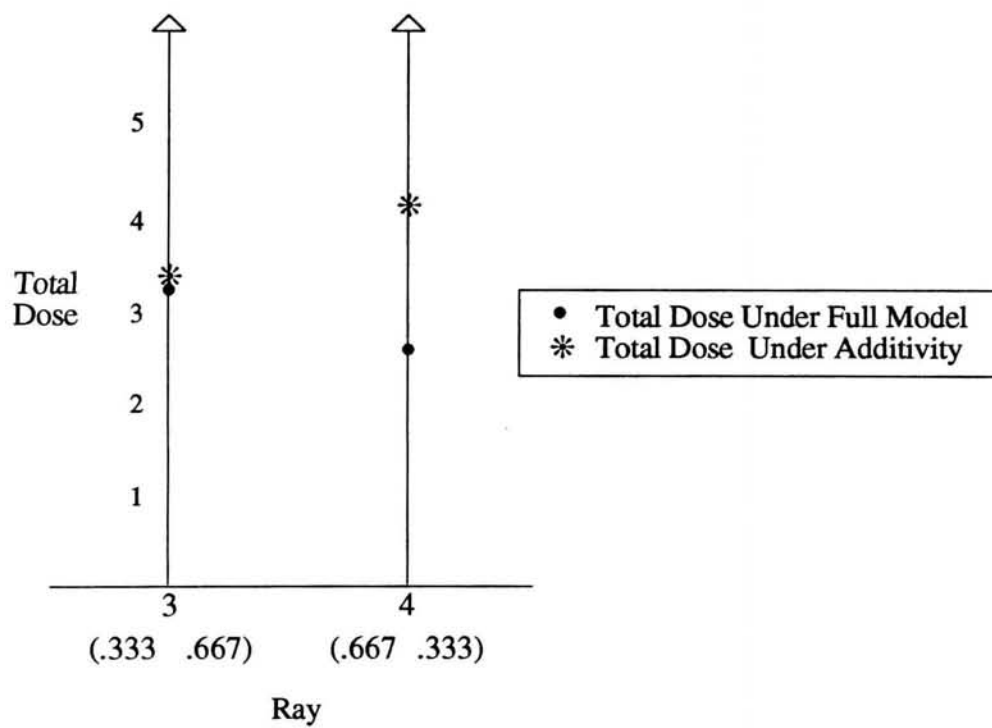


**Figure 7.5:** Parallel Isobologram ( $\pi=0.5$ ) for Two Agent Simulated Data

point, there is evidence of an antagonism. The non-significance of the synergistic interaction for Ray 3 is again noted by the closeness of the two points along this ray.

This second plotting technique can be extended to studies with any number of agents. In Figure 7.6 for  $\pi = 0.5$  the values of  $EDT_r(\pi)$  and  $EDT_r^A(\pi)$ ,  $r=5,6,\dots,15$ , are plotted for the 4 agent simulated data presented in Section 7.5. In this plot the rays are ordered by the observed p-values associated with the test for nonadditivity based on  $W_r^A$ . Alternative orderings of the rays, i.e., by types of interactions, may be more appropriate depending on the particular study. For this example, the plot clearly indicates at the 50% response level there are areas of the dose space where the agents are interacting synergistically and other areas where there is antagonism.

## 7.7 Summary

In this chapter methods for analyzing dose-response experimental data based on a ray design were presented. There are several advantages of this approach over an analysis based on response surface techniques where data are collected according to a factorial design. Here, if the investigator is interested only in a sub region of the N-dimensional dose space, data can be collected over as few as one non-axis ray. Alternatively, rays can be placed in several disjoint regions of the dose space. In both cases the actual number of observations may be much smaller than needed for a factorial design. For example, 426 observations were used in the simulated 8-dimensional data discussed in Section 7.7. In contrast, if a factorial design were used with 3 levels taken for each agent,  $3^8 = 6561$  observations would be taken. Even if a fraction of a factorial design was considered it is apparent that the ray design in a higher dimensional experiment may be cost effective.

It was also demonstrated in Chapter 5 that an isobologram, useful in a two agent dose-response surface analysis, is not adaptable to higher dimensional studies. Since the independent variable for these experiments is the 1-dimensional total dose rather than an

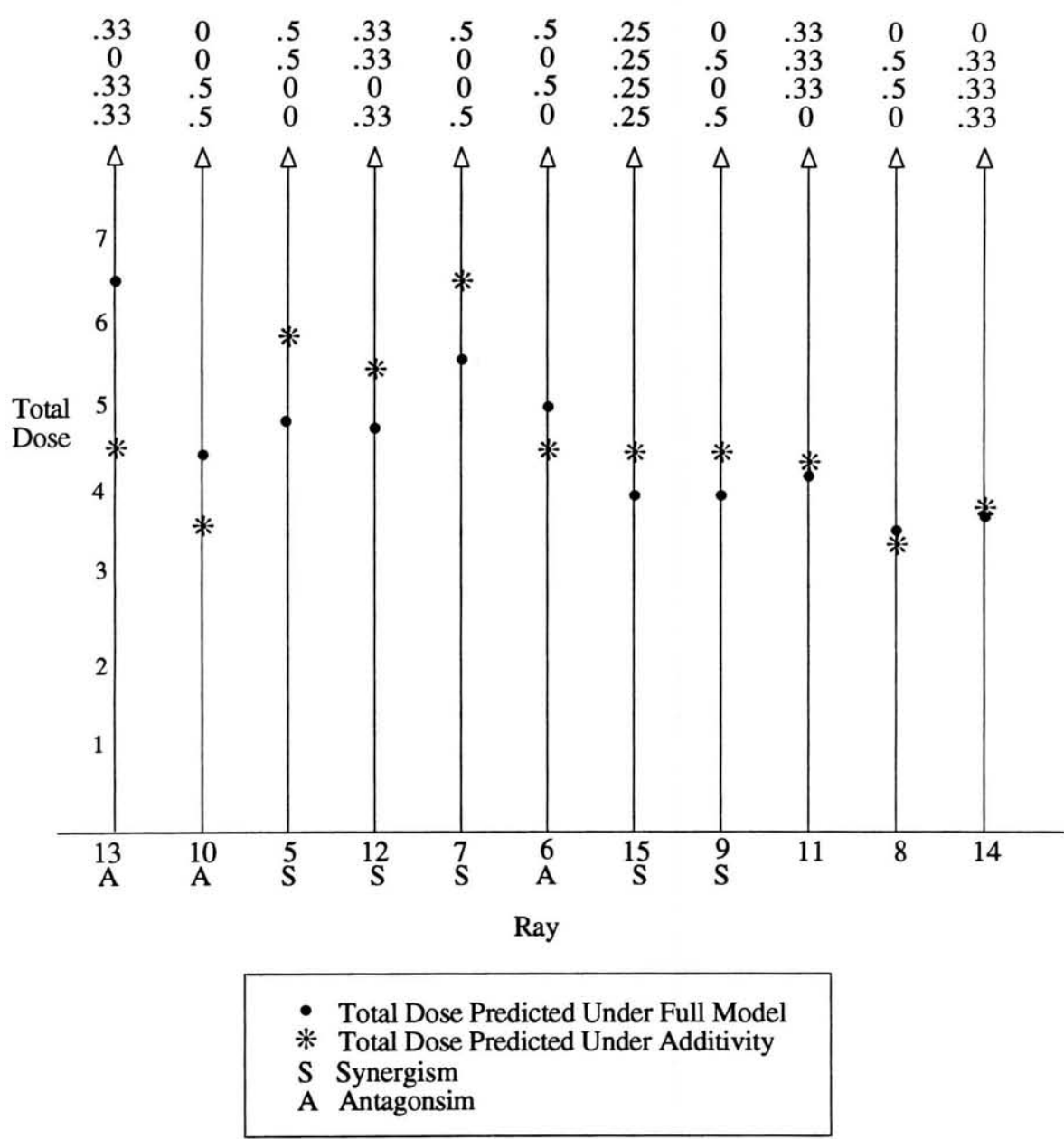


**Figure 7.6:** Parallel Isobologram ( $\pi = 0.5$ ) for 4-dimensional Simulated Data with Rays Ordered by Increasing Size of Observed P-values

N-dimensional vector of doses, several easy to interpret graphical techniques can be applied. Plotting the total dose against the fitted and observed data in an array of pairwise plots allows a visual assessment of the fit of the model. When the plot of the predicted dose-response curve under additivity is also plotted, the types of interactions that the model suggests can be visualized. The analyst does not need to study the set of parameter estimates in order to determine the character of the interactions. In addition, a parallel isobologram for a fixed response can be plotted. Here, along each ray, the predicted effective total doses under the fitted model and under additivity can be plotted. Again the types of interactions along each ray, at a fixed response of interest, can be easily observed.



## Chapter 8

### Extensions and Summary Comments

#### 8.1 Extensions

Several extensions can be made to the methods described in this dissertation for detecting and characterizing interactions. The dose-response relationships assumed in Chapters 7 were based on the logistic model. Here the dose-response curve along the  $r$ th ray is expressed as a linear function of the logit of the response, i.e.,  $\logit[P(t; \boldsymbol{\beta})] = \beta_0 + \beta_r t$ . Recall in Result 5.2.2 it was shown that this function is symmetric about  $\pi = 0.5$ . This constraint may, in fact, make it difficult to fit certain dose-response curves. For example, the rate of increase of a particular dose-response curve may be smaller for value of  $t > EDT_r(0.5)$  than for  $t < EDT_r(0.5)$ . The methods described in Chapter 7 can, however, be generalized to other transformations of the response besides the logit. Based on the generalized linear model (McCullagh and Nelder, 1989), a transformation of the response, or link, is written as a linear function of the doses. Various forms for this link function, including the logit, can be examined to determine which most adequately describes the data. Other forms for the dose-response model, such as the median effect equation given in (4.6.6), can be studied as well.

In order to generalize the methods of Chapter 7, models that account for extra variability in the data can also be considered. These models would be applicable when certain additional effects, such as litter, need be considered. As noted in Chapter 3, it was assumed that the variability in the data at each dose combination could be described by a

binomial distribution. This can be generalized to a beta-binomial distribution. In addition, the Quasi-likelihood approach, which further relaxes the distributional assumptions, can be considered.

Lastly, properties of the ray design can be examined to determine, along each ray, optimal levels of the total dose to consider in the experiment. For the examples described in this dissertation, it was assumed that the experimenter possessed prior knowledge of the dose-response surface sufficient to determine a range of total doses to examine along a ray. The development of two stage experimental designs could be useful in situations where there is insufficient prior knowledge.

## **8.2 Summary Comments**

The principal goal of this research was to derive methods for detecting and characterizing interactions in a study of a large number of agents. Analytic and graphical methods were considered. A summary of the new research presented in this dissertation is given below.

In Chapter 2, new plotting techniques useful in higher dimensional spaces were described and their usefulness illustrated in a repeated measures analysis. Specifically, it was shown that through the use of a parallel axis plotting system as well as a draftman's display of pair-wise plots, properties of higher dimensional data could be determined.

In Chapters 3 through 7, methods of detecting and characterizing interactions between any number of agents were considered. Well known properties of the logistic model, which was used to describe the dose-response relationships in this dissertation, were described in Chapter 3. In order to describe how the agents interact, several definitions and derivations were given in Chapter 4. This chapter summarized the results and assumptions previously made in an ad hoc, inconsistent manner throughout the literature on the subject. In Chapter 5, a technique for detecting and characterizing

interactions based on dose-response modeling was described. New graphical methods were developed in this chapter which were shown to be useful in interpreting the fitted model when a large number of agents are considered. In Chapter 6, it was also shown that certain properties of the logistic dose-response surface used in Chapter 5 are not applicable when a model is fit in terms of certain transformations for the doses. A new point-wise test to detect deviations from additivity was then derived which can be applied to studies of any number of agents. Lastly, in this research a method of detecting and characterizing interactions based on dose combinations that satisfy fixed ratios was derived and is described in Chapter 7. This technique was shown to be applicable to studies of a large number of agents. Several new graphical tools were introduced in this Chapter to assist in interpreting the fitted model.

## **REFERENCES**

## REFERENCES

- Agresti, A. (1990). *Categorical Data Analysis*. New York, NY: John Wiley & Sons.
- Ashford, J.R. and Smith, C.S. (1964). General Models for Quantal Response to the Joint Action of a Mixture of Drugs. *Biometrika* **51**, 413-428.
- Berenbaum, M.C. (1989). What is Synergy?. *Pharmacological Reviews*, **41**, 93-141
- Berenbaum, M.C. (1985). The Expected Effect of a Combination of Agents: The General Solution. *Journal of Theoretical Biology* **114**, 413-431.
- Berenbaum, M.C. (1981). Criteria for Analysing Interactions Between Biologically Active Agents. *Advances in Cancer Research.*, Vol. 35. New York, NY: Academic Press.
- Berenbaum, M.C. (1978). A Method for Testing for Synergy with Any Number of Agents. *The Journal of Infectious Diseases* **137**, 122-130.
- Berenbaum, M.C. (1977). Synergy, Additivism and Antagonism in Immunosuppression, A Critical Review. *Clinical and Experimental Immunology* **28**, 1-18.
- Bliss, C.I. (1939). The Toxicity of Poisons Applied Jointly. *Annals of Applied Biology* **26**, 585-615.
- Brunden, M.N. Vidmar, T.J. and McKean, J.W. (1988). *Drug Interaction and Lethality Analysis*. Boca Raton, Florida: CRC Press.
- Calabrese, E.J. (1991). *Multiple Chemical Interactions*. Chelsea, Michigan: Lewis Publishers.
- Carter, W.H., Gennings, C., Staniswalis, J., Campbell, E. and White, K. (1988). A Statistical Approach to the Construction and Analysis of Isobolograms. *Journal of American College of Toxicology* **7**, 963-973.
- Chambers, J.M., Cleveland, W.S., Kleiner, B., and Tukey, P.A. (1983). *Graphical Methods for Data Analysis*. Belmont, California: Wadsworth International Group.
- Chao, T.C. and Rideout, D.C. (1991). *Synergism and Antagonism in Chemotherapy*.

New York, N.Y.: Academic Press, Inc.

- Chao, T. C. and Talalay, P. (1984). Quantitative Analysis of dose-Effect Relationships: The Combined Effects of Multiple Drugs on Enzyme Inhibitors. *Adv. Enz. Res.* **22** 22-55.
- Cox, D.R. and Oakes, D. (1984). *Analysis of Survival Data*. New York, NY: Chapman & Hall.
- Dobson, A.J. (1990). *An Introduction to Generalized Linear Models*. New York, NY: Chapman & Hall.
- Finney, D.J. (1952). *Probit Analysis, Second Edition*. London: Cambridge University Press.
- Gennings, C. and Carter, W.H., Jr. (1995). Utilizing Concentration-Response Data from Individual Components to Detect Statistically Significant Departures from Additivity in Chemical Mixtures. *Biometrics*, In Press.
- Gennings, C., Dawson, K.S., Carter, W.H., Jr., and Myers, R.H. (1990). Interpreting Plots of a Multidimensional Dose-Response Surface in a Parallel Coordinate System. *Biometrics* **46**, 719-735.
- Gennings, C., Carter, W.H., Campbell, E., Staniswalis, J., Martin, T., Martin, B., and White, K. (1990). Isobolographic Characterization of Drug Interaction Incorporating Biological Variability. *The Journal of Pharmacology and Experimental Therapeutics* **252**, 208-217.
- Gershwin, M.E. and Smith, N.T. (1973). Interaction Between Drugs Using Three-Dimensional Isobolographic Interpretation. *Arch. Int. Pharmacodyn.* **201**, 154-161.
- Gessner, P. and Cabana, B. (1970). A Study of the Interaction of the Hypnotic Effects and of the Toxic Effects of Chloral Hydrate and Ethanol. *The Journal of Pharmacology and Experimental Therapeutics* **174**, 247-259.
- Greco, W.R., Park, H.S. and Rustum, Y.M. (1990). Application of a New Approach for the Quantitation of Drug Synergism to the Combination of cis-Diamminedichloroplatinum and 1- $\beta$ -D-Arabinofuranosylcytosine. *Cancer Research* **50**, 5318-5327.
- Harville, D.A. (1977). Maximum Likelihood Approaches to Variance Component Estimation and to Related Problems. *Journal of the American Statistical Association* **72**, 320-340.
- Hauck, W.W. (1983). A Note on Confidence Bands for the Logistic Response Curve. *The American Statistician* **37**, 158-160.
- Hauck, Jr., W.W. and Donner, A. (1977). Wald's Test as Applied to Hypotheses in Logit

- Analysis. *Journal of the American Statistical Association* **72**, 851-853.
- Hewlett, P.S. (1969). Measurement of the Potencies of Drug Mixtures. *Biometrics* **25**, 477-487.
- Hewlett, P.S. and Plackett, R.L. (1979). *The Interpretation of Quantal Responses in Biology*. Baltimore, Maryland: University Park Press.
- Hewlett, P.S. and Plackett, R.L. (1964). A Unified Theory for Quantal Responses to Mixtures of Drugs: Competitive Action. *Biometrics* **20** 566-575.
- Hochberg, Y. (1988). A Sharper Bonferroni Procedure for Multiple Tests of Significance, *Biometrika* **75**, 800-802.
- Hosmer, D.W. and Lemeshow, S. (1989). *Applied Logistic Regression*. New York, NY: John Wiley & Sons.
- Inselberg, A. (1985). The Plane with Parallel Coordinates, *The Visual Computer*, **1**, 69-91.
- Inselberg, A. and Dimsdale, B. (1987). Parallel Coordinates for Visualizing Multi-Dimensional Geometry. *Proceedings of Computer Graphics International*, Kunii, T.L., Editor. New York, N.Y.: Springer-Verlag.
- Jennrich, R.I. and Schluchter, Mark D. (1986). Unbalanced Repeated-Measures Models with Structured Covariance Matrices. *Biometrics* **42**, 805-820.
- Kelly, C. and Rice, J. (1990). Monotone Smoothing with Application to Dose-Response Curves and the Assessment of Synergism. *Biometrics* **46**, 1071-1085.
- Kotz, S., and Johnson, N.L. (eds.) (1982). *Encyclopedia of Statistical Sciences*. New York, N.Y.: John Wiley & Sons.
- Koziol, J.A., Maxwell, D.A., Fukushima, M., Colmerauer, M.E.M, and Pilch, Y.H. (1981). A Distribution-Free Test for Tumor-Growth Curve Analyses with Application to an Animal Tumor Immunotherapy Experiment. *Biometrics* **37**, 383-390.
- Laird, N., Lange, N., and Stram, D. (1987). Maximum Likelihood Computations with Repeated Measures: Application of the EM Algorithm. *Journal of the American Statistical Association* **82**, 97-105.
- Laird, N.M. and Ware, J.H. (1982). Random-Effects Models for Longitudinal Data. *Biometrics* **38**, 963-974.
- Lam, Y.M., Pym, J. and Campling, B.G. (1991). Statistical Models for Assessing Drug Interactions. *Proceedings of the Biopharmaceutical Section of the American Statistical Association* 214-219.

- Loewe, S. (1953). The problem of Synergism and Antagonism of Combined Drugs. *Arzneimittle forshung* **3**, 285-290.
- Machado, S.G. and Robinson, G.A. (1994). A Direct, General Approach Based on Isobolograms for Assessing the Joint Action of Drugs in Pre-Clinical Experiments. *Statistics in Medicine* **13**, 2289-2309.
- Madansky, A. A. (1989). Comparison of the Likelihood Ratio, Wald, and Rao Tests. *Contributions to Probability and Statistics, Essays in Honor of Ingram Olkin*. New York, NY: Springer-Verlag.
- Mantel, N. (1987). Understanding Wald's Test for Exponential Families. *The American Statistician* **41**, 147-148.
- Mardia, K.V. (1980). Test of Univariate and Multivariate Normality. *Handbook of Statistics, Vol. 1*. 279-320, P.R. Krishnaiah, ed., New York, NY: North Holland Publishing Co.
- Mathematical Society. (1993). Disproving the Obvious in Higher Dimensions. *What's Happening in the Mathematical Sciences*, **1**, 21-25.
- McCullagh, P. and Nelder, J.A. (1989). *Generalized Linear Model, Second Edition*. New York, NY: Chapman & Hall
- Morrison, D.F. (1976). *Multivariate Statistical Methods*. New York, NY: McGraw-Hill.
- Pregibon, D. (1981). Logistic Regression Diagnostics. *The Annals of Statistics*, **9**, 705-724.
- Rao, C. R. (1973). *Linear Statistical Inference and Its Applications, Second Edition*. New York, NY: John Wiley & Sons.
- SAS Institute Inc., SAS<sup>®</sup> Technical Reports p-229, *SAS/STAT<sup>®</sup> Software: Changes and Enhancements, Release 6.07*, Cary, NC: SAS Institute Inc., 1992. 620 pp.
- Serfling, R.J. (1980). *Approximation Theorems of Mathematical Statistics*. New York, NY: John Wiley & Sons.
- Steel, G.G. and Peckham, M.J. (1979). Exploitable Mechanisms in Combined Radiotherapy-Chemotherapy: The concept of Additivity. *International Journal of Radiat. Oncol. Biol. Phys.* **5**, 85-91.
- Tallarida, R.J. (1992). Statistical Analysis of Drug Combinations for Synergism, *Pain* **49**, 93-97.
- Tallarida, R.J. and Jacob, L.S. (1979). *The Dose-Response Relation in Pharmacology*, New York, N.Y.: Springer-Verlag.



- Ware, J.H. (1985). Linear Models for the Analysis of Longitudinal Studies. *The American Statistician* **39**, 95-101.
- Wedderburn, R.W.M. (1976). On the Existence and Uniqueness of the Maximum Likelihood Estimates for Certain Generalized Linear Models. *Biometrika*, **63**, 27-32.
- Wegman, E.J. (1990). Hyperdimensional Data Analysis Using Parallel Coordinates. *Journal of the American Statistical Association* **85**, 664-675.
- Weiss, R.E., and Lazaro, C.G. (1992). Residual Plots for Repeated Measures. *Statistics in Medicine* **11**, 115-124.
- Weller, E. (1992). *A Multivariate Rank Test Under Ordered Alternatives*. Unpublished Dissertation, Medical College of Virginia, Virginia Commonwealth University, Department of Biostatistics.
- Wessinger, W.D. (1986). Approaches to the Study of Drug Interactions in Behavioral Pharmacology. *Neuroscience and Biobehavioral Review* **10** 103-113.
- Wilkinson, L. (1992). Graphical Displays. *Statistical Methods in Medical Research*. **1**, 3-25.
- Wolfram, S. (1991). *Mathematica, A System for Doing Mathematics by Computer, Second Edition*. New York, NY: Addison-Wesley Publishing Company, Inc.

## **Appendix A**

## Appendix A

### Parallel Axis Plotting Program

```

/*****
/*
/* This SAS program plots points in two parallel axis plots.
/* The first plot are points that satisfy synergism and thesecond plot are points
/* that indicate antagonism.
/* User defines model and ranges of values they wish to examine in first data step.
/* Uses Proc Greplay to display both parallel axis plots on same page..
/*
/*****

%hscsps (figure58,,portrait);

/* format the labels for the parallel axes */

proc format;
  value xfmt 0='X1' 1='X2' 2='X3' 3='X4';

/* generate two data sets: syn and ant, which contain points that satisfy synergism
/* and antagonism respectively.

data syn ant;
  b0=-20;      b1=2;      b2=5;      b3=7;      b4=4;
  b12=.75;     b13=.8;     b14=.65;   b23=-.3;   b24=.6;    b34=-.5;
  b123=.5;     b124=.55;   b134=-.4;  b234=.45;
  b1234=.85;
  do x1=.5 to 2.5 by .5;
    do x2=.5 to 2.5 by .5;
      do x3=.5 to 2.5 by .5;
        do x4=.5 to 2.5 by .5;
          lpa=b0+b1*x1+b2*x2+b3*x3+b4*x4;
          lp=lpa+b12*x1*x2+b13*x1*x3+b14*x1*x4+b23*x2*x3+
            b24*x2*x4+b34*x3*x4+b123*x1*x2*x3+
            b124*x1*x2*x4+b134*x1*x3*x4+b234*x2*x3*x4+
            b1234*x1*x2*x3*x4;
          if lp>lpa then output syn;
          else if lp<lpa then output ant;
        end;
      end;
    end;
  end;
end;

```

```

        end;
    end;
end;

/* draw the line segments in the parallel axis system that represent the higher
/* dimensional synergistic points.
*/
*/

data picsyn;
    set syn;
    length function $ 8.; xsys='2'; ysys='2';
    function='move';y=x1;x=0;output;
    function='draw';y=x2;x=1;output;
    function='draw';y=x3;x=2;output;
    function='draw';y=x4;x=3;output;

/* draw the line segments in the parallel axis system that represent the higher
/* dimensional antagonistic points.
*/
*/

data picant;
    set ant;
    length function $ 8.; xsys='2'; ysys='2';
    function='move';y=x1;x=0;output;
    function='draw';y=x2;x=1;output;
    function='draw';y=x3;x=2;output;
    function='draw';y=x4;x=3;output;

/* Sets up a frame in which to draw the parallel axes. x=0 to 3 for the four
/* dimensional parallel axes. y=0 to 2.5 are possible values that each x1,x2,x3,x4
/* can assume.
*/
*/

data frame;
    do x=0 to 3;
        do y=0 to 2.5;
            output;
        end;
    end;
end;
format x xfmt.;

axis1 label=none value=(height=.5 in) order=0 to 3 by 1 minor=none major=none;
axis2 order=0 to 2.5 by .5 minor=none major=none label=none value=none;
title1 ' ';

proc gplot data=frame annotate=picsyn gout=fig;
    plot y*x/haxis=axis1 href=0 1 2 3 4 vaxis=axis2;
proc gplot data=frame annotate=picant gout=fig;
    plot y*x/haxis=axis1 href=0 1 2 3 4 vaxis=axis2;

proc greplay nofs;
    igout fig;
    tc template;
    tdef t2x1 1/ llx=20 ulx=20 lrx=80 urx=80

```

```
tdef t2x1 2/ lly=55 uly=80 lry=55 ury=80;  
            llx=20 ulx=20 lrx=80 urx=80  
            lly=20 uly=45 lry=20 ury=45;  
tempate t2x1;  
tplay 1:1 2:2;  
quit;
```

## **Appendix B**

## Appendix B

### Interaction Index Test

```

/*****
/*
/* This SAS program calculates the statistics used in the Interaction Index Test.
/* User inputs the data and programs any transformations of the doses needed.
/* User must also determine and program the functions defined by the Delta
/* Method. Analysis is described in Chapter 6.
/*
/*****

title 'log10 (dose+1)';
data rawdat;
  input x1 x2 r n;
  pobs=r/n;
  lx1=log10(x1+1);
  lx2=log10(x2+1);
cards;
0      0      0 30
5      0      1 10
10     0      2 10
25     0      3 10
130    0      4 10
265    0      7 10
670    0      9 10
0      5      0 10
0      25     0 10
0      55     4 10
0      280    4 10
0      565    4 10
0      1420   7 10
10     285    5 10
35     260    5 10
50     215    4 10
70     175    3 10
90     130    9 10
110    85     6 10
125    40     7 10
;

```

```

proc print data=rawdat;
title2 'Observed Data';

/* data set which contains the combination points (combo) and another data set which */
/* contains the axes data */

data combo axes;
  set rawdat;
  if x1=0 or x2=0 then output axes;
  else output combo;

/* determine the common intercept parameter and the slope parameters for each single */
/* agent dose-response curve. use the covout option to create a data set that contains */
/* the parameter estimates and the var-cov matrix for these estimates. */

proc logistic data=axes covout out=varcov;
  model r/n=lx1 lx2/covb;
  output out=pred p=phat;
proc print data=pred;
title2 'Predicted Values';

/* create data sets that contain the parameter estimates and the var-cov matrix for */
/* the parameter estimates from output from proc logistic. */

data betas varcov;
  set varcov;
  if _n_=1 then output betas;
  else output varcov;
  drop _link_ _type_ _name_ _lnlike_;

proc iml;
  start main;

  use betas;
  read all into beta;
  b0=beta[1,1]; b1=beta[1,2]; b2=beta[1,3];

  use varcov;
  read all into varcov;

  use combo;
  read all var {lx1 lx2} into lx;

  ten=j(nrow(lx),ncol(lx),10);
  one=j(nrow(lx),1,1);
  log10=j(nrow(lx),1,log(10));

  x=(ten##lx)-1;

  read all var {pobs} into pobs;

```



```

lpobs=log(pobs/(1-pobs));
ed1=ten[,1]##((lpobs-b0)/b1)-1;
ed2=ten[,1]##((lpobs-b0)/b2)-1;

ii=x[,1]/ed1 + x[,2]/ed2;

phi0=log10#(((ed1+one)#x[,1])/(b1#ed1##2)+((ed2+one)#x[,2])/(b2#ed2##2));
phi1=log10#(((ed1+one)#x[,1]#lx[,1])/(b1#ed1##2));
phi2=log10#(((ed2+one)#x[,2]#lx[,2])/(b2#ed2##2));
phi=phi0||phi1||phi2;

vars=diag(phi*varcov*T(phi))[,+];
wald=(1-ii)#(1-ii)/(vars);
pval=1-probchi(wald,1);

n=j(nrow(x),1,nrow(x));

ans=x||pobs||ed1||ed2||ii||wald||pval||n;
c={'x1','x2','pobs','ed1','ed2','ii','wald','pval','n'};
create ans from ans[colname=c];
append from ans;
finish main;
run main;

proc sort data=ans;
  by descending pval;

/* print results using Hochberg (1988) method for adjusting for multiple testing */

data ans;
  set ans;
  retain j done 1;
  length intact $10.;
  cut=.05/(n-j+1)*done;
  if ii<1 then intact='Synergism';
  else if ii>1 then intact='Antagonism';
  else intact='Additivity';
  j=j+1;
proc print;
  var x1 x2 pobs ed1 ed2 ii intact wald pval cut;
  title2 'Analysis Results';

```

## **Appendix C**

## Appendix C

### Ray Design Analysis

```

/*****
/*
/* This program performs the analysis of the ray designed data. The example is
/* described in Section 7.5.
/* User must input the ratios for each ray included in the study as well as the observed
/* data along each ray. This program then determines the maximum likelihood
/* estimates for the parameters, as well as a goodness-of-fit test.
/* Likelihood ratio, Wald and Score tests are used to determine if nonadditivity is
/* indicated along at least one nonaxis ray. Individual tests for nonadditivity are also
/* conducted along each nonaxis ray. A multiple testing adjustment is made using
/* Hochberg's procedure.
/*
/* Assume there are M rays, N agents, G observations in form r and n where n is
/* is the number of replications and r is the number of successes.
/*
/*****

```

```
libname save 'UD$VPH:[DAWSON.CHAPTER7]';
```

```
title1 '15 Ray - 4 Agent Analysis';
```

```
/* input the ratios, which sum to 1 which define each ray including the axis rays
```

```

data design;
  input ray a1 a2 a3 a4;
cards;
1 1 0 0 0
2 0 1 0 0
3 0 0 1 0
4 0 0 0 1
5 .5 .5 0 0
6 .5 0 .5 0
7 .5 0 0 .5
8 0 .5 .5 0
9 0 .5 0 .5
10 0 0 .5 .5
11 .333 .333 .333 0
12 .333 .333 0 .333

```

```

13 .333 0 .333 .333
14 0 .333 .333 .333
15 .25 .25 .25 .25
;

/* data set contains x1 x2 x3 x4 ray r n */

proc print data=save.data4;
title2 'Observed Data';

/* generate input for proc logistic */
/* N+1 columns of total doses and last two columns r and n */
/* G rows - one for each unique dose combination including origin */

data raydat;
  set save.data4;
  total=x1+x2+x3+x4;
  r0=1; r1=0; r2=0; r3=0; r4=0; r5=0; r6=0; r7=0; r8=0; r9=0;
  r10=0; r11=0; r12=0; r13=0; r14=0; r15=0;
  if ray=1 then r1=total;
  else if ray=2 then r2=total;
  else if ray=3 then r3=total;
  else if ray=4 then r4=total;
  else if ray=5 then r5=total;
  else if ray=6 then r6=total;
  else if ray=7 then r7=total;
  else if ray=8 then r8=total;
  else if ray=9 then r9=total;
  else if ray=10 then r10=total;
  else if ray=11 then r11=total;
  else if ray=12 then r12=total;
  else if ray=13 then r13=total;
  else if ray=14 then r14=total;
  else if ray=15 then r15=total;
keep r0 r1 r2 r3 r4 r5 r6 r7 r8 r9 r10 r11 r12 r13 r14 r15 r n total ray;

proc logistic out=varcov data=raydat covout maxiter=100;
  model r/n=r1 r2 r3 r4 r5 r6 r7 r8 r9 r10 r11 r12 r13 r14 r15;
  output out=pred p=phat;

/* total dose matrix */

data x;
  set pred;
  drop r n phat total ray;

data beta varcov;
  set varcov;
  if _n_=1 then output beta;
  else output varcov;
  drop _link_ _type_ _name_ _lnlike_;

```

```

/* calculate overall Wald test for nonadditivity */
/* calculate Wald Statistics to test for nonadditivity along each nonaxis ray. */

title3 'Wald Statistics';

proc iml;
  start main;

    use beta;
    read all into temp;
    beta=T(temp);
    m=nrow(beta)-1;

    use design;
    read all into temp2;
    design=temp2[,2:ncol(temp2)];
    n=ncol(design);

    use varcov;
    read all into varcov;

    c=j(m-n,m+1,0);
    c[,2:n+1]=(-1)#design[n+1:m,];
    c[,n+2:m+1]=I(m-n);

    restrict=c*beta;
    wald=t(restrict)*(inv(c*varcov*t(c)))*(restrict);
    df=m-n;
    pval=1-probchi(wald,df);
    print 'Overall Wald Test for Nonadditivity: ' wald ' df: ' df ' p-value: ' pval;

  start loop;
  do i=1 to m-n;
    ray=n+i;
    waldi=(restrict[i,1]**2)*(inv(c*varcov*t(c)))[i,i];
    pval=1-probchi(waldi,1);
    betai=beta[n+1+i,1];
    betaai=betai-restrict[i,1];
    outtemp=ray||m-n||betai||betaai||waldi||pval;
    outx=outx//outtemp;
  end;
  finish loop;
  run loop;
  c={'ray','num','beta','betaa','wald','pval'};
  create walldrays from outx[colname=c];
  append from outx;
  finish main;
run;

```

```
/* Use Hochberg multiple testing correction.
```

```
*/
```

```
proc sort data=waldrays;
  by descending pval;
title4 'Wald Test on Each Ray';
data waldrays;
  set waldrays;
  retain j 1;
  length intact $10.;
  cut=.05/(num-j+1)*done;
  if beta>betaa then intact='Synergism';
  else intact='Antagonism';
  j=j+1;
proc print;
  var ray beta betaa intact wald pval cut;
```

```
/* Goodness-of-fit test described in Chapter 3
```

```
*/
```

```
title3 'Goodness-of-Fit';
proc iml;
```

```
  start main;
```

```
  use x;
  read all into x;
```

```
  G=nrow(x);
```

```
/* pp1 = number of parameters
```

```
*/
```

```
  pp1=ncol(x);
```

```
  use pred;
  read all var {phat r n} into phat;
```

```
  use varcov;
  read all into iinv;
```

```
  V=x*iinv*T(x);
```

```
  t1=0; t2=0; t3=0; t4=0;
```

```
  chisq=0;
```

```
  start loop;
```

```
    do i=1 to g;
```

```
      phati=phat[i,1]; yi=phat[i,2]; ni=phat[i,3];
```

```
      chisq=chisq+(yi-ni*phati)**2/
```

```
        (ni*phati*(1-phati));
```

```
      t1=t1+(1-6*phati*(1-phati))*V[i,i];
```

```
      t3=t3+(ni-1)/ni;
```

```
      start loop2;
```

```
        do j=i to g;
```

```
          phatj=phat[j,1];
```

```

        t2=t2+ ni*phati*(1-phati)*(1-2*phati)*
              v[i,i]*v[i,j]*(1-2*phatj);
        t4=t4+(1-2*phati)*(1-2*phatj)*v[i,j];
    end;
    finish loop2;
    run loop2;
end;
ex=g-pp1-.5*t1+.5*t2;
vx=(1-pp1/g)*(2*t3+t4);
z=(chisq-ex)/sqrt(vx);
pval=1-probnorm(z);
df=g-pp1;
pvalold=1-probchi(chisq,df);
finish loop;
run loop;
finish main;
run main;
print 'Goodness-of-fit: McCullagh and Nelder, p.122';
print chisq df ex vx z pval;
print 'Usual Pearson goodness-of-fit ' pvalold;

/* individual goodness-of-fit statistics by observation */

data goodfit;
    set pred;
    chisqi=(r-n*phat)/sqrt(n*phat*(1-phat));
    if r=0 then
        di=sqrt(-2*n*log(1-phat));
    else if r=n then
        di=sqrt(-2*n*log(phat));
    else do;
        pi=r/n;
        lpi=log(pi/(1-pi));
        lphat=log(phat/(1-phat));
        di= sqrt(-r*lphat-n*log(1-phat) + r*lpi+n*log(1-pi));
        if pi<phat then di=-sqrt(2)*di;
        else di=sqrt(2)*di;
    end;
    keep r n phat chisqi di;
proc print;
title3 'By Observation Goodness of Fit';
run;

/* Overall Score test for nonadditivity */

title2 'Scores';

data rawadd;
    set save.data4;
    x0=1;

```

```

keep x0 x1 x2 x3 x4 r n;
proc logistic out=varcov2 data=rawadd covout maxiter=100;
  model r/n=x0 x1 x2 x3 x4/noint;
  output out=pred2 p=phata;

data x2;
  set pred2;
  drop r n phata;

data beta2;
  set varcov2;
  if _n_=1;
  drop _link_ _type_ _name_ _lnlike_;
data varcov2;
  set varcov2;
  if _n_ >1;
  drop _link_ _type_ _name_ _lnlike_;
run;

proc iml;

  start;
  use beta2;
  read all into betas;
  b0=betas[1,1];

  use pred2;
  read all var {r} into r;
  read all var {n} into ni;
  read all var {phata} into phat;

  use x;
  read all into x;
/* t is the g x m matrix of total doses
t=x[1:nrow(x),2:ncol(x)];

  g=nrow(t);
  m=ncol(t);
  n=ncol(betas)-1;

  temp=r-ni#phat;
  temp2=j(nrow(t),ncol(t),0);
  start loop;
  do i=1 to ncol(t);
    temp2[,i]=temp;
  end;
  finish loop;
  run loop;

  scores=j(m+1,1,0);
  scores[2:m+1,1]=T((t#temp2)[+,]);
*/

```



```
scores[1,1]=scores[+,1];

temp=ni#phat#(1-phat);
temp2=j(nrow(t),ncol(t),0);
start loop2;
do i=1 to ncol(t);
    temp2[,i]=temp;
end;
finish loop2;
run loop2;

ioj=(t#temp2)[+,,];
ijj=(t#t#temp2)[+,,];

i=j(m+1,m+1,0);
i[1,1]=exp(-b0)/((1+exp(-b0))**2);
i[1,2:m+1]=ioj;
i[2:m+1,1]=T(ioj);
i[2:m+1,2:m+1]=diag(ijj);

iinv=inv(i);

s=T(scores)*Inv(i)*scores;
df=m-n;
pval=1-probchi(s,df);
print 'Score Statistic ' s ' df: ' df ' pval: ' pval;
finish;
run;
```

## Vita

[REDACTED]